

Open Research Online

The Open University's repository of research publications and other research outputs

The Role of Inoculum in the Primary and Secondary Infection of Certain Plant Pathogens

Thesis

How to cite:

Bailey, Douglas John (1997). The Role of Inoculum in the Primary and Secondary Infection of Certain Plant Pathogens. PhD thesis. The Open University.

For guidance on citations see [FAQs](#).

© 1997 Douglas John Bailey

Version: Version of Record

Copyright and Moral Rights for the articles on this site are retained by the individual authors and/or other copyright owners. For more information on Open Research Online's [data policy](#) on reuse of materials please consult the policies page.

oro.open.ac.uk

UNRESTRICTED

**THE ROLE OF INOCULUM IN THE PRIMARY AND
SECONDARY INFECTION OF CERTAIN PLANT
PATHOGENS**

A thesis submitted for the degree of Doctor of Philosophy

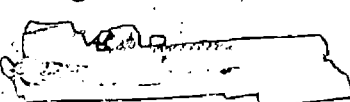
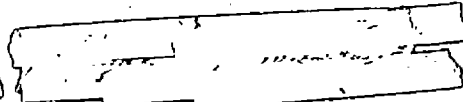
Department of Biology

The Open University

August 1997

Douglas John Bailey

B.Sc. (Hons.)

 
Date of submission: 8th August 1997
Date of award: 20th November 1997

ProQuest Number: C651972

All rights reserved

INFORMATION TO ALL USERS

The quality of this reproduction is dependent upon the quality of the copy submitted.

In the unlikely event that the author did not send a complete manuscript and there are missing pages, these will be noted. Also, if material had to be removed, a note will indicate the deletion.



ProQuest C651972

Published by ProQuest LLC (2019). Copyright of the Dissertation is held by the Author.

All rights reserved.

This work is protected against unauthorized copying under Title 17, United States Code
Microform Edition © ProQuest LLC.

ProQuest LLC.
789 East Eisenhower Parkway
P.O. Box 1346
Ann Arbor, MI 48106 – 1346

Abstract

The infection cycle of some economically important soil-borne plant pathogens involves a combination of primary infection from particulate inoculum residing in the soil and secondary infection as disease is spread from infected to susceptible hosts. This study examines the role of the two types of inoculum in the primary and secondary infection of soil-borne plant disease using a combination of experimentation and mathematical modelling.

The infectivity of inoculum can be quantified by the pathozone profile which measures changes in the probability of infection when inoculum occurs at different distances from the host. The study showed that the germinability of inoculum, the growth of the mycelial colony and the infectivity of mycelium at the surface of the host combine to dictate the shape of the pathozone profile for *Rhizoctonia solani* on radish. The ultimate shape of the pathozone depended on inoculum type and was particularly sensitive to changes in the density and distribution of the mycelium in the fungal colony. Mycelium from an infected radish plant grew much further and at a higher density than that from particulate inoculum (mycelial discs). This resulted in pathozone profiles that differed in shape. For particulate inoculum the profile rose and fell with distance whilst for an infected plant the decay was sigmoidal.

The characteristic shape of the pathozone for different inoculum types of *Rhizoctonia solani* was summarised using simple, non-linear models in which certain parameters were allowed to vary with time. Thus, the pathozone behaviour of single plants could be used to predict the progress of disease at the population level both in an unprotected crop and in a crop protected with the biological control agent *Trichoderma viride*. Predictions were particularly accurate for an epidemic restricted to primary infection or for an epidemic

dominated by secondary infection in the absence of biological control. The model underestimated the extent of secondary infection in the protected crop.

The contribution of inoculum type to the spread of disease was examined in a contrasting host-pathogen system involving the infection of wheat roots by the take-all fungus, *Gaeumannomyces graminis* var *tritici*. Two phases of disease progress were identified, an initial phase dominated by primary infection during which particulate inoculum decayed, and a subsequent phase involving an increase in secondary infection driven by the availability of susceptible host tissue. From a low density of initial inoculum this resulted in a disease progress curve which rose monotonically to an initial plateau and was sigmoidal thereafter. These results were consistent with observations from field data. The biological control agent, *Pseudomonas corrugata*, reduced the probability of infection on the seminal roots of a wheat plant from particulate inoculum. However, suppression of primary infection alone is not considered adequate for control of take-all over an entire season.

Declaration

With the exception of the work described below I hereby declare that all the studies presented in this dissertation are the original work of the author.

Two areas of mathematical modelling involved a contribution from other researchers. The precise derivation of the mathematical model used to predict the progress of disease from the pathozone behaviour of single plants for an epidemic involving monocyclic disease (Section 5.3.2) was performed in collaboration with Dr C. A. Gilligan.

Also, the mathematical prediction of disease progress from the pathozone behaviour of single plants for an epidemic involving polycyclic disease (Section 5.4.2) was performed in collaboration with Dr A. Kleczkowski.

Acknowledgements

The work described in this thesis was carried out in the Department of Plant Sciences at the University of Cambridge. Sincere thanks are due to my supervisors, Dr C. A. Gilligan for his continued support and encouragement and for his rigorous assessment of my work, and Dr I. Ridge for careful reading and marking of the thesis. I am also grateful to Sir J. H. Burnett for his constructive comments regarding the structure of the thesis. Thanks are also due to the members of the Botanical Epidemiology Group at the Department of Plant Sciences for providing an excellent working environment. In particular I would like to thank Dr W. Otten, Dr C. Thornton and Dr A. Kleczkowski for numerous and invaluable discussions which helped to facilitate the vital link between experimentation and mathematical modelling. I am also grateful to Mr B. Goddard for his technical assistance and computing expertise.

I am indebted to the late Professor T. ap Rees for his support during the conception and the first three years of this work and for the provision of facilities in the Department of Plant Sciences.

Finally, special thanks are reserved for my wife, Hayley, who continues to express restrained interest in my work and for the support of my friends and family.

Table of contents

Abstract	i
Declaration	iii
Acknowledgments	iv
Table of contents	v
List of figures	ix

Chapter 1 Introduction and literature review

1.1 Introduction	1
1.2 Background to study	1
1.2.1 Properties of inoculum	1
1.2.2 Disease progress curves	8
1.2.3 The mathematical description of disease	10
1.2.4 Host-pathogen systems	14
1.2.5 The pathogens	16
1.2.6 Specific biological control agents	22
1.2.7 Host susceptibility and the rhizosphere	25
1.3 The present investigation	27

Chapter 2 General materials and methods

2.1 Introduction	30
2.2 Experimental growth conditions	30
2.3 Soils	31
2.4 The hosts	32
2.5 Statistical analysis	32

2.6	The pathogens	33
2.6.1	Pathogenicity screening	34
2.6.2	Particulate inoculum	39
2.7	Biological control agents	48
2.7.1	<i>Trichoderma</i> and <i>Gliocladium</i>	48
2.7.2	<i>Pseudomonas corrugata</i>	54
Chapter 3	Inoculum and components of pathozone infection	
3.1	Introduction	56
3.2	Methods	57
3.2.1	Production of inoculum	57
3.2.2	Components of pathozone infection	57
3.2.3	Pathozone profiles	60
3.2.4	Derivation of model	61
3.3	Results	64
3.3.1	Estimation of the probability of germination	64
3.3.2	Estimation of the furthest extent of mycelial growth	64
3.3.3	Estimation of changes in hyphal density with distance	65
3.3.4	Estimation of the probability of infection given contact	71
3.3.5	Comparison of model predictions and experimental data	75
3.3.6	Stochastic realisations of model (3.16)	78
3.3.7	Sensitivity of model (3.16) to changes in parameter values	81
3.4	Discussion	82
Chapter 4	Fungal growth: A major determinant dictating the shape of the pathozone	
4.1	Introduction	89

4.2	Materials and methods	92
4.2.1	Microcosm experiment	92
4.2.2	Visualisation of the antigen	93
4.2.3	Quantification of mycelium	93
4.2.4	Comparison of growth from mycelial disc and infected plant inoculum	94
4.2.5	Predicting the probability of contact	94
4.2.6	The furthest extent of radial growth	95
4.3	Results	95
4.3.1	The active growth zone	95
4.3.2	The relationship between mycelial cover and hyphal density	100
4.3.3	Changes in μ and k over distance and time.	100
4.3.4	Estimating the probability of contact (P_2b)	103
4.3.5	The furthest extent of radial growth	103
4.4	Discussion	103
Chapter 5	Biological control of pathozone dynamics and disease progress	
5.1	Introduction	109
5.2	Pathozone dynamics of mycelial disc and infected plant inoculum	110
5.2.1	Introduction	110
5.2.2	Methods	111
5.2.3	Results	115
5.2.4	Discussion	122

5.3 Biological control of pathozone behaviour and disease progress caused by primary infection	126
5.3.1 Introduction	126
5.3.2 Materials and methods	127
5.3.3 Results	132
5.3.4 Discussion	140
5.4 Biological control of pathozone behaviour and disease progress including secondary infection	145
5.4.1 Introduction	145
5.4.2 Model derivation	146
5.4.3 Experiments	151
5.4.4 Results	153
5.4.5 Discussion	156
Chapter 6 The dynamics of primary and secondary infection in take-all epidemics	
6.1 Introduction	161
6.2 Disease progress of take-all	164
6.2.1 Materials and methods	164
6.2.2 Results	170
6.2.3 Discussion	183
6.3 Biological control of take-all using <i>Pseudomonas corrugata</i>	186
6.3.1 Introduction	186
6.3.2 Materials and methods	187
6.3.3 Results	189
6.3.4 Discussion	194

Chapter 7	Discussion and conclusions	200
References		209
Appendices		225

List of figures

1.1	The infection chain of a soil-borne plant pathogen.	9
2.1	Profiles describing changes in the probability of infection with distance for millet seed infested with <i>G. graminis</i> , chopped potato soil and mycelial discs infested with <i>R. solani</i> .	45
2.2	The effect of number of units of <i>Trichoderma</i> or <i>Gliocladium</i> growing from quinoa or poppyseed on the probability of infection by <i>R. solani</i> and on tap root length of radish seedlings.	52
3.1	Schematic representation of two properties of colony architecture used to estimate the probability of contact between mycelium growing out of a source of inoculum and host.	59
3.2	Histograms of the fitted distributions to the furthest extents of mycelial growth from CPS and MD inoculum.	66
3.3	Probability distributions for the number of hyphae passing through 2.34 mm sectors at different radial distances from the centre of colonies growing from CPS and MD inoculum.	67
3.4	Predicted and observed changes with distance from the centre of inoculum of the mean and clumping parameters of the negative binomial distribution for CPS and MD inoculum.	70
3.5	Changes in the probability of contact with the host with distance for different threshold numbers of hyphae.	72
3.6	Change in the probability of infection given contact with distance and with time for CPS and MD inoculum.	73
3.7	Summary of empirical observations of changes in the probability of infection with distance for CPS and MD inoculum using simple non-linear models.	76
3.8	Comparison of predicted and observed pathozone profiles for CPS and MD inoculum.	79

3.9	The effects of replication on stochastic realisations of the pathozone profile.	80
3.10	The effect of replication on the variance of the pathozone profile.	81
3.11	Sensitivity of a probability model (3.1) describing the pathozone profile to changes in parameters values.	83
3.12	Sensitivity of a probability model (3.1) describing the pathozone profile to changes in host susceptibility.	84
4.1	Sampling strategy used to detect changes in the density and distribution of mycelium at different distances from a unit of inoculum.	95
4.2	Calibration curve relating the number of hyphae present within a sampling unit with the area of sample covered by mycelium.	96
4.3	Scanned immunoblot images from a single colony of <i>R. solani</i> growing from a mycelial disc.	98
4.4	Scanned immunoblot images from a single colony of <i>R. solani</i> growing from an infected plant.	99
4.5	Surfaces describing changes in the mean density and clumping of mycelium over distance and time for mycelial disc and infected plant inoculum.	102
4.6	Predicted changes in the probability of contact of a host with distance and over time using immunoblotting by mycelial disc and infected plant inoculum.	104
4.7	Change in the furthest extent of mycelial growth from mycelial disc and infected plant inoculum.	105
5.1	Characteristic shapes of curves described by various non-linear models	113
5.2	The evolution of pathozone profiles for mycelial disc and infected plant inoculum.	116
5.3	Change in parameter values of simple non-linear models describing the evolution of pathozone profiles from mycelial disc and infected plant inoculum.	118
5.4	Response surfaces for pathozone profiles over distance and time from mycelial disc and infected plant inoculum.	120
5.5	Predictions of changes in the extent of the pathozone over time for mycelial disc and infected plant inoculum.	123

5.6	Profiles describing changes in the probability of disease with distance between the host and inoculum of either <i>R. solani</i> alone, <i>R. solani</i> with an additional food base (poppyseed) or <i>R. solani</i> with <i>Trichoderma</i> colonised poppyseed.	133
5.7	Change in parameter values over time for pathozone profiles described by the critical exponential function in the presence and absence of <i>Trichoderma</i> .	135
5.8	Response surfaces in the presence and absence of <i>Trichoderma</i> .	136
5.9	Predicted changes in the extent of the pathozone in the presence and absence of <i>Trichoderma</i> .	138
5.10	Comparison of predicted and observed disease progress curves for <i>R. solani</i> on radish seedlings in the presence and absence of <i>Trichoderma</i> .	139
5.11	Effects of changing parameter values of the critical exponential function on the shape of the pathozone profile.	141
5.12	Effects of changing $K (=exp -\theta_3)$ on disease progress caused by primary infection.	143
5.13	Diagrammatic illustration of the delays present in the primary and secondary infection of radish plants.	150
5.14	Surfaces describing the evolution of the pathozone for mycelial disc and infected plant inoculum.	154
5.15	Comparison of predicted and observed disease progress in the presence and absence of <i>Trichoderma</i> using the cellular automaton.	157
6.1	Change in the infectivity of particulate (infested millet) inoculum of <i>Ggt</i> over time.	171
6.2	Change in the number of main and lateral root axis over time from wheat plants growing in soil inoculated with either a low or high density of particulate inoculum.	173
6.3	Disease progress curves from wheat inoculated with either a low or a high density of particulate inoculum and fitted with the model for primary and secondary infection (model 1, excluding host growth and inoculum decay).	175
6.4	Disease progress curves from wheat inoculated with either a low or a high density of particulate inoculum and fitted with the model for primary and secondary infection (model 2, including growth of main root axis and inoculum decay).	177

6.5	Disease progress curves from wheat inoculated with either a low or a high density of particulate inoculum and fitted with the model for primary and secondary infection (model 3, including growth of both main root and lateral root axis together with inoculum decay).	178
6.6	Disease progress of take-all on the seminal and adventitious roots of wheat plants inoculated with a low density of particulate inoculum.	180
6.7	Disease progress of take-all on the seminal and adventitious roots of wheat plants obtained from field data.	182
6.8	Profiles describing changes in the probability of infection with distance between a wheat seminal root either colonised or uncolonised by <i>P. corrugata</i> and a unit of millet seed infested with <i>Ggt</i>	190
6.9	Change in the parameter values of a simple non-linear model describing the pathozone profile for <i>Ggt</i> on wheat in either the presence or absence of <i>P. corrugata</i> .	192
6.10	Response surfaces describing changes in the probability of infection with distance and time for the infection of wheat by <i>Ggt</i> in the presence and absence of <i>P. corrugata</i> .	193
6.11	Predictions of disease progress caused by primary infection of <i>Ggt</i> on the seminal roots of wheat in the presence and absence of <i>P. corrugata</i> .	195
6.12	Predicted effects from of controlling either primary or secondary infection using model 2 (describing the primary and secondary infection of wheat root over time and including terms for the growth of main root axis and for inoculum decay).	198

Chapter one

Introduction

1.1 *Introduction*

This investigation deals with the interpretation of disease progress described using simple, non-linear mathematical models. Differences in the shape of a disease progress curve are reflected in the parameter values of the models. In order to interpret the value of these parameters a clear understanding of the underlying biological components is crucial. The study focuses on the properties of inoculum as one major component affecting parameter estimates. However, it is recognised that the influence of inoculum cannot be examined in isolation and consideration is also given to changes in the host and in the environment. In this chapter current ideas regarding the properties of inoculum and the mathematical description of disease are introduced. This is followed by a description of two contrasting host pathogen systems which are used to relate the behaviour of inoculum to the progress of disease. The systems involve the infection of radish by *Rhizoctonia solani* Kühn and the infection of wheat by *Gaeumannomyces graminis* (Sacc.) Arx and Oliver. *tritici* Walker. Biological control agents can be used to influence the behaviour of inoculum and thus reduce disease. The current status of introduced biological control agents (*Trichoderma* spp. and *Pseudomonas* spp.) is also reviewed.

1.2 *Background to study*

1.2.1 *Properties of inoculum*

Inoculum has been defined as the viable material that can infect a host (Dimond and Horsfall, 1965) and features centrally in studies of botanical epidemiology both for foliar

and soil-borne plant pathogens. However, because of the relative ease with which the disease components of a foliar epidemic can be quantified, these have received more attention (Gilligan, 1987). Zadoks and Schein (1979) divide inoculum of aerial pathogens into dispersal and infection units. A dispersal unit is any device for spread and survival that can be recognised visually and counted, and for a foliar fungal pathogen it is represented by the spore. When a spore germinates in the presence of a suitable host, it produces a mycelial structure termed the infection unit which can also be quantified. For a foliar pathogen, the growth of mycelium makes little contribution to the distance over which the pathogen can spread to reach a susceptible host.

The same system of classification was applied to soil-borne fungi by Gilligan (1987). Soil-borne fungal pathogens exhibit greater diversity of inoculum, producing, in addition to spores and sclerotia, rhizomorphs and various soil or organic particles impregnated with living mycelium. These propagules are the initiators of mycelial growth and are equivalent to the spores of a foliar pathogen, dispersing the organism over time and space.

In contrast to foliar pathogens, direct contact between host and dispersal unit is not an essential pre-requisite with which to provide the soil-borne pathogen some chance of infection. Many of these subterranean parasites produce dispersal units capable of establishing a mycelial colony such that they need only to fall within a critical distance of a potential host to achieve this (Gilligan, 1985). Direct contact with the host is then achieved by the growth of mycelium through the soil to the host surface, a process that may be augmented by chemotropic response to the production of root exudate. This is particularly relevant to the zoosporic fungi (Deacon, 1996) but, as indicated by the response of mycorrhizal fungi to root exudate, may also be important for fungi that make contact via mycelial growth (Horan and Chilvers, 1990). The distances from which a pathogen can grow to make contact with the host depend on the pathogen and inoculum involved but may

range from only a few millimetres, as is common for *Gaeumannomyces graminis* (Gilligan and Simons, 1987) to many metres for tree pathogens such as *Armillaria mellea* (Garrett, 1956). Thus, the mycelial colony plays an enhanced role in the spread of soil-borne disease and is a major component of dispersal. Having infected the host, the multiplication of a soil-borne pathogen may be similar to that of a foliar pathogen, involving the production and release of dispersal units in the form of spores (eg *Plasmodiophora*, *Pythium* etc). However, because many soil-borne pathogens spread by the growth of mycelium outward from an infection unit to a susceptible host sited nearby, the dispersal unit may be represented, not by a discrete propagule, but by a single, viable hypha.

The growth and movement of mycelium through the soil is fuelled by the translocation of nutrients from the infection unit, the efficiency of which contributes to the spread of disease and to the colonisation of soil organic matter (Garrett, 1956; 1970). Mycelial growth has proved difficult to quantify directly, particularly *in situ*. The diameter of individual hyphae of a soil-borne pathogen are rarely larger than 10 μm which hinders visualisation and detection. Accordingly, most studies either record the effects of mycelial growth by measuring infection or colonisation whereby inoculum is defined according to its mycelial source or involves organisms in which mycelium is aggregated to form more easily observed cords (Boddy, 1993). Consequently, whilst a single viable hypha or section of a hypha is recognised as the smallest measurable unit of inoculum from which new mycelium may grow to initiate infection (i.e. an infection unit *sensu* Zadoks and Schein, 1979), for the purpose of this study I, as others have before, define inoculum according to the source from which the mycelial colony originates.

Inoculum is typically characterised by its infectivity which depends on the density, nutritional status and genotype of the hyphae that grow from it and interact with the surface of a susceptible host under the regimes imposed by a given environment. These components

are embodied in the term inoculum potential defined by Garrett (1956) as the energy of growth of a parasite available for infection of a host, at the surface of the host organ to be infected and do not include host susceptibility (termed disease potential by Grainger, 1956). Whilst the term 'inoculum potential' has been criticised as a biological entity which is impossible to quantify (Vanderplank, 1975) it is a useful concept which clearly identifies the components of inoculum that are responsible for infection.

The nutrient status of a unit of inoculum is affected by the quantity and quality of endogenous energy it can accommodate. Larger propagules, presumably having a higher reserve of endogenous energy, are typically more infective than smaller ones of the same type (Henis and Ben-Yephet, 1970). Also, differences in the quality of substrate from which inoculum is produced are manifested as differences in infectivity from inoculum units of equal size (McCoy and Krafts, 1984). It remains unclear what proportion of this increase in inoculum potential can be attributed to an increase in the density of mycelium contacting the host surface or an increase in the metabolic activity of individual hyphae. Exogenous nutrients in the form of host exudate also play a role in the infectivity of inoculum. Rhizodeposition, the loss of organic material from the roots as they grow through the soil, can provide an additional nutrient base on which the pathogen can multiply (Schroth and Hildbrand, 1964). If rhizodeposition can account for up to 40% of total photosynthates, this begs the question as to how the dependency of the pathogen on the different energy sources (endogenous or exogenous) changes over time.

The definition of inoculum potential given by Garrett (1956) implicitly incorporates the requirement that, to have any chance of infection, the pathogen must make contact with the host. Soil-borne pathogens can be classified according to those which can grow to the host, for example, *R. solani*, and those which depend on growth of the host to achieve contact, described by Schutte (1956) as translocating and non-translocating fungi respectively. The

same distinction was made, albeit within a nutritional context, by Lingappa and Lockwood (1964) and Ko and Lockwood (1967) with reference to fungal spores and according to their requirement for an exogenous source of carbon to stimulate germination. These contrasting ecological strategies were effectively examined by Baker *et al* (1967) who related inoculum density to disease in an early attempt to provide a rigorous mathematical account of inoculum potential. The spatial dependency of soil-borne pathogens on the disease they cause was described by a mathematical model, the so called surface density model, where change in the number of infections, s , with density of inoculum, I , is given by the formula $s = k(I)^m$ in which k is a constant. The magnitude of the parameter, m , was used to distinguish between pathogens which must occur at the rhizoplane ($m = 0.67$) to cause infection, and those which can grow towards the host and infect when they occur within the rhizosphere ($m = 1.0$).

Whilst this approach provided some necessary stimulation for further work, the basis on which the model was derived has been successfully criticised (Gilligan, 1979; Grogan *et al.*, 1980; Ferris, 1981; Leonard, 1980). These criticisms question the two dimensional nature of the rhizoplane (Grogan *et al.*, 1980), the dimensionality of inoculum and the location of the inoculum in relation to the host (Leonard, 1980). Gilligan (1979) proposed an alternative probabilistic model which relates the number of infected plants, N_i , to inoculum density, P , as:

$$N_i = N(1 - (1 - \phi)^P) , \quad (1.1)$$

where N is the number of hosts and P is the number of propagules occurring in a fixed volume of soil. The model is derived from the concept of the pathozone defined by Gilligan (1985) as the volume of soil surrounding a subterranean plant organ within which the centre of a propagule must occur if it is to have any chance of infecting the organ. The

parameter, ϕ , measures the probability of a single, randomly distributed propagule occurring within the pathozone of a single host and is given by the ratio of pathozone soil, v , to total soil volume, V . For a single root of length, L , uniformly susceptible along its length, the pathozone volume, v , was calculated by Gilligan (1985) as:

$$v = \pi L(r_r + z)^2, \quad (1.2)$$

and by Ferriss (1981) as:

$$v = \pi L((r_r + z)^2 - r_r^2), \quad (1.3)$$

where r_r is the radius of the root and z is the distance between the centre of the inoculum unit and the surface of the root. The latter differs by the exclusion of host volume from estimation of the pathozone. By rearrangement of equation (1.3), z , is given as:

$$z = \left(\frac{v}{\pi L} + r_r^2 \right)^{1/2} - r_r, \quad (1.4)$$

where, from equation (1.1) in which $\phi = v/V$:

$$v = \frac{1}{V} \left(1 - \left(\frac{N - N_i}{N} \right)^{1/r} \right) \quad (1.5)$$

The pathozone may extend beyond the influence of the rhizosphere when the inoculum unit of a pathogen is capable of germination, growth to and infection of a potential host in the absence of any host related stimulation. Furthermore, the pathozone is not restricted to a volume of soil surrounding a root but to any subterranean organ, such as a seed, hypocotyl, epicotyl or mesocotyl. The dimensions of the pathozone are characterised, not simply by the its size or volume, but by changes in the probability of infection when

inoculum occurs within different regions of the pathozone. This probability has been defined as the infection efficiency of inoculum (Gilligan, 1987) and may be experimentally determined by placing single, replicate units of inoculum at different distances from a host. The efficiency of infection is then calculated as the proportion of inoculum units that successfully infect the host from each distance. The relationship between inoculum efficiency and distance can be described by a curve, or pathozone profile, which typically declines with distance (Gilligan and Simons, 1987). This information can be used to refine the probability model (1.1) whereby not all the inoculum which occurs in the pathozone is certain to cause infection. The parameter ϕ is expanded to give $\phi = \theta\psi$ where θ is the probability that an inoculum unit occurs within the pathozone (formerly ϕ) and ψ is the conditional probability that it causes infection which depends on its location within the pathozone. By allowing the parameters describing the pathozone profile to become time dependent, the pathozone provides a potential link between the infection of a single host and the progress of an epidemic amongst a population of hosts.

Infectivity of inoculum has also been characterised by its longevity. Because the attentions of plant pathologists have been dominated by components of primary infection, enhanced decay of particulate inoculum, particularly between the growing seasons of an agricultural crop, represents an obvious disease control measure and a relatively simple variable with which to assess the performance of a given disease control strategy. Inoculum decay, a decline in the density of inoculum over time, has been described by three types of model assuming either simple, exponential decay (Yarwood and Sylvester, 1959); a delay followed by exponential decay (Dimond and Horsfall, 1965); or sigmoidal decay (Baker, 1971). The first model depends on the random death of inoculum units, the second on the presence of clumps of inoculum units and the last on a normal distribution describing the probability of death. Finally, a notable characteristic associated with soil-borne inoculum

and termed soil fungistasis can have an immense effect on the activity and thus the infectivity of inoculum (Lockwood, 1988). Soil fungistasis is the suppression of the germination and growth of fungi the cause of which has been attributed to the microbial production of inhibitory substances and to competition for available carbon compounds.

1.2.2 *Disease progress curves*

In combination with mathematical modelling, disease progress curves provide a powerful tool with which to describe, analyse and compare botanical epidemics (Gilligan, 1990b). Disease progress curves describe how the number or density of diseased host units change over time and reflect the behaviour of inoculum. Thus, in order to interpret, or better still, to predict the shape of a disease progress curve, a precise knowledge of inoculum dynamics is crucial (Pfender, 1982). The infection chain (Gilligan, 1987) provides a convenient framework within which to identify the mechanisms by which inoculum changes over time. For soil-borne diseases this includes two distinct processes of infection (Fig. 1.1). The chain is initiated by primary infection which involves mycelial growth or zoospore movement and infection of the host population from particulate inoculum residing in the soil. Additional particulate inoculum for primary infection can occur via the saprophytic colonisation of soil organic matter. Following primary infection, mycelium may grow from the infected plant to re-infect a susceptible region of the same plant (autoinfection *sensu* Robinson, 1969) or to pass infection to another, as yet, uninfected host, thereby continuing the spread of disease (alloinfection *sensu* Robinson, 1969). The infected plant is thus a secondary source of inoculum and a source of secondary infection.

During the early periods of research into botanical epidemiology, the spread of soil-borne disease by secondary infection was not considered important and investigations were either confined to, or assumed to result from primary infection. More recently, the

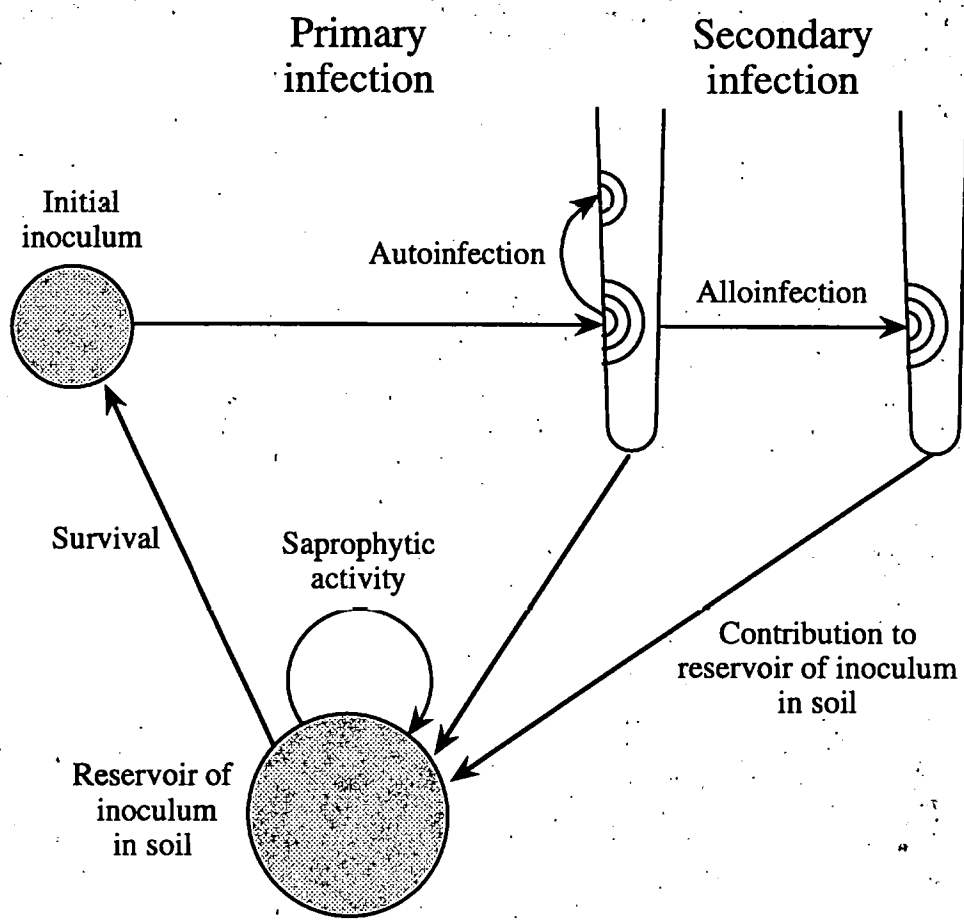


Fig. 1.1: The infection chain of a soil-borne fungal plant pathogen (modified from Gilligan, 1987)

contribution of secondary infection has been recognised in a minority of host-pathogen systems (Pfender and Hagedorn, 1983; Nelson *et al.*, 1989; Gilligan *et al.*, 1994). This does not, of course, mean that its occurrence is infrequent. Examples include the economically important and ubiquitous damping-off diseases caused by *Rhizoctonia* spp. and *Pythium* spp. and the root rot of peas caused by *Aphanomyces euteiches* (Pfender and Hagedorn, 1983).

The under-estimation of the contribution of secondary infection to the spread of soil-borne plant disease can be attributed to the way in which root diseases are assessed (Werker *et al.*, 1991). Following primary infection, secondary infection may occur by (i) spread along an existing root, (ii) spread from root to root on the same plant via the crown or via root to root contact or (iii) by spread from the root of an infected plant to the root of an uninfected plant. If the plant is defined as the unit of assessment, then increase in lesion number on the same plant is recognised simply as change in disease severity. This underestimate of secondary infection is most acute when primary infection affects a few roots on the majority of plants.

1.2.3 *The mathematical description of disease*

The mathematical description of disease progress was pioneered by J. E. Vanderplank (1963). Vanderplank distinguished between two types of disease spread and related them to the investment of money yielding either simple or compound interest. Simple interest disease results from the occurrence of a single cycle of infection during any one growing season and is caused by primary infection from particulate inoculum that has survived across the inter-cropping period. This monocyclic disease spread can be described by a monomolecular model where change in the number of diseased hosts, N_t , over time, t , is

given by:

$$\frac{dN_i}{dt} = r_p(N - N_i) , \quad (1.6)$$

in which r_p is the rate parameter for primary infection. The model describes a smooth, upwardly convex curve which rises to an asymptotic level of disease, N . In contrast, compound interest disease results from many cycles of infection in which the dominant source of inoculum is the infected host. The spread of disease is characterised by secondary infection in which disease is passed from an infected to a susceptible host that in turn becomes a fresh source of inoculum. The role of primary infection in this form of epidemic is relegated merely to the initiator of disease and makes no significant contribution to the further spread of disease. Polycyclic infection is described by the logistic model:

$$\frac{dN_i}{dt} = r_s N_i (N - N_i) , \quad (1.7)$$

in which r_s is rate parameter for secondary infection. The model describes a sigmoidal curve, symmetric about a point of infection, also rising asymptotically to N . Unfortunately, and probably due to the use of wilt diseases as an example of monocyclic disease, a general misconception evolved leading to the misnomer that all soil-borne pathogens were monocyclic and all air-borne pathogens polycyclic. Furthermore, the polarization between the two models resulted in mis-diagnosis of a pathogen's life history when this was inferred from the shape of a corresponding disease progress curve. The situation was further compounded by statements such as those of Bald (1969) who wrote that "during any one season, or the growth of an annual crop, most soil-borne pathogens will cause 'simple interest' diseases". However, it is now recognised that, because of the various influences

of, for example, host growth, the shape of the disease progress curve is not sufficient evidence with which to categorise the life history of a pathogen (Pfender, 1982).

The monomolecular and logistic models often fail to provide a satisfactory description of many epidemiological situations. Increased flexibility with which to describe different shapes of disease progress curve was achieved by adding 'shape' parameters, providing a suite of non-linear models for describing disease progress. These extend from the logistic model (*sensu* Vanderplank, 1963) to the Gompertz, Richards and Weibull functions which have, in their integrated forms, three, four and four parameters respectively.

In addition to an increase in the number of non-linear models available with which to describe a botanical epidemic, these models have also become increasingly sophisticated, including mathematical descriptions of the biological components which underpin their behaviour. The components of an aerial epidemic can be visualised and quantified more easily than those of soil-borne disease and have been more thoroughly examined. When the spore of an air-borne pathogen lands on the surface of a susceptible host plant, the host passes through a series of recognised pathological states. Initially it becomes infected and may express symptoms of disease such as the development of a necrotic lesion. As the infection progresses, the pathogen begins to sporulate and the host is classified as infectious. The period between infection and sporulation is the latent period. When the pathogen ceases to produce and release spores, the host is effectively removed from contributing to the spread of disease. In order to account for these different host states, the simple analytic model (equation 1.7) of Vanderplank describing polycyclic disease has been extended to include terms for the three categories by modifying the rate parameter, r_s , of model 1.7 to give:

$$\frac{dNi}{dt} = r_s (N_{i-p} - N_{i-p-l}) (N - N_i) \quad (1.8)$$

In equation 1.8, the amount of infection at time t depends on the amount of infectious tissue $t-p-I$ prior to the latent period, $t-p$. Jeger (1982) adopted a similar approach of host classification by adapting the SEIR (susceptible, exposed, infectious and removed) system of modelling from medical epidemiology which describes the progress of an epidemic using a series of linked differential equations.

The latent and infectious periods have not been identified (largely because of difficulties associated with quantification) as major components dictating the spread of soil-borne disease. Instead, changes in host density (Waggoner, 1986; Berger and Jones, 1985; Jeger, 1987; Brassett and Gilligan, 1988a; 1990) and decay of inoculum (Jeger, 1987; Gilligan, 1990a) have featured as sub-models in the description of disease below ground. The expansion of individual parameters by the use of sub-models is particularly appealing. It has the potential to cater for both the mathematical tractability of the model by allowing separate analytical solutions for each equation and for mathematical description of disease progress within a population of hosts which has a sound, biological basis.

Brassett and Gilligan (1988a) included the contributions of both primary and secondary infection to the spread of soil-borne plant disease by combining the two models (equations 1.6 and 1.7) described by Vanderplank. Change in the number of infected hosts, N_i , with time, t , is given by:

$$\frac{dN_i}{dt} = (r_p P + r_s N_i)(N - N_i) , \quad (1.9)$$

where P is the density of particulate inoculum and r_p and r_s are rate parameters for primary and secondary infection respectively. Equation 1.9 allows for overlapping periods of primary and secondary infection and produces disease progress curves which vary in shape from monotonic to asymmetrically sigmoidal and rising to an asymptote.

This model and the models of Vanderplank (1963), and Jeger (1987) are all examples of simple analytical models in which the underlying biological mechanisms that dictate disease progress have been subsumed within a few parameters. The models are in contrast to the complexity of large simulation models which include a detailed mathematical description of each of the biological components that contribute to disease progress and aim to predict disease progress as it is influenced by a changing environment. Jeger (1986) compared the relative merit of each approach in the context of mathematical modelling of botanical epidemiology. The large number of non-linear parameters involved in most simulation models make them mathematically intractable and the process of integration, in order to provide an analytical solution, impossible. It is therefore very difficult to estimate and interpret the values of parameters, however biologically meaningful, from disease progress data.

The approach taken in this study is to begin with a simple model such as that of Brassett and Gilligan (1988a) describing disease progress in which the parameters have some biological relevance, and to expand the model according to identified biological components that characterise a particular host-pathogen system. Thus, this study is concerned primarily with properties of inoculum included in the terms for primary ($r_p.P$) and secondary ($r_s.N$) infection of equation 1.9 together with host growth and availability (N) where deemed applicable.

1.2.4 *Host-pathogen systems*

The detailed study of even the most rudimentary epidemiological system poses considerable experimental problems regarding hypothesis testing and interpretation of results. Whilst the principal concern of this study is with the behaviour of inoculum, this is highly influenced by changes in the both the host and the environment. Furthermore, the

addition of another component, such as a biological control agent is likely to increase the dynamical interactions in a non-linear fashion.

This study investigates two contrasting host-pathogen systems as models for soil-borne plant epidemiology. These are the infection of radish (*Raphanus sativus* L.) by *Rhizoctonia solani* Kühn and the infection of wheat (*Triticum aestivum* L.) by *Gaeumannomyces graminis* (Sacc.) Arx and Oliver var. *tritici* Walker (*Ggt*), the take-all fungus. The selection of these two systems was based on increasing levels of epidemiological complexity and also represents the two ecological strategies identified by Schutte (1956) and Garrett (1970) in which contact between pathogen and host is determined largely by growth of the pathogen to the host (*R. solani*) or by growth of the host to the pathogen (*Ggt*). *Rhizoctonia solani* is typical of an unspecialised parasite (Garrett, 1970), with a wide host range and high competitive, saprophytic ability, usually infecting young, immature host tissue. As a damping-off pathogen, its spread is predominantly over the soil surface (Dr W. Otten, Pers Comm) and, as a result, the hypocotyl of the radish plant is targeted as the infection court. The experimental system used in this study is highly controlled with respect to the density and distribution of both host plants and inoculum. Also, because the growth of *Rhizoctonia* is rapid and experiments run for a maximum of 21 days, the influence of time-dependent environmental variables, such as soil moisture, is minimised. This means that, unlike many epidemics, the experimental set-up, is easy to repeat and, with accountable sources of variability, hypotheses are relatively easy to test.

In contrast to the static infection court of the radish plant, the infection of wheat by *Ggt* involves the pathogen's exposure to a continual input of young, mobile root material. The need to grow to the host to make contact is, therefore, of less importance and the saprophytic growth capability of *Ggt* is low. The dynamics of the system are further complicated by the potential for a functional response of the host to infection by way of

additional root production to compensate for roots which have become diseased.

Because the infection court is static and the radish plant only remains susceptible for a short period (Dodman and Fentje, 1970), the control of post-emergent damping-off by *R. solani* is potentially more amenable to biological control. A reduction in inoculum potential (*sensu* Garrett, 1956) at the hypocotyl surface during the period of susceptibility should reduce the rate at which the disease spreads. The control of take-all using an introduced biological control agent is more challenging because of the mobility of the growing root tip, which is the most susceptible region of the root (Deacon and Henry, 1980), and the continual production of roots. Hence, a major requirement for the control of take-all in such a system involves the mobility and/or longevity of the control agent.

1.2.5 *The pathogens*

Rhizoctonia solani

Rhizoctonia solani is a widespread, destructive and versatile plant pathogen which causes disease in an extensive range of host species. A combination of high pathogenicity and competitive saprophytic ability make this one of the most economically important pathogens world wide.

The genus *Rhizoctonia* was first described by de Candolle in 1815 (Parmeter and Whitney, 1970). It is a genus of the Basidiomycotina which is characterised by: branching near the distal septum of young, vegetative hyphae; formation of a septum in the branch near to the point of origin; constriction of the branch; dolipore septum; no clamp connection; no conidium (except monilioid cells); sclerotium not differentiated into rind and medulla; and no rhizomorph (Ogoshi, 1987). This characterisation divides the genus into three groups dependent upon the genus of their teleomorphic state, *Thanatephorus* Donk, *Ceratobasidium* Rogers and *Waitea* Warcup and Talbot.

Rhizoctonia solani Kühn was first identified by Julius Kühn in 1858 and is the major representative of the teleomorph *Thanatephorous cucumeris*. Distinct variants of the species are recognised but characteristics for classification into groups are vague. In plant pathology, the most commonly recognised form of classification to date is by way of anastomosis grouping (AG). The ability of hyphae produced by different isolates of *R. solani* to grow together, make contact and fuse has led to the identification of twelve anastomosis groups (AG-1, 2-1, 2-2, 3, 4, 5, 6, 7, 8, 9, 11 and BI) which have been further sub-divided according to cultural appearance and host range. Thus the fifteen intra-specific groups (ISG) AG-1 1A, AG-1 1B, AG-1 1C, AG2-1, AG2-2 IIIB, AG 2-2 IV, AG-3, AG-4, AG-5, AG-6, AG-7, AG-8, AG-9, AG-11 and AG-BI are recognised. More recently, classification of the *R. solani* complex has received the attentions of DNA-based systematics studies. Using isozymes, DNA/DNA hybridization, restriction length polymorphisms, polymerase chain reaction and DNA sequencing, the genetic isolation of these intraspecific groups has been demonstrated (Vilgalys and Cubeta, 1994). Classification by AG is used for the characterisation of isolates in the current investigation.

The life history (infection cycle) of *Rhizoctonia* begins with the germination of resting propagules (sclerotia or infested organic matter), the growth of a mycelial colony, contact with the host and infection of the host. This is followed by an identical series of processes governing the spread of the pathogen from the infected host to susceptible hosts. The mechanism and physiology of infection by *R. solani* which underlies the epidemiology of this host-pathogen system, is not well understood. Penetration of the plant can be achieved either through stomatal openings or through the intact plant surface. On making contact with the host surface, many isolates of *R. solani* produce infection structures such as appressoria or infection cushions. The production of infection cushions is a specific response to the topography of the host surface (Armentrout and Downer, 1987) or to

exudates produced by the root (Marshall and Rush, 1980a). Generally, more infection cushions are produced in the presence of a susceptible host than a resistant one (Kousic *et al.*, 1994). The infection cushion serves to fasten a high density of mycelium to the host surface and may be accompanied by the production of mucilage (Kenning and Hanchley, 1980). At the base of the infection cushion, lobed appressoria form as short, swollen side branches, achieving entry into the host by way of an infection peg produced at their tip. Direct penetration of the host is thought to be a predominantly mechanical process but may involve the aid of enzyme activity. *Rhizoctonia solani* produces cutinases *in vitro* (Baker and Bateman, 1978) but the relevance of this to *in planta* infection is, as yet, unclear. Once within the host, the endo-pectic enzymes released by *R. solani* are particularly efficient at degrading the middle lamella causing maceration and a collapse of structure ahead of the invading fungus (Cooper, 1983). When this process is severe a watery lesion forms and the seedling lodges (damping-off). Finally, cellulolytic enzymes damage the cell wall resulting in loss of ionic control and cell death. Using this suite of enzymes, both the structural and cytoplasmic content of the young host tissue becomes available to the pathogen.

One further group of compounds, the phenolics, are also produced in abundance by *R. solani*. The exact purpose of these compounds is not clear but they have been linked both with survival and pathogenicity (Reddy *et al.*, 1975).

Gaeumannomyces graminis

Gaeumannomyces graminis var *tritici* (*Ggt*) causes take-all, an economically important disease attacking the roots of wheat and barley crops (although its host range includes many other grass species which may act as an important carry-over of the pathogen between cereal crops). Crop losses due to take-all can, as the name implies, be devastating, but in general they are difficult to estimate and extremely variable. Even with no external

symptoms, a yield reduction of 9.0 % for winter wheat has been reported (Walker, 1975). The blackened root system of wheat plants due to take-all was first recognised in Australia in 1852 (Garrett, 1981). It was assigned to the ascomycete fungus *Ophiobolus graminis* by Prillieux and Delacroix in 1890 and was soon associated with stunted growth and white heads in wheat crops causing yield loss and shrivelled grain. Subsequently, the taxonomic characteristics of the pathogen were more clearly elucidated and it was renamed *Gaeumannomyces graminis* var *tritici* (Walker, 1972). Two other variants of *G. graminis* also exist, *G. graminis* var *avenae* which is an important pathogen of oats, and *G. graminis* var *graminis* which causes crown sheath rot of rice. *G. graminis* has a cosmopolitan distribution in temperate climates where soils have a pH of 6.0 to 8.5, have a temperature range of between 5 and 15°C, are near field capacity for much of the growing season and are well aerated.

The infection process of *Ggt* is described by Skou (1981). Surviving as a saprophyte in dead infected plant remains within the soil, *Ggt* attacks susceptible roots that pass nearby. Tropic growth of the hyphae to the root surface increases the probability of contact where the fungus can grow on all subterranean parts of the plant. The mycelium of *Ggt* consists of brown, thick-walled runner hyphae and hyaline infection hyphae which branch from the former. When the growing apex of an infection hypha touches the cell wall of the root hair or epidermal cell it swells up to form an appressorium-like structure with a narrow infection peg. A combination of mechanical pressure and degradative enzyme action combine to create a hole in the cell wall through which the hypha passes. The host responds by the formation of lignitubers which develop around the infecting hyphae but if the speed of their production is insufficient, cell death occurs. Penetration of all six layers of the cortex is followed by penetration of the endodermis and invasion of the stele. The phloem is rapidly colonised and destroyed near the point of invasion causing cessation of root growth

followed by senescence. The xylem is colonised more slowly and develops the characteristic blackening of the root due, in part, to the presence of fungal mycelium, but also due to coloured substances of plant origin. It is this stelar blackening which is used as the main criteria for successful infection of *Ggt*.

Despite being the subject of much literature, the epidemiology of take-all is poorly understood. In continuous wheat crops the effects of take-all often follow a recognised pattern. During the first year little crop loss occurs and only low levels of the pathogen are detectable, however, there is thought to be a build up of inoculum levels available for early infection of the second year wheat crop. Second year wheat crops show low initial levels of disease but infection spreads resulting in substantial crop loss. During the third successive wheat crop, the levels of particulate inoculum have risen so that early infection is severe with large yield penalties. Subsequent years may detect a reduction in disease levels due to the build up of antagonistic organisms, a phenomenon known as take-all decline (Rovira and Wildermuth, 1981). Notably, in this country, few data on the early infection of wheat by take-all exist (Gutteridge, Yarham, Pers. comm.) and the disease has rarely been studied according to the processes of primary and secondary infection.

Economically viable control measures have been restricted to crop rotation (*Ggt* is a poor competitive saprophyte and quickly loses viability) and the use of appropriate fertilisers or lime to manipulate rhizosphere pH (*Ggt* grows poorly in acidic conditions which can be induced by the addition of ammonia). The intensification of cereal farming in Britain during the 1930's led to an increase in the severity of the disease which was most prevalent on wet, alkaline soils. The Chamberlain system exploited the poor competitive ability of *Ggt* which involved under sowing each spring cereal crop with a legume that starved the pathogen of nitrogen during the fallow winter months and thereby reduced its survival. The post war availability of inorganic nitrogen fertilisers and the breeding of

wheat varieties responding to high input nitrogen led to an epidemiological dilemma. Whilst the input of nitrogen reduces the yield penalty suffered by take-all infested crops, by promoting the production of additional adventitious roots, it also increases the spread of disease resulting in a build up of inoculum with potentially devastating results in subsequent seasons.

As early as 1913, Masee, advocated the application of super-phosphate of lime to arrest the spread of take-all (Yarham, 1981). Subsequent work has shown a correlation between low levels of soil phosphate and a high incidence of take-all disease. Such a control measure has unwittingly employed tactics of biological control since the improved phosphate status of the soil was increasing the density of microbial populations antagonistic to *Ggt*. The role of these organisms in the biological control of *Ggt* has been recognised for many years. Garrett (1934) observed the suppression of *Ggt* following the addition of organic material and attributed this to the development of antagonistic micro-organisms. Attempts to develop biological control in soils have been complicated by variation in soil types and climate. Soils have been classified into decline and non-decline soils according to their ability to generate the phenomena of take-all decline. Cook and Rovira (1976) distinguished between general abiotic suppressive effects of a soil and its specific suppression due to antagonistic microbes from which Rovira and Wildermouth (1981) suggested that the important characteristic was whether they can be transferred into natural or fumigated soil. To date chemical treatments have been largely ineffective or too expensive to be economically viable although treatment with triadimefon (Baytan) has been practised in severe cases of the disease. Also, no genetic resistance has been identified (W. Hollins, Pers. comm).

1.2.6 *Specific biological control agents*

Although fungicides are convenient, the excessive use of broad spectrum or persistent chemicals may result in soil contamination, fungicide resistance or other harmful effects (Maloy, 1993). Biological control of plant pathogens using introduced organisms is an attractive alternative which has stimulated considerable research during the last three decades but has produced results which have been disappointing. Perhaps the most damning criticism has been the inconsistent performance of the control agent, the cause of which has been largely attributed to a lack of understanding of its behaviour in a specific environment (Cook, 1993). It is now recognised that the success of biological control will depend on a greater degree of skill in deploying the correct organism into the correct place at the correct time.

Trichoderma viride on *R. solani*.

The biology and systematics of the genus *Trichoderma* was recently reviewed by Samuels (1996). *Trichoderma viride* is a Hyphomycete and is characterised on oatmeal agar by fast growing hyaline colonies and may be distinguished from other species of *Trichoderma* by its relatively large (3.6-4.8 x 3.5-4.5 µm), roughened conidia (Domsch *et al.*, 1980). It is one of the most widely distributed of all fungi occurring in a range of forest, grassland and cultivated soils.

Many experimenters have demonstrated the control capability of *Trichoderma* spp. towards damping-off caused by *R. solani* (e.g. Lewis *et al.*, 1996; Coley-Smith *et al.*, 1991; Lewis and Papavizas, 1985; 1987; 1991). The potential use of *Trichoderma* species as biological control agents of soil-borne plant pathogens was first recognised by Weindling (1934) who isolated an antifungal metabolite (Gliotoxin) from a culture filtrate of *T. lignorum*. Later, Brian and McGowan (1945) described the production of viridin by

Trichoderma viride. Although both the organisms involved were later re-classified as a closely related species, *Gliocladium repens*, other antimicrobial substances (Trichodermin) have been associated with *Trichoderma viride* (Dennis and Webster, 1971). More recently, a review concerning the antifungal antibiotics produced by *Trichoderma* species was published by Ghisalberti and Sivasithamparam (1991).

The antagonistic activity of *Trichoderma* may not be limited to the production of antibiotics. Direct parasitism of *R. solani* by *Trichoderma* spp. has been observed using scanning electron microscopy (Elad *et al.*, 1983). This may not, of course, be a separate mechanism for control but may simply succeed antibiosis. Since most of the work investigating the mechanisms by which *Trichoderma* controls the growth of a pathogen has been carried out under laboratory conditions, the contribution of these mechanisms together with that of simple competition for nutrients in the soil environment remains unclear.

For a biological control agent to succeed, it must be active in the right place, at the right time. Damping-off disease affects the germinating seed and the hypocotyl of the radish plant. This means that the control agent must occur close to the host and remain active during the initial period of growth when it is most susceptible. For the control of damping-off of radish by *R. solani*, these conditions are relatively easy to satisfy. The control agent can be positioned near to the hypocotyl of the host by applying it at the time of sowing, and by culturing it on a nutrient base (for example, an autoclaved seed), the control agent is introduced in an actively growing condition capable of protecting the host during the early, most susceptible period of growth.

Pseudomonads on *Ggt*

The Pseudomonads are a group of non-spore forming, motile, Gram negative, soil-borne bacteria that, like *Trichoderma*, are common inhabitants of a variety of soil environments.

Also, like *Trichoderma* spp., the ability of *Pseudomonas* spp., and more specifically, the fluorescent Pseudomonads, to control disease has been known for some time (Burr *et al.*, 1978). They have been linked with control of pathogens such as *Fusarium solani* (Lim and Kim, 1995), *Sclerotinia* (Expert and Digat, 1995), *Pythium* (Zhou and Paulitz, 1994) and *Gaeumannomyces graminis* (Harrison *et al.*, 1993). *Pseudomonas* spp. produce antibiotics, notably phenazine which is an effective fungal growth inhibitor at very low concentrations (Thomashow *et al.*, 1990). The bacteria may also inhibit fungal growth of the pathogen by competing for available Fe(III) and by the production of hydrogen cyanide (Defago *et al.*, 1990).

Unlike the control of damping-off by *R. solani*, the control of take-all requires a highly motile control agent, capable of keeping pace with the growth of the entire root system. Root colonisation of wheat by a strain of *Pseudomonas* coated onto the seed was examined by Howie *et al.* (1987). Most of the long-distance movement of the bacteria was associated with a passive process, the organism being carried along with the root as it grew downward into the soil. Motility and adequate water availability were important for local movement (distances of a few millimetres) and subsequent rhizosphere colonisation.

The inconsistent performance of introduced *Pseudomonas* species has been attributed to variability in the ability to adequately colonise the root system. The density of bacteria declines with depth and over time. Moreover, the distribution of the organism is patchy, leaving large areas of the root system uncolonised (Weller, 1988). The search for so called 'rhizosphere competent' organisms capable of rapidly colonising the entire root system and remaining active for the duration of crop growth, is one of the current major objectives in bio-control of root infecting pathogens.

1.2.7 Host susceptibility and the rhizosphere

The components which affect disease progress are the infectivity of inoculum, the susceptibility of the host and the environment, all of which change with time (even within a controlled environment facility). Whilst the over-riding topic of this thesis concerns the behaviour of inoculum, its contribution to the progress of disease can only be assessed with any degree of confidence either by quantifying changes in the remaining components, which is beyond the scope of this study, or against a background of an informed understanding of the way in which the host and environment develop. Moreover, these two components are effectively coupled since, from the perspective of the pathogen, the environmental influence will be dominated by changes within the rhizosphere.

Various constitutive and pathogen induced mechanisms have been proposed for defence against invading pathogens and the contribution of each depends on the nature of a specific host-pathogen interaction. It is presently impossible to judge the relative importance of these defence mechanisms in any host-plant interaction (Ebel, 1986). All cells are expected to contain phenolic compounds capable of suppressing the growth and activity of the pathogen (Nicholson and Hammerschmidt, 1992). The sequence of events in a defence response can generally be thought to include host cell death and necrosis, accumulation of toxic phenols, modification of cell walls by phenolic substituents or physical barriers such as appositions or papillae, and, finally, the synthesis of specific antibiotics such as phytoalexins (Nicholson and Hammerschmidt, 1992). However, changes in either the constitutive or pathogen induced defence mechanisms as the host becomes older have not received much attention.

Because of the speed with which *R. solani* infects during the damping-off of radish seedlings, constitutive defence is likely to be most important. Host tissue typically becomes less susceptible to damping-off by *R. solani* as it ages. This has been attributed to changes

in the production of exudates as the host develops from the germinating seed to the established seedling (Dodman and Fentje, 1970). For bean seedlings, increase in resistance was correlated with an increase in the calcium pectate of the middle lamella, a substance particularly recalcitrant to the action of polygalacturonase (Bateman and Lumsden, 1965). The lignin component of cell walls also increases as plants become older and lignification of *Raphanus* spp. can be induced following infection by *Alternaria* (Vance, et al., 1980).

Wheat plants produce three types of roots, seminal, adventitious and lateral roots, which differ according to their site of initiation. Seven to eight seminal roots are produced from the seed, followed by the production of a large number of adventitious roots from the basal nodes of the stem. Lateral roots are produced from both the seminal and adventitious roots and arise from the pericycle, a layer of cells beneath the endodermis. Each root is composed of two principle layers, an outer cortex and an inner stele. The two layers are separated by the endodermis which is resistant to cell wall degrading enzymes and protects the stele from invasion (Hornby and Fitt, 1981). Two factors combine to dictate changes in the susceptibility of the root with age (and therefore time) to stelar infection; death of the root cortex (Deacon, 1987) and the resistance of the endodermis. Death of the root cortex has been implicated with increased susceptibility to infection by *Ggt* (Kirk and Deacon, 1986; Deacon, 1987) whereby senescence of these outer cells provides a nutrient base which may enhance the inoculum potential (*sensu*, Garrett, 1956) of the pathogen. However, changes in susceptibility are largely dominated by an increase in the resistance of the endodermis and nearby layers of cells as the root becomes older. The endodermis contains high, constitutive concentrations of phenols and quinones, inhibitors of fungal growth and capable of suppressing the activity of some cell wall degrading enzymes (Van Fleet, 1961), which increase as the root ages (Rengel *et al*, 1994). The formation of these substances and thus enhanced resistance can be elicited by exposing the root to 'weak' pathogens such as

species of *Phialophora radicicola* (Speakman and Lewis, 1978). The increase in phenols is closely linked to the production of lignitubers, formed in response to an invading organism. This provides an active mechanism for defence but changes in the efficiency of this mechanism with root age have not been investigated. Finally, lateral roots may provide sites of increased susceptibility (Hornby and Fitt, 1981).

In addition to host susceptibility, the rhizosphere also represents a potential barrier to the ingress of a plant pathogen both as a result of the localised compression of surrounding soil and the growth of soil microbes. Rhizodeposition (*sensu*. Whipps and Lynch, 1985) of a variety of materials is responsible for the growth of a population of organisms which surround the plant root and, depending on their competitive saprophytic ability (*sensu*. Garrett, 1970), these may out compete or directly antagonise a plant pathogen. Rhizodeposition varies according to the age of the root and at different positions along the root surface. As mentioned earlier, death of cortical cells represents a considerable input of organic matter into the rhizosphere stimulating the growth of the microbial population. In wheat, the zone just behind the root tip is a major site of rhizodeposition (McDougall and Rovira, 1970).

In conclusion, host susceptibility and interactions within the rhizosphere are likely to provide a reduction in the overall susceptibility of both radish and wheat to damping-off and take-all respectively as the host tissue ages.

1.3 *The present investigation*

This study was undertaken to examine and compare the behaviour of two types of inoculum which are responsible for two distinct processes of infection that occur during the progress of a soil-borne botanical epidemic. Particulate inoculum gives rise to a single cycle of primary infection and infected hosts cause secondary infection by continuing cycles of

disease spread. A principal theme of the investigation is to scale up from the behaviour of individuals to that of the population. To achieve this, a combination of experimentation and mathematical modelling is used to structure and test relevant hypotheses. Two contrasting host-pathogen systems are investigated; the infection of radish by *R. solani* on which most of the detailed studies were performed, and the infection of wheat by *Ggt*. The main objectives are: (i) to identify, examine and quantify the major components responsible for the shape of the pathozone, (ii) to compare the behaviour of particulate inoculum and of infected hosts with respect to pathozone dynamics, (iii) to interpret an epidemic according to the dynamics of the pathozone and (iv) to examine and predict the effects of a biological control agent, placed into the rhizosphere of a growing host, on the progress of disease.

The results of the investigation are structured into a general materials and methods chapter (chapter 2), four experimental chapters (chapter 3 through to chapter 6) and a general discussion (chapter 7). Most of the work (chapters 3 through to 5) was performed on the *Rhizoctonia*-radish system because it represents a relatively simple epidemiological system in which experiments only take between 10 and 20 days to complete. The investigation then progresses to the examination of a more complex epidemiological system involving the infection of wheat by *Ggt* (chapter 6).

The rationale behind the ordering of the chapters is as follows. Chapter 2 reports on the characterisation of isolates according to pathogenicity, the production of suitable types of inoculum and assays for the effectiveness of biological control agents. Chapter 3 describes how different infection components combine to determine the shape of the pathozone profile which describes changes in the probability of infection when inoculum occurs at different distances from the host. In chapter 4, the most important property of *Rhizoctonia* inoculum which dictates the shape of the pathozone, growth of the fungal colony, is examined in detail. The pathozone profiles associated with single, isolated radish plants are

compared for particulate inoculum and infected plants in chapter 5. Evolution of the pathozone over time is used to predict the progress of disease in monocyclic and polycyclic epidemics protected by the antagonist *Trichoderma viride*. Finally, chapter 6 examines the contribution of inoculum type to the spread of take-all on wheat roots.

Chapter two

General materials and methods

2.1 *Introduction*

This chapter deals with the materials and methods which are common to many of the experiments undertaken in the study and with preliminary work regarding the selection of isolates and the characterisation and production of inoculum. Details of experimental growth conditions, soil type, host type and statistical analysis are provided.

Because the study focuses principally on the behaviour of inoculum, a more detailed characterisation of isolates and of inoculum type is undertaken. Pathogenicity tests were performed on isolates of *Ggt* and *R. solani* and isolates of *R. solani* were characterised according to anastomosis grouping.

The need for standardisation of inoculum is twofold. Firstly it allows for experiments to be repeated and secondly it allows for more objective and efficient comparison between the results of different experiments. This is particularly important where the results from one experiment are used to predict the results of another. The entire study involved two types of experiment, placement experiments and population experiments. Placement experiments typically comprised of replicated location of single units of inoculum positioned at known distances from the host, whilst population experiments included large quantities of particulate inoculum positioned or distributed at random amongst a population of hosts.

2.2 *Experimental growth conditions.*

All experiments were conducted in plant growth cabinets (Sanyo Gallenkamp, Model

SGC/C/RO-HFL) in which plants were provided with 16 h of a mixture of fluorescent and incandescent light at $300 \mu\text{E} / \text{m}^2 / \text{s}$ every 24 h. Experiments involving *R. solani* were run at 23°C whilst for *Ggt* the temperature was 17°C both with regimes including a 15 min defrost every 3 h.

For *Ggt*, the relative humidity was maintained close to 60 %. For experiments involving *R. solani*, the relative humidity was maintained as high as possible by using sealed systems which included reservoirs of water where necessary.

2.3 Soils

Rhizoctonia solani has a high competitive saprophytic ability and can multiply rapidly using organic material within the soil as a source of nutrition. The organic material forms a secondary source of particulate inoculum and can add to primary infection. The effects of saprophytic multiplication on disease progress were not examined in this study and would be expected to interfere with pathozone behaviour. Consequently, experiments involving *Rhizoctonia* were performed in an acid washed, quartz sand (Hepworth Minerals and Chemicals, Redhill, Surrey. Grade 16/30). Samples of sand were tested for contaminant organisms capable of infecting radish.

Gaeumannomyces graminis var *tritici* is not a good saprophytic competitor and experiments were performed in a soil-sand mixture. A sandy clay loam soil (Soil 2, see Appendix I) was obtained from the Cambridge University Field Station from a site known to have been free of grass species for a minimum of five years. The soil was sieved through a 10 mm screen, air dried for 14 d followed by a further sieving through a 2 mm screen to remove stones and large pieces of debris. The soil was then baited (by growing wheat plants into samples of the soil and examining roots for disease) to certify that it was free from detectable inoculum of *Ggt* and mixed with sand in the ratio of two parts soil to one part

sand to aid drainage, aeration and, at the end of the experiment, the removal of soil prior to disease assessment. This soil-sand mixture (referred to in sections 2.6.2 and 6.2 as soil) was found to have a field capacity of 21% moisture corresponding to a water potential of -0.015 MPa and a pH of 7.0.

2.4 *The hosts.*

For experiments involving *Rhizoctonia*, the radish variety, Cherry Belle (Kings Crown) was used whilst for the investigation of take-all, seed of the winter wheat variety, Riband, was kindly supplied by T. W. Hollins (Plant Breeding International, Cambridge). Neither seed type had been chemically treated and was stored in the dark at 4 °C. Batches of seed were routinely tested for germinability and for the presence of contaminant organisms prior to use by germination on moist, sterile filter paper and examination under a dissecting microscope (x 20).

2.5 *Statistical analysis.*

Statistical analyses of the experimental data were carried out using the Genstat statistical software package (Anon, 1993) and the Facsimile modelling software package (1995) operating on a Vale 90 (Evesham Micros, Cambridge) personal computer (90 MHz, 16 Mb RAM). Three statistical techniques were used to analyse the experimental data. These were; the analysis of variance, analysis using a generalised linear model and parallel curve analysis.

The analysis of variance is particularly powerful for comparing population means (Campbell, 1989) and is used later in this chapter for identification of the most pathogenic isolates of *R. solani* and *Ggt* and to assess the phytotoxic effects of the biological control agents, *Trichoderma viride* and *Gliocladium virens*, on the tap root length of radish plants.

The analysis of variance is, however, restricted by three underlying assumptions (Mead and Curnow, 1990); (i) the data must be normally distributed, (ii) the variance must be homogeneous between treatments and (iii) that treatment effects are additive.

For epidemiological studies in which a quantal variable, such as the presence or absence of disease is under consideration, the underlying error structure is likely to be binomially rather than normally distributed. In some instances, it is possible to overcome the problem of data which are not normally distributed by using an appropriate transformation. Alternatively, generalised linear models can be used which take explicit account of the underlying error structure. Generalised linear models combined with polynomial contrasts are particularly useful for analysing trends in data. Hence, a generalised linear model, assuming a binomial error structure was also used later in this chapter to compare and assess the biological control potential of different inoculum densities of *Trichoderma viride* and *Gliocladium virens* on the damping-off of radish by *R. solani*.

Many biological processes are non-linear rather than additive and if an appropriate non-linear model can be identified with which to describe trends in data and which has biologically meaningful parameters, then parallel curve analysis (Ross, 1987) provides a particularly elegant technique with which to compare the affects of treatments in relation to specific biological properties. Parallel curve analysis was used throughout this investigation in which non-linear models were selected on the basis of the underlying biology of a system, shape and goodness of fit to data and the affects of treatments on parameters compared using the techniques outlined by Gilligan (1990b).

2.6 *The pathogens*

Isolates of *Ggt* were obtained from naturally infected wheat seedlings (see Appendix II) whilst isolates of *R. solani* were acquired from Dr C. A. Gilligan (Department of Plant

Sciences, University of Cambridge) together with information regarding their origin and the anastomosis groups to which they belong (see Appendix II). Twelve isolates of *Ggt* and seventeen isolates of *R. solani* were screened for variation in pathogenicity using sand/maizemeal inoculum and a simple agar based inoculum respectively.

2.6.1 Pathogenicity screening

Gaeumannomyces graminis.

Isolation

Using the method of Slope *et al.* (1978), as described by Cunningham (1981) in Asher and Shipton (1981), twenty eight isolates of *Ggt* were obtained from the roots of wheat plants grown on the University Farm near Cambridge. Sections of infected seminal roots were removed, washed in tap water and placed in 1% silver nitrate for 20 seconds. These sections were then rinsed once in 5% sodium chloride and twice in sterile distilled water before being plated onto tap water agar (15 g l⁻¹ agar)(Oxoid, England) with streptomycin (100 units ml⁻¹). Plates were incubated in the dark at 17 °C and examined every four days. Sections of colonies showing the characteristic curled hyphae of *Ggt* were removed to plates of potato dextrose agar (PDA)(Oxoid, England) and assessed for contamination before being transferred to quarter strength PDA slopes for storage in the dark at 4 °C.

Pathogenicity test

Sand/maizemeal inoculum was prepared for each of twenty isolates of *Ggt* using the method of Hollins *et al.* (1986). Aliquots of 100 g of dry sand, 2.8 g of maizemeal and 13 cm³ of distilled water were mixed in 250 cm³ conical flasks. After autoclaving at 121 kPa for 1 h on three consecutive days, agar plugs measuring 4 mm in diameter were removed from the growing edge of colonies of *Ggt* and were placed into the flasks. These were

incubated in the dark at 19 °C for 28 d after which time samples were removed for estimation of the density of colony forming units (CFU) and inspection for possible contamination. Twelve isolates were then selected for pathogenicity testing on the basis of having similar initial inoculum densities.

Sections of polyethylene tubing (Layflat Tubing, Isle of Wight) measuring 150 mm in length and with a internal diameter of 25 mm were stapled at one end and filled consecutively with 150 g of sand, 25 g of inoculum and 25 g of sand. A pre-germinated wheat seed was placed in the centre of each tube and covered with a final 25 g of sand. The experiment was set up with three replicates per treatment. Each tube was then weighed and water added to achieve a moisture content of 15% w/w. The tubes were packed into a plastic box and their bases covered in metal foil to prevent light reaching the root system. Tubes were transferred to a growth chamber at 17 °C with a light regime of 16 h day and 8 h night. After three weeks, plants were carefully removed from the tubes using a fine water jet and the root systems examined for disease.

Assessment of disease was based on the average lesion length per seminal root, where disease is defined as stelar discolouration.

Results.

Levels of disease were generally high (Table 2.1) with isolate ML1 achieving 41.20 mm of stelar discolouration per root. Only isolates NM2, NM5, ML3, ML5 and Δv recorded significantly lower levels of disease than ML1.

Table 2.1: *Results of the analysis of variance showing mean estimates of pathogenicity for different isolates of Ggt.*

Isolate	Lesion length per root (mm)
Av	16.7
BF1	36.5
BF3	33.4
BF4	32.5
Cv	32.6
ML1	41.2
ML2	40.0
ML3	30.5
ML5	30.5
NM1	33.4
NM2	20.8
NM5	26.8
LSD (p<0.05)	10.1

Rhizoctonia solani.

Anastomosis grouping

Isolates of *R. solani* are commonly divided into groups according to the ability of their hyphae to fuse or anastomose (Ogoshi, 1987). Isolates R3, R8, J262, J312 and J317 had been confirmed by previous researchers as being of AG3, AG4, AG2-1, AG4 and AG3 respectively; however, the anastomosis grouping of isolates R1, R2, R5, R10, R13 and R14 was only provisional, based on the host from which they were isolated. These isolates were therefore tested against reference isolates obtained from the International Mycological Institute (IMI) and against isolates R3 and R8 to confirm their grouping.

To test for the presence of anastomosis between isolates, standard microscope slides were sterilised and dipped into molten water agar. After allowing the agar to set, they were

placed in Petri-dishes on moist filter paper. Plugs of PDA measuring 2 mm in diameter were removed from the growing edge of two day old cultures of *R. solani* and placed 20 mm apart on the slides. The dishes were then sealed and incubated in the dark at 23 °C. After 2-3 days, slides were removed and stained with 2% trypan blue in acetic acid. Mycelium was assessed for hyphal fusion between colonies using a compound microscope at a magnification of x 100.

Pathogenicity test

To assess the isolates for variation in pathogenicity, Petri-plates of PDA measuring 9 cm in diameter were inoculated with *R. solani* and grown in the dark at 23°C until the colonies just filled the plates. These were covered with a 10 mm layer of vermiculite, moistened with 10 cm³ of distilled water and sown with 21 pre-germinated radish seeds placed just below the surface. The lids were replaced and sealed with parafilm. Two experiments were performed, eight isolates being tested in experiment 1 and 12 in experiment 2. In each experiment there were three replicates per isolate which were fully randomised and placed in a growth chamber at 23 °C with a light regime of 16 h day and 8 h night. After two days of incubation, lids were removed and plates transferred to sealed plastic containers. Plants were scored for disease (damping-off) after seven days.

Isolates failing to cause any damping-off in experiment 2 were omitted from the analysis. The LSD in experiment 2 is thus restricted to the comparison of the remaining isolates.

Results

The results of the anastomosis grouping and pathogenicity tests are given in Tables 2.2 and 2.3 respectively.

Table 2.2: *Hyphal fusion amongst test and between test and reference isolates. (+ fusion; - no fusion)*

	TEST ISOLATES					REFERENCE ISOLATES				
	R1	R2	R3	R5	R8	AG 1	AG 2-1	AG 2-2	AG 3	AG 4
R1	+	-	+	-	-	-	-	-	-	+
R2	-	+	-	+	-	-	+	-	-	-
R3	+	-	+	-	-	-	-	-	-	+
R5	-	+	-	+	-	-	+	-	-	-
R8	-	-	-	-	+	-	-	-	+	-
R10	-	-	-	-	+	-	-	-	+	-
R13	-	-	-	-	+	-	-	-	+	-
R14	-	-	-	-	+	-	-	-	+	-

Hyphal fusion was recorded between isolates R2, R5, and AG2-1 which, along with J317 and R3 in experiment 1 were significantly more aggressive against radish seedlings.

Table 2.3: *Results of analysis of variance comparing the pathogenicity of R. solani isolates on radish seedlings assessed by mean number of seedlings damped-off.*

Isolate	Suspected AG	Result of AG test	Expt 1	Expt 2
R1	4	4	6.33	0.00
R2	3	2-1	16.33	15.55
R3	4	4	20.00	7.22
R5	3	2-1	16.67	15.54
R8	3	3	3.67	
R10	3	3	5.00	
R13	3	3	4.67	
R14	3	3	4.00	
J317	2-1	-		18.89
J262	3	-		0.00
J312	4	-		3.89
AG1	1	1		3.88
AG 2-1	2-1	2-1		17.22
AG 2-2	2-2	2-2		0.00
AG3	3	3		0.00
AG4	4	4		0.55
LSD			6.92	3.03

Discussion

The *Ggt* isolate ML1 which recorded the greatest extent of stelar discolouration in the pathogenicity test was selected for the production and testing of inoculum type.

The redesignation of *R. solani* isolates R2 and R5 to anastomosis group 2-1 was supported by the results from the pathogenicity test. Ogoshi (1987) noted the association of AG2-1 isolates with the Cruciferae, to which *Raphanus sativus* belongs. Furthermore, ribosomal DNA sequence data shows a significant deviation between AG2-1 and AG3 (Vilgalys and Cubeta 1994). Isolate R3 was found to die suddenly in culture and this may be reflected by the inconsistent behaviour expressed in the pathogenicity tests. Alternatively, it was noted that this isolate was effective at causing pre-emergence damping-off but caused little disease once the radish seedlings had become established. This observation is consistent with the results of Benson and Baker (1974b) who reported a rapid decay in the ability of this isolate to cause disease once radish seedlings had become established. Consequently, small differences in the relative growth rates of pathogen and host may, therefore, be the crucial factor determining pathogenicity (Baker and Martinson, 1970). On the basis of its consistently aggressive behaviour with respect to the infection of radish, isolate R5 was selected for use in subsequent experimentation.

2.6.2 Particulate inoculum

This section deals with the production of inoculum using isolates selected on the basis of their performance in pathogenicity tests. Whilst the purpose of this study was not to complete a detailed comparison of different types of particulate inoculum, the nature of the techniques involved (i.e. placement and population experimentation) require that the inoculum used complies as near as is possible with the following criteria: that it can be produced rapidly, with ease and consistently in quantities that allow for its use in

population studies; that the individual units of inoculum are small, easy to handle and do not aggregate or fragment on mixing; that these units are all viable and have similar properties of saprophytic growth and infection with respect to each other and with those of natural inoculum; that their fungal biomass can be estimated and that they do not decay rapidly in storage. To assess the suitability of inoculum type for placement experiments, profiles for the probability of infection with distance (pathozone profiles) were generated.

The properties of three types of inoculum (one for *Ggt* and two for *R. solani*) were investigated with respect to the criteria listed above. Chopped potato soil (CPS), a mixture of potato and soil impregnated with fractions of mycelium, has been widely used as a source of inoculum for investigating the epidemiology of disease caused by *R. solani* (Benson and Baker, 1974a, 1974c; Gilligan and Simons, 1987). It can be produced to any unit size, would be expected to mix well, is considered to be representative of natural inoculum and to have good keeping qualities. Millet seed has similar properties to CPS inoculum, producing discrete inoculum units, but is likely to be an unnaturally rich substrate and is restricted to a unit size of between 2-3 mm in diameter. Both millet (for *Ggt*) and CPS (for *R. solani*) inoculum have been successfully utilised in placement experimentation (Gilligan and Simons, 1987). A third type of particulate inoculum, mycelial discs (MD), removed from a growing colony of *R. solani* was also examined. The consistent size of mycelial discs provides the potential to minimise variability between inoculum units. This will reduce the amount of replication required to detect differences between treatments and optimise the performance of placement experiments.

Inoculum was prepared and its potential for use in placement experimentation assessed by the production of profiles for the probability of infection with distance and the fitting of appropriate models.

Methods

Ggt/millet seed inoculum.

Millet seed inoculum was produced by addition of 12 g of millet (CPB Ltd, Cambs), 12 g of sand and 10 cm³ of distilled water to a 100 cm³ conical flask. This was autoclaved twice at 121 kPa for one hour with a three day interval between autoclavings and incubated for 28 days at 19 °C with six discs, 4 mm in diameter, cut from the margin of a colony of *Ggt* (Isolate ML1) growing on PDA agar. The inoculum was stored in the dark at 4 °C.

Profiles for the probability of infection with distance were produced with the use of soil packs (see Appendix III). These consist of 200 mm lengths of clear layflat tubing, 70 mm in internal diameter and partially sealed at one end using staples. The packs were filled with 300 cm³ of moist soil (10% water by weight) (see section 2.3 and Appendix I), stapled at the top leaving room for the emergence of a seedling and compressed to achieve enough rigidity to stand upright. A pre-germinated wheat seed was introduced into each through a small incision, which was then sealed with clear sticky tape. Water was added to achieve a moisture content of 20% w/w. After three days growth on an incline of 60° to the horizontal, a single inoculum unit (colonised millet seed) was introduced into each pack at a known distance from a selected root and 5 mm behind the root tip. The packs were then replaced in the growth chamber this time with the inoculated root uppermost to minimise disturbance from additional root growth, and covered with black plastic. The experiment was set up with 11 distances, these being at 1 mm intervals over the range 0-10 mm, and with 10 replicates per distance in a fully randomised block. Roots were assessed for infection (stelar discolouration) 15 days after inoculation.

R. solani/CPS inoculum

CPS was produced by mixing 906 g of loam soil (Soil 2, see Appendix I) with 170 g of

finely chopped potato in a 1l conical flask and adding distilled water to achieve a moisture content of 15% by weight. The flask was autoclaved at 121 kPa for 1 h on three consecutive days prior to the addition of a whole colony of *R. solani* (Isolate R5) grown on a 9cm Petri-plate. After three weeks incubation in the dark at 23 °C the inoculum was removed, air dried, ground and sieved to obtain units 1.0-2.0 mm in diameter. The inoculum was then stored in a sealed plastic container in the dark at 4 °C.

R. solani/MD inoculum

MD inoculum of *R. solani* was produced by growth of the pathogen over Millipore filters (0.45 µm pore size) (Schleicher and Schuell, Dassel, Germany) placed on a plate of potato dextrose agar. When the colony had overlapped the edge of the filter, the filter was removed from the plate and discs (of the mycelium only), 1.0 mm diameter, were cut out from the outer 5 mm by use of a micro-pipette. Discs of 1 mm diameter produced colonies of similar mean dimensions to those produced by CPS inoculum when grown on moist glass microfibre filters.

Profiles describing changes in the probability of infection with distance for *R. solani* on radish using either CPS or MD inoculum were generated using square Repli dishes (Sterilin, Twickenham) with twenty five compartments. 0.8 cm³ of distilled water was added to 8g aliquots of sieved sand (< 2 mm in diameter) placed into nine isolated compartments. A trough of sand was then removed to a depth of 5 mm with a small spatula and a radish seed sown. This was accompanied by either a single unit of CPS inoculum, 1-2 mm in diameter, placed at a known distance away, measured using callipers or by a unit of MD inoculum. The seed and inoculum were covered with sand and lids sealed on the Repli plates. After incubation for 48 h in a growth chamber, lids were removed and plates transferred to sealed, clear plastic containers with a reservoir of water in the base. The

experiment was set up as a fully randomised block with 18 replicates at distances 0,1,2,3,4,5,6,7,8,11,12 and 15 mm (CPS inoculum) or 0,1,2,4,7,10,15,20 mm (MD inoculum). Plants were removed after a further 48 h, washed and assessed for disease on the basis of the presence or absence of lesions visible to the naked eye.

Statistical analysis

The suitability of the inoculum for placement experimentation was assessed by fitting the data generated for profiles of the probability of infection with distance with three of the non-linear models used by Gilligan and Simons (1987) and an additional model, the critical exponential model. The models are given as;

I. $P = \beta \cdot \exp(-\alpha r)$

II. $P = \beta \cdot \exp(-\alpha r^2)$

III. $P = \beta / (1 + \exp(\phi_1(r - \phi_2)))$

IV. $P = (\theta_1 + \theta_2 \cdot r) \exp(-\theta_3 \cdot r)$

The first model (model I) is a simple exponential decline where β represents the asymptotic probability of infection and α is a measure of the reduction in probability of infection, P , as the distance from the host, r , increases. The second model (model II) allows for a less rapid decay in the probability of infection with distance when inoculum is placed close to the surface of the host. The third model (model III) is the logistic which produces a sigmoidal decline, symmetric about the point of inflection measured by the parameter ϕ_2 . The fourth model (model IV) is the critical exponential model which can accommodate an initial rise in the probability of infection followed by an exponential decay to zero. The parameter θ_1 represents the probability of infection at the host surface, θ_2 is a measure of

the increase in the probability of infection with distance, and θ_3 , a measure of the subsequent reduction in the probability of infection with distance.

Results

Of the three types of inoculum investigated, the *Ggt*/millet inoculum and *R. solani*/MD inoculum were the easier to prepare, producing inoculum of 100% germinability. In contrast, CPS was more difficult to generate, requiring careful preparation of potato and soil prior to mixing and rapid drying to avoid colonisation by air-borne contaminants. The germinability of CPS inoculum was inversely proportional to the size of inoculum units and was always less than 100% (Table 2.4).

Table 2.4: Results of characterisation for the millet, CPS and MD inoculum

	<i>Ggt</i> /Millet	<i>R. solani</i> /CPS	<i>R. solani</i> /MD
1. Production			
Time	4 weeks	4 weeks	1 week
Ease	Rapid	Slow	Very rapid
Quantity	Large	Large	Small
2. Inoculum units			
Size (mm)	2-2.5mm	Any up to 2 mm	Any
Handling	Easy	Easy	Easy
Aggregation	None after sieving	None after sieving	Yes
Fragmentation	None	Some	None
Germinability	100%	Inversely proportional to size	100%
Longevity	Variable	Variable	Not applicable

The logistic decay model produced the better description of the profile for the change in probability of infection with distance for the infection of wheat roots by *Ggt* grown on millet seed. The probability declined from an asymptote of 0.98 to an observed outer limit for the pathozone of 8 mm (Table 2.5; Fig 2.1a). The probability of causing infection on radish hypocotyls also decreased with distance between either CPS inoculum or MD

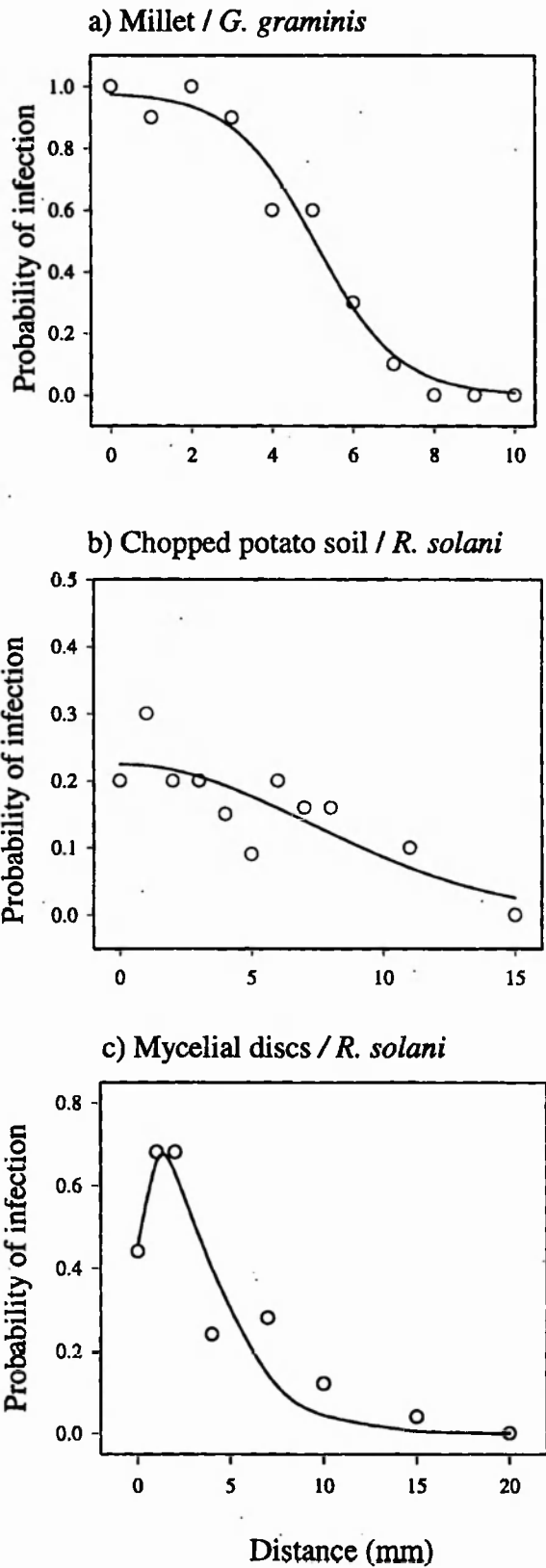


Fig 2.1: Profiles describing changes in the probability of infection with distance for a) millet seed infested with *G. graminis*, b) chopped potato soil infested with *R. solani* and c) mycelial discs of *R. solani*. Data are fitted with curves (solid lines) using selected models. See text for model selection.

inoculum and the host plant. The critical exponential model provided the most accurate fit to data generated using MD inoculum (Fig. 2.1c) but, because of the high levels of variability with the CPS inoculum, the critical exponential model (model IV) failed to converge and there was little to choose between the fit of any of the remaining three models to data generated by CPS inoculum (Table 2.5, Fig. 2.1b illustrating the fit of model II).

Table 2.5: Summary of non-linear models used to describe the relationship between the probability of infection of the host (y) and distance (r) for millet inoculum of Ggt and for CPS and MD inoculum of *R. solani*.

Inoculum	Model	Parameters (\pm s.e)	Res d.f	Residual deviance
Millet	I. $P = \beta \cdot \exp(-\alpha r)$	$\beta = 1.22 \pm 0.26$ $\alpha = 0.24 \pm 0.13$	9	2.43
	II. $P = \beta \cdot \exp(-\alpha r^2)$	$\beta = 1.00 \pm 0.10$ $\alpha = 0.03 \pm 0.02$	9	1.14
	III. $P = \beta / (1 + \exp(\phi_1 (r - \phi_2)))$	$\beta = 0.98 \pm 0.13$ $\phi_1 = 1.15 \pm 1.00$ $\phi_2 = 5.05 \pm 1.11$	8	0.51
	IV. $P = (\theta_1 + \theta_2) \exp(-\theta_3 \cdot r)$	Failed to converge		
CPS	I. $P = \beta \cdot \exp(-\alpha r)$	$\beta = 0.26 \pm 0.27$ $\alpha = 0.10 \pm 0.21$	9	0.26
	II. $P = \beta \cdot \exp(-\alpha r^2)$	$\beta = 0.22 \pm 0.19$ $\alpha = 0.01 \pm 0.02$	9	0.20
	III. $P = \beta / (1 + \exp(\alpha(r - \delta)))$	$\beta = 0.18 \pm 0.53$ $\phi_1 = 2.3 \pm 5.4$ $\phi_2 = 11.1 \pm 3.9$	8	0.20
	IV. $P = (\theta_1 + \theta_2) \exp(-\theta_3 \cdot r)$	Failed to converge	8	
MD	I. $P = \beta \cdot \exp(-\alpha r)$	$\beta = 0.64 \pm 0.34$ $\alpha = 0.16 \pm 0.15$	6	0.56
	II. $P = \beta \cdot \exp(-\alpha r^2)$	$\beta = 0.56 \pm 0.28$ $\alpha = 0.01 \pm 0.02$	6	0.42
	III. $P = \beta / (1 + \exp(\alpha(r - \delta)))$	$\beta = 0.70 \pm 1.17$ $\phi_1 = 0.32 \pm 0.64$ $\phi_2 = 5.28 \pm 15.0$	5	0.42
	IV. $P = (\theta_1 + \theta_2) \exp(-\theta_3 \cdot r)$	$\theta_1 = 0.49 \pm 0.48$ $\theta_2 = 0.68 \pm 0.19$ $\theta_3 = 0.41 \pm 0.74$	5	0.30

Discussion

The *Ggt*/wheat/millet system has been used successfully in the past to produce profiles for the probability of infection with distance (Gilligan and Simons, 1987) and for the quantification of other epidemiological variables (Gilligan, 1980a). In this study the system was also well behaved (Fig 2.1, Table 2.5) and the inoculum easy to produce, having similar saprophytic growth characteristics to that of colonised straw fragments (Dr M. J. Grose, Pers. comm.). This inoculum was therefore deemed acceptable for use in further investigation of the spread of take-all on wheat.

Results for the *R. solani*/radish/CPS system were less satisfactory. As well as the extra care required to produce the inoculum, two main disadvantages were recognised. Firstly, the inoculum is liable to fragment on mixing, particularly when wet, resulting in biased quantification of colony forming units during the sampling of population experiments: The problem can be reduced if the sample material is dried and therefore more stable prior to assay but this in turn requires that the pathogen retains germinability following desiccation. The second disadvantage is that the inoculum is always less than 100% germinable (Table 2.4) imparting unnecessary variability when generating profiles for the probability of infection with distance (Fig 2.1, Table 2.5) and reducing the maximum probability that the inoculum has for causing infection. The effect of reduced germinability on the variability of the pathozone profile is given by $(p(1-p))/n$ where p is the mean proportion of germinable inoculum and n is the degree of replication. The variability rises from zero at 0% germinability, peaks at 50% germinability, returning to zero again at 100% germinability. The effect of low germinability can be reduced if more than one inoculum unit is used. The probability that n propagules selected at random for the inoculation of a single host are all non-viable is given by the equation

$$\text{prob of non-viability} = (1-p)^n$$

where p is the mean germinability of the population. Consequently, the problems of non-germinability can be overcome by challenging a host with two or more units of inoculum.

In contrast to CPS inoculum, MD inoculum is guaranteed to be 100 % viable and together with the ease with which small quantities can be produced, it is ideal for use in placement experiments (involving the positioning of individual units of inoculum) or for population experiments (involving low densities of particulate inoculum).

Two other components, the characteristics of colony growth and the susceptibility of the host are also identified as likely contributors to the variability of the profile. Inoculum may vary with respect to both the distance and the density that hyphae can grow towards the host and the density of hyphae that arrive at the host. These components (inoculum germinability, mycelial growth and host susceptibility) are analysed further in chapter 3.

2.7 Biological control agents

2.7.1 *Trichoderma* and *Gliocladium*.

The performance of *Trichoderma* and *Gliocladium* has been assessed in glasshouse and field trials with inconsistent results. Two general strategies for the introduction of the biological control agent (BCA) into soil have been adopted (Whipps *et al.*, 1988; Chet, 1990). The first is to broadcast the BCA on a large scale, a practice which is not often considered economical. Large volumes of colonised bran mixtures have also been incorporated into soil (Maplestone *et al.*, 1991). However, the physical properties of bran make it inconvenient for use in the population and placement experiments planned for this investigation. The second, more efficient method involves the incorporation of the BCA into a pellet for sowing along with the crop seed (Lewis and Papavizas, 1985) and is the

basis for methods of experimental investigation used here. Both methods are most effective if the crop is introduced only when the BCA is actively growing and as such, its success may depend on the nutrient source on which it is introduced. One potential drawback of this method of deployment, detected in pilot studies, is the phytotoxicity of the control agent towards the host (radish). Thus the selection of an optimal density of the biocontrol agent is crucial.

The following experiment compares the performance of *Trichoderma viride* and *Gliocladium virens* introduced alongside radish seeds at different densities and growing on a different nutrient seed base. The phytotoxic effect of the organisms is assessed in the absence of the pathogen.

Bioassays: Quantification of the disease control potential and phytotoxicity of Trichoderma and Gliocladium

Methods

Inocula of *Trichoderma viride* (isolate Ex-PM) and *Gliocladium repens* (isolate TMD) (see Appendix II for details) were produced on blue poppy seed (*Papaver somniferum* L.) or quinoa seed (*Chenopodium quinoa* Willd). These seed types were selected in favour of bran formulations because of their size, uniformity and stability following heat sterilisation and colonisation by the BCA. 100 g of seed was mixed with 50 g of tap water in a 500 ml conical flask and autoclaved at 121 kPa for 1h. A $1.0 \times 10^7 \text{ ml}^{-1}$ conidial spore suspension of the BCA, obtained from a 14 d old culture grown on potato dextrose agar, was added to each flask at a rate of 10 ml per flask. Flasks were then incubated in the dark for 3 d at 23 °C.

Repli-plates (25 wells per plate, each measuring 15 x 15 x 12 mm in depth) were filled

with sand (0.5-1.0 mm in diameter and at 10% moisture by weight) and a single radish seed sown at a depth of 5 mm in the centre of each well. Beside each seed was incorporated 0, 1, 2 or 4 single quinoa or poppy seeds colonised with either *Trichoderma* or *Gliocladium*. At a distance of 2.0 mm from the radish seed on the other side of the BCA was placed a single mycelial disc of *R. solani* (isolate R5) measuring 1.0 mm in diameter. After covering the seeds and inoculum with sand, the lids of the plates were replaced, sealed with parafilm and incubated at 23°C with a 16 hour day. The experiment involved 10 replicates per treatment and was set up as a fully randomised design. After two days, the lids were removed and the plates sealed inside clear plastic containers. After a further 5 d, the seedlings were removed, washed and assessed visually for disease (damping-off).

To assess the phytotoxicity of *Trichoderma* and *Gliocladium*, the above treatments were repeated omitting *R. solani* and with five replicates per treatment. Plants were assessed for tap root length as a measure of phytotoxicity after 7 d incubation. Additional units were assessed to eliminate the possibility that poppy seed or quinoa seed alone were responsible for either disease control or phytotoxicity.

Statistical analysis

Because of the different nature of the two variables (quantal for the probability of damping-off and continuous for the measurement of tap root length) two different methods of analysis were used. A generalised linear model with the assumption of binomial error distribution was used to compare differences in the probability of disease caused by different numbers of *T. viride* and *G. virens* propagules grown on different seed types. Main effects and interactions were assessed by comparing the accumulated analysis of deviance values with the chi-squared distribution at $p \leq 0.05$.

To compare the phytotoxicity caused by different numbers of *T. viride* and *G. virens*

propagules grown on different seed types a simple analysis of variance was performed.

Results

When inoculum (a mycelial disc) of *R. solani* was placed at a distance of 1 mm from a radish seed, the probability of the seed becoming diseased after seven days was 0.6. The addition of either *Trichoderma viride* or *Gliocladium virens* significantly reduced the probability of disease caused by *R. solani*. This was detected as being highly significant by the generalised model analysis (Table 2.6).

Table 2.6: Summarised analysis of deviance of the effects of numbers of BCA units, seed (substrate) type and BCA on the probability of infection (damping-off) by *R. solani*.

Source	d.f	Deviance	Significance
Number (lin)	1	15.6	p≤0.001
Number (quad)	1	4.13	p≤0.05
Number (cubic)	1	0.64	n/s
Type of BCA	1	0.87	n/s
Seed	1	1.72	n/s
Number(lin).BCA	1	0.89	n/s
Number(quad).BCA	1	3.13	n/s
Number(cub).BCA	1	5.63	p≤0.05
Number.Seed	1	1.92	n/s
BCA.Seed	1	0.31	n/s
Number.BCA.Seed	1	0.02	n/s
Residual	148	158.89	

The placement of a poppy seed (food base) colonised with *Trichoderma* alongside the radish plant reduced the probability of damping-off from 0.6 to 0.1. When the food base was a quinoa seed, the probability of disease was reduced from 0.6 to zero (Fig. 2.2a). The

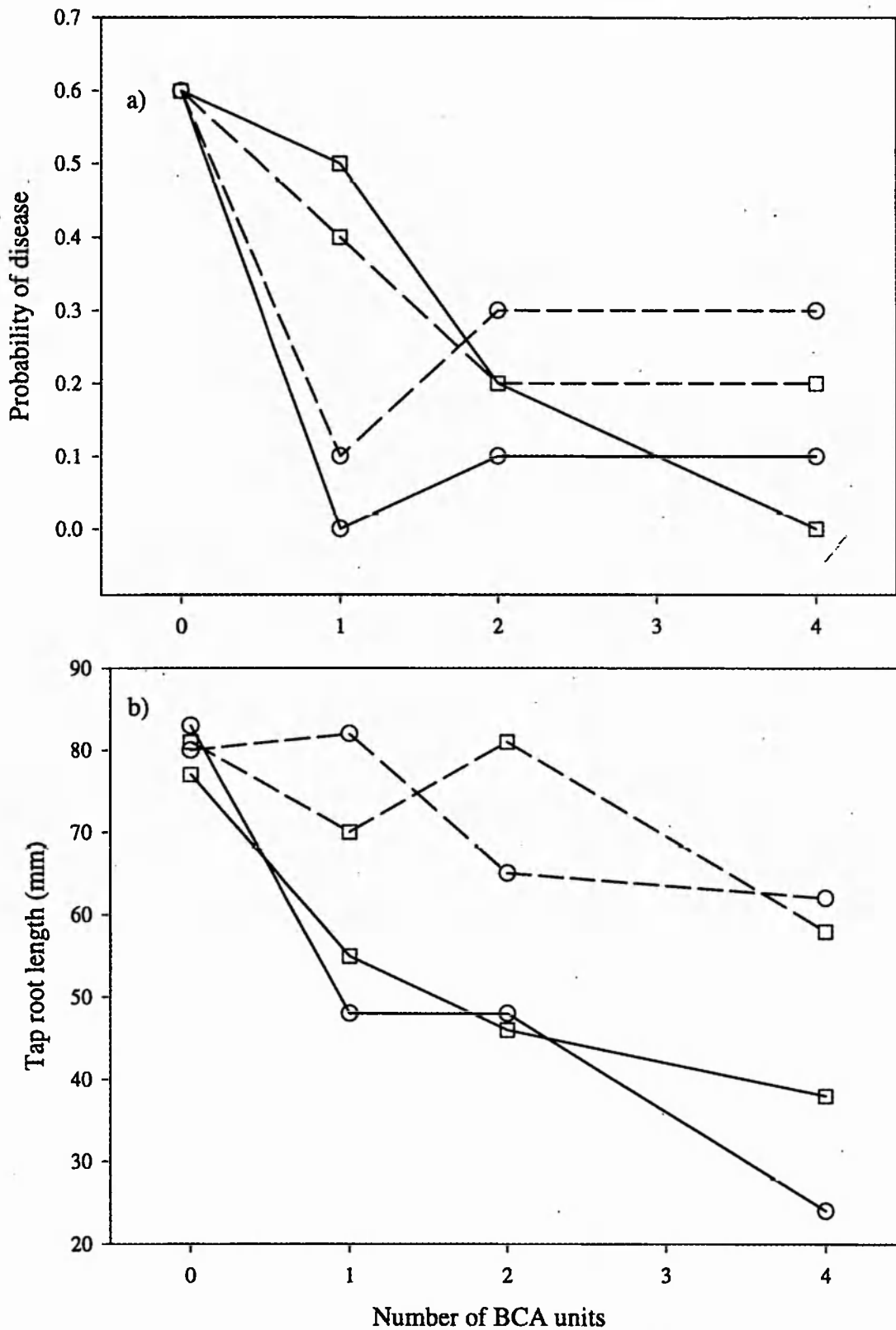


Fig 2.2: The effect of number of units of *Trichoderma viride* (circles) or *Gliocladium virens* (squares) growing from quinoa seed (solid lines) or poppyseed (dashed lines) on a) the probability of infection by *R. solani* and b) the mean tap root length of radish seedlings growing in the absence of *R. solani*.

addition of *Gliocladium* on either a poppy seed or a quinoa seed did not reduce the probability of disease by the same amount. When *Gliocladium* was added as a colonised poppy seed, the probability of disease was reduced from 0.6 to 0.4 and as a colonised quinoa seed from 0.6 to 0.5. As the number of BCA units was increased, from one to four, the difference between *Trichoderma* and *Gliocladium* disappeared, both providing significant levels of control. The different trends between *Trichoderma* and *Gliocladium* with respect to control of damping-off by different numbers of colonised seeds was detected in the analysis as a significant cubic interaction (i.e. Number(cub).BCA term).

Both *Trichoderma* and *Gliocladium* reduced the length of the radish tap root in the absence of *R. solani* (Fig 2.2b). The reduction was more severe when the number of BCA units was increased and for quinoa seed rather than for the poppy seed base (Table 2.7).

Table 2.7: Summary of analysis of variance showing the effects of number of BCA units, seed (substrate) type and type of BCA on the tap root length (mm) of radish seedlings and associated standard errors below.

Number of BCA units	<i>Trichoderma</i> on quinoa	<i>Trichoderma</i> on poppy seed	<i>Gliocladium</i> on quinoa	<i>Gliocladium</i> on poppy seed
0	83.0	80.0	77.0	81.0
1	48.0	82.0	55.0	70.0
2	48.0	65.0	46.0	81.0
4	24.0	62.0	38.0	58.0

	Number	BCA	Seed	Number. BCA	Number. Seed	BCA. Seed	Number. BCA. Seed
s.e.d	6.06	4.28	4.28	8.57	8.57	6.06	12.12
Rep	20	40	40	10	10	20	5

Conclusions

Trichoderma was selected for inclusion in future investigations on the basis of increased control with a single BCA unit (the placement of which saves time during experimentation) and with no detectable increase in phytotoxicity compared with *Gliocladium* at the same density (Fig. 2.2b). *Trichoderma* behaves as a partially selective antagonist which has the potential to harm both the plant and the pathogen, a property which may restrict its use as a control agent (Ousley *et al.*, 1993). The general loss of control when the number of units of *Trichoderma* was increased may be the result of this phytotoxicity whereby the presence of the BCA may have increased the susceptibility of the host to disease.

2.7.2 *Pseudomonas corrugata*

An isolate of *Pseudomonas corrugata* (strain R2140) was kindly supplied by Professor K. J. Killham (University of Aberdeen). The organism was originally isolated from the rhizosphere of a wheat root growing in take-all suppressive soil in Australia (Ryder and Rovira, 1993). *Pseudomonas corrugata* had been marked with the *luxAB* genes of *Vibrio harveyi* for the purpose of detection *in situ*. This property forms the basis for future work and was not exploited in this investigation. Russell (1996) compared the genetically altered (*luxAB*) marked strain of *P. corrugata* with the original wild type. No differences in growth or activity were detected. Since the wild type organism had performed well, providing significant levels of disease control in preliminary field trials (Prof K. J. Killham pers. comm.) its *luxAB* marked counterpart was selected as the biological control organism against *Ggt* on this basis.

To produce inoculum of *P. corrugata*, a 500 ml conical flask containing 200 ml of Luria broth (Oxoid) was inoculated with a culture of *P. corrugata*. The flask was incubated in an orbital incubator (125 rpm) at 25 °C for 16 h. This corresponds with the late log phase of

the culture containing 10^{10} cells ml^{-1} (Russell, 1996). Aliquots of 1.0 ml of the culture were pipetted into sterile Eppendorf tubes and these tubes were centrifuged at 12,000 g for 2 minutes. The supernatant was removed and the cells resuspended in 1 ml of phosphate buffered saline (PBS) (80 g NaCl, 2 g KCL, 11.5 g Na_2HPO_4 , 2.0 g KH_2PO_4 in 1 l RO H_2O). The centrifugation process was repeated twice more and the final culture diluted into a conical flask with PBS to provide 100 ml containing 1.0×10^7 cells ml^{-1} . The flask was placed on ice prior to inoculation of roots.

Chapter three

Inoculum and components of pathozone infection

3.1 Introduction

Changes in the probability of infection with increasing distance between an inoculum unit and the host are described by the pathozone profile. The objective of this chapter is to interpret and model the behaviour of inoculum in relation to the major components responsible for dictating the shape and variability of the pathozone profile and to identify an inoculum type suitable for the experimental derivation of pathozone profiles for the infection of radish by *R. solani*. The major components of pathozone infection were identified in chapter 2 as the germinability of inoculum, the growth of the resulting mycelial colony outwards to make contact with the host and the susceptibility of the host to disease once contact has been made. These components were represented in a model by the conditional probabilities P_1 , P_2 and P_3 respectively where the probability of disease from inoculum placed at distance r mm from the host $P(r)$ is given by:

$$P(r) = P_1 \cdot P_2(r) \cdot P_3(r) \quad (3.1)$$

For the infection of radish by *R. solani*, the probability of germination, P_1 , is independent of distance while the probability of reaching the host, P_2 , and of the susceptibility of the host on contact, P_3 , both depend on distance.

Each component is quantified separately for two types of inoculum, chopped potato soil (CPS) and mycelial discs (MD). Chopped potato soil inoculum is composed of a mixture of potato and soil impregnated with fractions of fungal mycelium. The amount and nutritional status of fungal mycelium varies between inoculum units reflecting variability

in germination, fungal growth and infection of naturally occurring inoculum. Mycelial discs, removed from a growing colony of *R. solani*, provide inoculum with actively growing mycelium, uniformly high viability and potentially less variability in colony growth and infectiveness. An inoculum type with these characteristics was considered necessary to minimise variability within profiles and thus maximise the chance of identifying treatment effects between profiles.

Using model (3.1) and empirically derived values of P_1 , P_2 and P_3 , the shape and variability of pathozone profiles for the two types of inoculum are predicted at a single time, specifically, when the mycelial colony had achieved its maximum size, and are compared with experimental data. Finally, the behaviour of the model is examined by assessing the sensitivity of shape and variability to different parameter values using a stochastic version of model (3.1).

3.2 Methods

3.2.1 Production of inoculum

Chopped potato soil and mycelial disc inoculum

Chopped potato soil (CPS) and mycelial disc (MD) inoculum were prepared according to the methods described in section 2.6.2. The CPS inoculum was obtained from the 1.0 mm to 2.0 mm diameter fraction, whilst MD inoculum was cut to a size of 1.0 mm diameter.

3.2.2 Components of pathozone infection

Inoculum germinability (P_1)

To assess the germinability of inoculum over time, 100 units of each inoculum type were plated onto potato dextrose agar immediately following preparation or after approximately

90 d (CPS) and 30 d (MD as whole plates) storage in the dark at 4 °C. The plates were incubated for 48 h at 23 °C and assessed for germination using a binocular microscope (magnification = x 20). Three batches of CPS inoculum, produced using three different soils (see Appendix 1 for details), were assessed for germinability. Of these, only one batch (soil 2) was selected for estimation of P_2 and P_3 .

Investigation of colony growth (P_2)

The growth of individual colonies was investigated on 11.0 cm diameter glass microfibre filters (Grade Gf/c, Whatman International Ltd, Maidstone, Kent) contained singly in 14.0 cm diameter plastic Petri-dishes. Aliquots of 5 cm³ sterile distilled water were added to each filter and plates were sealed with para-film. Plates were arranged in a fully randomised design and incubated in the dark at 23 °C. After 4 d incubation, colonies were stained with cotton blue in acetic acid and examined under a dissecting microscope (x 20). Growth of mycelial colonies on glass microfibre filters was selected because the furthest extent of mycelial growth produced under these conditions was not found to differ significantly from colonies generated directly on the surface of moist sand (Otten, Pers. comm.) and because of the relative ease and accuracy associated with the direct observation of mycelium.

Two properties associated with colony growth were investigated (Fig 3.1). The furthest extent of colony growth was examined for 100 replicates and a more detailed examination of changes in the number and distribution of hyphae with distance was performed on a randomly selected sub-sample of 35 of the same replicates.

Changes in host susceptibility (P_3)

Changes in the susceptibility of the host were estimated by combining information from

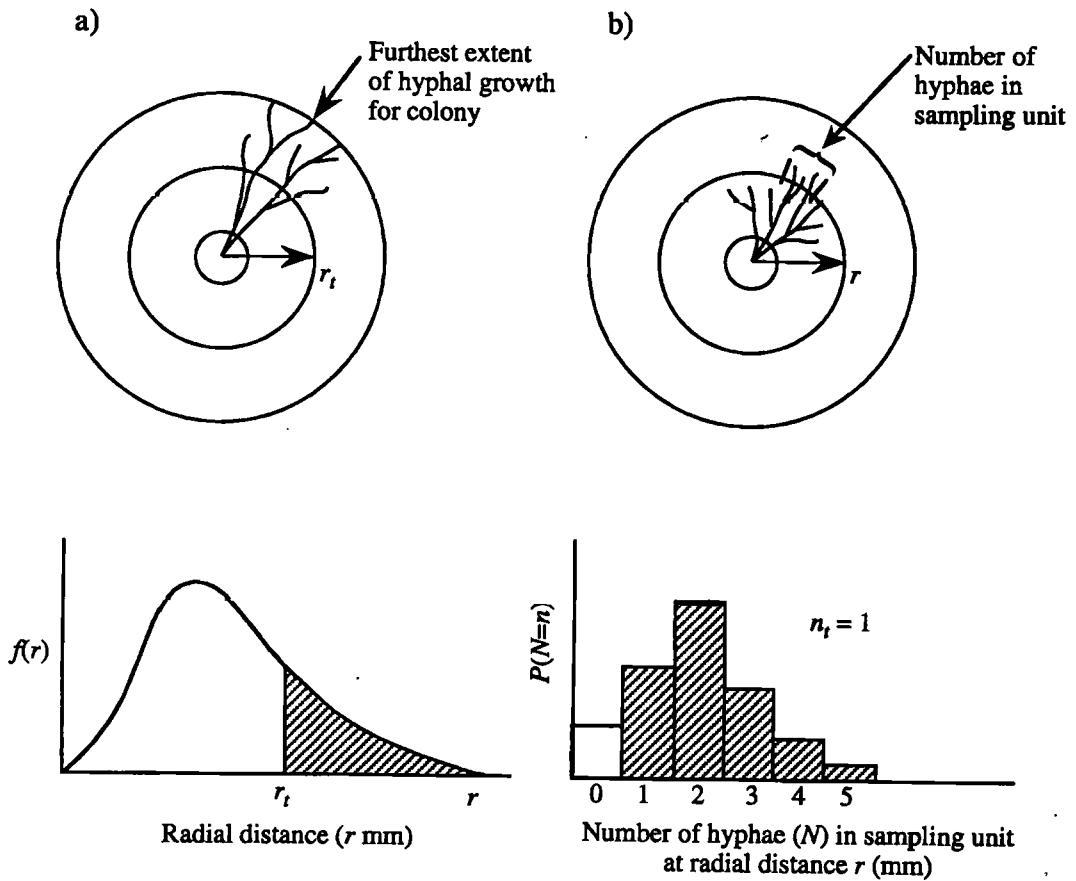


Fig. 3.1: Schematic representation of two properties of colony architecture used to estimate the probability of contact between mycelium growing out of a source of inoculum and a host.

a) The furthest extent of mycelial growth in replicate colonies is described by a continuous probability distribution. The threshold for infection is determined by the minimum distance between inoculum and host (r_t). The probability of contact (shaded area) is estimated by the proportion of inoculum units that can grow further than r_t .

b) The number of hyphae in a sampling unit equivalent to the host diameter is described by a discrete probability distribution with parameters that vary with distance. The threshold for infection is determined by the minimum number of hyphae required to contact the host (n_t). The probability of contact (shaded area) for a given distance is estimated by the proportion of sampling units with at least n_t hyphae.

two experiments. The first experiment estimated the time of contact by fungal mycelium arriving from inoculum placed at different distances from the host. The second experiment estimated changes in the relative susceptibility of the host over time for inoculum at a fixed location. Changes in susceptibility to inoculum placed at different distances from the host and thus making contact with the host at different times could then be estimated.

In the first experiment, growth curves for the expansion of fungal colonies generated by CPS and MD inoculum were produced on glass microfibre filters as before. The experiment included 9 replicates per inoculum type per time in a fully randomised design. Colonies were stained with 0.2% trypan blue in 95% acetic acid and measurements were made of the furthest extent of colony growth 1,2,3,4,5 and 7 d after introduction of the inoculum to the filters.

In the second experiment, changes in the susceptibility of the host over time were measured according to the methods described in 2.6.2 but with MD inoculum placed at a single distance (2 mm) from the surface of 0, 1, 2, 3, 4, 5, 6, 8, 10 or 12 d old radish seedlings. Each time was replicated 18 times in a fully randomised block.

3.2.3 Pathozone profiles

Pathozone profiles describing changes in the probability of infection when inoculum is placed at different distances from the surface of the host were generated according to the methods described in 2.6.2. The experiment was arranged in a fully randomised block design with 10 distances, 0, 1, 2, 3, 4, 5, 6, 8, 11 and 15 mm, each with 18 replicates.

The probabilistic model (3.1) is derived by empirical estimation of its components, (i.e. germinability, mycelial growth and infectivity at the host surface). The model is used to predict the shape of the pathozone profile for two types of inoculum. Ultimately, the dynamics of the pathozone will be used to predict disease progress amongst a population

of host plants. Model (3.1) is unnecessarily complex for this purpose (i.e it has many parameters). Consequently, four simple, non-linear models were fitted to the profiles in order to provide a summary of the principle features. Three of the models (models I, II and IV) were described in 2.6.2. The logistic model was replaced by an additional exponential model, $P = \beta \cdot \exp(1 - \exp(\alpha r))$, which allows for a more rapid decay in the probability of infection, P , with distance, r . The models were fitted by maximum likelihood under an assumption of a binomial distribution of errors due to the discrete nature of the response variate. The model of best fit was selected on the basis of minimal least squares and compared with predictions of model (3.1).

3.2.4 Derivation of model

Probability of germination (P_1) The probability that a unit of either CPS or MD inoculum germinates was assumed to remain independent of the distance at which it was placed from the surface of the host.

Probability of contact following germination (P_2)

The morphology of fungal colonies is notoriously variable both between species, for which it is historically used for the purpose of identification, but also within species. The architecture of a fungal colony can depend on the location and availability of nutrients. Thus, on an agar plate or in a nutrient rich, homogeneous soil environment, a fungal colony might be expected to develop with a regular and high mycelial density. Alternatively, if the colony develops in the absence of external nutrients, the distribution of mycelium is patchy (Ritz, 1995). Thus two forms of the model for contact of mycelium with the host, denoted P_{2a} and P_{2b} respectively, were examined.

The model for P_{2a} is based on two assumptions: (i) that colonies from germinating

inoculum units are radially symmetrical and (ii) that hyphal density is sufficiently high, such that, if the colony can grow at least as far as the host, contact is inevitable (Fig. 3.1a). This model also applies to directional growth towards a host.

The probability that the fungus contacts a host r mm away is estimated by the proportion of inoculum capable of growing at least r mm. The distance between inoculum and host therefore sets a threshold distance for growth, r_p , and the probability of contact is given by:

$$P_{2a} = P[\text{Fungus grows a threshold distance } r_p] = 1 - \int_0^{r_p} (f(r) | \theta) dr, \quad (3.2)$$

where $f(r)$ is the probability density function of a continuous distribution for the furthest extent of hyphal growth of individual inoculum units, with parameters θ . Frequency histograms were prepared for the furthest growth of hyphae from inoculum units of CPS and MD and the goodness-of-fit to normal, gamma and exponential distributions were tested by residual deviance and examination of residuals using maximum likelihood programme (MLP) (Ross, 1987).

The second form, P_{2b} , is estimated from the distribution of hyphal density arriving at the host surface. The model allows for sparse, radially-asymmetrical colony expansion (Fig. 3.1b). The probability of N hyphae arriving at a host is given by the density function of a discrete distribution: formally the probability that the random variable N takes a particular value, n , for inoculum at a distance r mm from the host, is given by:

$$P [N=n | r] = f [N | \theta (r)], \quad (3.3)$$

in which $\theta(r)$ are the parameters of the distribution, which change with distance.

If successful infection and disease requires a threshold density of hyphae, n_r , then P_{2b} is given by:

$$P_{2b} = P[N \geq n_r | r] = 1 - \sum_{N=0}^{N=n_r} f[N | \phi(r)] \quad (3.4)$$

Two distributions, the Poisson and negative binomial, were tested to describe the density of hyphae arriving at a host. The Poisson distribution applies to hyphae that are randomly and independently arranged at a given radius, while the negative binomial distribution allows for clumping of hyphae. Goodness-of-fit of hyphal density to the Poisson and negative binomial distributions at each distance was tested by chi-squared analysis. Simple exponential or hyperbolic functions were used to characterise the change in the mean and clumping parameter (for the negative binomial) with distance.

Probability of infection given contact (P_3)

The probability of infection over time was described by a monomolecular function, thus:

$$P_3(t) = \kappa_i(1 - \exp(-\beta_i(t - \delta_i))) \quad (3.5)$$

where κ_i , β_i and δ_i are parameters that relate the change in $P_3(t)$ with time. Equation (3.5) relates the susceptibility of the host to the time at which it encounters fungal mycelium. Time (t) in equation (3.5) was converted to distance travelled by the fungus, by analysis of growth curves derived from MD and CPS inoculum. The relationships were also monomolecular in shape where:

$$r = \kappa_r(1 - \exp(-\beta_r(t - \delta_r))) \quad (3.6)$$

Rearranging (3.6) to obtain t as a function of r and substitution in (3.5) yields:

$$P_3(r) = \kappa \left[1 - \gamma \left(\frac{\kappa_r}{\kappa_r - r} \right)^\beta \right], \quad (3.7)$$

where, $\kappa = \kappa_r$, $\beta = \beta_r/\beta_r$, $\delta = \beta_r(\delta_r - \delta_t)$, $\gamma = \exp(-\beta\delta)$.

3.3 Results

3.3.1 Estimation of the probability of germination (P_1)

Levels of germinability were similar for both inoculum types following initial preparation but varied with respect to their rate of decay during storage (Table 3.1). All units of MD inoculum were viable and, although not relevant because the inoculum is freshly prepared prior to use, suffered no observable decay after storage for 30 d. The rate of decay of CPS inoculum depends on the soil type from which it was prepared. The CPS inoculum (Soil 2) was chosen for further investigation prior to which the germinability had decayed to 68%.

Table 3.1: *Change of germinability during storage for different types of inoculum.*

Inoculum	Initial germinability (%)	Final germinability (%)	Duration of storage (days)	Linear decay rate (% day ⁻¹)
CPS (Soil 1)	91	85	90	0.047
CPS (Soil 2)	90	71	90	0.211
CPS (Soil 3)	86	30	90	0.620
MD	100	100	30	-

3.3.2 Estimation of the furthest extent of mycelial growth (P_{2a})

Germinable units of CPS inoculum produced mycelial colonies more variable in size

than those produced by MD inoculum. All grew a minimum of 3 mm, most grew about 10 mm but many grew further, reaching a maximum of 65 mm. In contrast, all colonies produced by MD inoculum grew to 21 mm but the number growing further tailed off rapidly to a maximum at 55 mm. Histograms of the furthest extent of hyphal growth from CPS inoculum could be adequately described by gamma and normal distributions and from MD inoculum, by exponential, gamma and normal distributions. However, visual observation of fitted curves suggests that the gamma function provided the best description of CPS inoculum, whilst a displaced exponential function provided an appropriate description for colonies produced by MD inoculum. The fitted functions for the two distributions are shown in Figures 3.2a and 3.2b.

Changes in the probability of a germinable unit of CPS and MD inoculum making contact with the host are given by:

$$P_{2a} = 1 - (0.123^{2.56}) (r^{2.56-1}) \frac{\exp(-0.123r)}{(\Gamma/2.56)}, \quad (3.8)$$

and

$$P_{2a} = \begin{cases} 1 & r < 21 \\ \exp(-0.131(r-21)) & r \geq 21 \end{cases}, \quad (3.9)$$

respectively and shown in Figures 3.2c and 3.2d.

3.3.3 Estimation of changes in hyphal density with distance (P_{2b}).

Histograms generated from counts of the number of hyphae passing through 2.34 mm sectors (equivalent to the host diameter) of the circumference at each distance, as indicated in Figure 3.1b, are shown in Figure 3.3. Hyphae became relatively more clustered (lower values of k) with distance for both types of inoculum and were adequately described by the negative binomial distribution at all distances except at 2 and 4 mm away from the centre

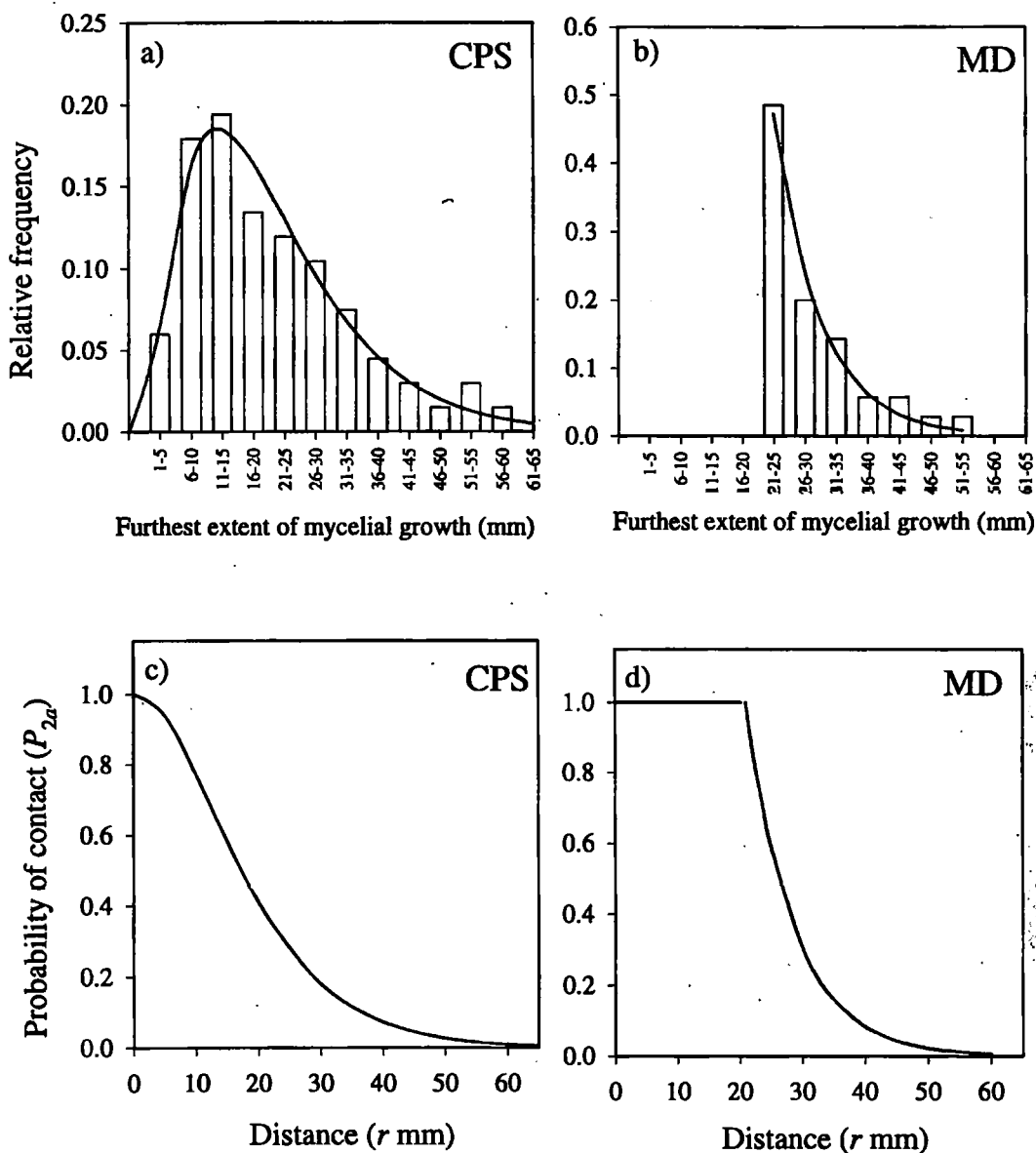


Fig. 3.2. Histograms and fitted distributions to the furthest extents of mycelial growth from four day old colonies of a) CPS and b) MD inoculum. CPS inoculum was described by a gamma and MD by a displaced exponential (for $r > 21$ mm) distribution. Figures c) and d) show the probabilities of contact with the host r mm away from inoculum of CPS and MD respectively (P_{2d} , equations 3.8 and 3.9).

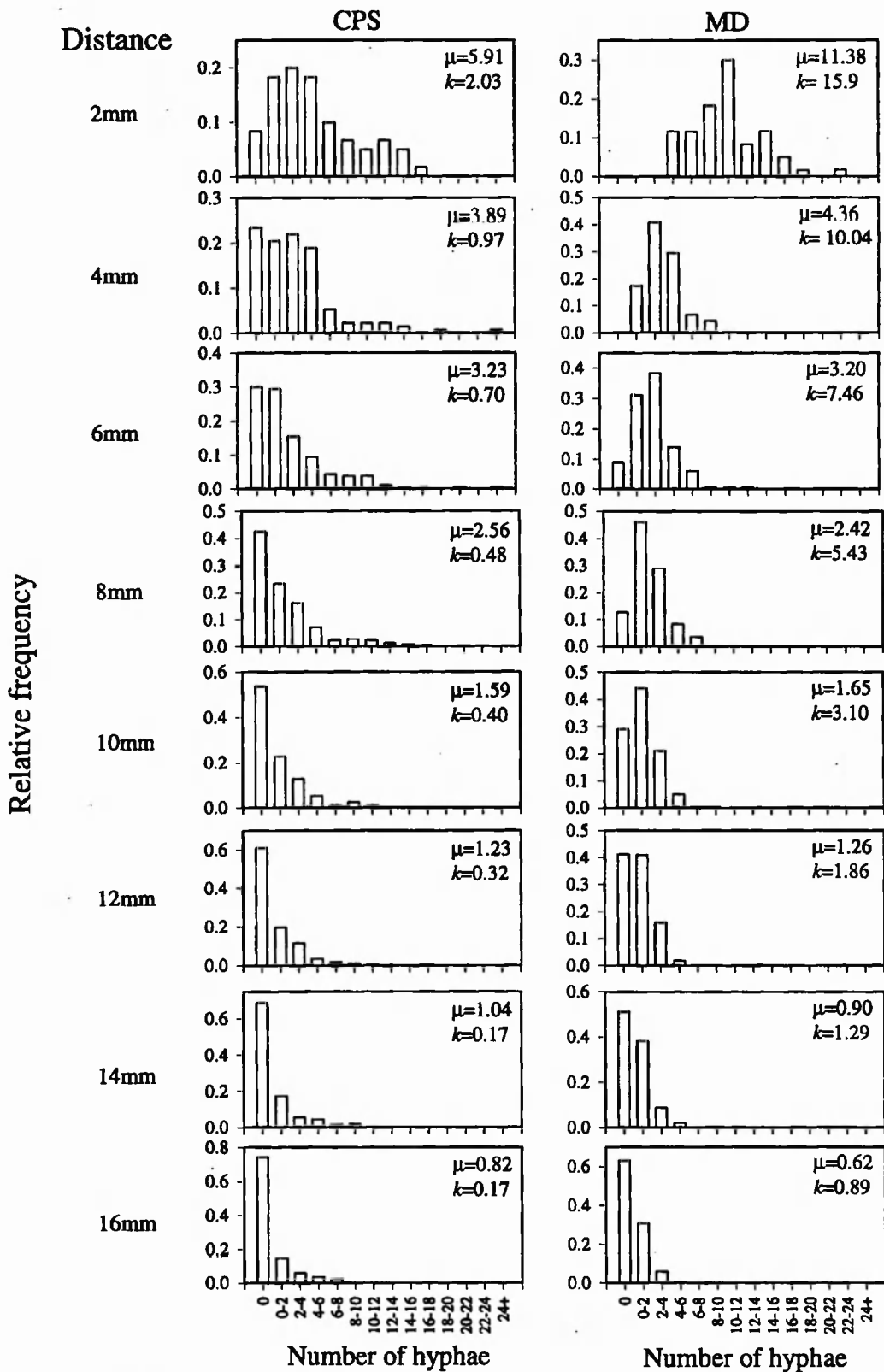


Fig. 3.3. Probability distributions for the number of hyphae passing through 2.34 mm sectors at radial distances, 2, 4, 6, 8, 10, 12, 14 and 16 mm from the centre of CPS and MD inoculum. The estimated values for the means and clumping parameters of the negative binomial distribution are shown. The estimates of k for MD inoculum placed at 2 and 4 mm from the host are obtained by extrapolation from the trends at larger distances. All other estimates were obtained by maximum likelihood estimation from fitting a negative binomial to the empirical frequency data.

of MD inoculum when the distribution of hyphae tended towards a Poisson distribution (Table 3.2).

Table 3.2: Results of fitting Poisson and negative binomial (N/B) distribution to data describing the number of hyphae present in 2.34 mm sections of the circumference at increasing distances from the inoculum unit.

Inoculum	Distance (mm)	Distribution	Residual deviance	d.f	Significance
CPS	2	Poisson	61.51	7	p<0.001
		N/B	2.66	6	n/s
	4	Poisson	125.9	6	p<0.001
		N/B	9.78	5	n/s
	6	Poisson	247.6	6	p<0.001
		N/B	3.44	5	n/s
	8	Poisson	388.8	6	p<0.001
		N/B	8.22	5	n/s
	10	Poisson	363.4	5	p<0.001
		N/B	11.52	4	p<0.05
12	Poisson	350.8	4	p<0.001	
	N/B	9.74	3	p<0.05	
14	Poisson	500.4	4	p<0.001	
	N/B	5.89	3	n/s	
16	Poisson	528.1	4	p<0.001	
	N/B	3.84	3	n/s	
MD	2	Poisson	5.56	5	n/s
		N/B	FTC*	FTC*	p<0.05
	4	Poisson	4.37	5	n/s
		N/B	FTC*	FTC*	p<0.05
	6	Poisson	12.95	6	p<0.05
		N/B	6.41	5	n/s
	8	Poisson	15.63	5	p<0.01
		N/B	2.07	4	n/s
10	Poisson	38.1	4	p<0.001	
	N/B	6.82	3	n/s	
12	Poisson	63.3	3	p<0.001	
	N/B	17.11	2	p<0.001	
14	Poisson	55.0	3	p<0.001	
	N/B	1.26	2	n/s	
16	Poisson	59.2	2	p<0.001	
	N/B	2.55	1	n/s	

* FTC = Fitting procedure failed to converge

The mean radial density of hyphae declined exponentially (CPS) or hyperbolically (MD) with distance from the centre of the inoculum unit (Fig. 3.4a). The degree of clustering, estimated by the k parameter of the negative binomial distribution, decreased exponentially at similar rates for both types of inoculum but over markedly different ranges (Fig. 3.4b). In summary, changes in the mean and clumping parameters with radial distance were given by :

$$\text{CPS } \mu(r) = 7.17 \exp(-0.15r), \quad (3.10a)$$

$$\text{MD } \mu(r) = 1/(a+0.059r), \quad (3.10b)$$

$$\text{CPS } k(r) = 2.68 \exp(-0.23r), \quad (3.10c)$$

$$\text{MD } k(r) = 25.2 \exp(-0.23r). \quad (3.10d)$$

The parameter, $a = 8.31 \times 10^{-7}$, in equation (3.10b) reflects the sharp increase in hyphal density close to the centre of MD inoculum. Since the functions for $\mu(r)$ are used relative to a comparatively low threshold density of hyphae required for infection to occur, the instability of the hyperbolic function for MD inoculum at low values of r does not cause any numerical problems.

The probability of contact by four or more hyphae is given by:

$$P_{2b} = 1 - \sum_{N=0}^{N=n_1} \binom{N+k(r)-1}{k(r)-1} \left(\frac{\mu(r)}{\mu(r)+k(r)} \right)^N \left(1 + \frac{\mu(r)}{k(r)} \right)^{-k(r)} \quad (3.11)$$

where $\mu(r)$ and $k(r)$ are defined by (3.10).

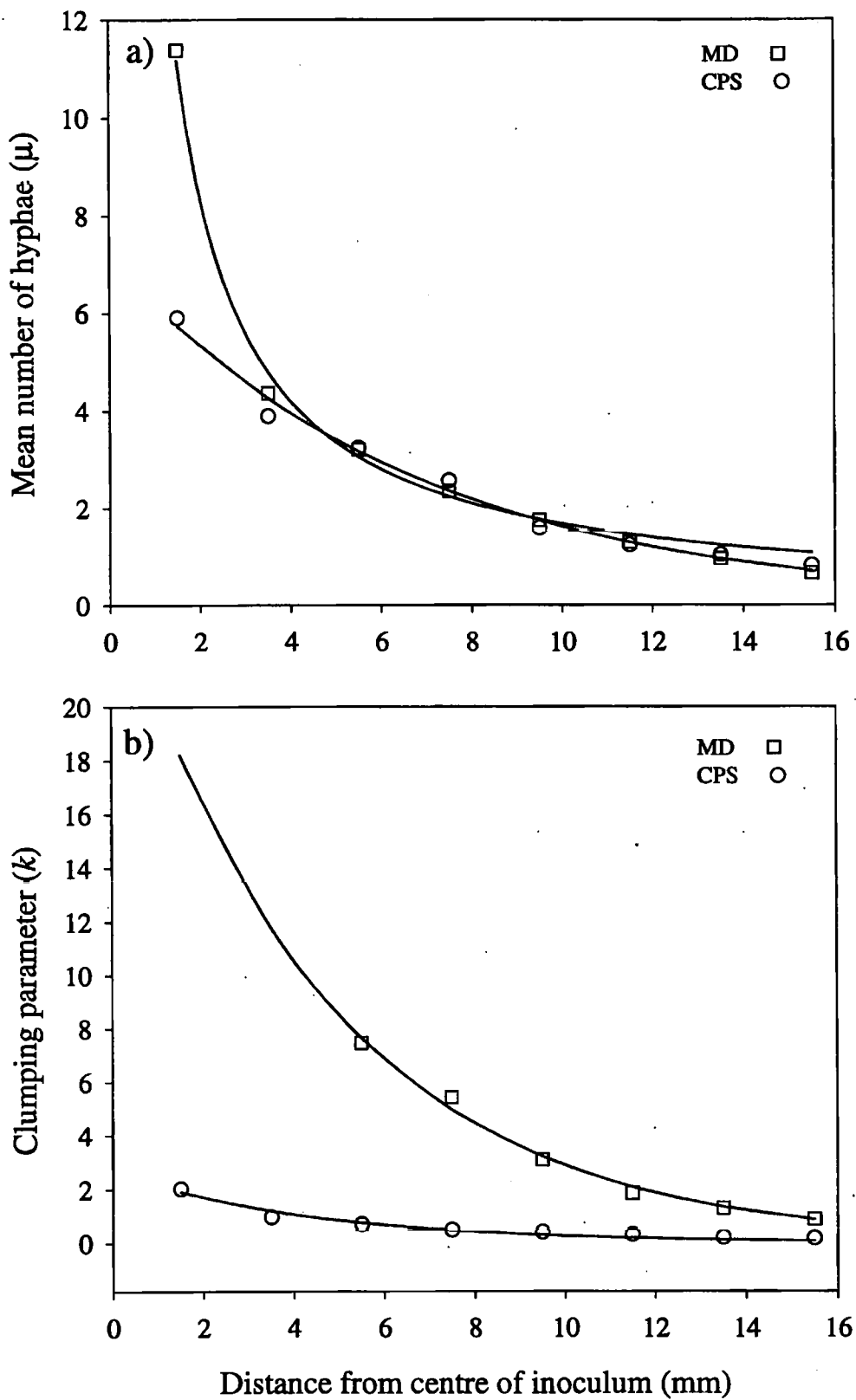


Fig. 3.4. Observed and estimated (equation 3.10) changes with distance of a) the mean (μ) and b) the clumping parameter (k) of the negative binomial distribution from the centre of four day old colonies growing from CPS (circles) or MD (squares) inoculum.

The expression is greatly simplified when the threshold is a single hypha where:

$$P_{2b} = 1 - \left(1 + \frac{\mu(r)}{k(r)} \right)^{-k(r)}, \quad (3.12)$$

which for CPS and MD inoculum yields:

$$\text{CPS } P_{2b} = 1 - [1 + 2.67 \exp(0.07r)]^{-k(r)},$$

$$\text{MD } P_{2b} = 1 - \left[1 + \frac{\exp(0.23r)}{25.3a + 1.493r} \right]^{-k(r)},$$

where $k(r)$ is defined by (3.10c and 3.10d). The probability of contact by one ($n_i = 1$) or four ($n_i = 4$) hyphae is shown in Figure 3.5 for each type of inoculum. For MD inoculum both curves were sigmoidal, whereas for CPS, the curves switch from sigmoidal to exponential as the threshold n_i increases.

3.3.4 Estimation of the probability of infection given contact (P_3)

When MD inoculum was placed at the surface of an ungerminated seed, the probability of infection was estimated to be 0.5 (Fig. 3.6b). If inoculum was placed at the surface of older host material, the probability of disease increased. The maximum probability of infection was attained when hosts were three days old at the time of inoculation. It was noted that this coincided with cessation of physical disruption to the rhizosphere soil caused by the germinating seedling. The relationship between $P_3(t)$ and time was described by:

$$P_3(t) = 1 - \exp(-0.91(t+0.74)). \quad (3.13)$$

Growth curves of both inoculum types could be described by a monomolecular function of the form (3.6) where the asymptotic extent of colony growth was estimated at 23.6 mm

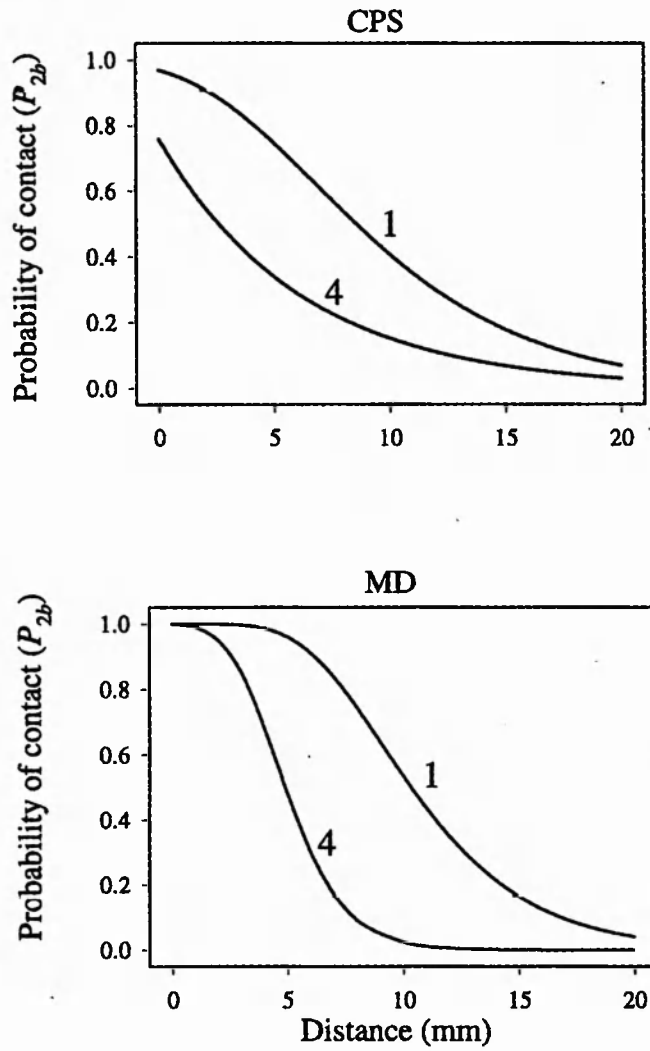


Fig. 3.5. The probability of contact (P_{2b}) with the host with a threshold of $n_t = 1$ or 4 hyphae for CPS and MD inoculum.

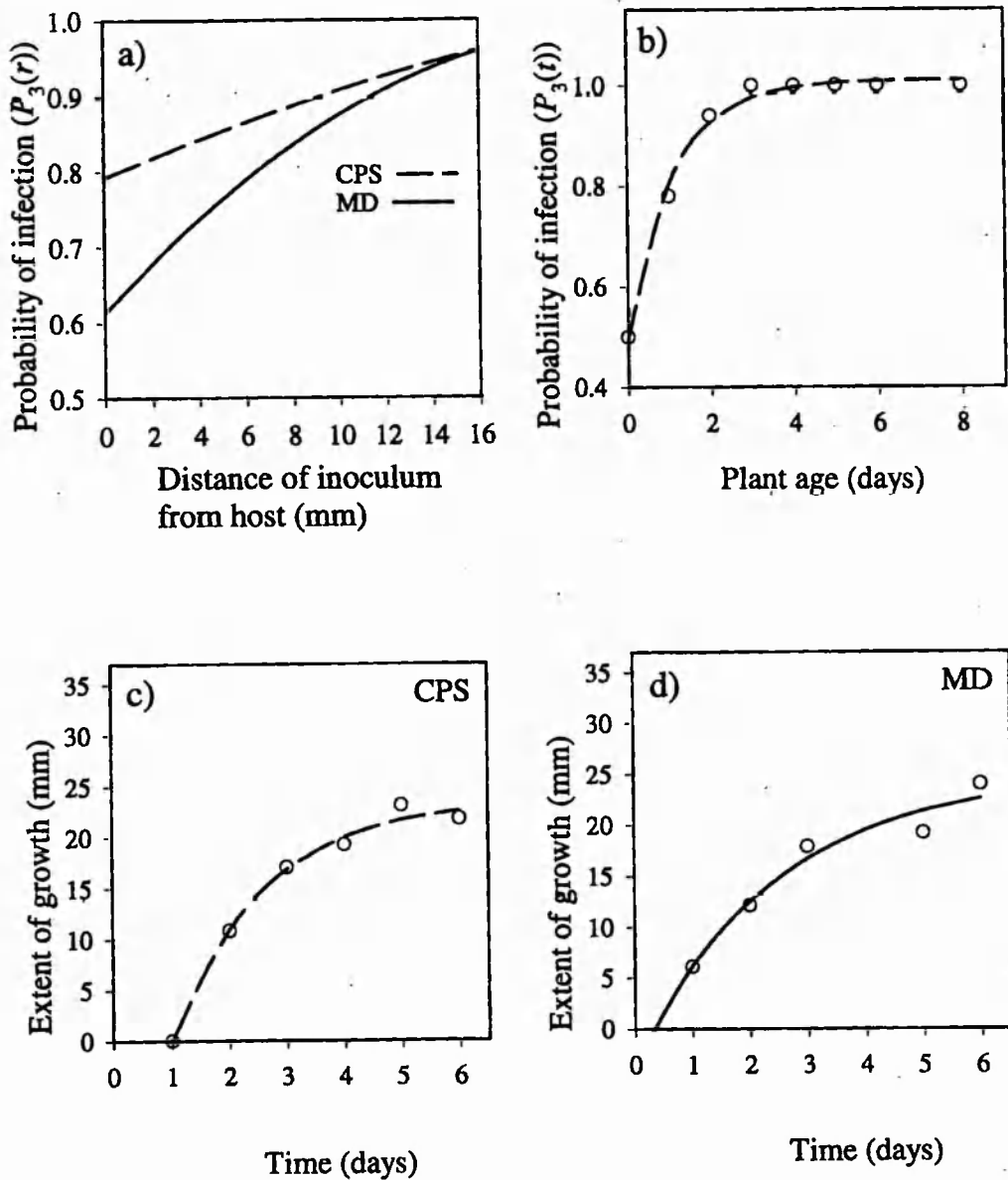


Fig. 3.6. a) Probabilities of infection given contact, $P_3(r)$, with distance from the host for CPS and MD inoculum (equation 3.15). b) Change in susceptibility of radish seedlings, $P_3(t)$ with time (equation 3.13). c) and d) mean extent of mycelial growth over time for CPS and MD inoculum (equation 3.14).

and 25.0 mm for CPS and MD inoculum respectively (Table 3.3).

Table 3.3: Summary of model fitting to curves describing the growth of mycelium with time for mycelial disc and chopped potato soil inoculum.

Inoculum	Parameter estimate +/- s.e	d.f	Residual mean square	Variance accounted for (%)
Chopped potato soil	$\kappa = 23.6 \pm 1.18$ $\beta = 0.62 \pm 0.11$ $\delta = 1.00 \pm 0.075$	2	3.12	93.5
Mycelial disc	$\kappa = 25.0 \pm 3.11$ $\beta = 0.41 \pm 0.18$ $\delta = 0.31 \pm 0.039$	3	1.40	98.1

When the growth curves were compared using equation (3.6) they differed only in respect of the δ parameter (Table 3.4). This difference reflects a significant delay in the germination of CPS inoculum.

Table 3.4: Summary of analysis of variance for comparison of curves describing the growth of mycelium from chopped potato soil and mycelial disc inoculum.

Inoculum	d.f	Residual mean square	Significance
CPS vs MD			
Common curve	8	31.43	p<0.001
Separate curves	5	10.44	
Varying κ	7	31.21	n/s
Varying β	7	29.91	n/s
Varying δ	7	14.95	p<0.05

The average extent of hyphal growth from CPS and MD inoculum (Fig. 3.6c and Fig. 3.6d)

was given by:

$$\text{CPS } r = 23.6 (1 - \exp(-0.62(t-1.00))), \quad (3.14a)$$

$$\text{MD } r = 25.0 (1 - \exp(-0.41(t-0.31))), \quad (3.14b)$$

yielding probabilities of infection given contact [$P_3(r)$] of:

$$P_3(r) = \left[1 - 0.205 \left(\frac{23.6}{23.6-r} \right)^{-1.47} \right], \quad (3.15a)$$

for CPS inoculum and

$$P_3(r) = \left[1 - 0.385 \left(\frac{25.0}{25.0-r} \right)^{-2.22} \right], \quad (3.15b)$$

for MD inoculum. It follows that the more rapid arrival of hyphae from MD inoculum coincides with a period when the host is less susceptible (Fig. 3.6a). It is noted, however, that with substantially further delay, the susceptibility once again may be expected to decline.

3.3.5 Comparison of model predictions and experimental data

When inoculum of either CPS or MD was placed at increasing distances from the host, the probability of infection declined (Fig. 3.7). The furthest outer limit of the pathozone was observed to be 11 and 15 mm for CPS and MD inoculum respectively. There was no noticeable difference between inoculum types in the shape of this decay and all three of the models used previously by Gilligan and Simons (1987) as well as Model IV produced significant fits to the data. However, it was noted that model II produced the best description of the profile generated using CPS inoculum whilst model IV gave the lowest residual deviance for MD inoculum (Table 3.5).

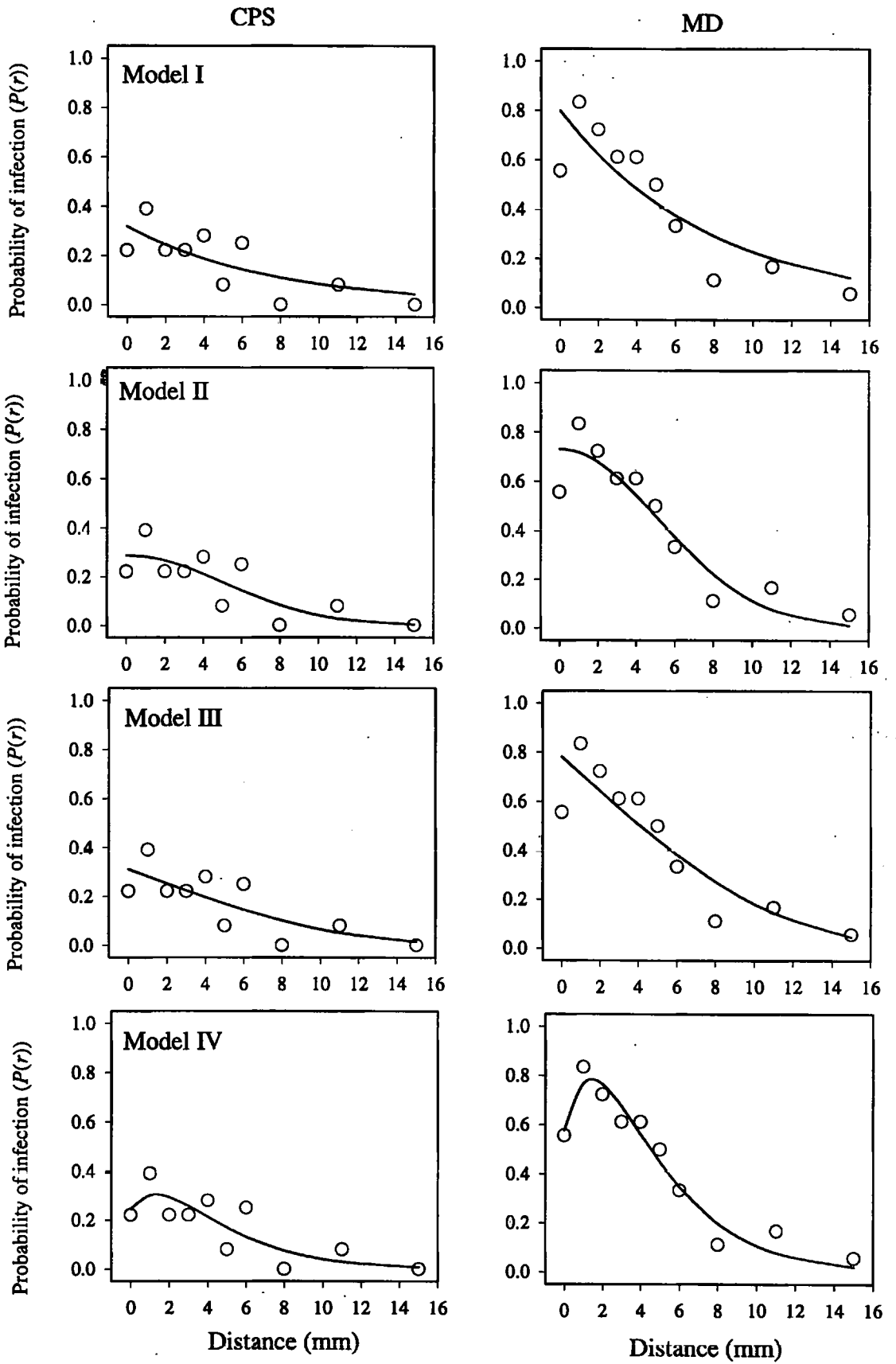


Fig. 3.7. Empirical observations (circles) obtained from placement experiments for the pathozone profile of the probability of infection (and disease) with distance of CPS and MD inoculum from radish after four days. Models I, II, III and IV are used to summarise the shape of the data.

CPS was less infective than MD inoculum. The probability of infection by a unit of CPS inoculum placed at the surface of the host was estimated, by the fitting of model II, to be 0.28 whilst that from MD inoculum was estimated to be 0.58 by model IV (Table 3.5).

The data produced when CPS inoculum was placed at increasing distances from the host were more variable than that produced using MD inoculum. This was reflected in the higher value for residual deviance and lower goodness of fit estimates.

Table 3.5: Summary of non-linear models used to describe the relationship between the probability of infection of the host (P) and distance (r) comparing chopped potato soil and mycelial disc inoculum of *R. solani*.

Inoculum type	Model	Parameters \pm s.e	Res d.f	Residual deviance	Goodness of fit
CPS	I. $P = \beta \cdot \exp(-\alpha r)$	$\beta=0.35 \pm 0.390$ $\alpha=0.17 \pm 0.269$	8	0.517	60.7
	II. $P = \beta \cdot \exp(-\alpha r^2)$	$\beta=0.28 \pm 0.252$ $\alpha=0.17 \pm 0.031$	8	0.452	65.6
	III. $P = \beta \cdot \exp(1 - \exp(\alpha r))$	$\beta=0.32 \pm 0.303$ $\alpha=0.10 \pm 0.104$	8	0.464	64.7
	IV. $P = (\theta_1 + \theta_2 r) \exp(-\theta_3 r)$	$\theta_1=0.72 \pm 0.120$ $\theta_2=0.56 \pm 1.71$ $\theta_3=0.68 \pm 0.32$	7	0.496	62.2
MD	I. $P = \beta \cdot \exp(-\alpha r)$	$\beta=0.863 \pm 0.57$ $\alpha=0.141 \pm 0.14$	8	0.296	76.2
	II. $P = \beta \cdot \exp(-\alpha r^2)$	$\beta=0.695 \pm 0.36$ $\alpha=0.013 \pm 0.01$	8	0.226	89.3
	III. $P = \beta \cdot \exp(1 - \exp(\alpha r))$	$\beta=0.790 \pm 0.44$ $\alpha=0.085 \pm 0.056$	8	0.237	87.8
	IV. $P = (\theta_1 + \theta_2 r) \exp(-\theta_3 r)$	$\theta_1=0.583 \pm 0.44$ $\theta_2=0.466 \pm 0.59$ $\theta_3=0.700 \pm 0.14$	7	0.191	93.1

These empirical profiles were compared with the predictions of the two forms of the model $P(r) = P_1 \cdot P_2(r) \cdot P_3(r)$ (Fig. 3.8). The model based on the furthest extent of mycelial growth failed to describe the profiles for either CPS or MD inoculum (Fig. 3.8a). The model based on hyphal density, however, matched the shape and magnitude of the data for both inoculum types when a threshold of four hyphae arriving at the host was required for successful contact leading to infection. The resultant model ($P = P_1 \cdot P_2 \cdot P_3$) is given by:

$$P = P_1 \cdot \left[1 - \sum_{N=0}^{N=4} \binom{N+k(r)-1}{k(r)-1} \left(\frac{\mu(r)}{\mu(r)+k(r)} \right)^N \left(1 + \frac{\mu(r)}{k(r)} \right)^{-k(r)} \right] \cdot \left[1 - \gamma \left(\frac{\kappa_r}{\kappa_r - r} \right)^{-\beta} \right], \quad (3.16)$$

where values for $\mu(r)$ and $k(r)$ are given in (3.10) and values for the parameters (κ , γ , κ_r and β for P_3) are given in (3.15). The model predicts an exponential decline in the shape of the profile for CPS inoculum and an initial rise then decay for MD inoculum. This is consistent with the shapes produced by the non-linear models II and IV respectively.

3.3.6 Stochastic realisations of model (3.16)

A stochastic version of the model for $P(r) = P_1 \cdot P_{2b} \cdot P_3$ was used to simulate experiments with different levels of replication (Fig 3.9). The corresponding variances for P and each of the three components, based on a binomial distribution of errors, are shown in Fig. 3.10. Whereas the trend in the pathozone profile of MD inoculum settles close to the deterministic prediction with 20 replicates, that for CPS required substantially more replication (Fig. 3.9). Furthermore, variability at distances close to the host are associated with changes in host susceptibility whilst variability beyond about 4 mm is caused by properties of the inoculum (germinability and colony growth).

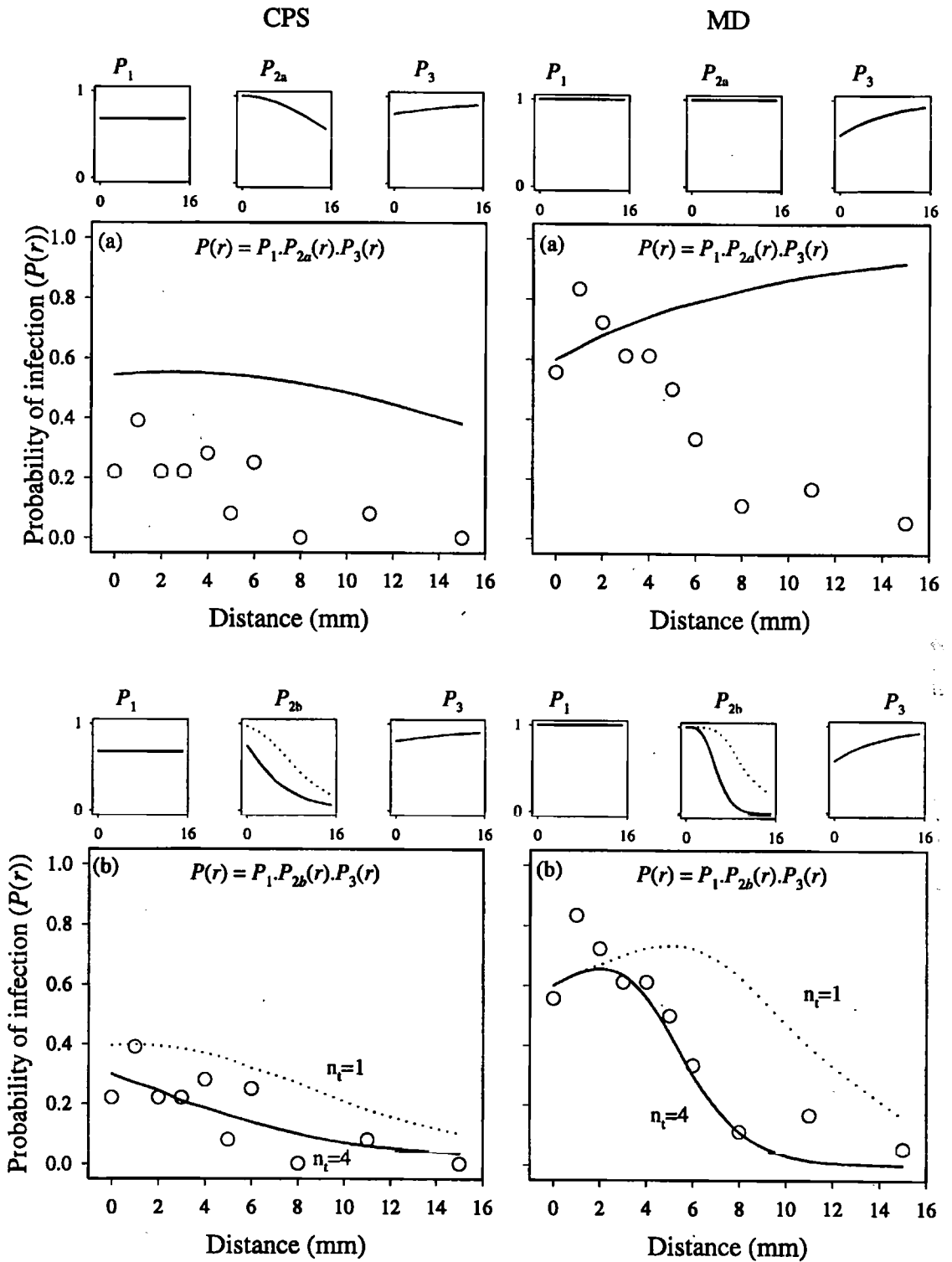


Fig. 3.8. Comparison of predicted profiles using $P(r) = P_1 \cdot P_2(r) \cdot P_3(r)$ for a) $P_{2a}(r)$ and b) $P_{2b}(r)$ with empirical observations for CPS and MD inoculum. The upper boxes show the shapes of the individual probability components on a common scale (0-1 and 0-16 days). The predicted curve for model P_{2b} is shown for two thresholds of hyphal density contacting the host, $n_1=1$ and $n_1=4$.

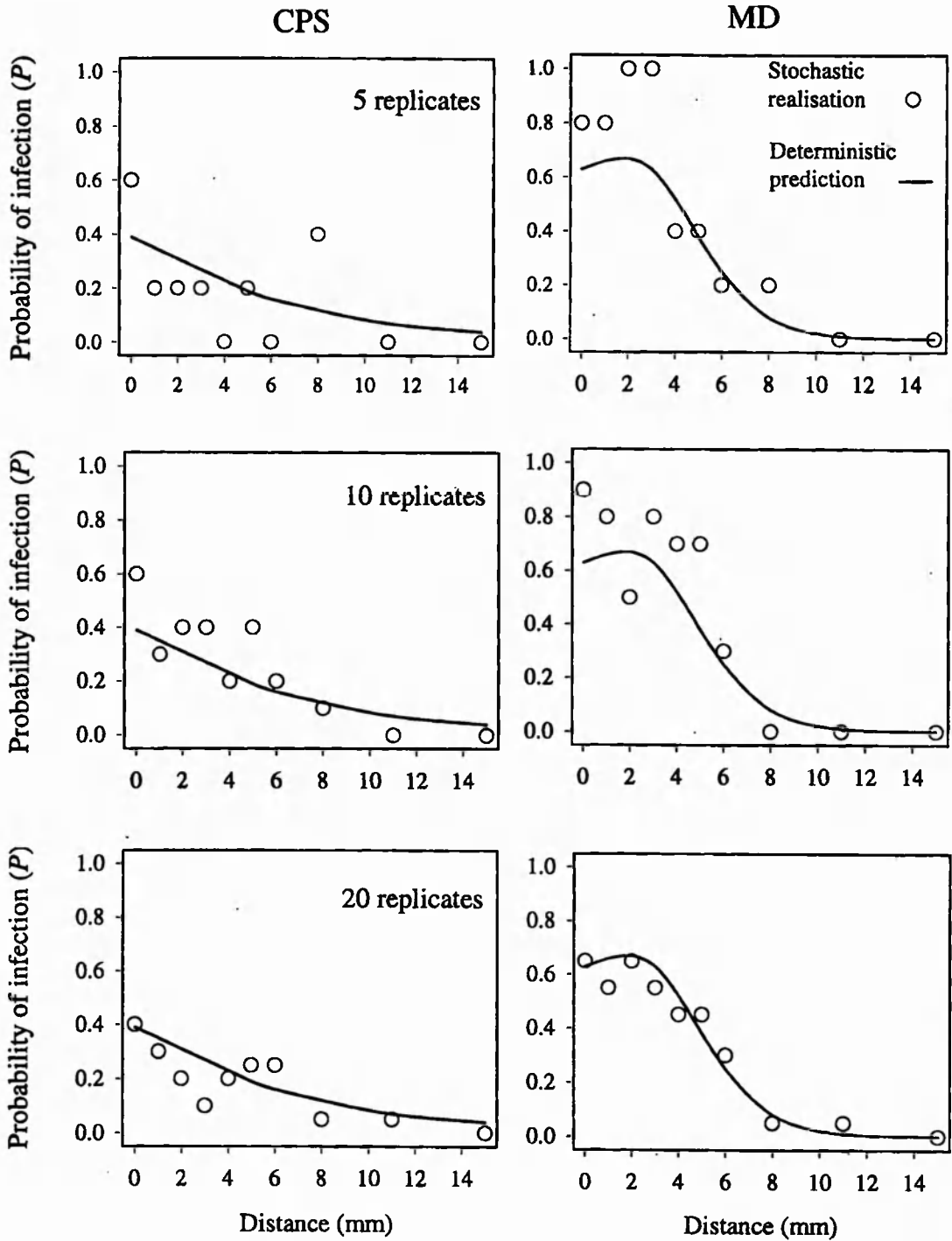


Fig. 3.9. Effects of replication on stochastic realisations (circles) of the pathozone profiles for the proportion of infected radish plants by CPS and MD inoculum. The lines represent deterministic predictions equivalent to large numbers of replicates.

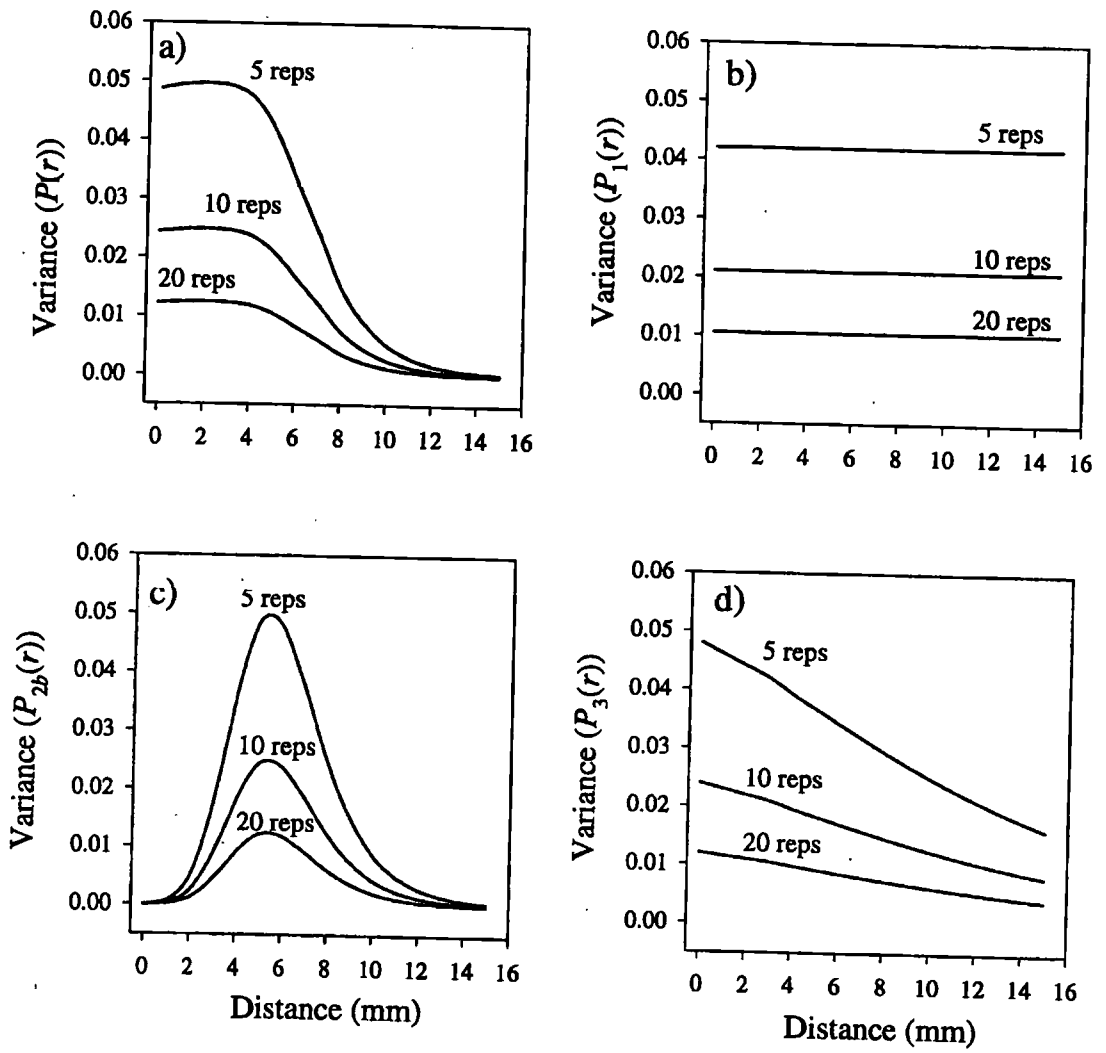


Fig. 3.10. Effect of changing replication on the variance of a) the probability of infection, and the three components: b) P_1 , c) P_{2b} and d) P_3 for MD inoculum.

3.3.7 Sensitivity of the model to changes in parameters values

The sensitivity of the model to changes in the parameters was examined with respect to the deterministic and stochastic output. There were 20 replicates in the stochastic simulations. Reduction in the germinability of inoculum reduces the maximum probability of infection (Fig. 3.11a). Reduction in the maximal hyphal density and of the dilution of hyphal density with distance both affect the magnitude and shape of the profile (Fig. 3.11b and Fig. 3.11c). In particular, increasing hyphal density moves the distance from which maximal infection occurs to the right in the profile. Clustering of inoculum reduces the probability of infection (Fig. 3.11d) but the rate of clustering with distance has relatively little effect (Fig. 3.11e). When the susceptibility of the host was allowed to decline rather than increase with distance, the maximum was eliminated (Fig. 3.12a and Fig. 3.12b)

3.4 Discussion

The objectives of this chapter were to develop and test a biological model (3.1) capable of predicting the shape and variability of the pathozone profile. Profiles generated from CPS and MD inoculum were compared and the latter was identified as being more suitable for investigation of factors affecting pathozone behaviour. The main reason for this was the consistently high degree of germinability (100%) (Table 3.1) which increases the sensitivity of the profile to treatment effects.

Much has been written on the description of colony architecture (Jennings and Rayner, 1984; Gow and Gadd, 1995) and the spatial dynamics of hyphal growth (Regalado *et al.*, 1996; Ritz and Crawford, 1990) whilst others have examined chemotactic responses usually restricted to zoosporic fungi (Deacon, 1996). Little attention has been given to the consequences of these changes on the ability of the pathogen to infect a host. Two forms of the model (3.1) were tested which differed with respect to hypotheses concerning colony

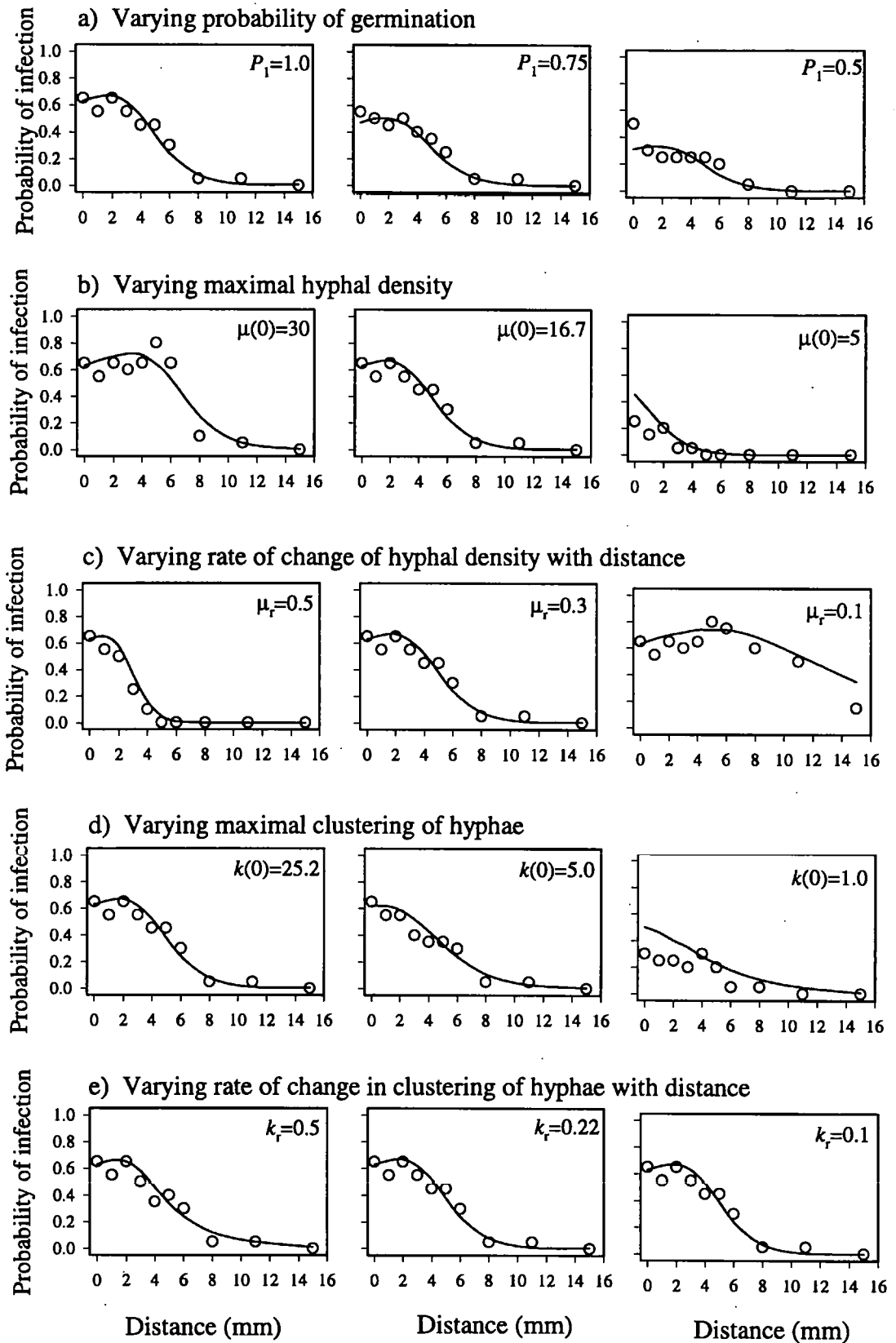


Fig. 3.11. Effect of changing a) P_1 b) mean hyphal density close to the host and c) the rate of change of hyphal density with distance; d) the degree of hyphal clustering close to the host and e) the rate of change of hyphal clustering with distance on stochastic (circles) and deterministic predictions (line) for pathozone profiles of MD inoculum. Stochastic predictions are based on 20 replications.

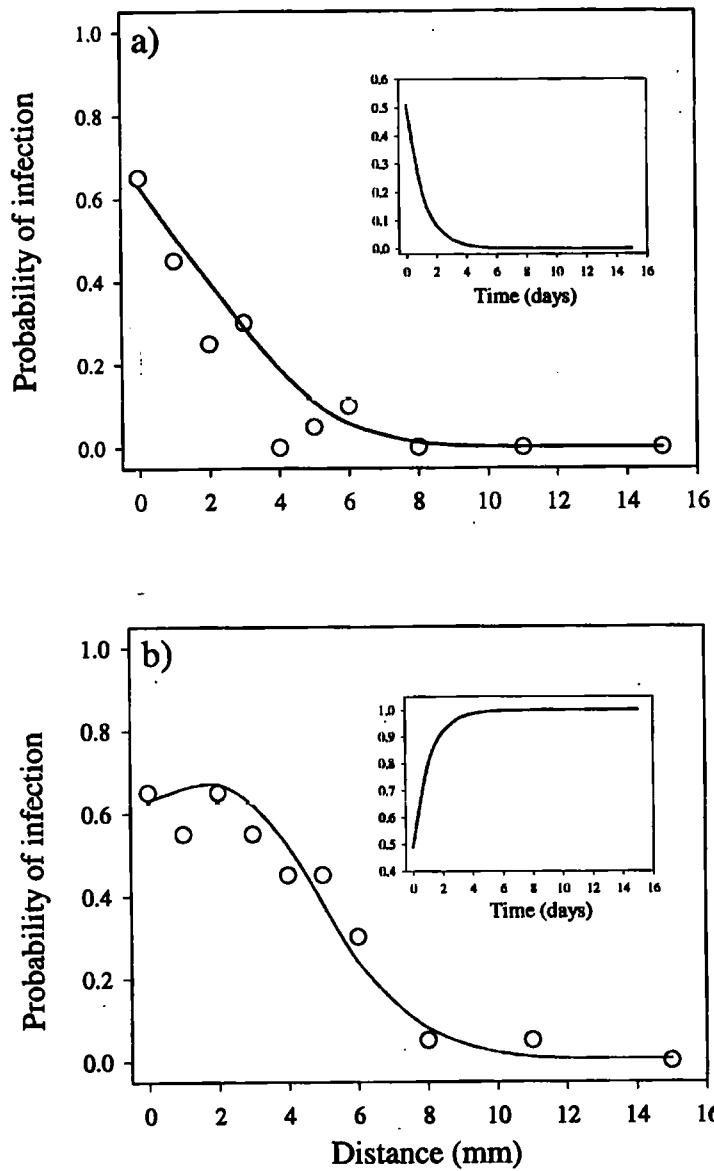


Fig. 3.12. Comparison of a) decreasing and b) increasing host susceptibility with distance on deterministic predictions of the pathozone profile for MD inoculum. Insets show the temporal changes of P_3 during the course of infection.

growth and the probability of a germinable inoculum unit making contact with the host. The first form, which assumed radially symmetric growth of high mycelial density, (P_{2a}) failed to predict either the shape or the magnitude of pathozone profiles produced by either type of inoculum (Fig. 3.8a).

The second form of the model involved contact of the host by a critical density of hyphae from a fungal colony that was spatially inhomogeneous in its local radial density of mycelium (P_{2b}). This was estimated from the density of hyphae in host-sized sampling units around concentric circles centred on the inoculum unit. The distributions differed for CPS which was more variable than MD but each could be approximated by a negative binomial distribution with parameters (μ and k) that decline with distance. Large values of k indicate randomness and small values clustering. So, as the density of hyphae decreases with distance from the source of inoculum, the hyphae tend to become more aggregated. The probability of contact, $P_{2b}(r)$, with the host depends on the mean hyphal density and the degree of clustering, both of which vary with distance (Fig. 3.4). This also yields sigmoidal curves for $P_{2b}(r)$ that vary with the threshold density of hyphae required for infection to be possible (Fig. 3.5). The magnitudes of the curves for $P_{2b}(r)$ are such that when $n_i = 4$, the shape and magnitude of experimentally derived profiles from both types of inoculum could be predicted (Fig. 3.8b). Thus, it is possible to interpret the pathozone behaviour of both types of inoculum in relation to the three stochastic components: germination, growth of the fungal colony to make contact with the host, and the susceptibility of the host following contact.

For the infection of *R. sativus* by *R. solani*, germination was assumed to be independent of distance (this is consistent with independent experimental evidence, not shown). The fall-off in the probability of infection with distance was determined instead, by the interactions between fungal growth and the changing susceptibility of the host. The

susceptibility of the host increased monotonically during the period of exposure to inoculum (Fig. 3.6b). This means that mycelium arriving after growth through the soil encounters a more susceptible host on contact than does mycelium from inoculum placed close to the host surface. Thus the probability of infection increases with distance between inoculum and host. Changes in host susceptibility with distance between inoculum and host are off-set by reduction in the density and nutritional status of hyphae that reach the host from more distant inoculum resulting in a decline in the probability of infection with distance. The outcome of this interaction predicts a pathozone profile which may decline exponentially or sigmoidally or give rise to a curve which rises close to the host surface and then decays asymptotically to zero. For MD inoculum, the shape of the profile reflects initially an increase in host susceptibility since the probability of contact remains constant at 1.0 for inoculum located near to the host (Fig 3.5). After this, the profile decays exponentially along with the probability of contact. The absence of a pronounced maximum in the profile for CPS is due to an immediate rapid decline in the probability of contact as the distance between inoculum and host is increased. The effects of changes in host susceptibility are diminished by a delay in germination of MD inoculum compared with CPS inoculum.

Increasing susceptibility of the host with time was counter intuitive, since most evidence suggests that the seedlings become more resistant to infection by damping-off fungi as the plant ages. Careful inspection during infection showed that the reduction in successful infection for inoculum located close to the host is most likely due to the disruption of fungal mycelium by the expansion and germination of the host. Thus, mycelium from CPS inoculum makes contact with the host when it is more fully established and more susceptible to infection than that from MD inoculum (It is noted that P_3 might be more accurately defined as the net infectivity of mycelium making contact with the surface of the

host). The flexibility of model (3.16) derived from the components of infection suggests that the summary models I, II and III used by Gilligan and Simons (1987) and the critical exponential model (model IV) are special cases of this more versatile model. The model (3.16) also explains the difference in the shape of the pathozone profiles produced by the two types of inoculum where CPS is best described by an exponential decay and MD by the critical exponential model (Table 3.6).

Although model (3.16) can predict the shape of the pathozone profile related to a specific type of inoculum and allows for flexibility in shape relating to the interaction of underlying biological mechanisms, it is over parameterised for the purpose of curve fitting and parameter estimation. It has ten parameters, one for P_1 , five for P_{2b} (n , and two each for μ and k with distance) and four for P_3 ($\kappa = 1$, γ , κ , β). However, even the most complicated profile which has four characteristic properties (an intercept at $r = 0$, a maximum, a point of inflection and a lower asymptote which is unequivocally zero) can be described by as few as three parameters. Thus, for the purpose of investigating the effect of, for example, the presence of a biological control agent on the behaviour of the pathozone, it is expected that selection from a suite of parsimonious, nonlinear models such as the summary models I to IV will be necessary.

Examination of stochastic predictions of the model (3.16) shows the importance of having adequate replication which is necessary, not only to define the profile, but in the analysis of such factors as biological control. Early work on pathozone profiles was based on as few as 10 replicates at each distance (Gilligan, 1980b; Gilligan and Simons, 1987) but these findings suggest a minimum of 15 and preferably 25 replicates even with an inoculum low in variability such as mycelial discs.

The stochastic simulations also identify a limitation of the model. An increase in the infectivity (or potential) of inoculum to cause disease was simulated by increasing the

maximal hyphal density (Fig. 3.11b). This is equivalent to simulation using a different type of inoculum and had the effect of moving the peak of the profile distally and of increasing the width of the pathozone. However, in this model, P_3 is independent of P_2 and estimates of the probability of infection when a more potent inoculum is placed at the surface of the host were constrained by P_3 . This is biologically unreasonable for inoculum producing colonies of different size. A more versatile reformulation of the model may be given by:

P_1 = Probability of germination,

P_2 = Probability of contact by n hyphae,

P_3 = Probability of disease caused by n hyphae.

The disruptive effects of the germinating host are now incorporated into P_2 as the infectivity of mycelium at the surface of the host. P_3 reflects the variability in susceptibility of the host population which can be summarised as a threshold for the number of hyphal contacts necessary to cause disease. The problems associated with quantification of the relevant variables to test this new model are substantial since the minimum requirement would involve measurement of the degree of mycelial contact in the presence of a germinating host plant. To this end, a novel immunological technique termed immunoblotting is being developed (see chapter 4). Furthermore infectivity may not be related simply to the number of hyphal contacts necessary to cause disease but to the nutritional and physiological status of these hyphae.

Chapter four

Fungal growth: A major determinant dictating the shape of the pathozone

4.1 Introduction

In the previous chapter (chapter 3), the mycelial colony was identified as the dominating factor determining the shape of the pathozone profile for *Rhizoctonia solani*.

A considerable amount of literature exists describing the growth of fungal colonies over agar media from a wide range of species (Trinci, 1971; 1979). At the periphery of the colony, exponential growth and regular branch formation result in a circular, two dimensional structure. The rate of colony expansion is a function of the average length of the terminal hyphae which contribute protoplasm to the apical extension of the leading edge of the colony and this constitutes the peripheral growth zone (Cooke and Rayner, 1984). Behind the peripheral growth zone is a region in which hyphae branch and anastomose thus establishing the colony structure as a network of mycelium. Consequently, the growth of hyphae in these two regions dictates the density and distribution of mycelium in the entire fungal colony. Characteristically, the mycelia of a fungal colony growing on a nutrient rich agar plate develop at a high density and are regularly distributed both within the peripheral growth zone (Prosser, 1995) and also, as fractal analysis has established, within the centre of the colony (Ritz and Crawford, 1990). Following an initial phase of exponential increase, the colony maintains a constant rate of radial growth.

For a colony in which the density of mycelium is high, contact with a host plant depends only on the size of the colony. In chapter 3, the probability of the pathogen locating a potential host was found to depend, not simply on the furthest extent of mycelial growth,

but on changes in the density and distribution of mycelium with distance from the inoculum unit. Thus, changes in the probability of contact by one or more hyphae (P_{2b}) with distance, r , was given as:

$$P_{2b}(r) = 1 - \left(1 + \frac{\mu(r)}{k(r)} \right)^{-k(r)}, \quad (4.1)$$

where the mean and clumping parameters, μ and k , depend on distance. By combining the probability of contact by a threshold density, in this case $n_t = 4$, of hyphae with the probability of germination (P_1) and the net infectivity of mycelium at the host surface (P_3), at each distance, it was possible to predict the shape of the pathozone profile. This prediction was made for a single time only, specifically, when the mycelial colony had achieved its maximum size and the nutrition of the inoculum unit had been exhausted. However, prediction and interpretation of pathozone dynamics will ultimately require quantification of fungal growth over time.

This chapter investigates the dynamics of fungal growth from single units of inoculum over a natural substrate. The effect of time and distance on the mean density, μ , and the degree of mycelial aggregation of hyphae, k , in relation to the rate of radial expansion is characterised using simple mathematical models for replicate colonies growing from particulate (mycelial disc) and infected plant inocula over the surface of sand. The two types of inoculum differ markedly in nutrient status and are responsible for the primary and secondary infection of soil-borne plant disease caused by *R. solani*. By characterising the behaviour of μ and k , a method for predicting changes in the probability of contacting a host, P_{2b} , with distance from the inoculum unit and over time is described.

Rhizoctonia solani spreads most rapidly over the surface of soil (Otten, pers. comm.). However, problems arise in quantification of mycelial growth *in situ* which has been

limited to only a few techniques. Detection using radio-isotopes has provided useful information regarding the spread of *Gaeumannomyces graminis* (Robinson and Lucas, 1962) and of translocation in the mycorrhizal colonisation of various root systems (Finlay and Read, 1985) but requires that the specimens be frozen to enhance resolution. Some root-rotting pathogens produce mycelial cords that can be visualised simply with the aid of low power microscopy or image analysis (Bolton *et al.*, 1991) but the hyphae of *R. solani* are comparatively small. More recently, the development of molecular tools showing high specificity towards a target organism offers the opportunity to overcome these limitations. For example, Rattray *et al.*, (1995) monitored the colonisation of wheat roots by a strain of the bacteria, *Enterobacter cloacae* transformed with the *Lux* operon. The development of DNA based assays such as the polymerase chain reaction (Keller *et al.*, 1995; Smalla *et al.*, 1993) offer potentially high sensitivity and specificity but such assays do not distinguish between living and dead biomass and are also destructive.

In this chapter a technique involving monoclonal antibody technology, termed immunoblotting, is used which, combined with computer-aided visualisation, has the potential to quantify the growth of mycelium non-destructively, *in situ* and over time. Immunoblotting was first described by Dewey *et al.* (1997). As the mycelium of *Rhizoctonia* spreads over the soil surface, extracellular water soluble antigens are rapidly immobilised on a polyvinylidene difluoride membrane (PVDF). The bound antigen is detected by incubating the membrane in a *R. solani*-specific immunoglobulin M (IgM) monoclonal antibody (MAb) supernatant followed by an anti-mouse IgM gold conjugate and subsequent silver enhancement. The antigen, a catechol oxidase, detected by the IgM MAb used in this study is produced only by the actively growing hyphal tips of the fungus. Hence, immunoblotting detects only mycelium in the two regions of active growth. The two regions are referred to collectively in this report as 'the active growth zone'.

The immunoblotting technique became available late in the course of the study and the results presented here are restricted to exploratory work to relate the behaviour of fungal pathogens in the rhizosphere to disease progress at the population level. The techniques and those described in subsequent chapters represent a framework for this 'scaling up' process.

4.2 Materials and methods

4.2.1 Microcosm experiment

Mycelial discs were produced according to the methods described in section 2.6.2. Infected plant inoculum was produced in seed trays (320 mm x 200 mm) filled with sand (grade 0.5-1.0 mm diameter and 10 % water by weight). Radish plants were sown at equal spacing at a rate of forty per tray. Alongside each seed and at a distance and depth of 2 mm a mycelial disc of *R solani* (Isolate R5) was positioned. The trays were covered with clear plastic lids and incubated at 23⁰C with a day length of 16 h. After seven days, infected plants were carefully extracted from the sand and placed into distilled water.

Mycelial colonies were grown in clear plastic trays measuring 60 x 120 x 15 mm (1 x w x d) and filled with sand (grade 0.5-1.0 mm diameter and 10 % water by weight). Into the centre of each tray was placed either a mycelial disc at a depth of 2 mm or an infected radish seedling. The infected seedling was transplanted into a hole and supported with a fine glass rod measuring 1.2 mm in diameter. Each tray was covered with a nylon mesh (45 µm aperture; Cadish, Finchley, London) and incubated at 23⁰C with a 16 h day. The experiment was fully randomised with five replicates per inoculum type.

To detect antigen-producing regions of the colony, PVDF transfer membranes (Millipore) were activated by immersion in methanol for 2 min, and rinsed three times in reverse osmosis (R.O.) H₂O. The activated membranes were applied to each tray for 16 h immediately or after 24, 48 or 72 h incubation. Membranes were removed, placed between

filter paper to dry and stored at 4 °C in the dark prior to development.

4.2.2 *Visualisation of the antigen*

Membranes were reactivated according to the procedure described above and placed in 100 ml of tris buffered saline (TBS) containing 0.3% (w/v) casein (TBS/c; 3g tris, 8 g NaCl, 0.2g KCl, R.O. H₂O, pH 8.3) for 1 h at room temperature. The membranes were then incubated in MAb supernatant diluted 1:1 (v/v) with 10% tissue culture medium for 24 h. The membranes were given three consecutive rinses in TBS/c and then incubated for a further 16 h in TBS/c containing a 1 in 250 dilution of goat anti-mouse IgM + IgG immuno-gold conjugate (British Biocell International, BLGAF20). Both primary antibody and secondary antibody gold conjugate incubation steps were performed at room temperature, with gentle agitation in sealed dishes. Finally, the membranes were given three consecutive rinses in TBS/c, a single rinse in R.O. H₂O and then developed in silver enhancer (British Biocell International, SEKB250) for a maximum of 45 min. Enhancement was stopped by rinsing the membranes in several changes of R.O. H₂O and the membranes were air dried at room temperature between layers of Whatman filter paper (grade N° 1).

4.2.3 *Quantification of mycelium*

Data were collected by direct scanning of immuno-blots using a high resolution optical scanner (Umax pro 1200 x 1200 dpi) from immunoblots detecting growth over the periods 0 to 16 h, 16 to 40 h, 40 to 64 h and 64 to 88 h (referred to hereafter as days 1, 2, 3 and 4 respectively). Some of the images were discoloured by residual antigenic material. These regions are not associated with the active growth zone of the colony and were removed using the software package 'Adobe photoshop' (California USA). Contiguous sampling units measuring 1.1 mm in diameter (0.95 mm²) and covering the entire circumference of

radii increasing at 1.1 mm intervals from the inoculum unit (Fig. 4.1) were individually scanned by computer for the area of the sample covered by mycelium (mycelial cover).

4.2.4 *The relationship between hyphal density and mycelial cover.*

Changes in mycelial cover, c , with distance and over time were converted to numbers of hyphae using a calibration curve relating the number of black pixels per sample unit to hyphal density (number of hyphae per sample unit) (Fig 4.2). The calibration curve was generated by randomly selecting five sites from an immunoblot, each site containing 1, 3, 5, 7 or 9 hyphae and assessing each site for mycelial cover (area covered by black pixels after scanning).

By careful alignment of the immunoblots, each sample site was maintained in the same position for each time of observation. Therefore, the number of actively growing hyphae in each sample site could be counted for each time of observation. The sample size was increased to twice the initial size representing a host 2.2 mm in diameter by adding the numbers of hyphae detected in neighbouring sample units. By accumulating the results over time, changes in the total number of hyphae entering each sample site was quantified over time.

4.2.5 *Estimation of the probability of contact, P_{2b} .*

Frequency histograms of the number of hyphae per sampling unit were fitted with the negative binomial function. Changes in the parameters of μ and k over distance, r , and time, t , were both described by exponential functions where:

$$\mu(r) = \mu_1(t) \cdot \exp(-\mu_2(t) \cdot r^{\mu_3(t)}) \quad (4.2)$$

$$k(r) = (k_1(t) \cdot \exp(-k_2(t) \cdot r)) \quad (4.3)$$

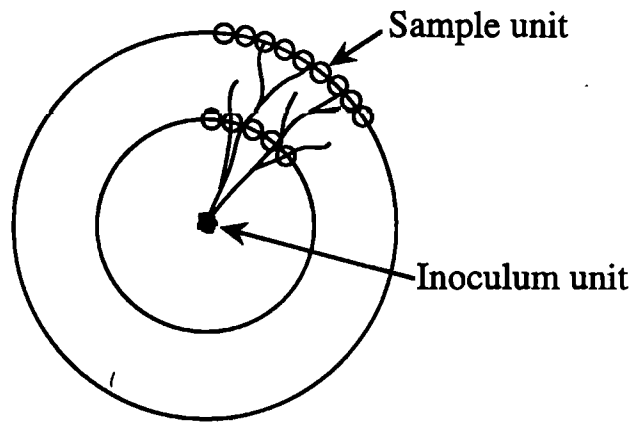


Fig 4.1: Sampling strategy used to detect changes in the density and distribution of mycelium at different distances from a unit of inoculum. Sample size is 1.1 mm diameter.

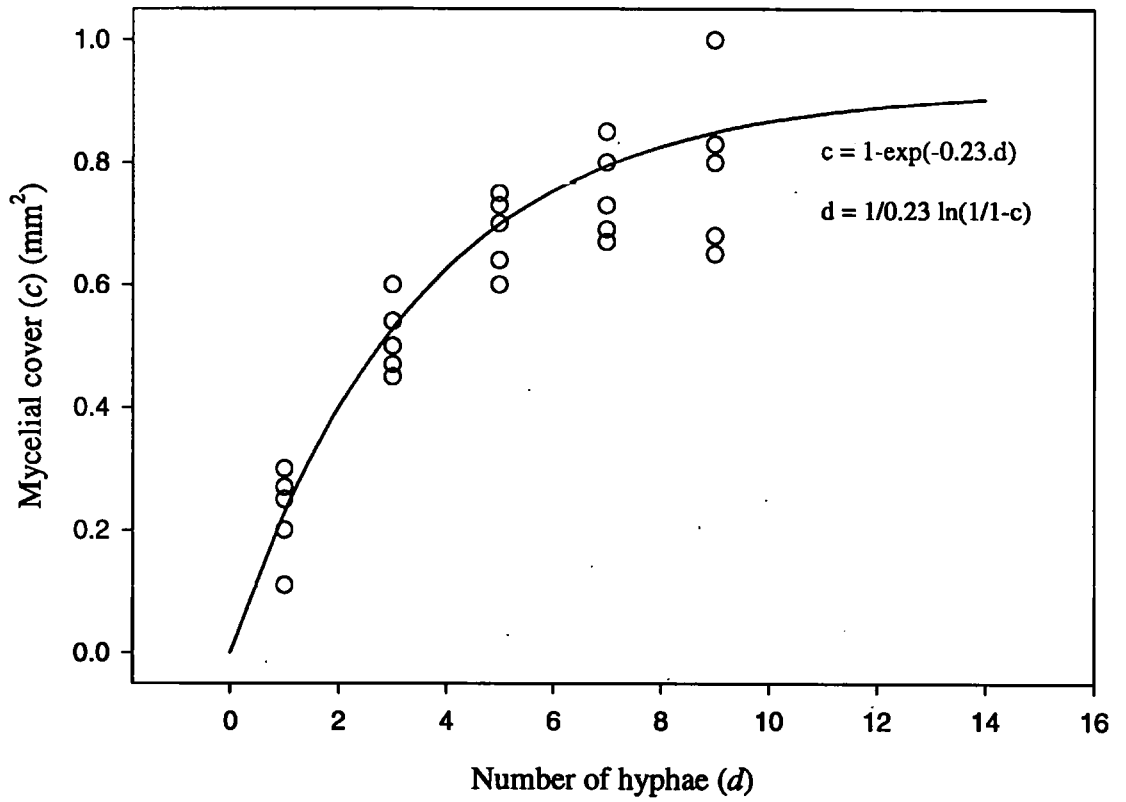


Fig. 4.2: Calibration curve relating the number of hyphae present within a sampling unit 1.1 mm in diameter (d), with the area of the sample covered by mycelium (c).

Both equations describe an exponential decay to zero where, for equation (4.2), the parameter μ_3 was included to provide an accurate description of the lower levels of mycelial density detected furthest from the inoculum unit.

Changes in the parameters $\mu_1(t)$, $\mu_2(t)$, $\mu_3(t)$, $k_1(t)$ and $k_2(t)$ were described by either an exponential decay or a monomolecular increase over time. This provided two surfaces, one for $\mu(r,t)$ and one for $k(r,t)$, for each type of inoculum. The model for P_{2b} (4.1) based on $n_i = 4$ is then;

$$P_{2b} = \left[1 - \sum_{N=0}^{N=4} \binom{N+k(r,t)-1}{k(r,t)-1} \left(\frac{\mu(r,t)}{\mu(r,t)+k(r,t)} \right)^N \left(1 + \frac{\mu(r,t)}{k(r,t)} \right)^{-k(r,t)} \right], \quad (4.4)$$

where $\mu(r,t)$ and $k(r,t)$ are given by the surfaces in 4.2 and 4.3.

4.2.6 The furthest extent of radial growth

Changes in the extent of radial growth were measured as the furthest detectable hypha at each time of observation.

4.3 Results

4.3.1 The immunoblots

Immunoblotting detected a zone of active mycelium (the active growth zone) which grew outwards from each inoculum unit over time (Figs. 4.3 and 4.4). The active growth zone grew further and faster from infected plant inoculum. After four days growth from mycelial discs, the colonies had a diameter of approximately 20 mm whilst, from an infected plant the colony had grown to over 40 mm in diameter.

The magnified regions of the immunoblots (Fig. 4.4) indicate the regions removed during the cleaning process. This assists with quantification of the wave of mycelium that

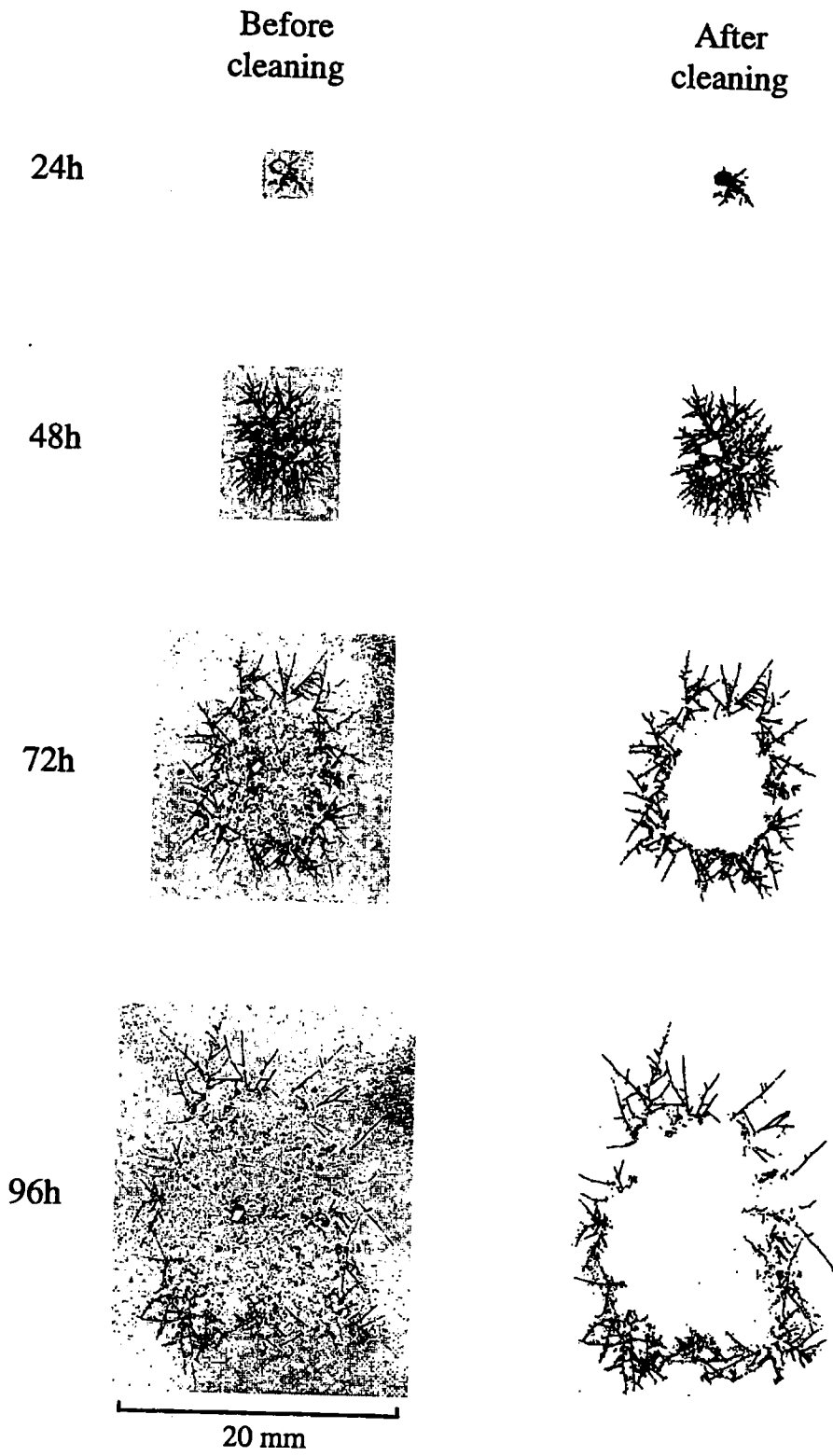


Fig 4.3: Scanned immunoblot images from a single colony of *R. solani* growing from mycelial disc inoculum before and after cleaning.

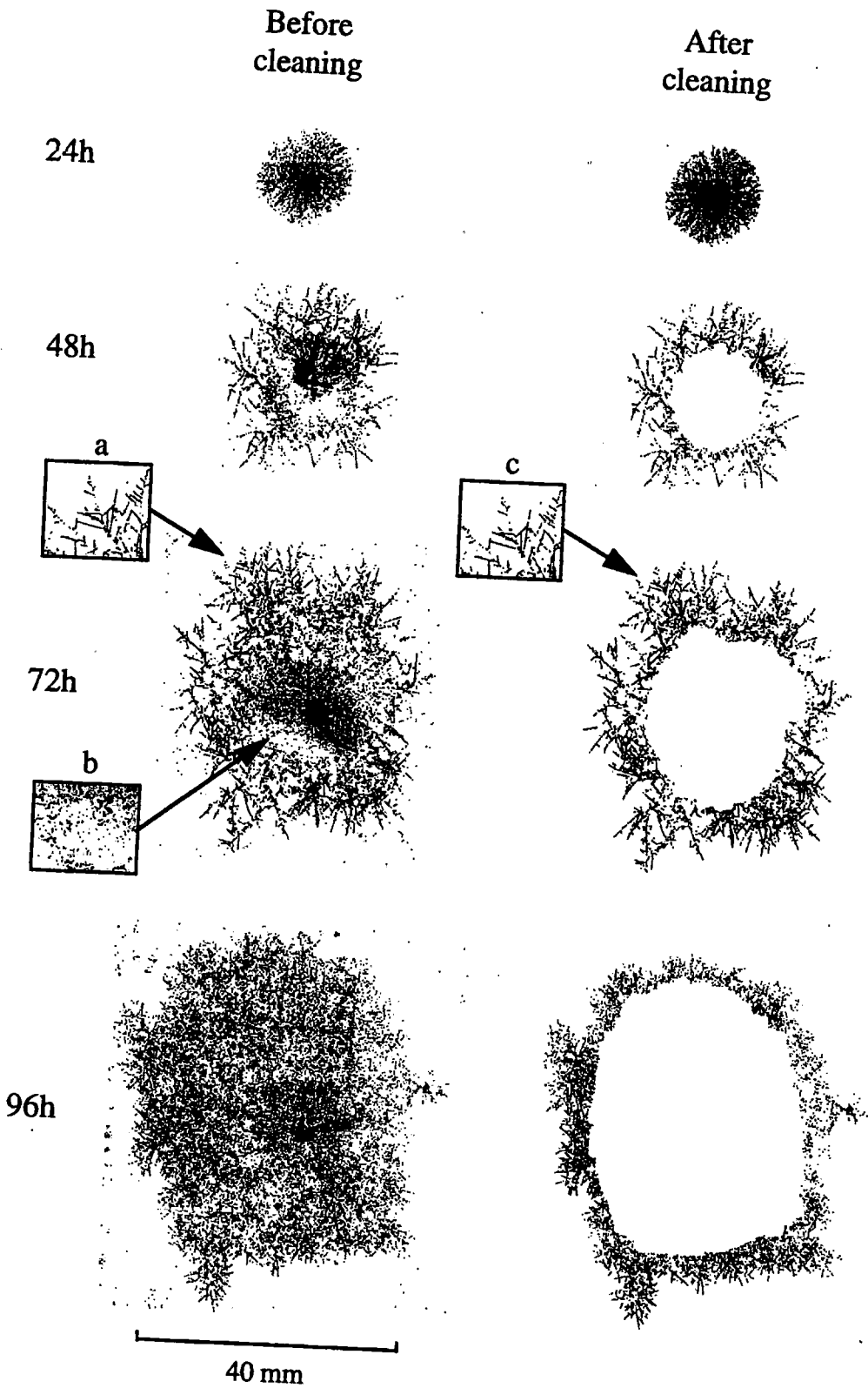


Fig 4.4: Scanned immunoblot images from a single colony of *R. solani* growing from infected plant inoculum before and after cleaning. Magnified sectors show a) intact mycelium detected by immunoblotting, b) antigenic material removed prior to analysis and c) intact mycelium after (and unaffected by) the cleaning process.

is detected by immunoblotting to which continuous models, based on reaction-diffusion equations and not considered further here, may be fitted.

4.3.2 *The relationship between mycelial cover and hyphal density*

The mycelial cover, c , detected in each 1.1 mm sampling unit was converted to numbers of hyphae (hyphal density), d , using a calibration curve (Fig. 4.2). The relationship was described by the monomolecular function:

$$c = 1 - \exp(-0.23.d) , \quad (4.5)$$

which, rearranging in terms for d gives:

$$d = \frac{1}{0.23} \ln\left(\frac{1}{1-c}\right) . \quad (4.6)$$

4.3.3 *Changes in μ and k over distance and time.*

Frequency distributions describing hyphal density, d , at each distance were fitted with the negative binomial function to provide estimates for the mean, μ , and the clumping parameter, k over distance for mycelial disc and infected plant inoculum at each time. Surfaces for $\mu(r,t)$ and $k(r,t)$ were given by:

$$\mu(r) = \mu_1(t) \cdot \exp(-\mu_2(t) \cdot r^{\mu_3(t)}) \quad (4.7)$$

and

$$k(r) = (k_1(t) \cdot \exp(-k_2(t) \cdot r)) , \quad (4.8)$$

where, for colonies growing from MD inoculum,

$$\mu_1(t) = 22.3(1 - \exp(-5.60(t-0.83))) , \quad (4.9a)$$

$$\mu_2(t) = 1.61 \exp(-76.7 t) , \quad (4.9b)$$

$$\mu_3(t) = 0.95 \exp(-0.18 t) , \quad (4.9c)$$

$$k_1(t) = 3.56 (1 - \exp(-1.62 t)) , \quad (4.10a)$$

$$k_2(t) = 1.15 \exp(-0.29 t) , \quad (4.10b)$$

and from infected plant inoculum

$$\mu_1(t) = 24.1 (1 - \exp(-12.8(t-0.66))) , \quad (4.11a)$$

$$\mu_2(t) = 1.94 (1 - \exp(-0.024 t)) , \quad (4.11b)$$

$$\mu_3(t) = 2.3 \exp(-0.25 t) , \quad (4.11c)$$

$$k_1(t) = 33.9 \exp(-12.4 t) , \quad (4.12a)$$

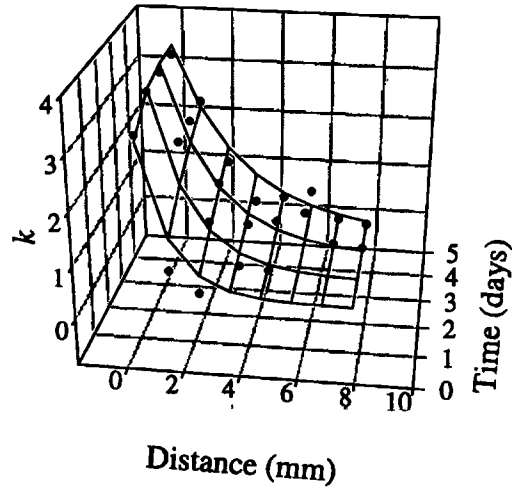
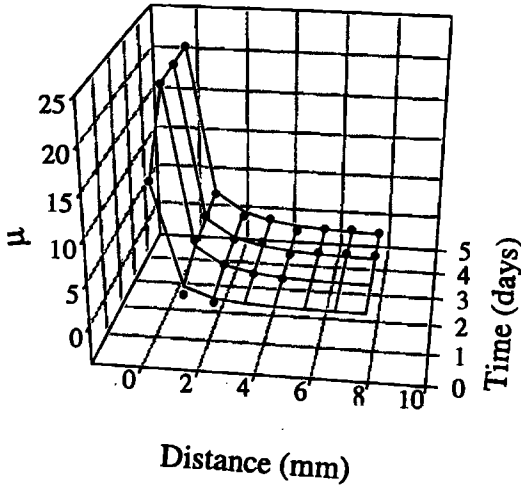
$$k_2(t) = 0.30 \exp(-0.0027 t) . \quad (4.12b)$$

The surfaces for $\mu(r,t)$ and $k(r,t)$ for both types of inoculum are shown in Figure 4.5. They exhibit some general properties. The mean mycelial density, μ , decayed rapidly with distance to a low level. However, this low density of mycelium was maintained for some considerable distance and time. Similarly, there was a concomitant reduction in the clumping parameter, k (ie. increase in clumping), with distance.

Both the mean density of mycelium, μ , and the degree of clumping k increased with time for colonies growing from mycelial disc inoculum but changed little for colonies growing from an infected plant.

The rise and fall of μ and k with distance for infected plant inoculum detected after 3 and 4 days growth is due to variability in the growth of replicate colonies.

a) Mycelial disc inoculum



b) Infected plant inoculum

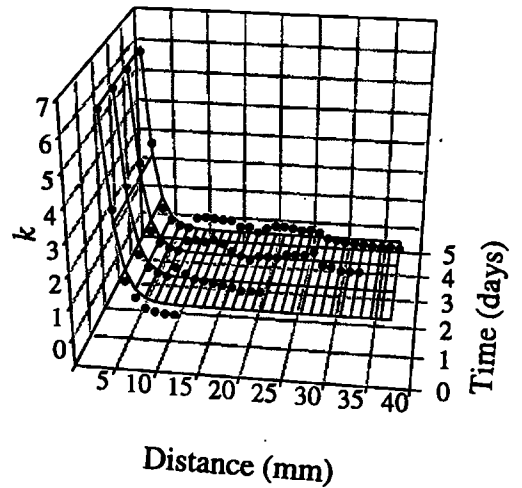
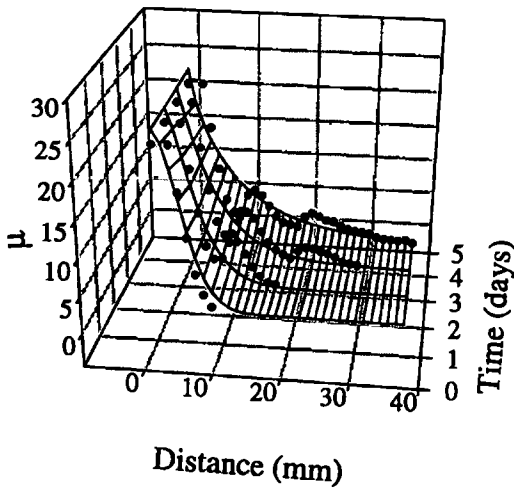


Fig. 4.5: Surfaces describing changes in the mean density (μ) and clumping (k) of mycelium over distance and time from a) mycelial disc and b) infected plant inoculum. Data (solid points) was derived by fitting the negative binomial distribution to numbers of hyphae present in 2.2 mm samples at each distance from the inoculum unit.

4.3.4 Predictions for the probability of contact, P_{2b} .

The surfaces describing the behaviour of μ and k were used in model (4.4) to predict changes in the probability of contact, P_{2b} , by four or more hyphae over distance and time for a host measuring 2.2 mm in diameter (Fig. 4.6). The probability of contact decayed exponentially with distance at all times for mycelial disc inoculum (Fig. 4.6a). The probability of contact by mycelium growing from an infected plant decayed sigmoidally with distance at all times (Fig. 4.6b). The decay in the probability of contact with distance results from the combined influence of μ and k . The maximal probability of contact for a host occurring near the centre of the colony reflects the combination of high and less aggregated (high k) mycelial density. Since both μ and k decay with distance, the probability of contact is reduced. However, even the low densities of mycelium, which occur at some distance from the centre of the colony, make a significant contribution to the probability of contact.

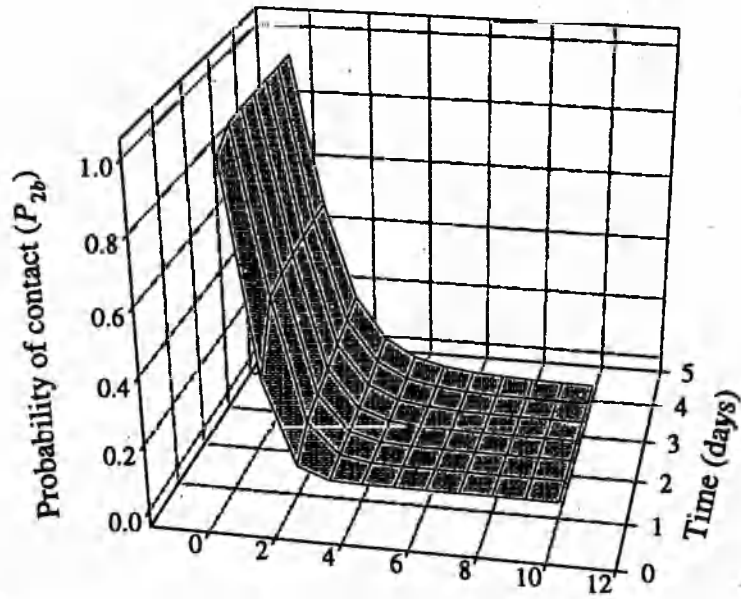
4.3.5 The furthest extent of radial growth

Radial growth of the fungal colony was linear over time for both mycelial disc and infected plant inoculum (Fig. 4.7). Colonies from infected plant inoculum grew at about twice the rate of those from mycelial discs.

4.4 Discussion

Immunoblotting, combined with image analysis, permits the non-destructive, *in situ*, visualisation and quantification of colony growth. Using a simple calibration, it was possible to convert pixel images to mycelial densities and assess the characteristic behaviour of hyphal density by fitting the negative binomial distribution in which μ and k vary with distance and time. This enables quantification of mycelial behaviour in nutrient scarce environments and computation of the probability of contact by certain threshold densities

a) Mycelial disc inoculum



b) Infected plant inoculum

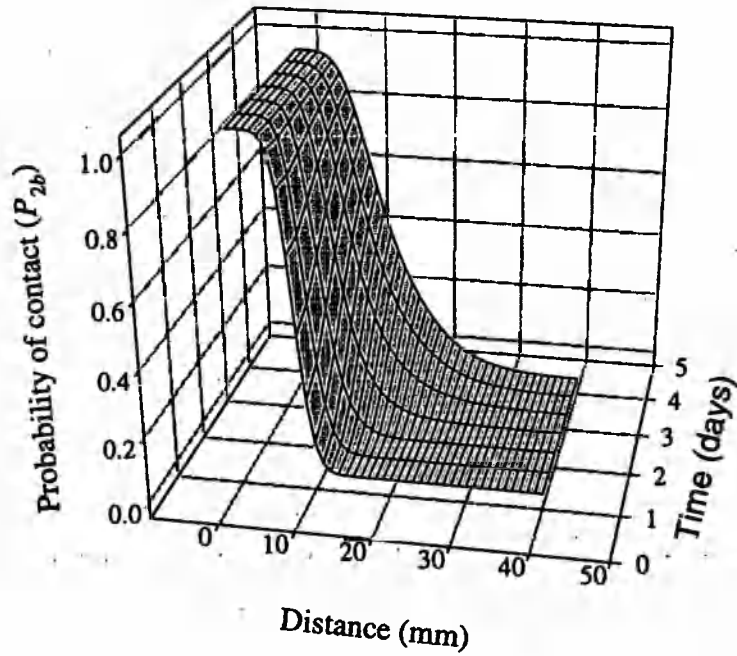


Fig. 4.6: Predicted changes in the probability of contact with distance and over time by four or more hyphae growing from a) mycelial disc or b) infected plant inoculum

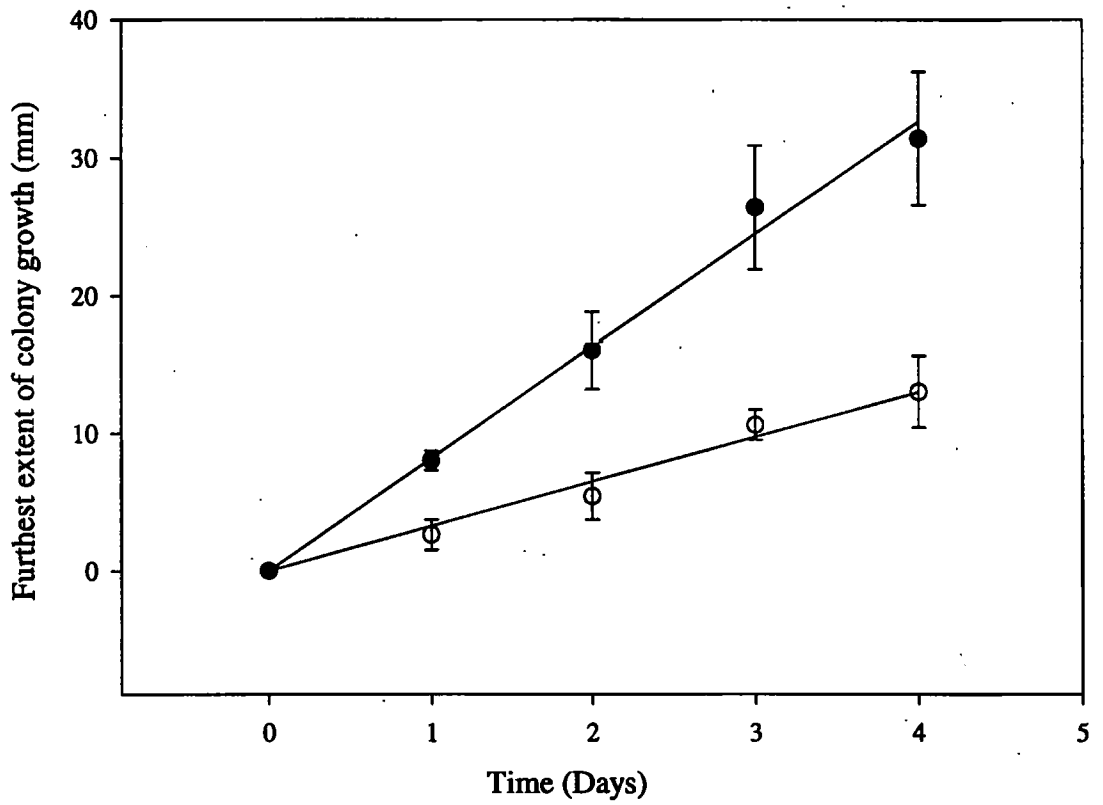


Fig. 4.7: Change in the furthest extent of detectable mycelium from mycelial disc (open circles) and infected plant (closed circles) inoculum.

of hyphae. The techniques were used to compare fungal growth from mycelial disc inoculum (used in chapter 3) with infected plant inoculum and to infer differences relating to the probability of contact, P_{2b} .

Growth of soil-borne fungi *in situ* from a single unit of inoculum has received little attention, though notable exceptions occur (eg. Boddy, 1993; Bolton and Boddy, 1993). The results of this experiment suggest that the fundamental, underlying mechanisms which dictate colony growth and architecture when external nutrients are abundant and homogeneously distributed (Cooke and Rayner, 1984), apply equally well to situations in which nutrients from a point source of inoculum become growth limiting. Thus, irrespective of the type of inoculum, a wave of actively growing mycelium, equivalent to the peripheral growth zone combined with a zone of branching immediately behind, as described by Cooke and Rayner (1984), was detected moving outwards from the centre of the colony over time (Figs. 4.3 and 4.4).

The early growth of fungal colonies on nutrient-rich, homogeneous agar media produces mycelial structures which typically exhibit a constant radial growth rate and maintain a high density of regularly distributed mycelium (Cooke and Rayner, 1984; Trinci *et al.*, 1979; Trinci, 1984; Ritz and Crawford, 1990). These broad characteristics were compared with growth from single units of mycelial disc or infected plant inoculum over the surface of sand. The density of mycelium did not remain constant, but declined rapidly with distance (Fig. 4.5). The reduction in mycelial density with distance was associated with a concomitant increase in aggregation (reduction in k). However, as the mycelial density increased in any given location over time, so the mycelium became less clumped.

Whilst the density and distribution of hyphae were subject to considerable variation over distance and time, the rate of radial expansion was constant during the first four days of growth (Fig. 4.7). It appears that when *R. solani* grows from a unit of inoculum into a

nutritionally poor environment it conserves a linear growth rate at the expense of a decline in mycelial density. This growth pattern is consistent with the observation that, as nutrients become limiting, some fungi are capable of selectively withdrawing cytoplasm from selected hyphae to maintain the growth of others (Dickinson and Bottomly, 1980; Cooke and Rayner, 1984; Paustian and Schnurer, 1987a and 1987b). It also accounts for the particularly long tails to the curves describing changes in mycelial density with distance after several days growth. The growth strategies of several soil-borne fungi have been examined. Rayner and Coates (1987) refer to a dimorphic growth capability in *R. solani* whereby the pathogen switches from slow-dense to fast-diffuse growth depending on the availability of nutrient resource. Thus the organism shifts between an exploitative mode (*sensu* Ritz and Crawford, 1990) in the presence of a suitable substrate when the internode length is low and branch length high, to an explorative mode with a longer internode length and acute branch angle as nutrients are exhausted. This nutritionally driven ability to change modes (or 'gears', *sensu* Rayner and Coates, 1987) also allows the pathogen to increase inoculum potential in the presence of a suitable host prior to infection.

The significance of this dimorphic growth strategy was translated into the probability of locating a potential host using model (4.4) in which changes in the mean density of mycelium and the aggregation of mycelium over distance and time were used to predict the changes in the probability of contact (P_{2b}) by four or more hyphae. The profile for P_{2b} is dominated by the transition of high probabilities of contact near to the centre of the colony resulting from high densities of mycelium and a less clumped distribution to low probabilities that occur at larger distances. Whilst mycelium located further from the centre of the colony has a low probability of locating a single host, for a population of host plants, the probability of a host occurring increases with distance. Consequently, mycelium that occurs further from the centre of the colony can make an important contribution to the

progress of disease.

Although there was no qualitative difference in the shapes of surfaces describing the dynamics of μ and k , the higher mycelial densities close to the centre of the colonies from infected plant inoculum transformed the curve for the probability of contact from exponential to sigmoidal with distance. Furthermore, the higher hyphal densities and more rapid growth of colonies from an infected plant would be expected to enhance the probability of contact with the population of host plants that occur further from the centre of the colony.

This study quantifies the dynamics of fungal growth *in situ* into a nutritionally poor environment and provides a significant contribution to the scaling-up process, linking components of infection to pathozone dynamics of individual plants. Although, these results suggest that an infected plant would be considerably more infective than a mycelial disc, it is not possible to insert the results for P_{2b} into the probability model (model 3.1) in order to predict the evolution of their associated pathozone profiles. This is because the probability that the mycelium is infective once it reaches the surface of the host, P_3 , is not independent of the density of mycelium but most likely increases as the density of mycelium contacting the host increases. Consequently, P_3 should be defined for each inoculum type separately or the model adjusted (see section 3.4). Furthermore, the model does not allow for the period between contact and the development of disease (damping off) which may also depend on the rate at which mycelium makes contact with the host and thus on inoculum type.

Chapter five

Biological control of pathozone dynamics and disease progress.

5.1 Introduction

The spread of damping-off disease by *R. solani* is via the growth of mycelium. Mycelium spreading from an infected radish plant grows faster, further and more densely than that from particulate inoculum (Chapter four). Fungal growth outwards from a source of inoculum is a major determinant of the shape of the pathozone (Chapter three). Consequently, the dynamics of the pathozone will behave differently for the two types of inoculum.

It has long been recognised that successful control of disease may be effected by changing the behaviour of fungal plant pathogens in the rhizosphere or pathozone. Yet little information is available to describe this behaviour or the quantitative effects of these responses on the dynamics of epidemic development.

In this chapter, the relationship between pathozone behaviour and the dynamics of damping-off disease caused by *R. solani* on populations of radish seedlings is examined. This represents a model system in which the contribution of primary and secondary infection to the spread of disease can be easily controlled by manipulation of host density. Section 5.2 identifies, compares and describes, using simple non-linear summary models, the generic shapes of pathozone profiles associated with mycelial disc and infected plant inoculum as they evolve over time. This is necessary because the probability model (3.16), which includes individual components of pathozone infection, is over-parameterised for the purpose of curve fitting.

Thus, the probability of infection, $P(r,t)$, depends on distance (r) and time (t):

$$P(r,t) = f (r \mid \theta(t)) ,$$

where $\theta(t)$ are the time varying parameters. The model $P(r,t)$ is obtained from placement experiments (Henis and Ben-Yephet, 1970; Gilligan, 1980b), introduced in chapter 2 in which replicates comprise single plants challenged with propagules of inoculum placed at known distances from hypocotyls of radish. For accurate model selection and to identify the distances at which to place inoculum, large numbers of replicates and additional distances were included. This information was used to optimise the performance of further placement experiments.

In sections 5.3 and 5.4, $P(r,t)$ is used to predict disease progress curves in the presence or absence of the biological control agent, *Trichoderma viride* in a population of radish seedlings exposed to randomly distributed inoculum of *R. solani*. This enables scaling up from individual to population behaviour. Two types of epidemic are examined; one in which disease progress is caused by primary infection alone (5.3) and a more complicated situation in which disease is caused by a combination of primary and secondary infection (5.4).

5.2 Pathozone dynamics of mycelial disc and infected plant inoculum

5.2.1 Introduction

In chapter three, a simple probability model (3.16), incorporating terms for inoculum germinability, colony growth and infectivity of mycelium at the host surface, was presented to explain the shape of pathozone profiles generated by different types of particulate inoculum. The number of parameters in model (3.16) is expected to increase further still when the model is expanded to account for the evolution of the pathozone over time. As

an alternative, a suite of non-linear models varying in shape, with fewer parameters but retaining some degree of biological integrity is presented here.

Investigation of mycelial disc inoculum (chapter three) suggested that the critical exponential function may provide an adequate description of its pathozone profile. But whether or not the shape of this profile is maintained as the pathozone evolves over time is not yet known, nor is the characteristic shape of the pathozone associated with infected plant inoculum. The objectives of this investigation are therefore, to identify, compare and describe the shapes of the pathozone profiles generated by the two types of inoculum as they evolve over time using simple non-linear models which summarise the essential features of the profiles.

5.2.2 Methods

Inoculum

Mycelial disc inoculum (MD) and infected plant (IP) inoculum were produced according to the methods described in sections 2.6.2 and 4.2.1 respectively.

Placement experiment

A placement experiment was performed to generate pathozone profiles over time for each type of inoculum. Soil packs were used in place of repli-plates (section 2.6.2) because of the larger pathozone width anticipated for infected plant inoculum. Soil packs were prepared by adding 60 g of moist sand (0.5-1.0 mm in diameter and 10% water by weight) to 100 mm lengths of clear plastic tubing (Layflat, Isle of Wight) stapled at one end. After sealing the open end with three staples, the packs were compressed by hand to increase rigidity. Single units of inoculum were placed at either 0, 1, 2, 5, 10, 15 or 20 mm (mycelial disc inoculum) or 0, 10, 20, 30, 40, 50 or 60 mm (infected plant inoculum) from the host

with 25 replicates per distance. Placement of both host seed and inoculum was achieved via small incisions made in the plastic using a scalpel. For treatments involving infected plant inoculum, the diseased cotyledon was allowed to protrude from the soil pack.

The packs were arranged into a fully randomised design within a growth chamber and incubated at 23 °C with a 16 h day for 9 d. The number of plants diseased (damped-off) was assessed after emergence from day 5 onwards.

Modelling changes in pathozone profile over time

The pathozone profiles for the probability of infection over time from mycelial disc and infected plant inoculum were empirically described by the general model:

$$P(r,t) = f (r \mid \theta(t)) , \quad (5.1)$$

where $\theta(t)$ are the time varying parameters. Data generated by each type of inoculum were assessed visually and described by an appropriate non-linear summary model selected on the basis of the shape of the pathozone profiles. The following models were considered:

$$\text{Model I. } P = \beta \cdot \exp(-\alpha r)$$

$$\text{Model II. } P = \beta \cdot \exp(-\alpha r^2)$$

$$\text{Model III. } P = \beta \cdot \exp(1 - \exp(\alpha r))$$

$$\text{Model IV. } P = (\theta_1 + \theta_2 r) \exp(-\theta_3 r)$$

$$\text{Model V. } P = \beta / (1 + \exp(-\phi_1 (r - \phi_2))) .$$

The properties of models were described in 2.6.2 and 3.2.2 and their characteristic shapes, for the appropriate parameter space, are plotted in Figure 5.1.

The selected models were fitted separately to each of the pathozone profiles. Fitting was

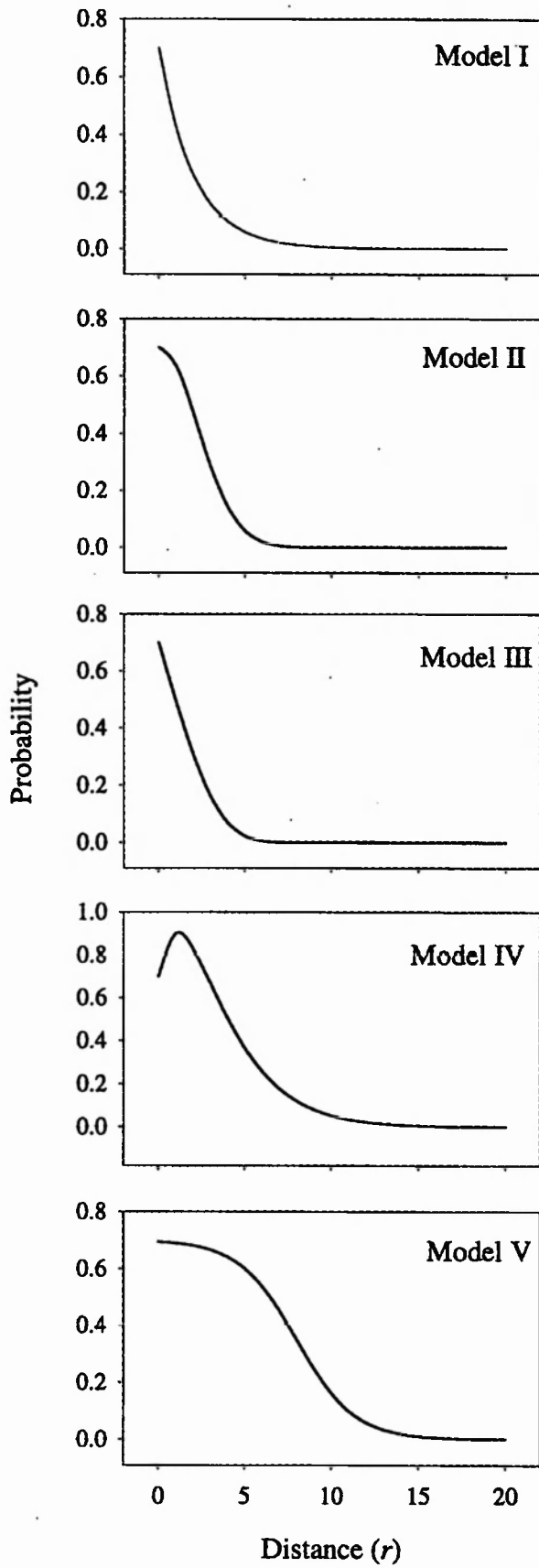


Fig. 5.1: Examples of the shapes of curves produced by the suite of models used to describe the pathozone profile, $P(r)$

done using GENSTAT (Anon, 1993) under an assumption of binomial errors because of the quantal nature of the response variate. This gave separate estimates of $P(r)$ for ten profiles corresponding to five sampling times (days 5...9) for each type of inoculum. The models (one for each type of inoculum) were then tested for common parameters over the five times of observation using the methods of Gilligan (1990b). This involved the computation of F values using the formula:

$$F = \frac{RD_1 - RD_2}{d.f_1 - d.f_2} / \frac{RD_{full}}{d.f_{full}}$$

where RD_1 and RD_2 are the residual deviances of the two models being compared and RD_{full} is the residual deviance of the full model in which all parameters are released to vary with time. The first model has fewer parameters varying with time than the second and the relevant degrees of freedom of each model are given by $d.f_1$, $d.f_2$ and $d.f_{full}$.

Trends of parameter estimates varying significantly over time were described by simple, non-linear sub-models. This produced a non-linear response surface that describes the change in the pathozone profiles over time.

Computation of the extent of pathozone influence.

In this experiment, the extent of pathozone influence, R , was defined as the furthest distance beyond which the probability of infection is less than 5%: R is solved iteratively for a given time (t) by setting $P(R,t) = 0.05$ in equation (5.1), given by:

$$P(R,t) = f(r | \theta(t)) - 0.05 \quad (5.2)$$

5.2.3 Results

Mycelial disc inoculum

The shape of the pathozone profile generated by mycelial disc inoculum and first elucidated in Chapter 3 was reproduced in this experiment (Fig. 5.2a). The probability of disease increased as the distance between inoculum and host increased, reaching a maximum when inoculum was placed at a distance of 2.0 mm from the surface of the host and declining asymptotically to zero thereafter. The outer limit of the pathozone of 20 mm was achieved after seven days incubation. The shape of the profiles did not appear to alter significantly over time, although accurate observation of disease prior to day 4 was not possible because of the non-destructive nature of assessment.

Changes in the probability of disease, P , with distance between inoculum and host, r , were adequately described at all times of assessment by the critical exponential model:

$$P=(\theta_1+\theta_2.r) \exp(-\theta_3.r) . \quad (5.3)$$

θ_1 is an estimate of the probability of disease when inoculum is placed at the surface of the host, θ_2 is a measure of the amplitude of the rise and fall in infectivity, whilst the intrinsic rate at which infectivity decays as the distance between inoculum and host increases is given by θ_3 . For ease of fitting, the model was reparameterised in the form:

$$P=(\theta_1+\theta_2.r)K^r , \quad (5.4)$$

where $K = \exp(-\theta_3)$. Releasing the K parameter to vary with time produced the most significant reduction in residual deviance and no further significant improvement to the fit was obtained by the release of more parameters. (Table 5.1).

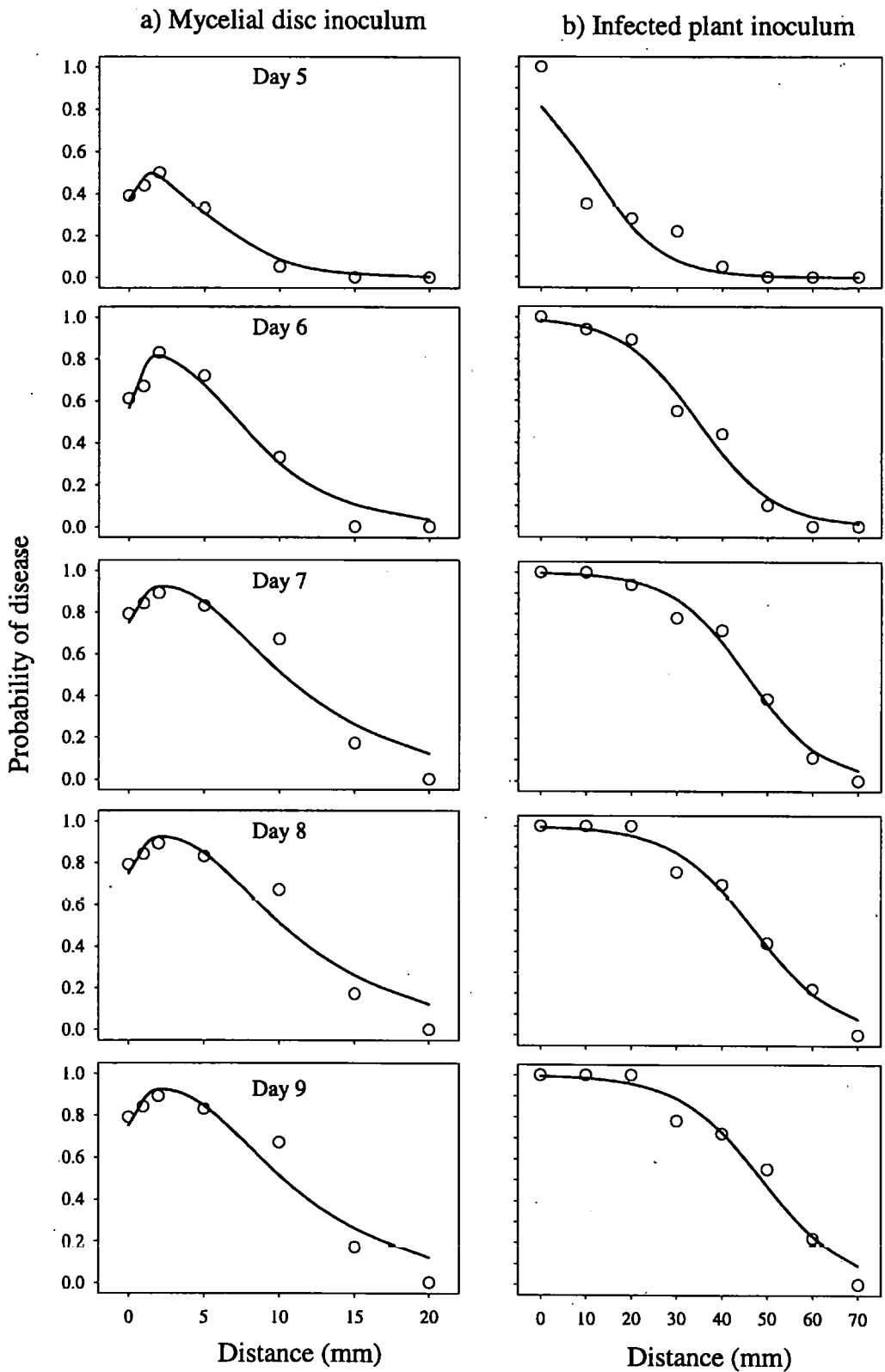


Fig. 5.2: Profiles describing changes in the probability of disease with distance between the host and a) mycelial disc inoculum or b) infected plant inoculum at different times after introduction of the inoculum. Data were fitted individually with the critical exponential function $P(r) = (\theta_1 + \theta_2 r) \exp(-\theta_3 r)$ for mycelial disc inoculum or the logistic function $P(r) = 1/(1 + \exp(\phi_1(r - \phi_2)))$ for infected plant inoculum

Table 5.1: Results of fitting the critical exponential model (model 5.4) to disease data generated by mycelial disc inoculum. A single curve was fitted first and then the effects of releasing different parameters on the residual deviance were assessed by performing an approximate F test.

Model	Res d.f	Res deviance
1. No parameters vary with time	32	4.89
2. θ_1 varies with time	28	FTC*
3. θ_2 varies with time	28	2.39
4. K varies with time	28	2.28
5. θ_1 and θ_2 vary with time	24	2.12
6. θ_1 and K vary with time	24	1.70
7. θ_2 and K vary with time	24	2.19
8. all parameters vary with time (full model)	20	1.62

* optimisation failed to converge

The trend of increase of K with time was monotonic (Fig. 5.3a). Whilst θ_1 did not have a significant influence on the goodness of fit of model (5.4) when released to vary over time, it is biologically reasonable to assume that it increases with time (Fig. 5.3a) in response to changes in the density of fungal mycelium arriving at the surface of the host. Both parameters were therefore described by a monomolecular function of the form:

$$b (1 - \exp(-r (t-c))) . \quad (5.5)$$

Accounting for the increase in the value of these parameters with time, model (5.4) was expanded to give:

$$\begin{aligned}
 P &= (\theta_1(t) + \theta_2, r) K(t)^r \\
 \theta_1(t) &= b_{\theta_1} (1 - \exp(-r_{\theta_1} (t - c_{\theta_1}))) \\
 K(t) &= b_K (1 - \exp(-r_K (t - c_K))) .
 \end{aligned} \quad (5.6)$$

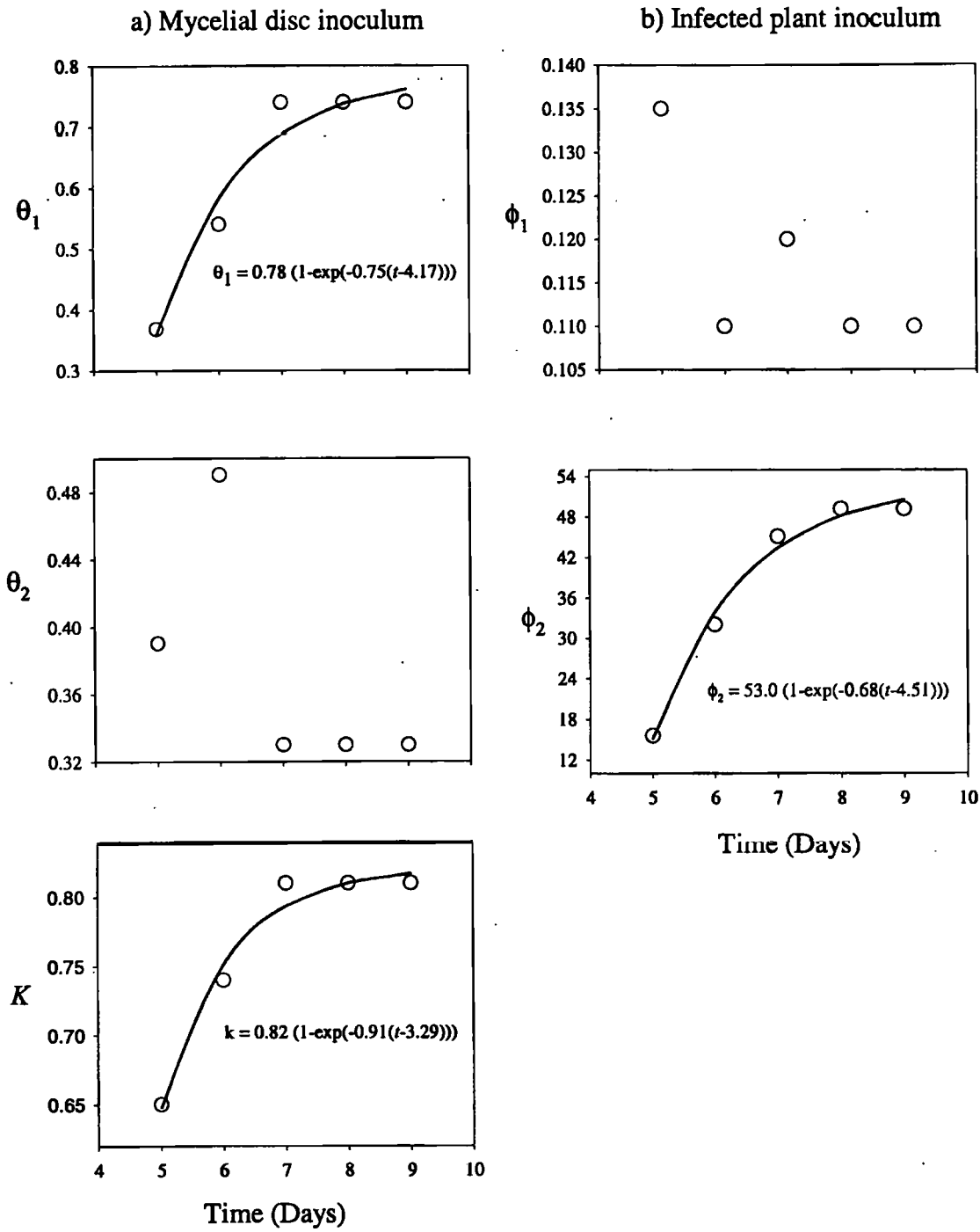


Fig. 5.3: Change in parameter values over time for pathozone profiles described by the critical exponential function, $P(r) = (\theta_1 + \theta_2 r) \exp(-\theta_3 r)$ for mycelial disc inoculum (a) and the logistic function, $P(r) = 1/(1 + \exp(\phi_1(r - \phi_2)))$, for infected plant inoculum (b). Fitted curves to relate parameter changes to time are all of the form $y = b (1 - \exp(-r(t-c)))$

Fitting model (5.6) to data generated using mycelial disc inoculum produced the following parameter estimates:

$$\theta_1(t) = 0.75 (1 - \exp(-1.09 (t - 4.39))) , \quad (5.7a)$$

$$\theta_2 = 0.34, \quad (5.7b)$$

$$K(t) = 0.81 (1 - \exp(-1.40 (t - 3.72))). \quad (5.7c)$$

The fitted model provided both a good qualitative (shape) and quantitative description (Fig. 5.4a). The quantitative fit was compared with that of the full model in which all parameters were allowed to vary in an unstructured manner with time (ie. Full model in Table 5.1). No significant increase in residual deviance was detected (Table 5.2).

Table 5.2 Comparison of the goodness of fit of the critical exponential model with time dependent parameters θ_1 and K (model 5.6) with the critical exponential model in which all parameters were allowed to vary in an unstructured manner with time (model 5.4, full model Table 5.1)

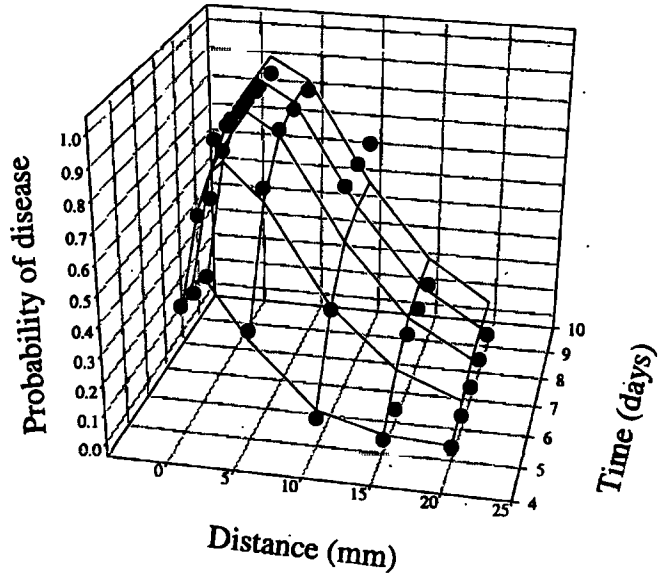
Model	Res d.f	Residual deviance
Model 4.2	28	1.76
Full model	20	1.62 $F=0.22_{8,20 \text{ d.f}}$

Infected plant inoculum

The pathozone profiles generated by infected plant inoculum differed in shape from those generated by mycelial disc inoculum (Fig. 5.2b). The initial rise in infectivity as the distance between inoculum and host increased was absent at all times of observation and the shape of the profiles changed over time from an exponential decline at day 4 to a sigmoidal decline thereafter. A logistic decay of the form:

$$P(r) = \frac{\beta}{(1 + \exp(\phi_1(r - \phi_2)))} , \quad (5.8)$$

a) Mycelial disc inoculum



b) Infected plant inoculum

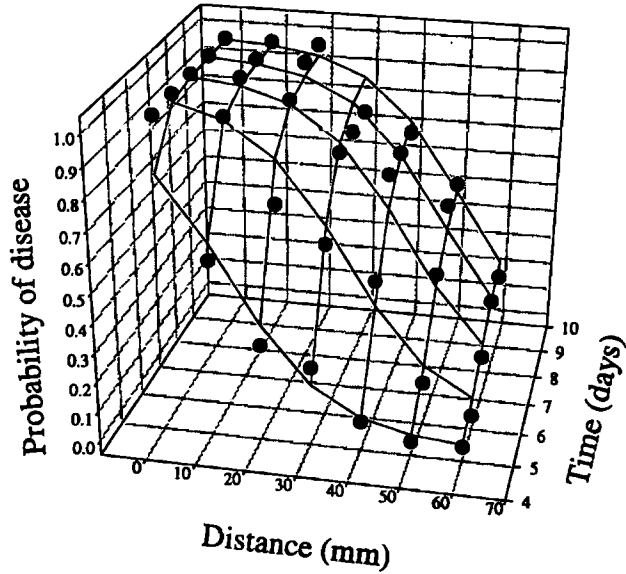


Fig. 5.4: Response surfaces for a) mycelial disc inoculum of the form, $P(r,t) = (\theta_1(t) + \theta_2(t)r) K(t)^r$ and b) infected plant inoculum of the form $P(r,t) = 1/(1 + \exp(\phi_1(r - \phi_2(t))))$. Points represent data.

was used to describe the profiles. By fixing the upper asymptote, β to 1.0 it was possible to reproduce profiles which declined either exponentially (at $\phi_2 \leq 0$ and $P < 0.5$) or in a sigmoidal manner (at $\phi_2 > 0$ and $P > 0.5$). The parameter ϕ_1 is an estimate of the rate of decay of infectivity with distance and ϕ_2 is a locational parameter identifying the point of inflection of the curve.

Only ϕ_2 was found to vary significantly with time (Table 5.3), increasing monotonically to a maximum of 52 mm (Fig. 5.3b).

Table 5.3: Results of fitting the logistic model (5.8) to disease data generated by infected plant inoculum. A single curve was fitted first and then the effects of releasing different parameters on the residual deviance were assessed by performing an approximate F test.

Model	Res d.f	Res deviance
No parameters vary with time	33	9.35
ϕ_1 varies with time	29	7.74
ϕ_2 varies with time	29	1.42
Both parameters vary with time (full model)	25	1.37

Changes in this parameter over time were described by a monomolecular equation of the form (5.5) and included in model (5.8) to give:

$$P(r) = \frac{1}{(1 + \exp(\phi_1(r - \phi_2(t))))} \quad (5.9)$$

$$\phi_2(t) = b_{\phi_2} \cdot (1 - \exp(-r_{\phi_2}(t - c_{\phi_2})))$$

Fitting model (5.9) to data generated using infected plant inoculum produced the following parameter estimates:

$$\phi_1 = 0.105, \quad (5.10a)$$

$$\phi_2(t) = 52.9 (1 - \exp(-0.73(t - 4.58))) \quad (5.10b)$$

The model fitted well to data (Fig. 5.4b) and produced no significant increase in residual deviation compared with the full model of Table 5.3 (Table 5.4).

Table 5.4 Comparison of the goodness of fit of the response surface model (5.9) with that of the logistic model (5.8) in which all parameters were allowed to vary in an unstructured manner with time (Full model, Table 5.3)

Model	Res d.f	Residual deviance
Model 4.4	31	1.53
Full model	25	1.37 $F=0.49_{6,25 \text{ d.f}}$

The extent of the pathozone (R) was calculated for $P(r,t) = 0.05$, giving, after least squares fitting (Fig. 5.5) for mycelial disc inoculum:

$$R = 23.5(1 - \exp(-0.99(t-4.41))) , \quad (5.11)$$

and for infected plant inoculum

$$R = 78.1(1 - \exp(-0.70(t-3.96))) . \quad (5.12)$$

The pathozone from mycelial disc inoculum began to grow after 4.41 days to a maximum of 23.5 mm. The growth of the pathozone from an infected plant was initiated earlier, after 3.96 days and grew to a maximum of 78.1 mm (Fig. 5.5).

5.2.4 Discussion

The success of *R. solani* in causing disease depends on the delivery of an appropriate suite of pectinolytic and cellulolytic enzymes to the site of infection (Weinhold and Sinclair, 1996). This, in turn, is closely correlated with changes in the density of mycelium at the host surface (Weinhold and Motta, 1973). As the inoculum unit germinates and

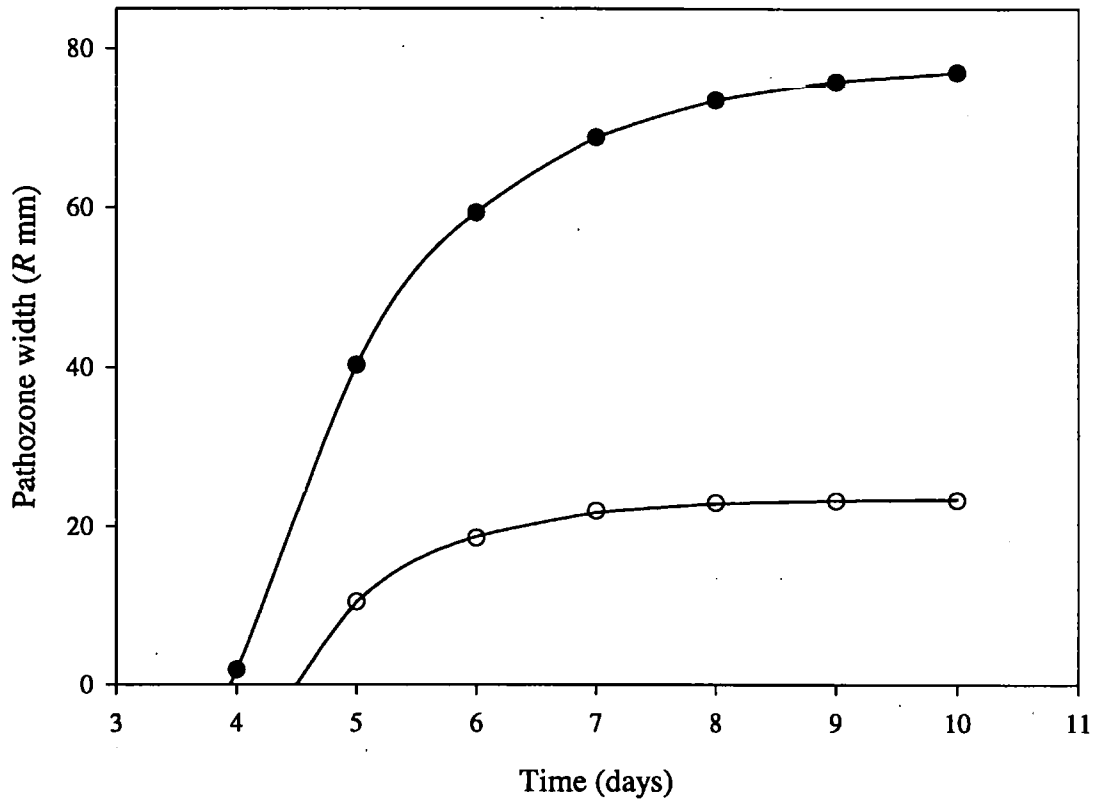


Fig. 5.5: Change in the extent (R) of pathozone influence over time for for mycelial disc (open circles) and infected plant (closed circles) inoculum beyond which less than 5 % of propagules succeed in causing disease.

grows to the host, the density of mycelium at the surface of the host increases, but the rate of increase declines when inoculum is placed further from the host, both because of an increase in the area of soil that the colony must explore if it is to have any chance of locating potential sources of food, and because the nutrients available for growth of the colony become exhausted as it performs this spatial exploration (See Chapter 4). The rate at which the fungus can multiply on the surface of the host may be further reduced by the germinating host which disrupts fungal mycelium as it approaches through the rhizosphere (Chapter 3). Differences in the shapes of the pathozone profiles produced by mycelial disc and infected plant inoculum can be interpreted with respect to these processes.

Mycelial discs contain a relatively small amount of nutrient and produce small colonies of low mycelial density, thus the probability of locating a host declines rapidly with distance and time. In combination with this, the instant germinability of mycelial disc inoculum means that, if the inoculum is located near to the host, the mycelium it produces is disrupted by the germinating radish seedling and has little chance of recolonisation after the host has established. As a result, mycelial disc inoculum placed near to the surface of the radish seed is less infective than that placed a little further away. The infectivity of an inoculum unit achieves an optimum when it is placed at a distance of about 2.0 mm from the host. The density of mycelium reaching the hypocotyl from inoculum placed at this distance is still relatively high but the disruptive influences of the host have subsided by the time the mycelium enters the rhizosphere. As the distance between inoculum and host is increased further, the probability of contact declines to zero. The shape of the pathozone when inoculum occurs at different distances close to the host was confirmed in a separate experiment (results not shown) involving 50 replicates and distances 0, 1, 2, 3 and 5 mm.

In contrast to MD inoculum, an infected plant provides a substantial source of nutrition and quickly produces large colonies of high mycelial density capable of rapid colonisation,

penetration and delivery of a large dose of host degrading enzymes. Although germination is almost immediate and therefore the mycelium from inoculum close to the host presumably suffers from some interference caused by contact with the germinating seed, recolonisation is likely to be equally rapid and no noticeable effects on infectivity (decrease in the probability of infection) were detected. By the time the radish seedlings had emerged, all the replicates in which infected plant inoculum was placed at the host surface, had contracted disease. Thus it is possible that the shape of the pathozone profile prior to this time might show a similarity in shape to that associated with mycelial disc inoculum. It is also likely that such rapid colonisation results in, not only pre-emergent damping-off, but complete failure of the seed to germinate (Baker, 1970).

The pathozone profiles generated using infected plant inoculum were, as a result, different in shape from those produced by mycelial disc inoculum and were described using a different non-linear model. Because of this, no direct comparison of parameters was possible. Comparing the growth in the widths of the pathozones, R , over time, infected plant inoculum produced a pathozone that was initiated more rapidly and extended to over three times the width of that produced by mycelial disc inoculum (Fig. 5.4).

The contrasting infectivity displayed by the two types of inoculum is somewhat arbitrary (clearly, particulate inoculum can be more or less infective than an infected plant depending on the size and nutrient status of the inoculum units) but I consider the contrast to represent a realistic situation which may occur in many horticultural and agricultural ecosystems. The different behaviour of each type of inoculum offers the opportunity to investigate the effects of factors which display a non-linear or threshold response to inoculum infectivity, in particular, the potential of a biological agent to control disease.

The aim of this section was to identify simple non-linear summary models with which to describe and compare the evolution of pathozone profiles over time from two types of

inoculum using the minimum number of parameters necessary. This was achieved, although different models were selected to describe profiles generated by each type of inoculum. The two models can be used to predict the progress of disease amongst a population of radish seedlings. Model (5.6), based on the critical exponential model and associated with mycelial disc inoculum, can be used to estimate disease progress by primary infection alone (Gilligan, 1985), whilst both this model and model (5.9), which describes the evolution of profiles from infected plant inoculum using a logistic function, are required for the estimation of disease progress caused by a mixture of primary and secondary infection. These estimates are made and tested in sections 5.3 and 5.4 respectively. The next step is to model the effects of a biological control agent (in this instance *Trichoderma viride*) on the evolution of the pathozone (Baker, 1990).

5.3 Biological control of pathozone behaviour and disease progress caused by primary infection.

5.3.1 Introduction

Epidemics of plant disease are often divided into those resulting from or dominated by primary infection and those in which primary infection is followed by many cycles of secondary infection (Vanderplank, 1963). Because there is little opportunity for the escalation of errors caused by the non-linear, multiplicative processes associated with many cycles of secondary infection, accurate forecasting of disease resulting from primary infection alone has a better chance of success. Moreover, and because of this non-linearity, the accurate forecasting of disease (and disease control) in which secondary infection makes a significant contribution depends on the accuracy and variability of estimates associated with primary infection. This section expands the work of section 5.2 by examining the pathozone behaviour associated with particulate inoculum when a biological control agent

is placed directly into the rhizosphere of a germinating radish seedling. Baker (1990) noted that modelling of biological control systems in phytopathology had received limited attention (but see Rouse and Baker, 1978) and recognised the potential of the pathozone as a mechanism by which these systems could be studied. Here, the progress of epidemics in the presence or absence of the biological control agent, and resulting exclusively from primary infection, is forecast using a probability model featuring pathozone dynamics, and the outcome of model predictions are tested in a simple experimental microcosm.

5.3.2 Materials and Methods

Inoculum

Mycelial disc inoculum of *R. solani* and poppy seed inoculum of *T. viride* were prepared as described in sections 2.6.2 and 2.7.1 respectively

Placement experiment

A placement experiment was used to compare the effects of *T. viride* on the probability of infection by *R. solani*. Single propagules (colonised poppy seed) of *T. viride* were introduced alongside germinating seeds of radish in soil packs (see section 5.2.2) containing single propagules (mycelial discs) of *R. solani* placed at 0, 2, 5, 10, 15 or 20 mm from the seed. The seed was positioned at a depth of 5.0 mm and the inoculum at a depth of 2.0 mm. There were 15 replicates per treatment organised into a fully randomised design which included a full set of replicated controls containing uncolonised, sterile poppy seed. Plants were assessed visually for disease (lodging due to damping-off) after 5, 6, 7, 8 and 9 d incubation.

Population experiment.

Predictions made using a model for monocyclic disease (model 5.25, specified later) were assessed by growing populations of 40 radish plants (spaced at 40 mm apart to reduce the risk of secondary infection) in seed trays measuring 320 mm by 200 mm and containing 3.0 kg of sand (Grade 0.5-1.0 mm diameter) moistened with tap water (10% tap water by weight). Propagules of the pathogen (mycelial disc inoculum) were positioned at randomly selected coordinates at a rate of 100 units per tray. In half of the replicates (three replicates) each radish seedling was protected by a single propagule of *T. viride* (as colonised poppy seed), carefully positioned beside the seed at the time of sowing in such a way as to reduce the chance of displacement during germination of the host.

Individual trays were covered with clear plastic lids and incubated at 23 °C (16 h light and 8 h dark) in a fully randomised design. The number of diseased (damped-off) plants was recorded at daily intervals for 10 d following inoculation and the possibility of secondary infection (i.e. by spread from plant to plant) minimised further by the removal of plants soon after they were diagnosed as diseased.

Modelling changes in the pathozone profile over time

The pathozone profile for the probability of infection over time from mycelial disc inoculum was empirically described by the model:

$$P(r) = (\theta_1 + \theta_2 r) \exp(-\theta_3 r) , \quad (5.3)$$

identified in 5.2.3 as providing a simple and accurate, non-linear description of the profile, having an intercept at $r = 0$, a maximum, a point of inflection and a lower asymptote of zero.

The model was reparameterised in the form:

$$P(r)=(\theta_1+\theta_2r) K^r \quad , \quad (5.4)$$

where $K = \exp(-\theta_2)$, for ease of fitting (Ross, 1987). This form greatly improved convergence. Fitting was done using GENSTAT (Anon, 1993) under an assumption of binomial errors because of the quantal nature of the response variate.

As in the previous section, model (5.4) was fitted separately to each of the pathozone profiles. This gave separate estimates of θ_1 , θ_2 and K for ten profiles corresponding to five sampling times (days 5...9) with and without *T. viride*. The model was then tested for common parameters over the five times of observation using the methods of Ross (1987) and Gilligan (1990b). One parameter, θ_2 , did not change over time. Trends in the remaining parameters (θ_1 and K) were examined and the model fitted in the form:

$$\begin{aligned} P &= (\theta_1(t) + \theta_2 r) K(t)^r \\ \theta_1(t) &= b_{\theta_1} (1 - \exp(-r_{\theta_1} (t - c_{\theta_1}))) \\ K(t) &= b_K (1 - \exp(-r_K (t - c_K))) \end{aligned} \quad (5.6)$$

This produced a non-linear response surface that describes the change in the pathozone profiles over time, in the presence or absence of *T. viride*. The effect of *T. viride* was also assessed by testing for common parameters in (5.4) between pairs of profiles with and without *Trichoderma* at each time separately.

Computation of the extent of pathozone influence.

In this experiment, the extent of pathozone influence was defined as the distance beyond which the probability of infection is less than 5%: R is solved iteratively for a given time (t) by setting $P(R, t) = 0.05$ in equation (5.6), given by:

$$P=(\theta_1(t)+\theta_2.R) K(t)^R - 0.05 = 0 . \quad (5.13)$$

Prediction of disease progress from pathozone behaviour

The expected progress of disease in a population of radish plants in which secondary infection was prevented was computed from pathozone profiles. The method follows that of Gilligan (1985) except that allowance was made for a non-monotonic pathozone profile with time-dependent parameters.

The probability of a single radish seedling, growing in a microcosm, and becoming diseased by a single, randomly distributed unit of mycelial disc inoculum, ϕ , is given by:

$$\phi = \theta\psi , \quad (5.14)$$

where θ is the probability that a propagule lies within the pathozone and ψ is the conditional probability that it is capable of causing disease given that it occurs within the pathozone. For the radish-*Rhizoctonia* system with inoculum confined to a plane, θ is independent of time but ψ increases with time as mycelium growing from inoculum further out in the pathozone, reaches the host.

For a single time, if the area of the microcosm is A and the area of the pathozone is a then $\theta = a/A$ where a is given by:

$$a = \pi[(R + h)^2 - h^2] . \quad (5.15)$$

R is the radius of the pathozone and h is the radius of the host. ψ is obtained as:

$$\psi = \int_0^R f(r).P(r)dr , \quad (5.16)$$

where:

$$f(r) = \frac{2(r+h)}{(R+h)^2 - h^2}, \quad (5.17)$$

is the density function for the occurrence of a propagule at a particular distance between r and $r+\Delta r$ from the surface of the host and $P(r) = (\theta_1 + \theta_2 r) \cdot \exp(-\theta_3 r)$ is the probability of infection from a distance r . For a fixed time:

$$\phi = \frac{2\pi}{A} \int_0^R (r+h) (\theta_1 + \theta_2 r) \exp(-\theta_3 r) dr, \quad (5.18)$$

which, after solution and further manipulation gives,

$$\phi = B [1 - (1 + CR) \exp(-\theta_3 R)], \quad (5.19)$$

$$B = \frac{2\pi}{\theta_3^3 A} [(\theta_1 \theta_3 + \theta_2) (1 + \theta_3 h) + \theta_2], \quad (5.20)$$

$$C = \frac{2\pi}{\theta_3^2 AB} [(\theta_1 \theta_3 + \theta_2) + \theta_2 (1 + \theta_3 h + \theta_3 R)]. \quad (5.21)$$

For changing time:

$$\phi(t) = B(t) [1 - (1 + C(t)R(t)) \exp(-\theta_3(t)R(t))], \quad (5.22)$$

$$B(t) = \frac{2\pi}{\theta_3^3(t)A} [(\theta_1(t)\theta_3(t) + \theta_2) (1 + \theta_3(t)h) + \theta_2], \quad (5.23)$$

$$C(t) = \frac{2\pi}{\theta_3^2 AB(t)} [(\theta_1(t)\theta_3(t) + \theta_2) + \theta_2 (1 + \theta_3(t)h + \theta_3(t)R)]. \quad (5.24)$$

If $\theta\psi$ is the probability that a single plant becomes diseased by a single propagule of mycelial disc inoculum then the number of seedlings that are expected to contract disease, N_d , when N seedlings are grown and p propagules are dispersed at random within the microcosm is:

$$N_d(t) = N [1 - (1 - \phi(t))^p] . \quad (5.25)$$

The parameters for the population dynamics given in equation (5.25) are all derived from pathozone behaviour studied around single plants. Equation (5.25) was used to predict the progress of infection and disease, together with 95% confidence intervals (based on binomial expectations), in the presence or absence of *T. viride*. These predictions were compared with the observed data from the population experiment. Equation (5.25) is therefore a prediction of population behaviour scaled up from the behaviour of individuals.

5.3.3 Results

Placement experiment

The shape of the pathozone profiles associated with mycelial disc inoculum and described in section 5.2 are repeated here for comparison with the *T. viride* treatment. The probability of disease with distance increased to a maximum and then decreased asymptotically to zero both in the absence and presence of *T. viride* (Fig. 5.6a and 5.6c). The presence of *T. viride* decreased the probability of disease at all distances and all times. Incorporation of a food base (poppy seed), without *T. viride* greatly increased disease (Fig. 5.6b). I conclude that the poppy seed alone was not inhibitory to *R. solani* and that the advantage of an additional food base close to the host was not sufficient to offset the potential for *T. viride* to reduce disease. The results for the poppy seed control are not considered further.

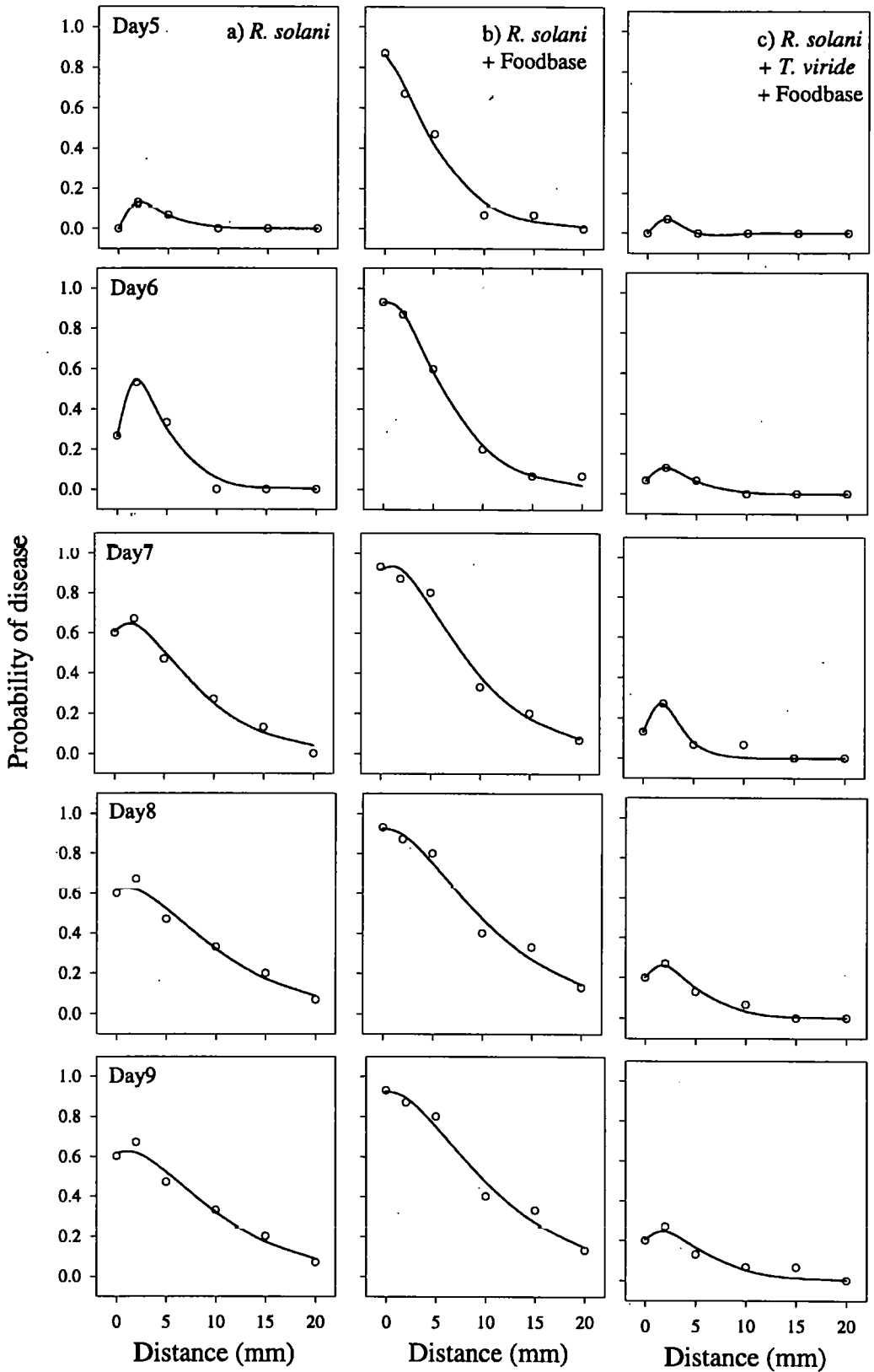


Fig. 5.6: Profiles describing changes in the probability of disease with distance between the host and a) *Rhizoctonia solani*, b) *R. solani* and an additional food base (poppy seed) placed alongside the host, c) *R. solani* with *Trichoderma viride* colonised poppy seed placed alongside the host at different times after introduction of the inoculum. Data were fitted individually with the critical exponential function $P(r) = (\theta_1 + \theta_2 r) \exp(-\theta_3 r)$.

The critical exponential model provided a good description of the disease profiles at each time for *R. solani* in the presence or absence of *T. viride* (Fig. 5.6a and 5.6c). Both θ_1 and $K = \exp(-\theta_3)$ increased asymptotically with time and were adequately described by a monomolecular function (Fig. 5.7). The other parameter, θ_2 decreased approximately linearly with time. However formal testing for common parameters across time and within treatments suggested that θ_2 could be assumed to be common, whilst θ_1 and K varied with time.

Fitting model (5.6) to data generated in the absence of *T. viride* produced the following parameter estimates:

$$\theta_1(t) = 0.61 (1 - \exp(-1.05 (t - 5.02))) , \quad (5.26a)$$

$$\theta_2 = 0.22, \quad (5.26b)$$

$$K(t) = 0.81 (1 - \exp(-2.22 (t - 3.99))), \quad (5.26c)$$

and in the presence of *T. viride*,

$$\theta_1(t) = 0.26 (1 - \exp(-0.41 (t - 5.09))) , \quad (5.27a)$$

$$\theta_2 = 0.16, \quad (5.27b)$$

$$K(t) = 0.74 (1 - \exp(-0.75 (t - 3.99))) . \quad (5.27c)$$

The response surfaces for $P(r,t)$ are shown in Figure 5.8, in which the inhibitory affect of *T. viride* on the probability of disease is shown over distance and time.

It was not possible to fit model (5.1) to the combined data for the presence and absence of *T. viride*, in which θ were allowed to vary with treatment and time. However, disease profiles with and without *T. viride* were compared separately at each time, using model

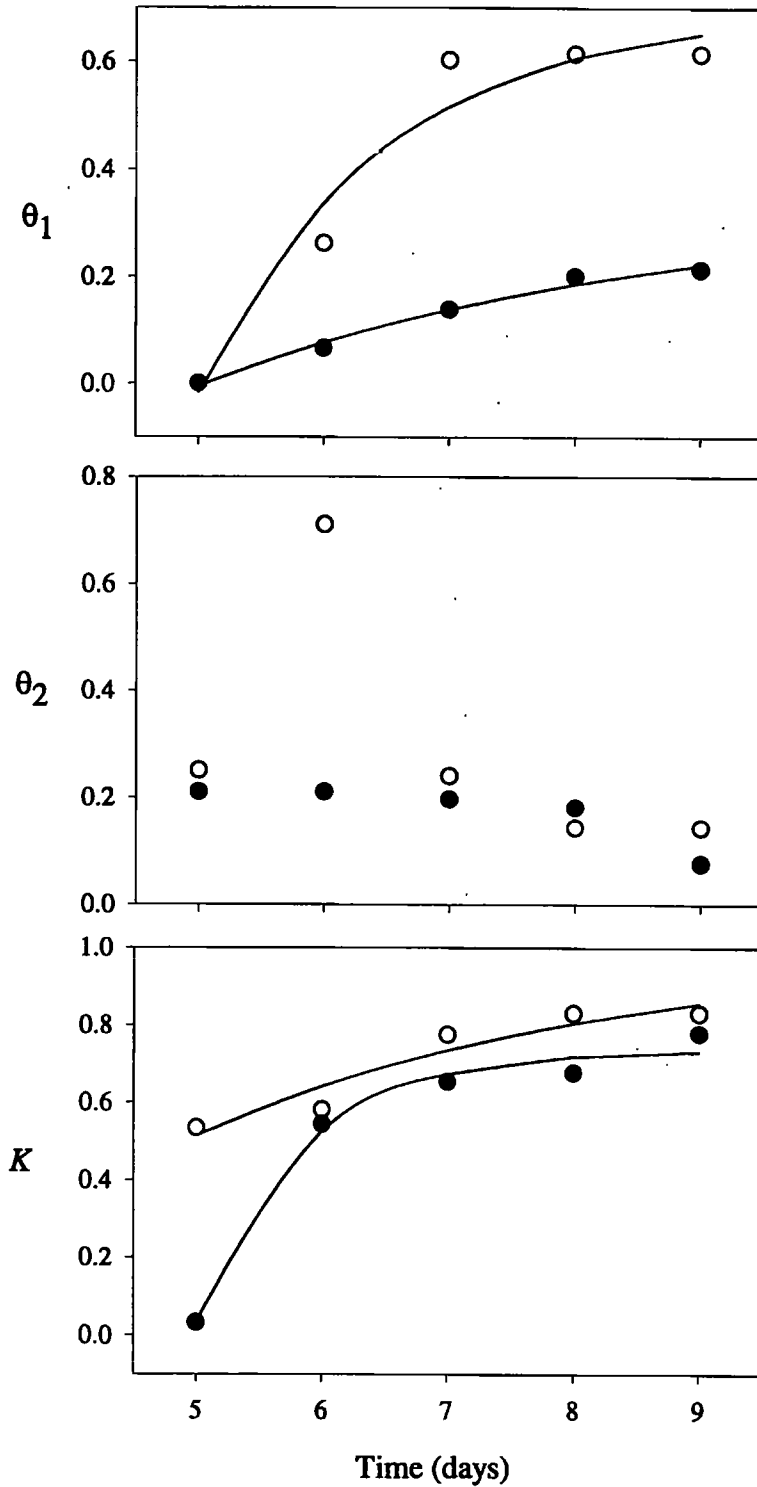
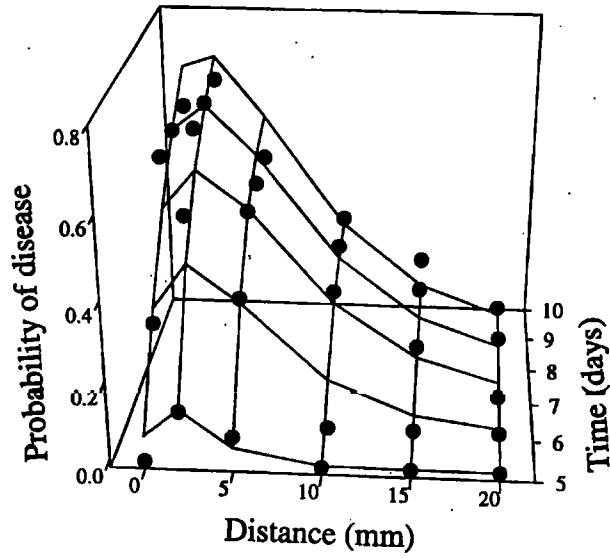


Fig. 5.7: Change in parameter values over time for pathozone profiles described by the reparameterised critical exponential function, $P(r) = (\theta_1 + \theta_2 r)K^r$, in the presence (closed circles) and absence (open circles) of *Trichoderma viride*. Fitted curves for θ_1 and K were of the form $y = b(1 - \exp(-r(t - c)))$.

a) *Trichoderma* absent



b) *Trichoderma* present

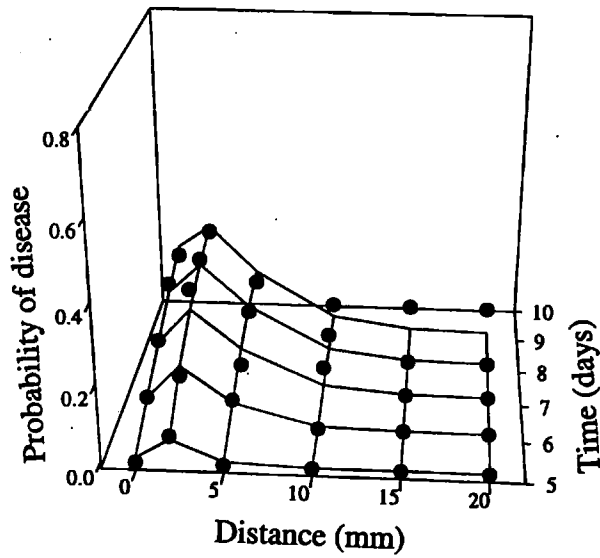


Fig. 5.8: Response surfaces of the form $P(r,t)=(\theta_1(t)+\theta_2 r) K(t)$ a) in the absence of *T. viride*, with $\theta_1(t) = 0.61(1-\exp(-1.05(t-5.02)))$, $K(t) = 0.81(1-\exp(-2.22(t-3.99)))$, $\theta_2 = 0.22$ and b) in the presence of *T. viride*, $\theta_1(t) = 0.26(1-\exp(-0.41(t-5.09)))$, $K(t) = 0.74(1-\exp(-0.75(t-3.99)))$, $\theta_2 = 0.16$.

(5.4). The model failed to converge when testing for common parameters at days five and six. Beyond day six, as the amount of disease increased, fitting of common models was possible. Successive release of parameters revealed that the control of disease by *T. viride* was associated with a reduction in the intercept parameter, θ_1 .

The extent of the pathozone was calculated for $P(r,t) = 0.05$, using model (5.13), giving in the absence of *T. viride*:

$$R = 22.6(1 - \exp(-0.65(t-4.64))) , \quad (5.28)$$

and in the presence of *T. viride*

$$R = 13.8(1 - \exp(-0.38(t-4.63))) . \quad (5.29)$$

It may be seen that *T. viride* reduces the absolute extent of the pathozone from 22.6 mm for *R. solani* and radish when *T. viride* is absent, to 13.8 mm when the biological control agent is present. (Fig. 5.9).

Population experiments

Predictions of disease progress in the presence and absence of *T. viride* were made by incorporating the parameter estimates obtained by analysis of the pathozone profiles into model (5.25) and then comparing these with experimentally derived disease progress curves (Fig. 5.10a). *Trichoderma* reduced the progress of disease from a maximum of 42% in the absence of biocontrol to 13%. The average disease progress curve for the biocontrol treatment was sigmoidal with an asymmetrical point of inflection approximately seven days after sowing. The average disease progress curve in the unprotected crop rose smoothly without inflection towards an asymptote. Similar trends were detected for the increase in variance (Fig. 5.10b). The models for disease progress based on the behaviour of the

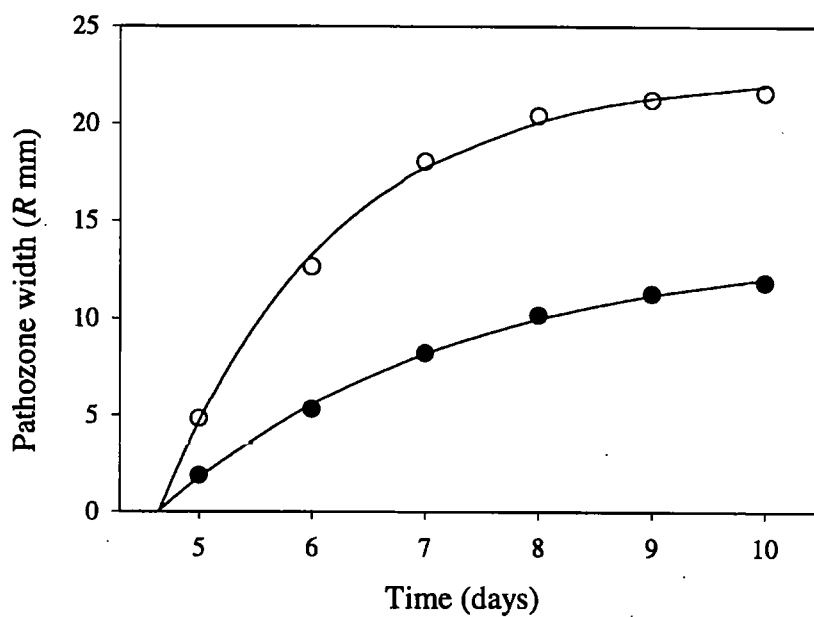


Fig. 5.9: Change in the extent (R) of pathozone influence, beyond which more than 5% of propagules succeed in causing disease, for *Rhizoctonia solani* and radish over time, in the presence (closed circles) and absence (open circles) of *Trichoderma viride* placed at the host surface. The fitted curves are given by equations 5.28 and 5.29.

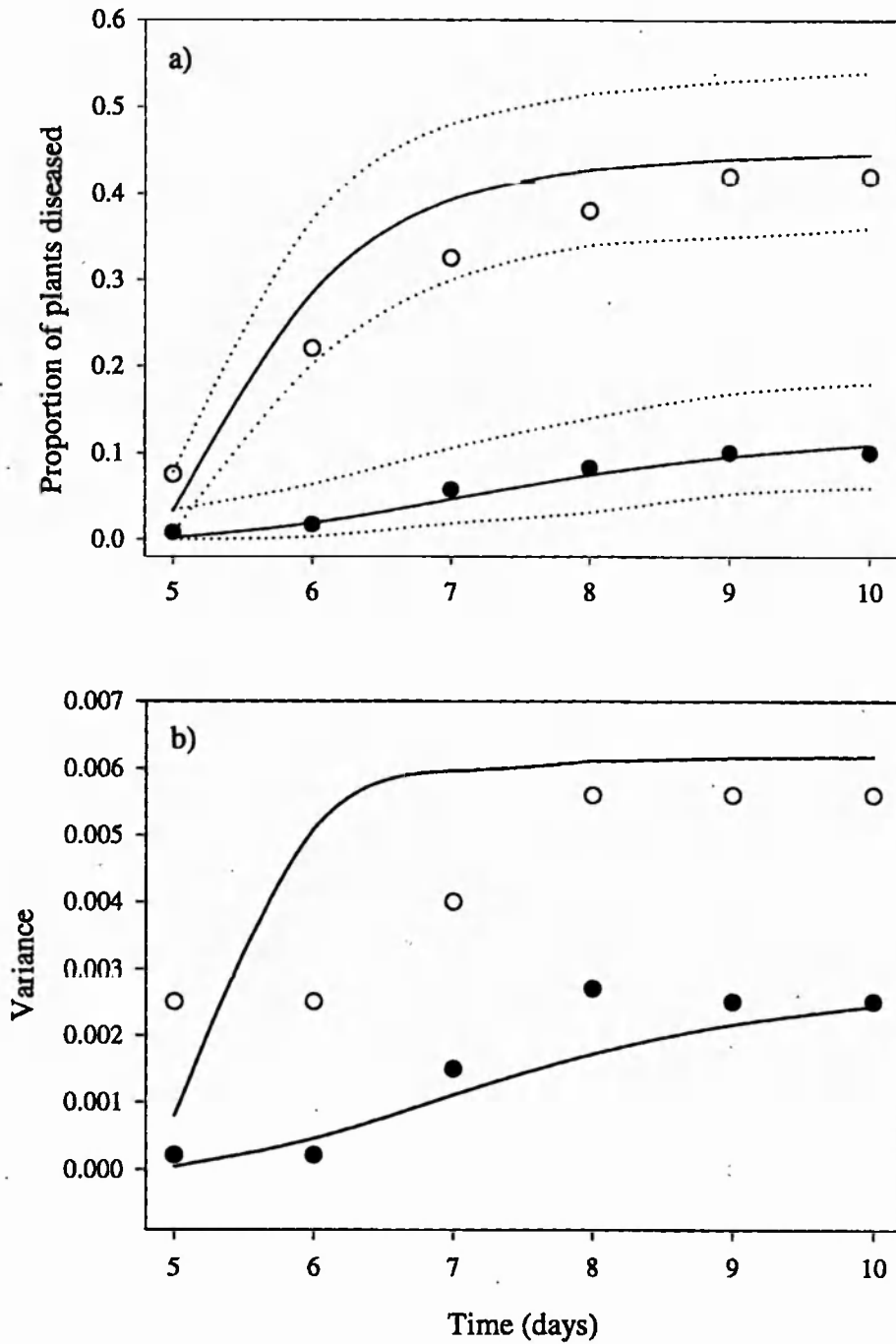


Fig. 5.10: a) Comparison of observed (circles) and predicted (lines) disease progress curves for *Rhizoctonia solani* in populations of radish plants in the presence (closed circles) and absence (open circles) of *Trichoderma viride* placed in contact with host plants. Data represent the means of three replicates. The dotted lines represent 95% confidence intervals about the predicted curve based on binomial sampling. b) Comparison of empirical (circles) and predicted binomial variance (lines).

pathozone surrounding individual host plants closely predicted the average and the variability of the disease progress curves in both the unprotected and in the protected crops.

5.3.4 Discussion

The biological control agent, *T. viride*, reduces the extent of pathozone influence and the infection efficiency of *R. solani* infecting radish. The change in pathozone behaviour can be used to predict changes in disease progress amongst a population of plants.

The similarity of the pathozone behaviour associated with mycelial disc inoculum in the absence of *T. viride* with the results reported in the previous section was reassuring. Fitting the same model (model 5.4), the same parameters, θ_1 and K , were identified as being responsible for changes in the evolution of pathozone profiles over time and fitting model (5.6) to the entire data set produced a three dimensional surface of similar shape and with similar parameter estimates to those obtained in the previous experiment.

The critical exponential model provides a simple, non-linear description of the shape of the pathozone profile. The model has three parameters and certain features of the model are summarised in Figure 5.11d. The pathozone profile characterises the infection efficiency of inoculum which is defined as the probability of infection with distance of inoculum from the host (Gilligan, 1985; Gilligan and Simons, 1987). The pathozone profile is also used to define the extent of pathozone influence theoretically, beyond which the probability of infection is less than 5%. Two parameters, θ_1 and $K = \exp(-\theta_1)$ increase monotonically with time, towards limiting values (Fig. 5.7). θ_1 defines the probability of infection for inoculum located at the surface of the host (Figs. 5.11a and d). The effect of *T. viride* on the pathozone behaviour of mycelial disc inoculum was associated with a reduction in the value of θ_1 . This means that its effect is independent of the distance between inoculum and host and results in the failure of an additional proportion of the inoculum of *R. solani* to cause

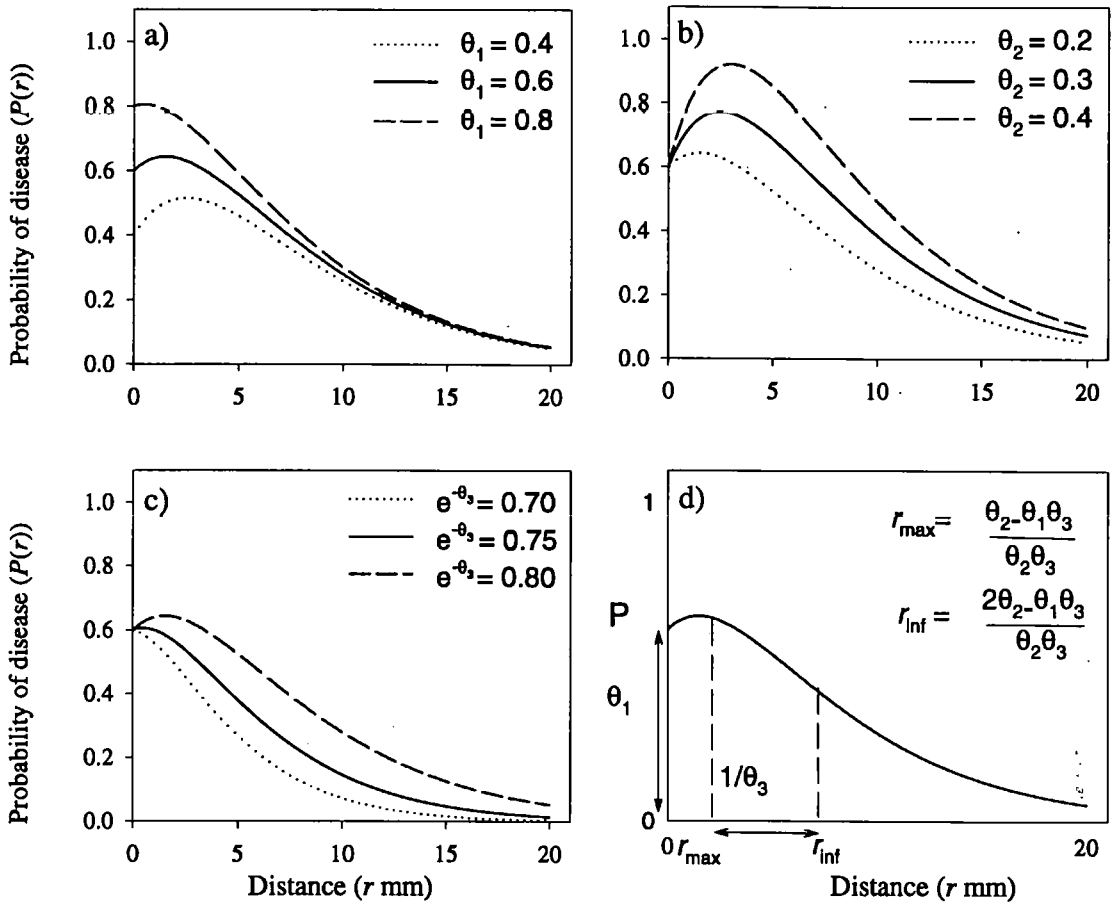


Fig. 5.11: Effects of changing a) θ_1 , b) θ_2 and c) $k (= \exp -\theta_3)$ on the shape of the profile described by $P(r) = (\theta_1 + \theta_2 r)k^r$. d) Relationships amongst parameters showing characteristic features (intercept θ_1 , maximum r_{\max} , and inflection r_{inf}) of the function. Default values for the parameters were $\theta_1 = 0.6$, $\theta_2 = 0.2$ and $k = 0.8$.

disease. The reason may be due to either a quantitative reduction in the proportion of mycelium arriving at the surface of each of the host plants or because only a proportion of the propagules of *T. viride* are capable of controlling disease. Formally, $1/\theta_3$ defines the distance between the maximum and the point of inflection. In practice, θ_3 has a marked effect on the furthest extent of the pathozone (Fig. 5.11c). Hence the change in K over time reflects the expansion of the pathozone as mycelium reaches and infects the host from more distant inoculum.

Prediction of the course of disease progress from pathozone behaviour (Fig. 5.10) matched both the shape and the magnitudes of independent disease progress curves with and without *T. viride*. Consequently it may be concluded that the effects of the biological control agent on pathozone dynamics were sufficient to cause the substantial reduction in disease progress observed in the population experiments.

A practical implication for optimisation of biological control comes from analysis of the sensitivity of disease progress curves to parameters that characterise the shape of the pathozone. The asymptotic level of infection and disease is particularly sensitive to K (Fig. 5.12a). Even a small decrease in K , due for example, to the presence of a biological control agent, can result in a comparatively large reduction in the asymptotic level of disease. In this experiment, the effect of *T. viride* was associated with a reduction in θ_1 . However, whilst the addition of *T. viride* did not significantly affect K , a small but consistent reduction was noted (Fig. 5.7). Differences in K reflect changes in spatial distribution of propagules within the pathozone combined with the efficiency of infection. The probability of inoculum occurring in the pathozone, $f(r)$ increases with r (Fig. 5.12b), while infection efficiency ($P(r)$) increases slightly with distance and then declines exponentially (Fig. 5.11). The product of $f(r) \cdot P(r)$, is a measure of the contribution of inoculum that falls in concentric zones to infection. Consequently, the pathozone profile can be subjectively

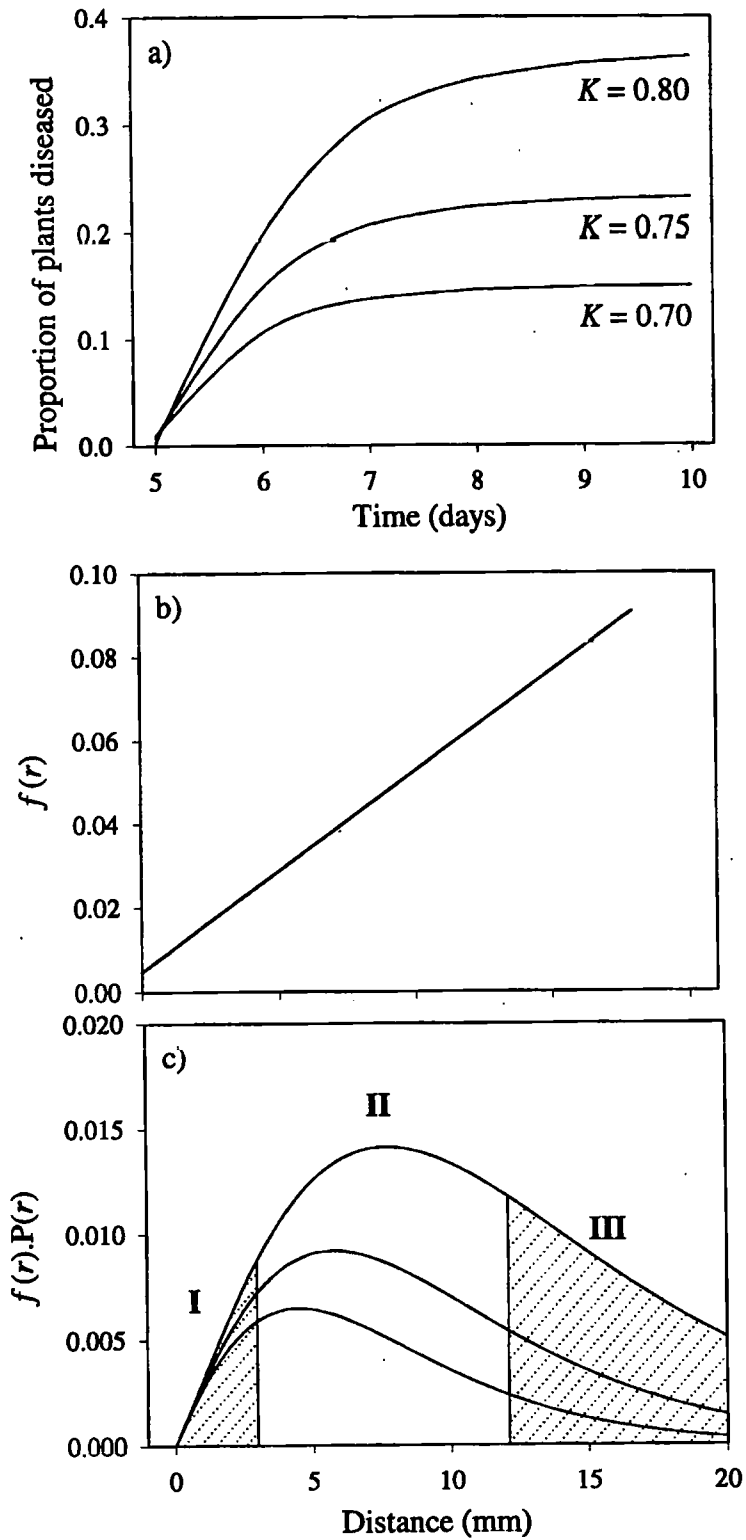


Fig. 5.12: a) Effects of changing $K = \exp(-\theta_3)$ on disease progress curves; the disease progress curves were computed from equations (5.14-5.25), with the asymptotic value of K (equation 5.6) changing. b) Relationship between $f(r)$ and radial distance, r . c) Relationship between the product $f(r)P(r)$ and radial distance, r , measured from the host surface.

The three curves correspond to $K = 0.80$ (upper curve), $K = 0.75$ (middle curve) and $K = 0.70$ (lower curve). See text for interpretation of regions I, II and III.

divided into three regions, an inner region (I) dominated by low values of $f(r)$, an outer region (III) dominated by low values of $P(r)$ and an intermediate region (II), between 3-12 mm from which most successful infections occur. From this it can be concluded that successful biological control must be able to inhibit potential infections that arise from inoculum in the intermediate region, where there is optimisation of inoculum location and infection efficiency.

In the population experiments, one hundred units of inoculum were placed at random allowing for considerable interaction as mycelial colonies develop. Various authors have argued for the presence of facultative synergism between interacting units of inoculum (Henis and Ben-Yephet, 1970; Benson and Baker, 1974a). Certainly, the ability of different fungal colonies to anastomose, and thus reduce intraspecific competition, would provide a basis for such a process (Cooke and Whipps, 1993). However, the successful prediction of disease progress from pathozone behaviour of single plants exposed to single units of inoculum suggests that synergism is not an important component of primary infection in this system (I note, however, that the presence of two opposing processes cannot be ruled out).

In this experiment, the variability of disease between replicate microcosms, both in the presence and absence of *T. viride*, was predicted by the assumption of a binomial error distribution (Fig. 5.10b). Although interactions between mycelial colonies must have occurred, secondary infection and its associated non-linearity was controlled by reducing host density. As a result, the simplicity of this system is reflected in an equally simple derivation of variability. Predictions of disease progress and associated variability in the presence of secondary infection promises to provide a more resilient challenge.

5.4 Biological control of pathozone behaviour and disease progress including secondary infection

5.4.1 Introduction

In the last section biological control of disease progress amongst a population of host plants was predicted simply by the examination and characterisation of the pathogen's behaviour as it infects a single host plant. This scaling up of pathozone behaviour to disease progress was limited to primary infection which involves a single infection cycle whereby particulate units of inoculum germinate, grow, and make contact with the host almost simultaneously. In this section, the scaling up of pathozone behaviour and prediction of disease progress is extended to an epidemic which includes the combined processes of primary and secondary infection. The procedure is complicated by the presence of overlapping cycles of secondary infection which introduce additional time (age)-dependent factors on the changes in host susceptibility and inoculum infectivity and which lead to the spatial dependency of one infection upon another.

In this host-pathogen system the two types of inoculum which lead to primary and secondary infection are represented by mycelial discs of the pathogen *R. solani* and infected radish plants respectively. Characterisation of the pathozone behaviour associated with each type of inoculum has shown that infected plants are considerably more infective than mycelial discs (Fig. 5.2) resulting in a pathozone profile which extends to a greater distance and is intrinsically different in shape. Thus the disruptive effects of the germinating host, which lower the probability of infection when mycelial discs are placed close to the host surface and give rise to a profile in which the probability of infection rises and then falls with distance (Fig. 5.2a), are overcome by the dense, rapidly growing mycelium produced by infected plants. This results in a pathozone profile which decays sigmoidally with distance between inoculum and host (Fig. 5.2b). The relative potency of infected plants to

spread infection provides the potential for a soil-borne epidemic in which secondary infection makes a significant contribution.

Two types of epidemiological model were derived, one which describes the pathozone behaviour of single, isolated plants and a second which describes the population behaviour of an entire epidemic. The essential features of the pathozone behaviour associated with mycelial disc and infected plant inoculum were encapsulated within rate parameters of the pathozone models and used to transfer the information to a population model where it could be scaled up for the prediction of disease progress. The spatial dependency of secondary infection was introduced by imposing the structure of a probabilistic cellular automaton on the behaviour of the model. The cellular automaton allows placement of plants and inoculum in a given spatial structure whereby disease progress can be simulated by calculating changes in the probability of disease transmission between inoculum and susceptible hosts over time.

5.4.2 Model derivations

Pathozone behaviour of mycelial disc and infected plant inoculum

In the previous section (5.3), the description of pathozone behaviour focused primarily on changes in the probability of disease with distance between inoculum and host using a simple non-linear model. The evolution of the pathozone was achieved by allowing selected parameters of the non-linear model to vary with time. In this section, an alternative model is derived which is based on changes in the probability of disease with time from inoculum placed at a single distance from the host surface. Thus for mycelial disc inoculum, the probability of a plant becoming diseased, Y_p , at time t is given by:

$$\frac{dY_p}{dt} = r_p(1 - Y_p), \quad (5.30)$$

and the probability of becoming diseased from an infected plant, Y_s , is

$$\frac{dY_s}{dt} = r_s(1 - Y_s) . \quad (5.31)$$

These models do not, as yet, account for the decay in infectivity as inoculum becomes exhausted, changes in host susceptibility as the host ages or the delays prior to infection for the pathogen to germinate, multiply and penetrate the host and, if the inoculum is not in direct contact with the host, the time taken to grow the distance, x , between inoculum and host. Accordingly, the rates of infection, r_p and r_s , are expanded where:

	Spatial decay due to	Time decay due to	Delay prior
Rate =	location of inoculum from host	x changes in host susceptibility	x to the onset of infection

giving:

$$r_p(x,t) = \phi_p(x)\psi_p(t)H(t-p_6-p_4x) , \quad (5.32)$$

$$r_s(x,t) = \phi_s(x)\psi_s(t)H(t-s_6-s_4x) , \quad (5.33)$$

where the step function, $H(t)$, is 0 if $H < 0$ and 1 if $H > 0$ and is used to describe the delay in the onset of infection. The parameters p_4 and s_4 allow for a delay in infectivity from inoculum occurring at different distances from the host in addition to p_6 and s_6 which represent the delay due to the infection process after contact with the host has been made.

For particulate inoculum, the spatial decay was described by a critical exponential

function of the form:

$$\phi_p(x) = C_p(1+a_5x)\exp(-p_2x) , \quad (5.34)$$

and for secondary infection by the Gaussian function:

$$\phi_s(x) = C_s\exp(-s_2x^2) , \quad (5.35)$$

where the constants C_p and C_s are parameterised as $\mu \beta$ and $\xi \xi$ respectively. The time decay is assumed to be exponential giving:

$$\psi_p(t) = \exp(-p_3(t-p_6)) , \quad (5.36)$$

and:

$$\psi_s(t) = \exp(-s_3(t-s_6)) . \quad (5.37)$$

This provides the following descriptions of the evolution of pathozone profiles from primary and secondary inocula from which parameter estimates for r_p and r_s can be obtained:

Primary (mycelial disc):

$$Y_p(x,t) = 1 - \exp(-p_1(1+p_5x)\exp(-p_2x)(1 - \exp(-p_3(t-p_6)))H(t-p_6-p_4x)) . \quad (5.38)$$

Secondary (infected plant):

$$Y_s(x,t) = 1 - \exp(-s_1\exp(-s_2x^2) \cdot (\exp(-s_3s_4x) - \exp(-s_3(t-s_6)))H(t-s_6-s_4x)) . \quad (5.39)$$

Disease progress involving primary and secondary infection

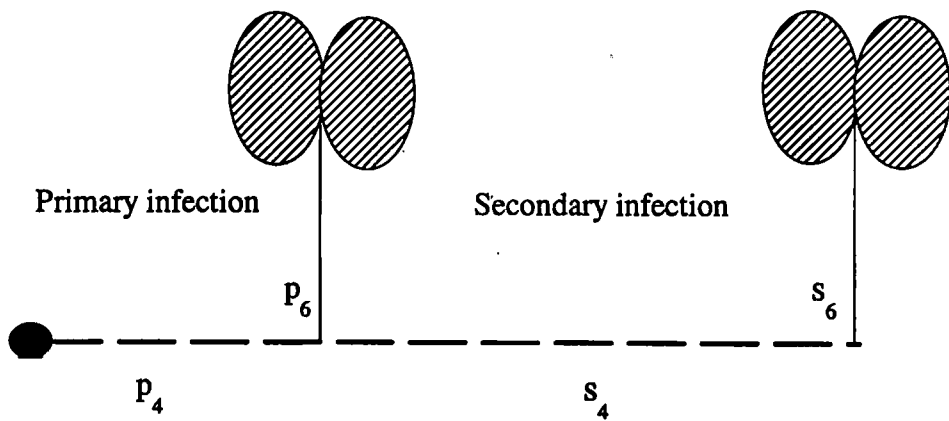
The rates $r_p(x,t)$ and $r_s(x,t)$ are the probabilities of disease transmission used in a spatial

contact process (cellular automaton) describing the population dynamics of *R.solani* on radish. Figure 5.13 illustrates the infection cycle and identifies the occurrence of delays with respect to parameters of the models (5.38 and 5.39). Parameters p_4 and p_6 can be estimated directly from placement experiments and applied to the cellular automaton. However s_4 and s_6 , estimated in the same way are unreliable for use in predicting disease progress. This is because the placement experiments involving infected plants are performed out of context with the population experiment. In these experiments, the delays associated with p_4 and p_6 are circumvented by the introduction of radish plants as seeds and, as a result, the pathogen makes contact with a host which is younger and potentially more susceptible. In addition, when an infected plant was placed near to the host surface, all were infected by day 4. In order to produce a more reliable estimate of the delays s_4 and s_6 (given hereafter as $T (= s_4 + s_6)$) a separate experiment was performed (see below).

For the simulation of disease progress using the cellular automaton, fifty hosts were distributed on a 5 by 10 lattice spaced 20 mm apart. Ten units of particulate inoculum were distributed at random positions within a rectangle containing the lattice. Each host was in one of the three discrete states, susceptible, latent or infectious. Simulations of disease progress were started at $t = p_6$ and were updated with a time step Δt of 0.1 days. The model involved the following transitions:

1. Susceptible to latent host via primary infection.

Transition occurs between time t and $t + \Delta t$ with the probability $r_p(x,t)\Delta t$, if a primary inoculum unit is located at a distance, x in a square with length x_d , centred at the susceptible host (x_d is the distance between hosts).



- p_4 = growth of mycelium from mycelial disc to primary host
- p_6 = multiplication and infection at the surface of the primary host
- s_4 = growth of mycelium from infected primary host to secondary host
- s_6 = multiplication on and infection of secondary host

Fig. 5.13: Diagrammatic illustration of the infection processes involving primary and secondary infection and the location of delays represented by the parameters of models 5.38 and 5.39.

2. Susceptible to latent host via secondary infection.

Transition occurs between time t and $t + \Delta t$ with the probability $\exp(-s_3(p_6 - s_6)) r_s(x_d, t) \Delta t$, if an infectious host is located at a distance of 20 mm. This includes four hosts in the centre of the lattice, three at the edge and two in the corners. The correction factor $\exp(-s_3(p_6 - s_6))$ allows for the delay prior to the formation of secondary inoculum.

3. Latent to infective host

The fixed latent period is T .

The number of infected hosts at time, t , was given as the sum of latent and infective hosts.

5.4.3 Experiments

Placement experiments

Placement experiments were used to characterise the pathozone behaviour of mycelial disc and infected plant inoculum in the presence and absence of the biological control agent *T. viride*. The results of part of this experiment were reported in section 5.2. This section also examines the effect of *T. viride* on the pathozone behaviour of infected plants in which single units of this inoculum were placed at 0, 10, 20, 30, 40, 50 or 60 mm away from the host.

The techniques of parallel curve analysis, used in section 5.2 to identify the effects of *T. viride* on the pathozone associated with mycelial disc inoculum, were used here to examine infected plants. Although equation 5.39 represents an alternative description of the pathozone for an infected plant it includes five parameters which complicates comparison of profiles by parallel curve analysis. Hence, pathozone profiles produced in the absence

and presence of *T. viride* were compared at each time of observation using the simpler logistic function 5.8:

$$P(r) = \frac{1}{(1 + \exp(\phi_1(r - \phi_2)))}$$

Population experiment

Predictions made using the cellular automaton were assessed by growing populations of 50 radish plants spaced at 20 mm apart in seed trays measuring 200 mm by 100 mm and containing 1.0 kg of sand (Grade 0.5-1.0 mm diameter) moistened with tap water (10% tap water by weight). The increased density of host plants (20 mm compared to 40 mm for the examination of primary infection, section 5.3.2) allowed for significant levels of secondary infection. Propagules of the pathogen (mycelial disc inoculum) were positioned at random at a rate of 10 units per tray. In half of the replicates (five replicates) each radish seedling was protected by a single propagule of *T. viride* (as colonised poppy seed), carefully positioned beside the seed at the time of sowing in such a way as to reduce the chance of displacement during germination of the host.

Individual trays were covered with clear plastic lids and incubated at 23 °C (16 h light and 8 h dark) in a fully randomised design. The number of diseased (damped-off) plants was recorded at daily intervals for 20 days following inoculation.

Estimation of T

Under conditions identical to those of the population experiments, 25 radish seeds were sown in a 5 by 5 lattice and the centre plant (either with or without a poppyseed colonised by *Trichoderma*) challenged with a unit of mycelial disc inoculum placed at a distance of 3 mm to optimise the probability of its becoming diseased. For those replicates in which

the centre plant damped-off and provided an infected plant as a source of inoculum, the mean time taken to re infect a surrounding plant was recorded as T .

5.4.4 Results

Pathozone behaviour

The relationship between the probability of infection and distance between mycelial disc inoculum and the host radish plant was described in section 5.3. The probability increased initially with distance and then declined asymptotically to zero at each time of observation. This relationship was described by the same shape of curve when the biological control agent, *T. viride*, was placed into the rhizosphere of the host (Fig. 5.6) but the probability of infection was reduced at each distance and at each time. When infected plants were used as the source of inoculum, a different shaped curve was produced and was described by a logistic function (Fig. 5.14). The addition of *T. viride* caused a significant reduction in the ϕ_2 parameter of the logistic model (5.8) after seven days growth and the significance of this reduction increased over time (Table 5.6).

Table 5.6 Summary of parallel curve analysis comparing pathozone profiles of infected plants generated in the presence and absence of the biological control agent *Trichoderma viride*.

Model	d.f	Residual deviance				
		5	6	7	8	9
a) No parameters vary	10	0.66	0.21	0.34	0.80	0.52
b) ϕ_2 varies	9	0.61	0.21	0.23	0.25	0.09
c) ϕ_1 varies	9	0.60	0.21	0.34	0.78	0.51
d) Both ϕ_1 and ϕ_2 vary	8	0.55	0.21	0.23	0.22	0.09
a) compared with d)	2,8	0.80 ^{n/s}	0.00 ^{n/s}	2.09 ^{n/s}	10.5 ^{**}	19.1 ^{***}
b) compared with d)	1,8				0.54 ^{n/s}	0.00 ^{n/s}

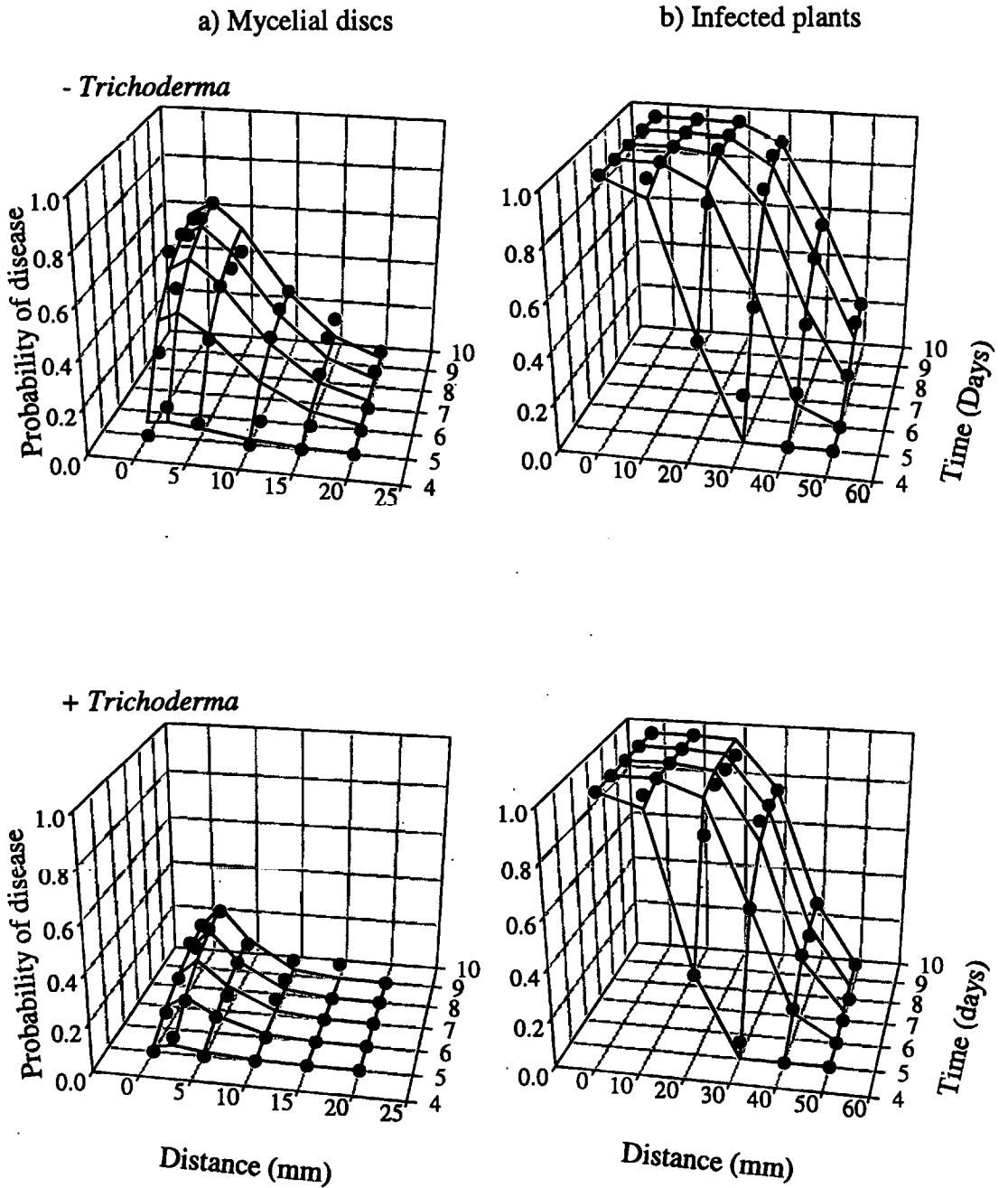


Fig. 5.14: Evolution of the pathozone for a) mycelial discs and b) infected plants in the absence (- *Trichoderma*) and presence (+ *Trichoderma*) of the biological control agent *Trichoderma viride*.

Models 5.38 and 5.39, used as alternatives to the simpler (fewer parameters) critical exponential (5.6) and logistic (5.9) models provided an accurate description of pathozone behaviour for both types of inoculum in the presence and absence of *T. viride* (Fig. 5.14). The parameter values estimated from the fitting process are given in Table 5.7 together with the estimate of T.

Table 5.7: Parameter estimates (\pm s.e) of models (5.38) and (5.39) describing the effects of *Trichoderma viride* on the pathozone behaviour of mycelial disc and infected plant inoculum

Parameter	- <i>Trichoderma</i>	+ <i>Trichoderma</i>
P ₁	1.09 \pm 0.200	0.28 \pm 0.078
P ₂	0.28 \pm 0.027	0.49 \pm 0.050
P ₃	0.55 \pm 0.200	0.37 \pm 0.200
P ₄	- -	- -
P ₅	0.49 \pm 0.150	1.55 \pm 0.380
P ₆	4.90 \pm 0.082	4.77 \pm 0.190
S ₁	14.9 \pm 4.09	15.6 \pm 2.52
S ₂	0.00098 \pm 0.0002	0.0016 \pm 0.0003
S ₃	0.36 \pm 0.190	0.75 \pm 0.210
S ₄	0.052 \pm 0.006	0.034 \pm 0.008
S ₅	- -	- -
S ₆	3.73 \pm 0.150	4.20 \pm 0.155
T	1.82 \pm 0.84	1.80 \pm 1.14

Population dynamics

In the absence of *T. viride*, the progress of disease in experimental microcosms was approximately linear with respect to time until day 15 at which point it began to slow (Fig.

5.15a). *Trichoderma* reduced the mean levels of disease. Disease progress in the presence of *Trichoderma* was also linear but proceeded with a slower mean rate which showed no sign of retarding until day 18. Examination of individual replicates (not shown) identified the progress of disease within a single microcosm as largely responsible for this. The variability between replicate microcosms also increased with time which was initially more rapid in the absence of *T. viride*. However, by twenty days, although the mean level of disease was only half of that in the unprotected crop, the variance between replicates of the protected crop was greater.

The cellular automaton provided an accurate prediction of the mean level of disease progress in the absence of *T. viride* and during the early phase of disease progress in the presence of *T. viride*. After thirteen days the model over-estimated the reduction of disease caused by adding the biological control agent (Fig. 5.15a). Similarly, the model provided a good description of the variability between replicate microcosms in the absence of *T. viride*, but failed after thirteen days in the presence of the control agent (Fig. 5.15b). (It should be noted that whilst the simulations consistently provided accurate descriptions of mean disease progress amongst five replicates, predictions of variability were less repeatable).

5.4.5 Discussion

The pathozone dynamics of the two types of inoculum were affected differently by the presence of the biological control agent, *T. viride*. When mycelial discs were used as a source of inoculum, *Trichoderma* reduced the probability of disease by the same proportion, which did not depend on the distance at which the inoculum was placed from the surface of the host. In contrast, *T. viride* did not control disease when infected plants were placed close to the host and was increasingly more effective when this inoculum was

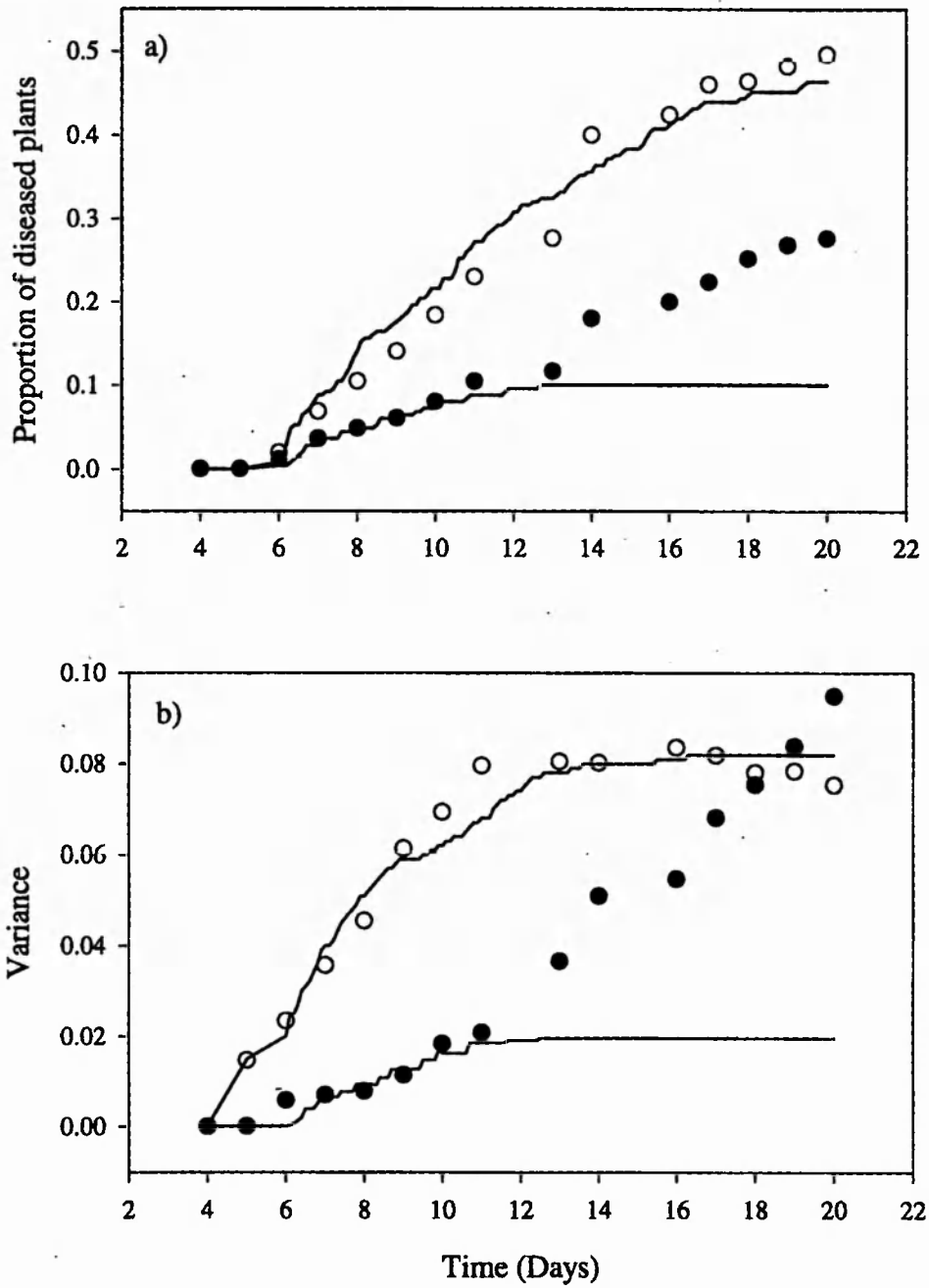


Fig. 5.15: a) Comparison of predicted (lines) and observed (symbols) disease progress in the absence (open circles) and presence (filled circles) of the biological control agent, *Trichoderma viride*. b) Comparison of empirical (symbols) and predicted (from model simulation) variance between five replicate microcosms.

positioned further away. This is interpreted in terms of the presence of a threshold density of mycelium which is necessary to cause disease. When infected plants are placed near to the host, the threshold is quickly and easily reached and the probability of disease is independent of the distance between inoculum and host. The effects of *T. viride* are therefore undetected. As the distance increases, the effects of inoculum exhaustion and a reduction in the density of mycelium as the colony extends into an increasing area of soil, reduces the density of mycelium that make contact with the host surface. The density falls below the threshold and the probability of disease is reduced. The effects of *T. viride* begin to have a significant impact in this region of the profile and become more pronounced over time as the inoculum becomes weakened by exhaustion. These processes were subsumed into the equations (5.38) and (5.39) which provided an accurate description of the pathozone dynamics associated with the two types of inoculum.

By transferring the information encapsulated in equations (5.38) and (5.39) into the rate parameters r_p and r_s for use in the cellular automaton, it was possible to predict disease progress that would occur within a microcosm containing a population of 50 radish plants. The prediction of mean disease in the absence of *T. viride* were very accurate, reproducing both the shape and the magnitude of the disease progress curve. Three factors contribute to the success of the model; the form in which the pathozone behaviour associated with mycelial disc and infected plant inoculum is accurately characterised; the incorporation of a delay prior to the onset of secondary infection; and the dependency of secondary infection on the spatial distribution of disease.

The pathozone behaviour of the two types of inoculum combine changes in infectivity and host susceptibility with time and distance from the host into the parameters r_p and r_s . This effectively sets a clock which modifies the rate at which disease is transmitted by secondary infection and allows for cessation of disease progress before all hosts have

become infected. Combined with the highly non-linear increase of disease by secondary infection, this can account for large variability in the asymptotic levels of disease between identical replicates from the small, stochastically generated differences that develop after primary infection. This phenomenon has recently been termed dynamically generated variability (Kleczkowski, Bailey and Gilligan, 1996).

Clearly, for the spread of a soil-borne pathogen such as *R. solani* causing damping-off disease amongst a seedling crop, the assumptions implicit in models of the form:

$$\frac{dN_i}{dt} = r.N_i(1-N_i) \quad ,$$

regarding complete mixing between infective, N_i , and susceptible, $(1-N_i)$, plants is invalid. The growth of the mycelial colony from an infected plant restricts mixing (contact) to neighbouring plants only. This reduction in contact between infected and susceptible plants is imposed by the structure of the cellular automaton.

Predictions of disease progress and the dynamics of variability between replicates in the presence of *T. viride* were accurate during the early stages of the epidemic in which disease progress was dominated by primary infection. However, the model predicted cessation of disease progress after 12 days during which time disease continued to spread within the experimental microcosms and variability between replicates increased. This may be interpreted as the disappearance of the disease control afforded by the presence of *T. viride* and may be linked with a transformation from an early phase of mycelial growth together with a concomitant production of antibiotics to a phase of spore production. Indeed, as a result, secondary infection may be fuelled not simply by the breakdown in disease control afforded by *Trichoderma* but by access of *R. solani* to the poppy seed as an additional food source.

In summary, this chapter features techniques by which the pathozone behaviour of single, isolated radish plants can be used to predict the progress of an epidemic. Predictions were particularly accurate for primary infection where even small differences in pathozone behaviour, caused for example, by the presence of a biological control agent, can have a large effect on the progress of disease. Prediction of disease progress in an epidemic dominated by secondary infection was also possible by incorporating information regarding pathozone behaviour into a cellular automaton based model. Whilst predictions of disease progress were accurate in the absence of the biological control agent *T. viride*, the model failed during the latter stages of an epidemic controlled by *T. viride*. This highlights the need for more research into the influence of longer-term, time-dependent interactions between the control agent, the pathogen and the host.

Chapter six

The dynamics of primary and secondary infection in take-all epidemics

6.1 Introduction

The infection of radish by *Rhizoctonia solani* represents a relatively simple epidemiological system. It involves a single cohort of regularly spaced hosts that each provide a static infection court (the hypocotyl). *Rhizoctonia solani* has a high competitive saprophytic ability (Garrett, 1970) and when spreading rapidly over the soil surface creates an epidemiological system which simplifies its direct observation and quantification and accounts for the success of the immuno-blotting technique for *in situ* detection. Furthermore, because the hypocotyl is the primary target for infection (damping-off), once *Trichoderma* is placed nearby, limited colonisation of the host is adequate to suppress disease.

In chapters three to five, three components (inoculum germinability, mycelial growth and infectivity at the host surface) were quantified and successfully used to predict the shape of the pathozone profile. The evolution of the pathozone on individual plants was summarised by a simple non-linear model which was subsequently used to predict disease progress amongst a population of radish plants. Placement of a biological control agent, *Trichoderma viride*, near to the hypocotyl of a potential host plant suppressed the evolution of the pathozone and consequently reduced the spread of disease. In summary, the epidemic was characterised by overlapping phases of primary and secondary infection in which spatial spread was facilitated by mycelial growth of the pathogen.

Whilst the infection of wheat by *Gaeumannomyces graminis* (Ggt) still includes primary infection from particulate inoculum and secondary infection as disease spreads from

infected to susceptible roots, it involves a more complex epidemiological system. In addition to the decay in infectivity of particulate inoculum, the pathogen is provided with a continuous supply of susceptible roots, initially in the form of seminal roots growing from the seed, and thereafter by an indeterminate number of adventitious roots that grow from the crown. Moreover, the rate at which new, susceptible roots are produced may depend on the number of roots diseased (Skou, 1975). This means that the spread of disease involving both primary and secondary infection amongst a population of roots belonging to a number of different plants is unlikely to be easily predicted from the pathozone dynamics of single, isolated roots.

Much effort has been directed at investigation of the practical aspects of take-all epidemiology (Yarham, 1981). However, the intrinsic shape of the disease progress curve and the underlying biological factors that determine disease dynamics are poorly understood. Studies consisting of a sequential sampling regime have involved field plots (Brassett and Gilligan, 1988b; Werker *et al.*, 1991). The data are highly variable because of the temporal and spatial patchiness of disease. Changes in environmental variables, notably temperature and moisture, influence growth of the pathogen (Cook, 1981) and thus the shape of the disease progress curve. In view of this variability, the frequency of sampling and the quantity of data collected are often inadequate for testing detailed, epidemiological hypotheses, largely because of the labour and time required to collect the data. Also, data collection is often restricted to the most dynamic period of disease progress which accounts only for a portion of the disease progress curve. Growth and infection of wheat in microcosms offers the opportunity to control this variability and thus provide a more efficient and sensitive analysis of disease progress.

Consequently, for this host-pathogen system, the order of investigation was reversed. Instead of predicting disease from pathozone dynamics, I first identified the intrinsic shape

of the disease progress curve and then interpreted disease dynamics according to underlying biological components. The model proposed by Brassett and Gilligan (1988a) is used as the basis of the investigation of disease progress. Change in the number of infected roots, N_i over time, t , is given by:

$$\frac{dN_i(t)}{dt} = (r_p P + r_s N_i(t))(N - N_i(t)) , \quad (6.1)$$

where P is the density of particulate inoculum and r_p and r_s are rate parameters for primary and secondary infection respectively. The model predicts a disease progress curve which varies in shape from monotonic for an epidemic dominated by primary infection to sigmoidal when secondary infection makes the most significant contribution to disease.

The chapter is divided into two sections. In section 6.2 the model (6.1) is fitted to disease progress data and interpreted according to changes in particulate inoculum, P , and root growth, N , over time. Two disease progress curves are produced under controlled conditions in microcosms, one from a high density of particulate inoculum to represent an epidemic dominated by primary infection, and one from a low inoculum density, allowing for significant secondary infection. The progress of disease is examined alongside the constraints imposed by inoculum decay and host growth and terms for the behaviour of these components are included in model (6.1) to show how they dictate the shape of the disease progress curve. Disease progress on the seminal and adventitious roots is examined in isolation and compared with predicted levels of primary infection in order to confirm that substantial levels of secondary infection occur. The characteristic behaviour of disease on the seminal and adventitious root systems is then used to compare the dynamics of disease progress in a controlled environment with corresponding data collected from a field experiment.

In section 6.3, the effects of a biological control agent, *P. corrugata*, on the pathozone dynamics of seminal wheat roots are examined. The techniques described in section 5.3 are used to predict disease progress caused by primary infection amongst a population of seminal roots from pathozone behaviour of single roots in the presence and absence of the biological control agent. Finally, the principal characteristics of control afforded by *P. corrugata* are extrapolated to predict disease progress in relation to primary and secondary infection of the total root system.

6.2 Disease progress of take-all

6.2.1 Materials and methods

Inoculum

The inoculum used in all experiments consisted of *Ggt* (isolate ML1) grown on foxtail millet grains (*Setaria italica*) which provided small, uniform infection units. Methods for the production of this inoculum are described in section 2.6.2

Host species

The winter wheat variety Riband was used throughout the experiments. Seeds were selected for uniformity of size, surface sterilised for 5 minutes in 5% sodium hypochlorite (0.5% w/v available chlorine) and rinsed twice in sterile distilled water. These were incubated for 48 h at 19°C and selected for uniformity of germination.

Controlled environment

Compared to other soil-borne fungi, *Ggt* has an exceptionally high water potential requirement and cannot grow at less than -4.5 MPa (Cook, 1981). Soil was therefore maintained near to field capacity (-0.015 MPa) during experiments using a soil moisture

probe (Type 2900F. Soilmoisture Equipment Corp, Santa Barbara, USA). Experiments were run at 15°C with a light regime of 16 h light and 8 h dark.

Production of disease progress curves

Two batches of inoculum were prepared with 15 and 240 propagules per litre of soil respectively. Pots measuring 160 mm in depth and with an internal diameter of 150 mm were filled with 880 cm³ of soil, then 880 cm³ of inoculum followed by a further 550 cm³ of soil. Five pre-germinated wheat seeds were planted in the centre of each pot and covered with 350 cm³ of soil and finally 175 cm³ of sand to prevent excessive evaporation. The pots were allowed to stand in water until saturated after which they were transferred to a growth cabinet.

The experiment involved 40 pots (20 for each inoculum density). The pots were fully randomised between two growth chambers and sampled over a twelve week period by washing away soil and carefully separating the roots. Roots were then examined under a binocular microscope and the numbers of diseased and healthy roots per plant on both the seminal and adventitious root systems were recorded where disease was defined as stelar discolouration.

Two additional pots were included to estimate the number and average length of roots passing through the inoculum layer. This information was then utilised in the simple probability model for the estimation of primary infection on seminal roots.

Models describing disease progress

Three models were fitted to disease progress data. The generic model (model 6.1) was that derived by Brassett and Gilligan (1988a) and described again here for the purpose of clarity.

Change in the number of infected roots, N_i over time, t , is given by:

$$\frac{dN_i(t)}{dt} = (r_p P + r_s N_i(t))(N - N_i(t)) , \quad (6.1)$$

where P is the density of particulate inoculum and r_p and r_s are rate parameters for primary and secondary infection respectively. The second model included the dynamics of particulate inoculum (P), measured in a separate experiment, and the dynamics of host growth (N). Change in the number of infected roots, N_i , over time, t , is given by:

$$\frac{dN_i(t)}{dt} = (r_p P(t) + r_s N_i(t))(N(t) - N_i(t)) , \quad (6.2)$$

where P and N are functions of time. In a pilot experiment, lateral root formation was observed as a potential route for the transmission of disease. Consequently, a further model in which secondary infection also included a term for change in the total number of lateral roots (it was not possible to distinguish easily between infected and uninfected lateral roots) over time ($l(t)$), was examined. The model is given as:

$$\frac{dN_i(t)}{dt} = (r_p P(t) + r_s N_i(t) l(t))(N(t) - N_i(t)) . \quad (6.3)$$

The models were fitted to disease progress data using the numerical curve fitting software package FACSIMILE (AEA technology U.K.) The goodness of fit was assessed by comparing residual deviance, trends of residual error, errors associated with individual observations and parameter estimates for primary and secondary infection.

Decay of particulate inoculum

The decay of particulate inoculum, P , was examined in a separate experiment. Ten soil packs (Appendix III) were prepared using 200 mm lengths of clear, layflat tubing, 70 mm in diameter. The tubing was partially sealed at one end using staples and filled with 300 ml of moist soil (10 ml water per 100 g dry soil/sand). Packs were sealed at the top allowing enough room for the emergence of a coleoptile and then compressed to achieve enough rigidity to stand upright. Pre-germinated seeds were introduced into the pack by making a small incision, inserting the seed and then resealing with clear, adhesive tape. Soil moisture was adjusted to achieve near field capacity and the packs placed in the growth chamber. Ten propagules were introduced into each pack at random and one propagule removed from each on each sampling occasion. These propagules were tested for their ability to cause disease by placement against fresh wheat roots grown under the conditions described above.

The experiment was set up as a fully randomised block, with ten sampling times. Decay of Ggt may occur immediately or following a delay (Hornby, 1981). Thus, two simple non-linear models were fitted using MLP (Ross, 1987). These were :

$$P = \beta_p \cdot \exp(-\alpha_p \cdot t) , \quad (6.4)$$

$$P = \beta_p \cdot \exp(-\alpha_p \cdot t^2) . \quad (6.5)$$

Model (6.4) is an exponential decay whilst model (6.5) allows for an initial period during which inoculum decay is less rapid. The fitting procedure was constrained to estimate β_p below 1.0.

Primary infection of the seminal roots.

The asymptotic level of primary infection was estimated using the probability model described by (Gilligan, 1985). This model assumes a fixed number of host units which is represented by the rapid growth of seminal roots through an inoculum layer. The volume of pathozone soil, v , surrounding a single root growing through an inoculum layer can be estimated from the equation:

$$v = \pi L((r_r + w + r_i)^2 - r_r^2) \quad (6.6)$$

where r_r is the radius of the root, r_i is the radius of a propagule, w is the distance across which the pathogen can grow to cause infection and L is the length of root passing through the inoculum layer. Thus the probability of a single, randomly dispersed inoculum unit falling into the pathozone soil which surrounds a single root is given by v/V where V is the total volume of soil within the inoculum layer.

For N roots passing through the inoculum layer in which P propagules have been randomly dispersed, the number of roots containing at least one propagule within the surrounding pathozone is given by:

$$N_i = N - [N \cdot \exp(-\phi P)] \quad \text{where } \phi = v/V \quad (6.7)$$

The infection of a host does not depend solely on the presence of an inoculum unit within the pathozone but on its distance from the root surface. Typically, the probability of infection declines as the distance between inoculum and host increases (Gilligan & Simons, 1987). The probability of infection, ϕ , is then $\theta\gamma$ where θ is the probability that an inoculum unit occurs within the pathozone (formerly ϕ): γ has two components, γ_1 and γ_2 , which represent, respectively, the probabilities of occurring a certain distance from the root surface and of infection at that distance (Gilligan, 1985).

Changes in the probability of infection or infection efficiency, γ_2 , were determined in a placement experiment which involved the positioning of single inoculum units at known distances from the host surface and scoring for the proportion of successful infections from replicate units. Soil packs were prepared as described for estimates of inoculum decay. After 7 days growth a single, isolated root, at least 50 mm in length was selected. An inoculum unit was introduced into each pack at a known distance from the selected root and 5 mm behind the root tip. Roots were inspected for disease (stelar discolouration) 21 days after inoculation. The experiment was fully randomised with 11 distances (0, 1, 2, 3, 4, 5, 6, 7, 8, 9 and 10 mm) between root and inoculum with 15 replicates for each distance.

The model used to describe the decay in the probability of infection, P_i , with distance, r , between inoculum and root was:

$$\gamma_2 = \beta_\gamma \cdot \exp(-\alpha_\gamma \cdot r^2) \quad (6.8)$$

The model had been tested previously and consistently provided accurate descriptions of the pathozone profiles of *Ggt* on wheat (Gilligan and Simons, 1987). It describes a sigmoidal decline where β_γ represents the asymptotic probability of infection and α_γ is a measure of the reduction in the probability of infection as the distance between inoculum and host, r , increases.

By accounting for the probability that a unit of inoculum is located a certain distance from a root and the probability that it infects from that distance, ϕ can be estimated from:

$$\phi = \frac{\pi L \beta}{\alpha V} [\exp(-\alpha \cdot r_r^2) - \exp(-\alpha(r_i + w)^2)] \quad (6.9)$$

(Gilligan, 1985; 1990a).

Field data

Field data describing disease progress was obtained from Rothamsted Experimental Station. Disease progress curves from a large field plot experiment (CS 212) at Rothamsted Experimental Station were examined. The experiment involved plots of first, second, fourth, fifth (or fifth and sixth in 1989) and continuous wheat crops assessed over a period of two years. Plants were assessed for total and diseased seminal and adventitious roots from mid April to harvest.

6.2.2 Results

Decay of particulate inoculum

The decay of inoculum was examined to assess the duration over which primary infection was possible and to obtain an estimate for the decay rate, α_p of particulate inoculum. The curve for the decay of inoculum was best described by the function $P = \beta_p \exp(-\alpha_p t)$ the fitting of which generated the lowest residual deviance (Table 6.1, Fig. 6.1).

Table 6.1. Summary of non-linear models used to describe the relationship between the number of propagules capable of causing disease (P) and time (t).

Model	Parameters (\pm s.e)	Residual deviance
$P = \beta_p \exp(-\alpha_p t)$	α 0.037 \pm 0.0181 β 1.00 (constrained)	53.82 on 8 d.f
$Y = \beta_p \exp(-\alpha_p t^2)$	α 0.00514 \pm 0.00613 β 0.90 \pm 0.140	83.96 on 8 d.f

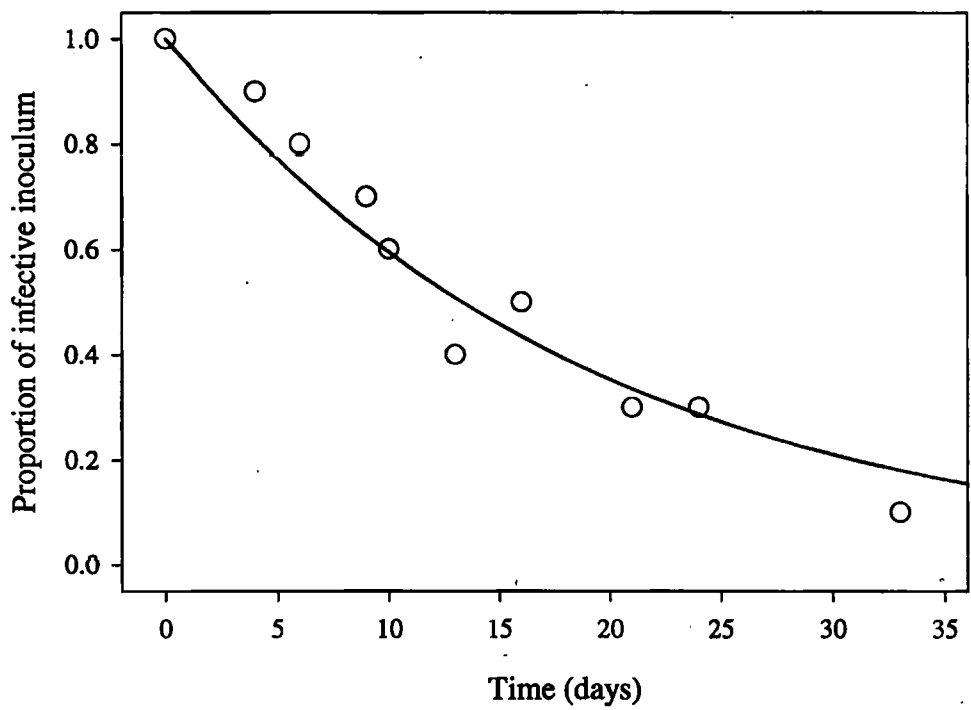


Fig. 6.1: Change in the infectivity of particulate (infested millet) inoculum of *G. graminis* over time (circles) fitted with the function $P = \beta_p \cdot \exp(-\alpha_p \cdot t)$

When extrapolated, the plot shows that less than 5% of inoculum was capable of causing disease after 57.6 days

Host growth

Two variables of host growth were monitored during the production of disease progress data. These were changes in the number of main root axes and of lateral roots over time. Main roots were produced at a constant rate throughout the duration of the experiment (Fig. 6.2a). The rate of production of main roots was greater at the higher inoculum density than the lower. A fitted regression line produced rates of 0.81 and 0.92 roots per day respectively (Table 6.2).

Table 6.2: *Summary of linear regression describing growth of main root axes over time at low ($P=15$ units l^{-1}) and high ($P=240$ units l^{-1}) densities of particulate inoculum.*

Model and inoculum density	Parameter estimates \pm s.e	Residual mean square and Goodness of fit
$N = m.t + c$		
1. $P = 240$ units l^{-1}	$m = 0.81 \pm 0.05$ $c = -6.52 \pm 2.89$	48.15 on 13 d.f (95.1%)
2. $P = 15$ units l^{-1}	$m = 0.92 \pm 0.04$ $c = -1.92 \pm 2.47$	35.39 on 13 d.f (97.1%)

The production of lateral roots was sigmoidal over time for both low and high inoculum density (Fig. 6.2b) and was described by a simple logistic function (Table 6.3)

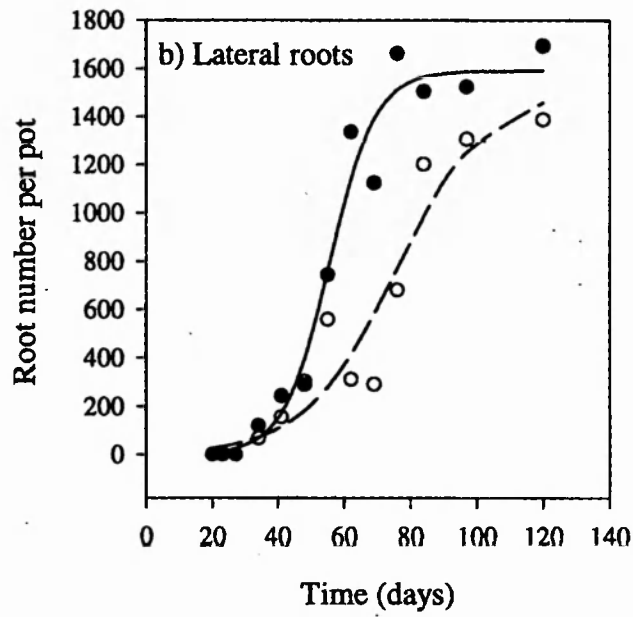
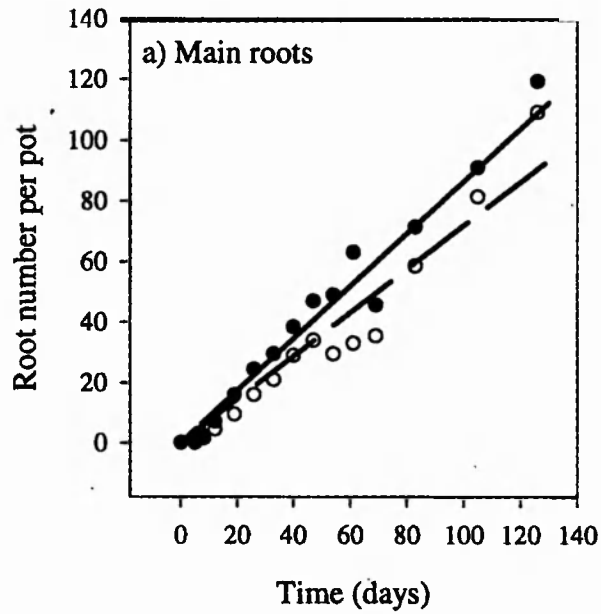


Fig. 6.2: Change in a) the number of main roots and b) the number of lateral roots over time at a low (open circles) and high (closed circles) initial density of particulate inoculum.

Table 6.3: Summary of non-linear curve fitting describing growth of lateral roots over time

Model and inoculum density	Parameter estimates \pm s.e	Residual mean square and Goodness of fit
$l = \beta_i / (1 + \exp(-\alpha_i(t - \delta_i)))$ 1. $P = 240 \text{ units l}^{-1}$	$\beta_i = 1520 \pm 202$ $\alpha_i = 0.072 \pm 0.019$ $\delta_i = 75.67 \pm 5.66$	25681 on 10 d.f (90.2%)
2. $P = 15 \text{ units l}^{-1}$	$\beta_i = 1591 \pm 74.6$ $\alpha_i = 0.140 \pm 0.03$ $\delta_i = 55.6 \pm 1.7$	17178 on 10 d.f (96.5%)

Disease progress curves and model fitting

Disease progress from a high initial inoculum density was monomolecular in shape resulting in 90% of roots becoming diseased after 140 days whilst that from a low initial inoculum density was not (Fig. 6.3a). From a low inoculum density change in the percentage of diseased roots over time was initially monomolecular, reaching a plateau after 50 days when 20% of roots had become diseased. This was followed by a sigmoidal increase in infection which culminated in an asymptote of 90% root disease after 140 days. During the experiment, plants were assessed for crown infection by *Ggt*. This did not appear until after 120 days suggesting that the predominant route for secondary infection was directly from root to root and not via the crown.

Each of models (6.1), (6.2) and (6.3) were fitted to the data in turn. Model (6.1) over-estimated disease during the later stages (after 60 days) of disease progress at the high inoculum density and produced parameter estimates that suggested an epidemic completely dominated by primary infection (Table 6.4). Moreover, model (6.1) could not reproduce the shape of curve necessary to describe disease progress at low inoculum density (Fig.

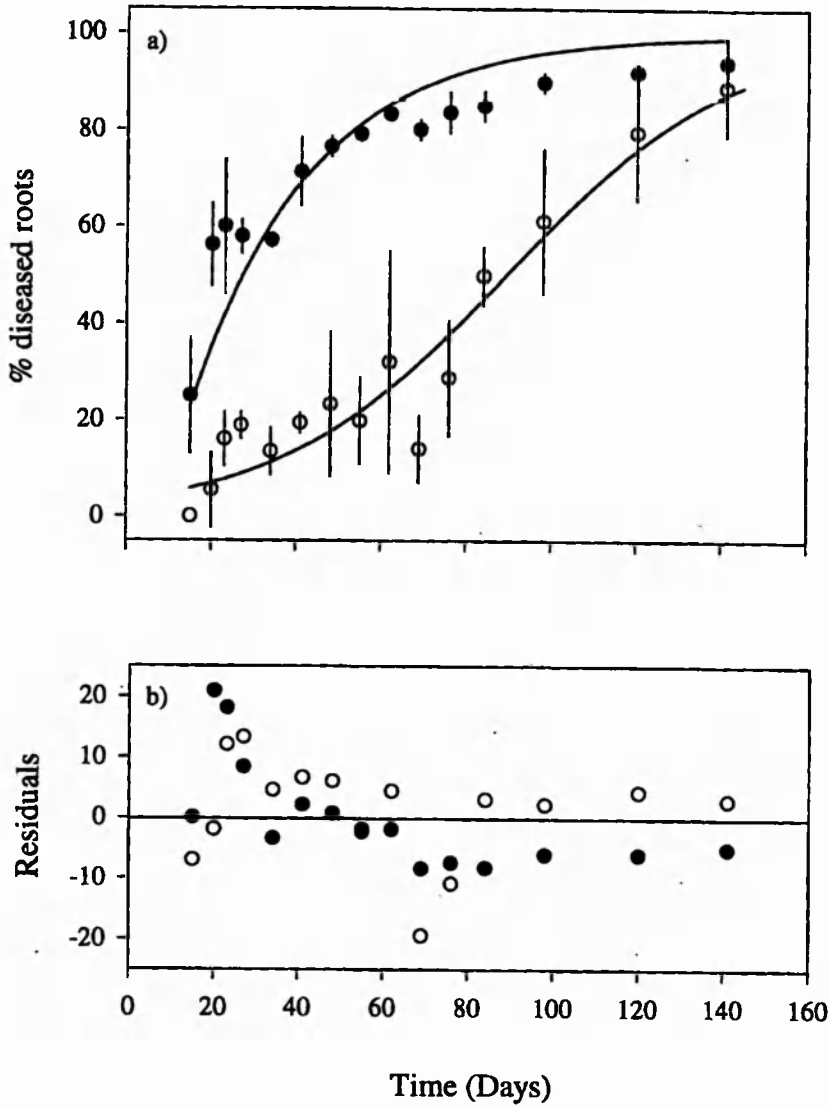


Fig. 6.3: a) Disease progress of take-all on wheat from low (open circles) and high (closed circles) initial densities of particulate inoculum. Vertical lines represent standard error of replicate observations. Data are fitted with model 6.1 where $dN_i(t)/dt = (r_p P + r_r N_i(t)) (N - N_i(t))$. b) Plot of residuals.

6.3a). The rate of disease progress increased (as opposed decreasing) during the initial phase of the epidemic, thereby under-estimating levels of primary infection. This resulted in high levels of residual variation in the same region of the curve (Fig 6.3b).

Table 6.4: Summary of curve fitting to data describing the progress of take-all on roots of wheat seedlings.

Model	Inoculum density	Parameter estimates	95% confidence limits	Residual deviance
Model 6.1	Low	$r_p = 4.7 \times 10^{-4}$ $r_s = 2.9 \times 10^{-2}$	2.27×10^{-4} to 9.75×10^{-4} 1.77×10^{-2} to 4.91×10^{-2}	12.6 _{12 d.f}
	High	$r_p = 1.5 \times 10^{-4}$ $r_s = 1.5 \times 10^{-6}$	1.46×10^{-4} to 1.78×10^{-2} Parameter not determined	13.0 _{14 d.f}
Model 6.2	Low	$r_p = 1.98 \times 10^{-3}$ $r_s = 8.19 \times 10^{-4}$	1.42×10^{-3} to 2.76×10^{-3} 6.86×10^{-4} to 9.77×10^{-4}	7.32 _{12 d.f}
	High	$r_p = 2.63 \times 10^{-3}$ $r_s = 2.00 \times 10^{-3}$	2.26×10^{-3} to 3.00×10^{-3} 1.55×10^{-3} to 2.64×10^{-3}	3.47 _{13 d.f}
Model 6.3	Low	$r_p = 5.00 \times 10^{-3}$ $r_s = 1.50 \times 10^{-3}$	3.50×10^{-3} to 7.14×10^{-3} 8.40×10^{-4} to 2.81×10^{-3}	28.4 _{12 d.f}
	High	$r_p = 1.43 \times 10^{-3}$ $r_s = 1.05 \times 10^{-3}$	1.15×10^{-3} to 1.77×10^{-3} 7.76×10^{-4} to 1.43×10^{-3}	13.3 _{13 d.f}

In contrast, model (6.2), which includes terms for inoculum decay and growth of main root axis, reproduced the shapes of disease progress curves for both initial densities of inoculum (Fig. 6.4a). Residual deviance, trends in residuals and fit to individual observations (Fig 6.4b) were all improved and parameter estimates suggested a contribution of both primary and secondary infection to the progress of disease (Table 6.4). Inclusion of a term for the transmission of disease by lateral roots (model 6.3) significantly reduced the fit of the model to disease progress curves generated from both low and high inoculum densities (Fig. 6.5a) resulting in large residual deviance (Fig. 6.5b).

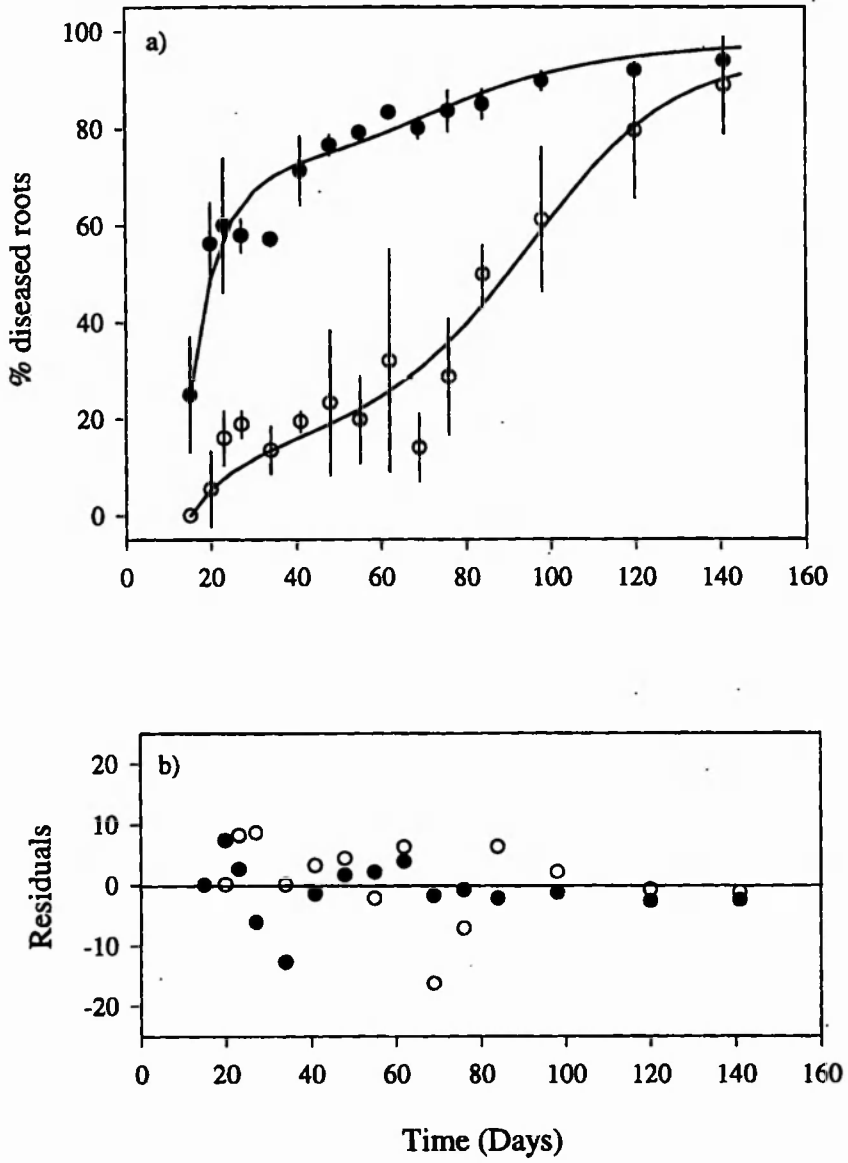


Fig. 6.4: a) Disease progress of take-all on wheat from low (open circles) and high (closed circles) initial densities of particulate inoculum. Vertical lines represent standard error of replicate observations. Data are fitted with model 6.2 where $dN_i(t)/dt = (r_p P(t) + r_s N_i(t)) (N(t) - N_i(t))$. b) Plot of residuals

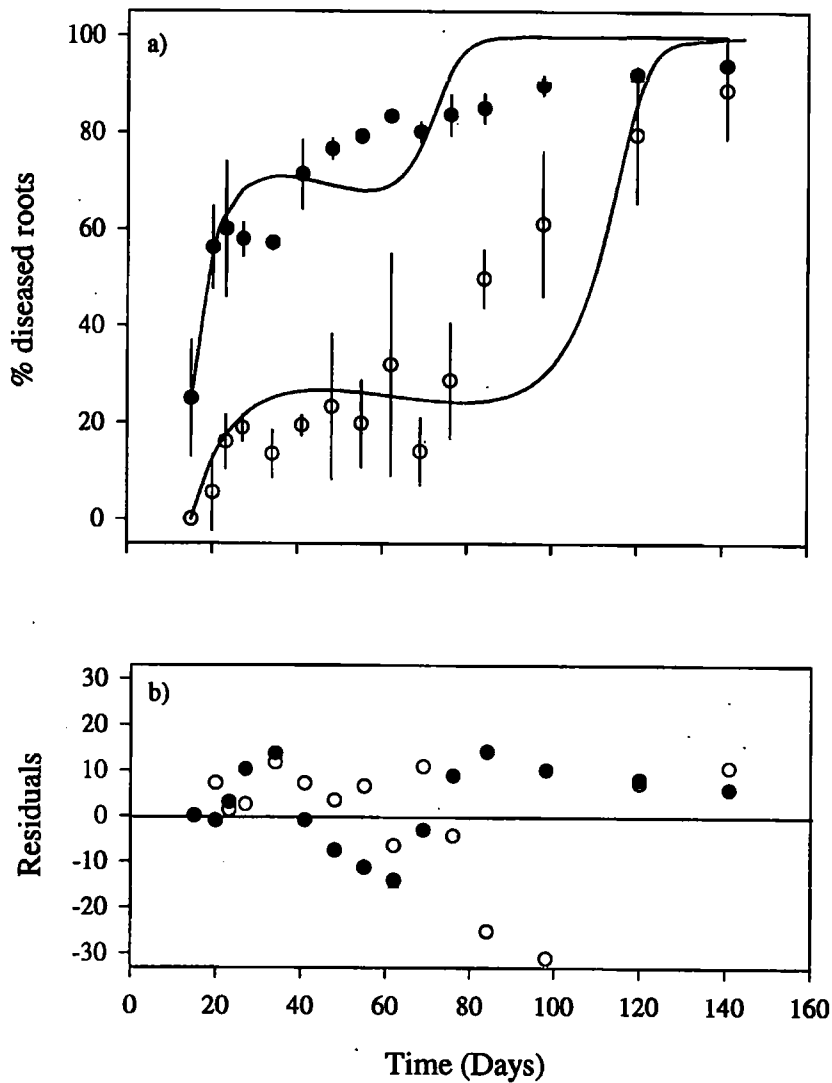


Fig. 6.5: a) Disease progress of take-all on wheat from low (open circles) and high (closed circles) initial densities of particulate inoculum. Vertical lines represent standard error of replicate observations. The data are fitted with model 6.3 where $dN_i(t)/dt = (r_p P(t) + r_s N_i(t) \cdot I(t)) (N(t) - N_i(t))$. b) Plot of residuals

Disease progress on seminal and adventitious roots

The progress of disease from the low density of particulate inoculum was examined on seminal and adventitious roots separately. On the seminal root system the shape of disease progress was similar to that on the entire root system. Disease increased monotonically, without a point of inflection, to an initial plateau when about 35% of roots were diseased (Fig. 6.6a). This was followed by an increase in the rate of infection which slowed as 100% of seminal roots became diseased. Disease progress on the adventitious roots was sigmoidal, increasing at 30 days from no disease to around 80% of roots diseased after 140 days (Fig. 6.6b).

Primary infection of seminal roots.

In order to predict the asymptotic level of disease caused by primary infection on the seminal roots of wheat plants, information regarding changes in the probability of infection when inoculum occurs at different distances from the root (pathozone dimensions) was required. The pathozone dimensions of a growing wheat root were examined in a placement experiment. Changes in the probability of disease with distance were described by the exponential function:

$$\gamma_2 = \beta_\gamma \cdot \exp(-\alpha_\gamma \cdot r^2) \quad (6.8)$$

The results of curve fitting are summarised in Table 6.5.

Table 6.5: *Summary of curve fitting using model 6.8 to relate changes in the probability of disease with distance between inoculum and root.*

Model	Parameter estimates \pm s.e	Residual deviance
$\gamma_2 = \beta_\gamma \cdot \exp(-\alpha_\gamma \cdot r^2)$	$\beta_\gamma = 1.00 \pm 0.063$ $\alpha_\gamma = 0.032 \pm 0.005$	0.014 on 9 d.f

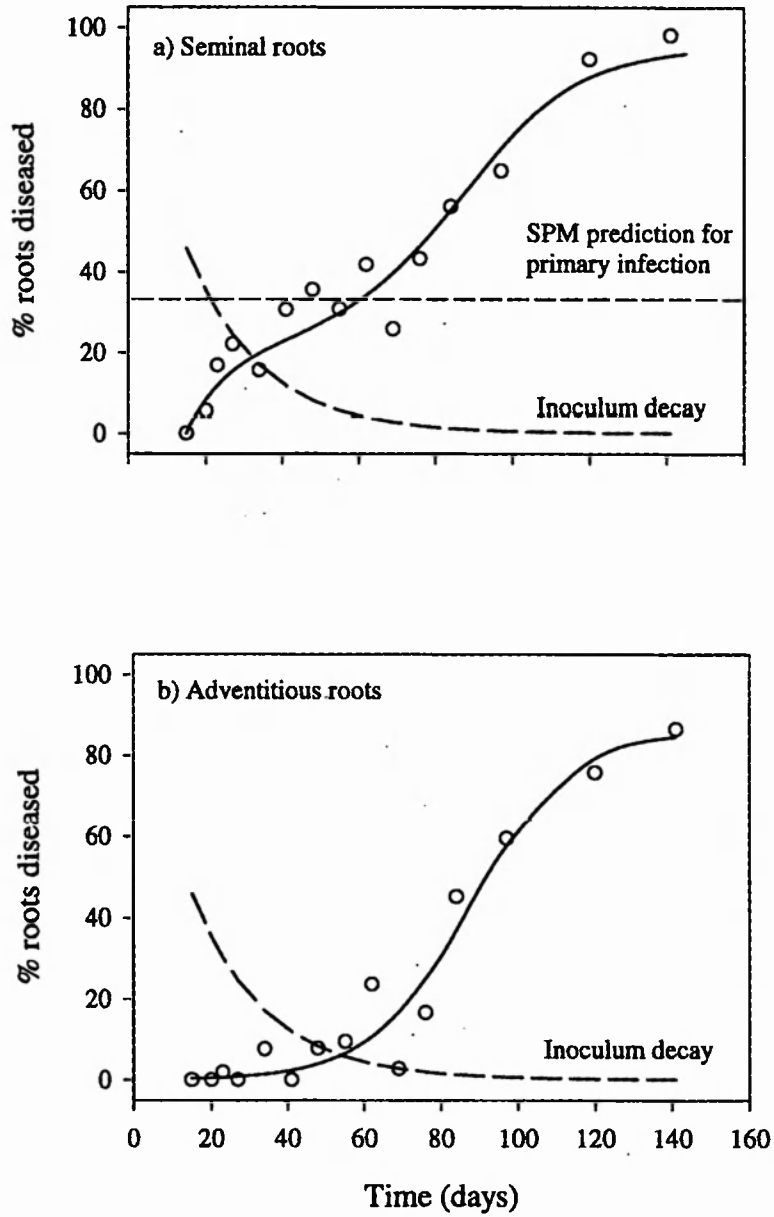


Fig. 6.6: Disease progress of take-all on a) seminal roots and b) adventitious roots of wheat from a low initial density of particulate inoculum. Decay of particulate inoculum (dashed lines) and estimates of primary infection from a simple probability model (SPM) are also shown

Using equation (6.9) to estimate ϕ for the probability model (6.7), the asymptotic level of disease caused by primary infection was predicted. Estimates of variables are listed in Table 6.6.

Table 6.6: *Values of variables used to estimate numbers of diseased seminal roots.*

Variable	Estimate
Root number (N)	25
Mean root length (L)	8.0 cm
Root radius (r_r)	0.05 cm
Inoculum unit radius (r_i)	0.1 cm
Pathozone width (w)	0.8 cm
Total soil volume (V)	883.6 cm ³

At low inoculum density, an average of 13 inoculum units were randomly distributed within the inoculum layer (volume = 883.6 cm³) from which the model predicts that primary infection would be responsible for 37.2 % of seminal roots becoming diseased. The location of this estimate with respect to disease progress on seminal roots is shown in Fig 6.6a. It corresponds to the level of the initial plateau.

Field data

Examples of typical disease progress curves from field data of experiment CS 212 (Continuous wheat) are shown in Figure 6.7 for total roots, seminal roots and adventitious roots. Time has been transformed to day degree above 5°C in order to minimise the effects of changing temperature. Curves for the percentage of infected total, seminal and adventitious roots increased over time. Another consistent feature was the high levels of disease on seminal roots (5-15%) at the beginning of disease assessment compared with the absence of diseased adventitious roots (0%).

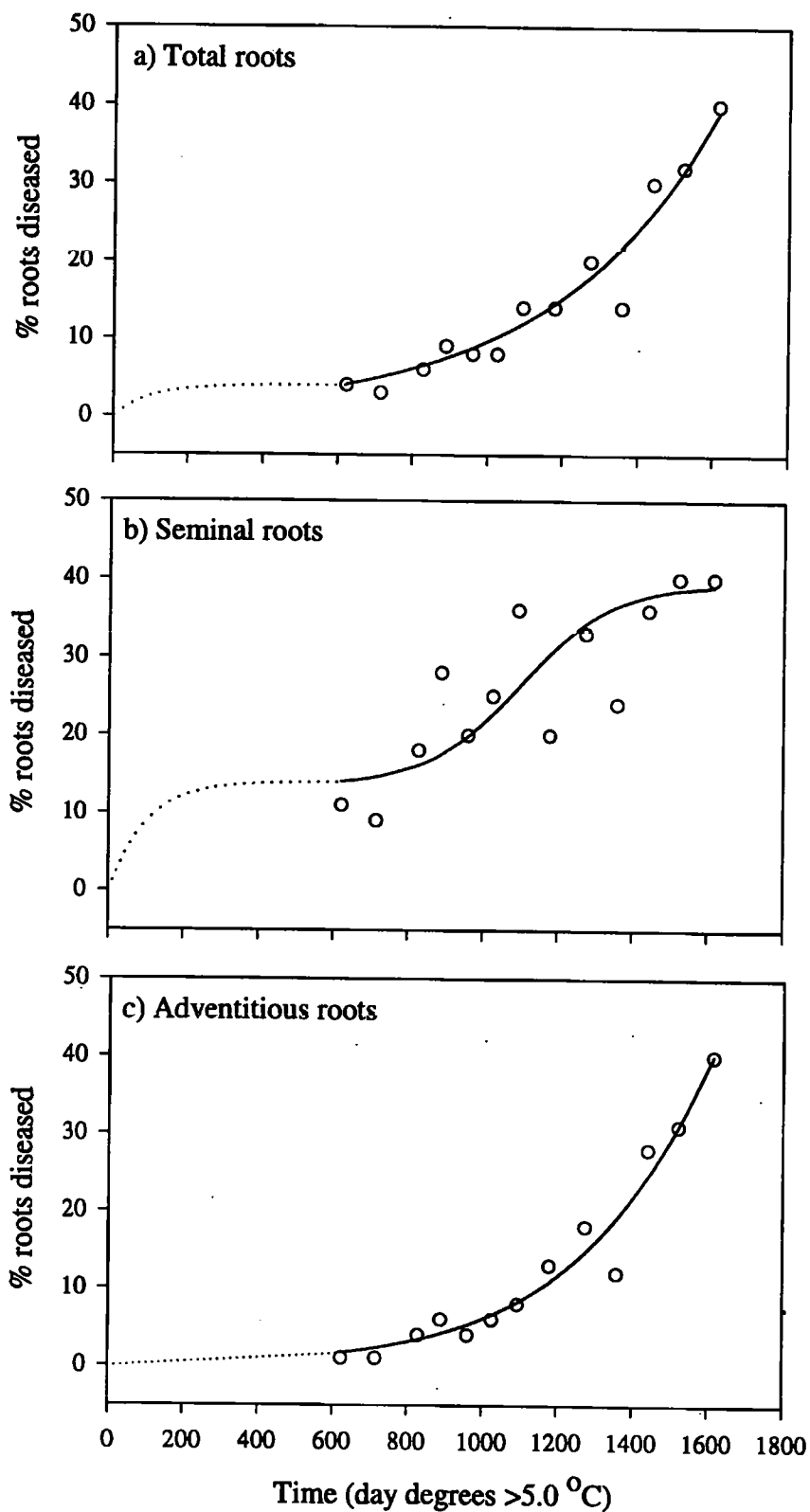


Fig. 6.7: Disease progress of take-all on a) total, b) seminal and c) adventitious roots of a continuous wheat crop grown in a field trial at IACR, Rothamsted. Symbols represent field data with solid lines (exponential for total and adventitious roots and logistic for seminal roots) used to summarise trends in data. Dashed lines represent the expected course for disease progress during the early stages of an epidemic for which no data was available.

6.2.3 Discussion

The objectives of this section were to determine the intrinsic shape of the disease progress curve describing an epidemic of take-all on wheat roots and to produce a biologically plausible mathematical model based on a coherent understanding of the dynamics of inoculum and host growth. The results suggest that there is an initial phase of primary infection as roots grow through the soil and make contact with particulate inoculum. This is followed by a phase of secondary infection from root to root stimulated by the production of susceptible roots and the spread of disease from infected roots. Two factors, decay of particulate inoculum and the growth of susceptible roots, were identified as having a major influence on the shape of the disease progress curve, particularly at low densities of initial particulate inoculum.

Decay of particulate inoculum slowed the rate of primary infection even in the presence of available susceptible roots and was responsible for the initial plateau at the low density of initial inoculum. The simple exponential rate of decay of particulate inoculum is in accordance with the findings of Yarwood and Sylvester (1959). Scott (1969) also found an exponential decay in the survival of *G. graminis* in colonised fragments of nodal wheat straw under laboratory conditions. Alternative dynamics for inoculum decay have been proposed by Diamond and Horsfall (1965) who suggested an initial lag phase when propagules are composed of more than a single inoculum unit (or in this case viable fragments of mycelium). The data provided no evidence of this.

Further evidence for the presence of consecutive phases of primary and secondary infection was provided by assessing disease progress on the seminal and adventitious roots separately. On the seminal roots, the shape of the disease progress curve was similar to that on the entire root system. Estimates of disease on seminal roots using the simple probability model predicted an asymptotic level of disease from the low density of initial inoculum

which corresponded to the height of the initial plateau (Fig. 6.6a). Disease progress on the adventitious roots did not begin until almost all particulate inoculum had lost its ability to infect. This may be due, in part, to their later emergence. From this, I conclude that, at the lower density of initial inoculum, there was an initial period of primary infection largely restricted to the seminal root system followed by the secondary infection of both seminal and adventitious roots.

The rate at which disease spread following primary infection was controlled by the availability of susceptible roots. As the number of main roots entering the soil increases, the probability that an infected root is located within the pathozone of a susceptible root increases.

One of the major criticisms of microcosm experiments is their poor relationship to the more complex ecological systems that they aim to simulate. The consistency of results describing inoculum decay and disease progress obtained from the experiments performed here under the controlled conditions of a growth cabinet at the lower initial inoculum density compared favourably with field data. The decay of particulate inoculum under field conditions has been described by several researchers (Shipton, 1981). Longevity is affected by biotic and abiotic conditions but typically decays sigmoidally or exponentially over time. Hornby (1981) presented data describing the decay in infectivity of particulate inoculum varying in size. Inocula were buried in October in outdoor pits and assayed for infectivity over a 16 month period. Decay was exponential with only the coarsest fragments (> 4.0 mm) remaining infective after May of the following year. Disease progress data were also consistent with field data. All disease progress curves showed high (between 5 and 15%) infection of seminal roots at the beginning of the sampling period in mid-April followed by an exponential increase. During the same period, levels of disease on adventitious roots was initially zero rising exponentially thereafter. These observations are consistent with the

second phase of an epidemic involving secondary infection, primary infection having already taken place.

The generic model (Model 6.1) describing disease progress from two sources of inoculum (particulate inoculum and infected roots), and therefore including terms for primary and secondary infection, failed to describe the dynamics of disease at the low initial density of particulate inoculum. When the dynamics of inoculum decay and host growth were included (model 6.2) the model described both the initial plateau and the sigmoidal increase to a second plateau thereafter.

Whilst the model fits the data well, the disparity between parameter estimates for r_s at the two inoculum densities (Table 6.4) suggests the model is still deficient in some respect. The inclusion of a term allowing lateral roots to stimulate the transmission of disease did not improve the fit of the model. However, because of the difficulty in scoring roots, no distinction was made here between infected and uninfected lateral roots. Also, temporal separation of the two phases of disease spread has not been explained. Three potential causes are considered: i) a latent period during which a root is infected and shows symptoms of disease but is not yet infectious; ii) change in root susceptibility and; iii) change in r_s with increase in host density, N . The latent period of aerial pathogens is a commonly studied component of the infection cycle (Zadoks and Schein, 1979) but has received little attention in the epidemiology of soil-borne plant pathogens (Gilligan, 1987). Changes in host susceptibility are usually linked with damping-off pathogens such as *Rhizoctonia* and *Pythium* spp. Whilst wheat roots are assumed to become more resistant to infection as they age, relatively little is known about differences in the susceptibility of the seminal roots compared with the adventitious roots. Finally, the rate of secondary infection may depend on the density of host roots in a non-linear fashion. For example, percolation theory suggests a threshold density of roots at which the pathogen would be able to spread

unconstrained by the proximity of nearby hosts (Bunde and Havlin, 1991).

The description of disease progress with two plateaux is not restricted to the infection of wheat by *Ggt* (Amorim *et al.*, 1993, for *Ustilago scitaminea* on sugarcane; Rupe and Gbur, 1995, for *Fusarium solani* on soybean) and various mathematical models have been derived to describe such dynamics (Hau *et al.*, 1993; Gilligan and Kleczkowski, 1997). However, to my knowledge, this is the first example which involves primary and secondary infection by a soil-borne plant pathogen based on the empirical description of underlying biological components.

6.3 Biological control of take-all using *Pseudomonas corrugata*.

6.3.1 Introduction

In recent years, *Pseudomonas* spp. have undergone extensive investigation for their ability to control take-all (Weller, 1988; Thomashow *et al.*, 1990). They are one of many species of so-called rhizobacteria that are commonly isolated from around the roots of wheat plants and are associated with the phenomenon of take-all decline (Cook and Weller, 1987). A variety of mechanisms by which they are able to suppress the growth of organisms such as *Ggt* has been proposed. These include competition for nutrients, competition for iron (III), the production of antibiotics and the production of hydrogen cyanide. In particular, Bull *et al.* (1991) demonstrated that the antibiotic, phenazine, plays an important part in the suppression of *Ggt* which has been directly isolated from the wheat rhizosphere (Thomashow *et al.*, 1990). The effect of these mechanisms on the spread of take-all has been observed as the suppression of primary infection and a reduction in the growth of lesions (Bull *et al.*, 1991). However, the effects of these processes have not been investigated in relation to pathozone behaviour of *Ggt* or to the sequential primary and secondary infection of disease dynamics identified in the previous section.

In this experiment, the antagonistic bacterium *Pseudomonas corrugata* (R2140) is applied to the growing root of a wheat plant challenged with particulate inoculum of *Ggt*. The dynamics of the pathozone were examined and used to predict the effect of *P. corrugata* on the progress of disease caused by primary infection using the techniques developed in Chapter 5. The characteristics of disease control described by pathozone behaviour are then assessed in relation to primary and secondary infection of take-all using model (6.2).

6.3.2 Materials and methods

Inoculum

Inocula of *Ggt* (Isolate ML5) and *P. corrugata* were prepared as described in section 2.6.2.

Placement experiment

Soil packs were prepared according to the methods described in section 2.6.2. The soil sand mixture was replaced with moist sand (Grade 1-2 mm diameter and 10% tap water). Sand was preferred to the soil-sand mixture used previously because of the improved visualisation of disease *in situ* combined with the need to assess disease non-destructively over time. Packs were sealed at the top allowing enough room for the emergence of a coleoptile and then compressed to achieve enough rigidity to stand upright. Pre-germinated seeds were introduced into the pack by making a small incision, inserting the seed and then resealing with clear, adhesive tape. The packs were placed in the growth chamber (15°C and a 16 h day) at an angle of 60° to the horizontal. After 7 days growth a single, isolated root, at least 70 mm in length and with the distal 30 mm visible was selected within each soil pack. Half the packs (selected roots) were treated with *P. corrugata*, applied to the exposed

end of the root at a rate of 100 μl (of the 1.0×10^7 cells ml^{-1}) per cm of root (to give an initial density of 1.0×10^6 cells per cm root). Single inoculum units (infested millet seed) of *Ggt* were introduced into each pack at a known distance (0, 2, 5, 8, 11, 15, 20 and 25 mm) from the selected root and 5 mm behind the root tip. The packs were fully randomised and replaced into the growth cabinet. Roots were inspected for disease (stelar discolouration) 8, 11, 14, 17 and 21 days after inoculation.

Modelling changes in the pathozone profile over time

The pathozone profiles for the probability of infection over time from millet seed inoculum were empirically described by the model:

$$P(r) = \beta \cdot \exp(-\alpha \cdot r^2) \quad (6.9)$$

The model serves as a simple, non-linear description of the profile, having an intercept at $r = 0$, a maximum, a point of inflection and a lower asymptote of zero. Fitting was done using GENSTAT (Anon, 1993) under an assumption of binomial errors because of the quantal nature of the response variate.

The pathozone model (6.9) was fitted separately to each of the pathozone profiles. This gave separate estimates of β , and α for ten profiles corresponding to five sampling times (days 5...9) with and without *P. corrugata*. The model was then tested for common parameters over the five times of observation using the methods of Ross (1987) and Gilligan (1990b). Both parameters varied significantly with time, β rising monotonically to an asymptote and α declining exponentially to zero.

The model was extended to give:

$$P(r,t) = \beta(t) \cdot \exp(-\alpha(t) \cdot r^2) \quad (6.10)$$

where the specific forms of $\beta(t)$ and $\alpha(t)$ are given below. This produced a non-linear response surface that describes the change in the pathozone profiles over time, in the presence and absence of *P.corrugata*. To examine the effects of *P. corrugata* on the dynamics of the pathozone, model (6.10) was fitted to all data and tested for common parameters over the two treatments (with and without *P. corrugata*) using the methods of Ross (1987) and Gilligan (1990b).

Predictions of disease progress

The effects of *P. corrugata* on the progress of disease of wheat seminal roots was predicted using model (6.7) in which the parameter of β and α of ϕ are time dependent and given by (6.10). Thus:

$$N_i(t) = (N - (N \cdot \exp(-\phi(t)P)) \text{ where } \phi(t) = v(t)/V . \quad (6.11)$$

The consequences of the control afforded by *P. corrugata* were investigated in relation the epidemiology of take-all using model (6.2)(varying inoculum and host growth).

6.3.3 Results

Changes in the pathozone over time

Placement of the *G. graminis* inoculum at different distances from a wheat seminal root had a marked effect on the probability of infection. The probability of infection declined with distance at all times but increased over time (Fig. 6.8a). The observed asymptotic probability of infection when inoculum was positioned at the surface of the root increased from 0.3 after 8 days to 1.0 and the outer limit of the pathozone increased from 5 mm to 25 mm after 21 days. (This was much larger than the pathozone dimensions detected in soil in the previous experiment)

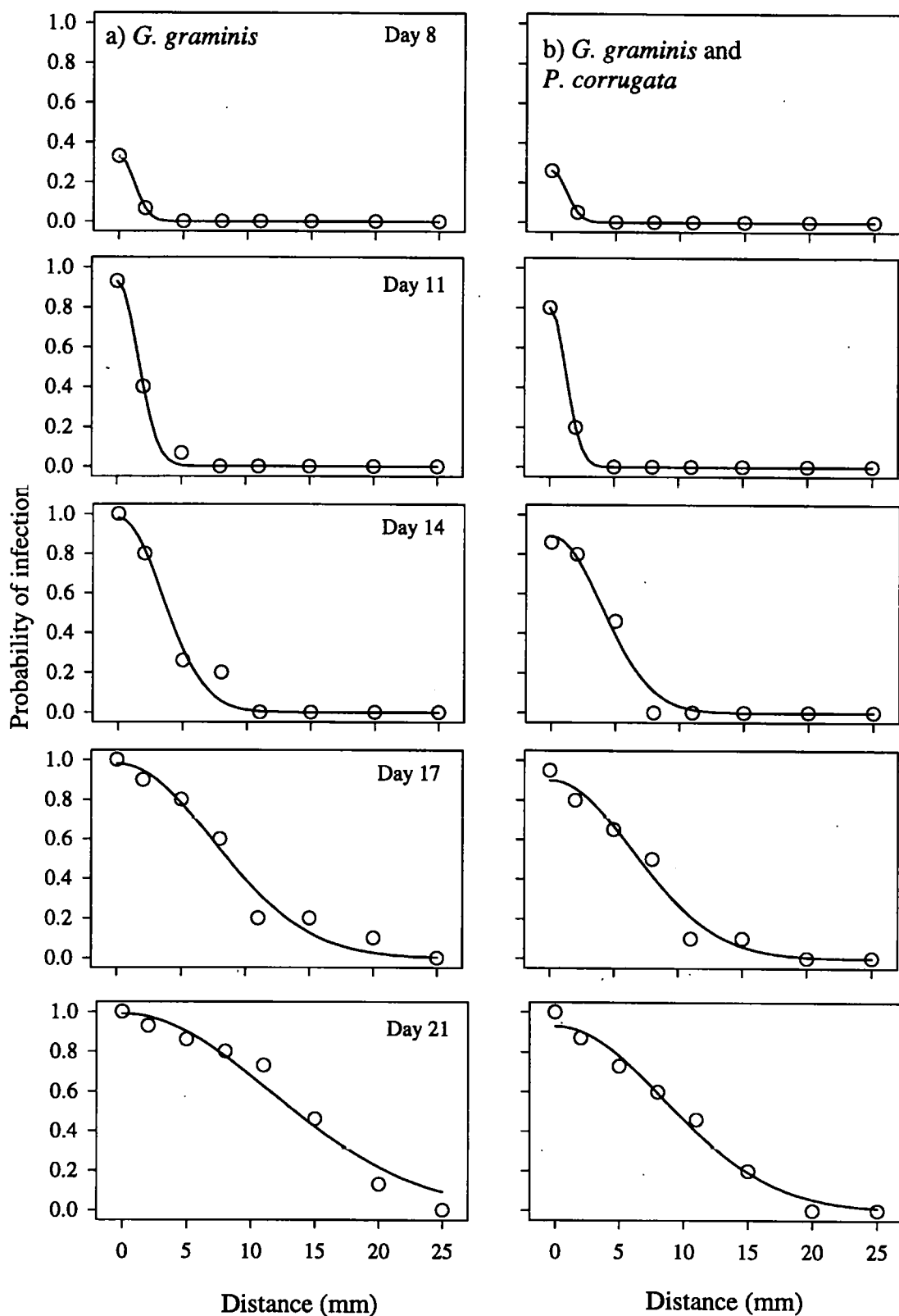


Fig. 6.8: Profiles describing changes in the probability of disease with distance between a) a wheat root and millet seed infested with *G. graminis* or b) a wheat root colonised with *P. corrugata* and millet seed infested with *G. graminis*. Data are fitted with the function $\beta = \exp(-\alpha \cdot r^2)$

The same general trends in pathozone behaviour were observed when *P. corrugata* was applied to the root surface (Fig. 6.8b). The presence of *P. corrugata* reduced the final width of the pathozone to 20 mm.

Model (6.9) provided an accurate description of the profiles describing changes in the probability of infection of wheat seminal roots by *Ggt* both in the presence and absence of *P. corrugata* (Fig. 6.8). The parameter β reflects the probability of infection when inoculum of *Ggt* is placed at the surface of the host whilst α is a measure of the rate at which the probability of infection decays with distance. β increased monotonically over time (Fig. 6.9a) whilst α declined exponentially (Fig. 6.9b). Change in β over time, t , was described by the function:

$$\beta(t) = \beta_1(1 - \exp(-\beta_2(t - \beta_3))) , \quad (6.12)$$

and for α by:

$$\alpha(t) = \alpha_1 \exp(-\alpha_2 t) . \quad (6.13)$$

Fitting model (6.10), where $\beta(t)$ is given by (6.12) and $\alpha(t)$ by (6.13), yields in the absence of *P. corrugata*:

$$\beta(t) = 0.98(1 - \exp(-0.64(t - 7.45))), \quad \alpha(t) = 3.81 \exp(-0.0001t) \quad (6.14a)$$

and in the presence of *P. corrugata*:

$$\beta(t) = 0.96(1 - \exp(-0.44(t - 7.39))), \quad \alpha(t) = 2.78 \exp(-0.0001t) \quad (6.14b)$$

The corresponding surfaces for $P(r,t)$ are given in Figure 6.10.

The effects of *P. corrugata* on the evolution of the pathozone were formally compared using model (6.10). Significant differences were detected between the parameters α_1 and

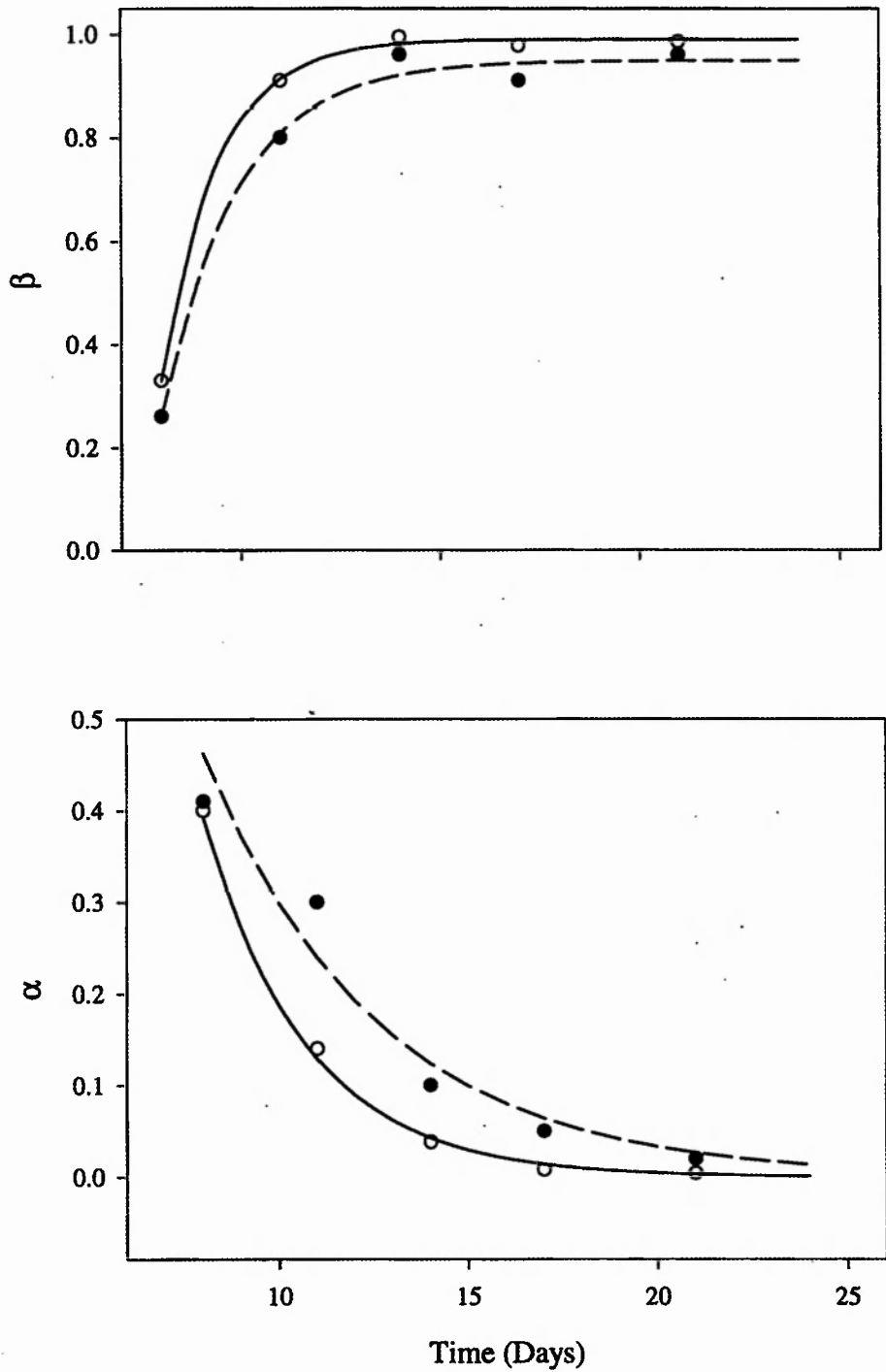
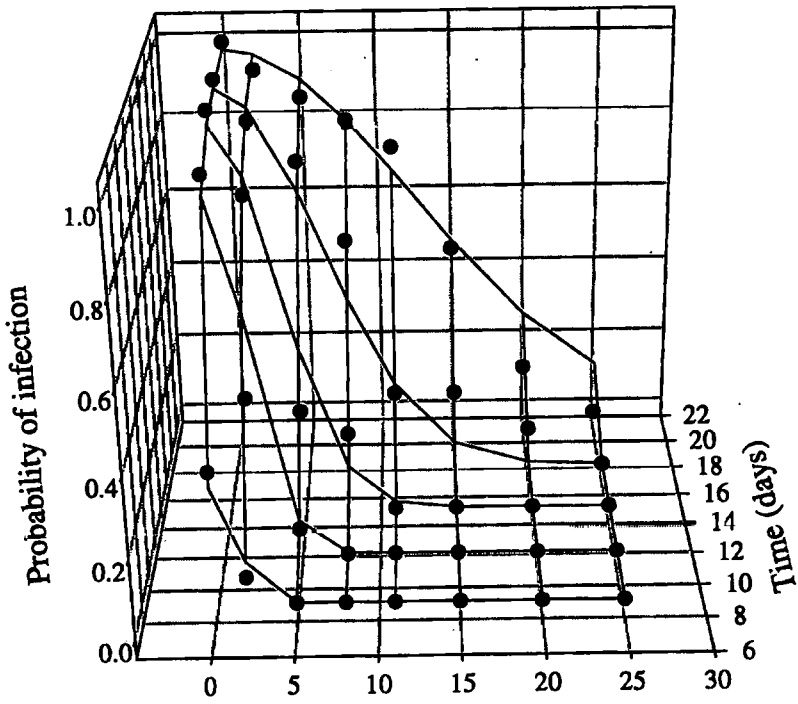


Fig. 6.9: Change in parameter values β and α over time for pathozone profiles described by the exponential function, $P(r) = \beta \cdot \exp(-\alpha \cdot r^2)$, in the presence (closed circles) and absence (open circles) of *P. corrugata*. Fitted curves were of the form $\beta(t) = \beta_1(1 - \exp(-\beta_2(t - \beta_3)))$ and $\alpha(t) = \alpha_1 \cdot \exp(-\alpha_2 \cdot t)$.

a) - *P. corrugata*



b) + *P. corrugata*

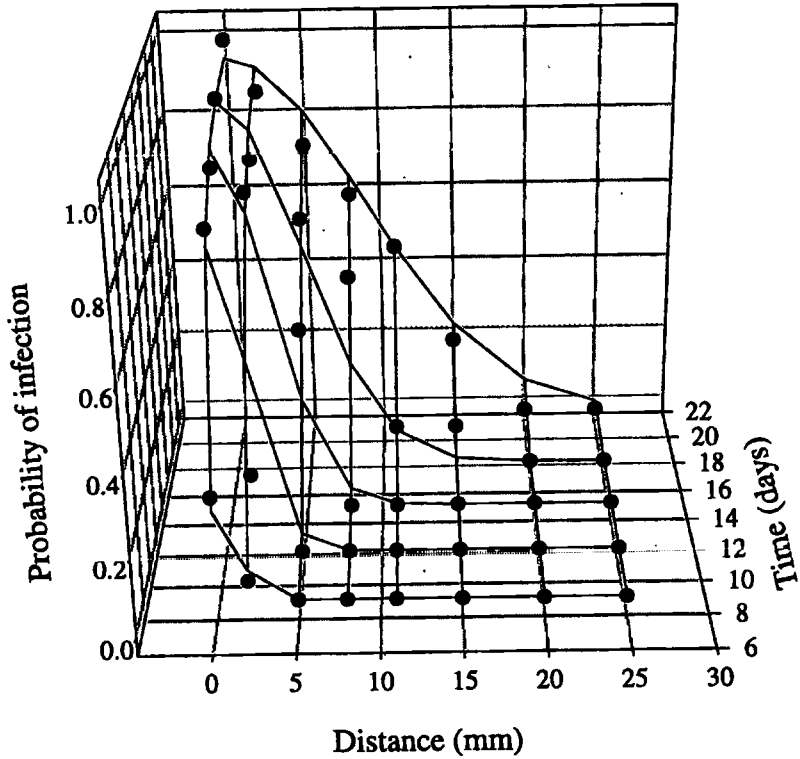


Fig. 6.10: Response surfaces of the form $P(r,t) = \beta(t) \cdot \exp(-\alpha(t) \cdot r^2)$ in a) the absence and b) the presence of *P. corrugata*.

α_2 of $\alpha(t)$ (Table 6.7) which accounted for most of the variability between treatments.

Table 6.7: Summary of parallel curve analysis comparing pathozone evolution from *Ggt* in the presence and absence of the biological control agent *P. corrugata*

Model	d.f	Residual deviance
Common model	75	4.68
β_1 varies	74	4.23
β_2 varies	74	4.44
β_3 varies	74	4.63
α_1 varies	74	3.75
α_2 varies	74	3.71
Full model	70	3.57

Predictions of disease progress

Using model (6.11), the progress of disease was predicted for protected and unprotected wheat roots (Fig. 6.11) in a similar microcosm system involving growth of wheat roots through an inoculum layer in the presence and absence of *P. corrugata*. Both disease progress curves increased monotonically with time. *P. corrugata* reduced the asymptotic prediction of disease from 90% to 77% infection.

6.3.4 Discussion

In this investigation, the pathozone profile of *Ggt* on wheat was described by the model $P = \beta \cdot \exp(-\alpha \cdot r^2)$. The probability of infection (also known as infection efficiency), P , of inoculum placed at the surface of the root is given by β whilst α describes changes in the infection efficiency of *Ggt* as the distance, r , between inoculum and root increases. The probability of infection declines with distance. This may be the result of a reduction in the

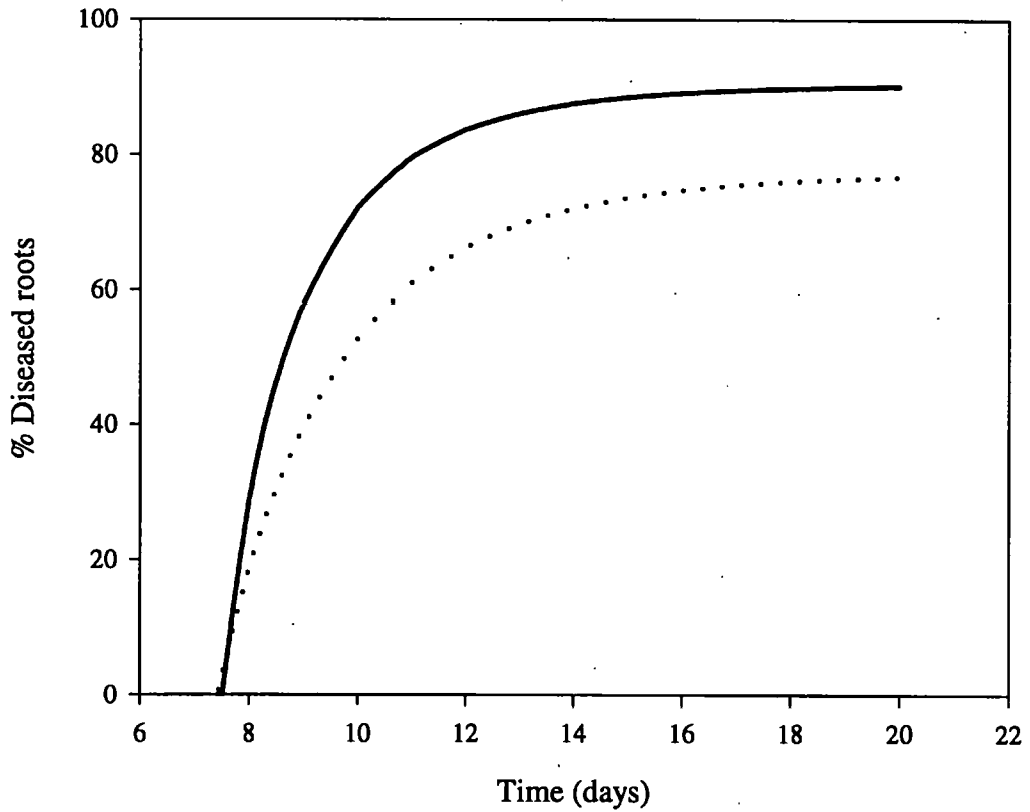


Fig. 6.11: Predictions of disease progress of *G. graminis* on seminal wheat roots in the presence (dashed line) and absence (solid line) of *P. corrugata* using $P(r,t) = \beta(t) \cdot \exp(-\alpha(t) \cdot r^2)$. Parameters estimates for $\beta(t)$ and $\alpha(t)$ were derived from placement experiments.

inoculum potential caused by a reduction in the density of mycelium making contact with the host, or by an increase in host resistance over the time taken for mycelium to grow outwards from an inoculum unit and make contact with the root. The parameter β increased monotonically over time as inoculum placed at the surface of the host germinated, colonised and infected the root (Fig. 6.9). When *P. corrugata* was applied to the surface of the root, parallel curve analysis did not detect any significant difference in β . Thus, the infection efficiency of inoculum placed at the surface of the root was not affected. Over the period of the experiment, α was significantly higher when *P. corrugata* was present. This means that *P. corrugata* suppressed disease from inoculum placed further from the root surface. The ability of *P. corrugata* to control *Ggt* depends on the relative densities of the two organisms (Bull *et. al.*, 1991) which may have favoured the biological control agent only when inoculum was placed away from the root surface. It is precisely this type of non-linear relationship that can account for the variable success of a biological control agent.

The differences in pathozone behaviour between protected and unprotected roots were used to predict disease progress on the seminal roots of a population of wheat plants. Both disease progress curves increased monotonically with time (Fig. 6.11). *Pseudomonas corrugata* reduced the asymptotic prediction of disease from 90% to 77% infection. Although this represents only a modest amount of disease control, I have demonstrated that small differences in the central region of the pathozone profile can have a large effect on disease progress (Chapter 5 section 5.3.4 and Fig. 5.12). *Pseudomonas corrugata* displays the potential to affect this region of the profile and suppresses the overall infectivity of particulate inoculum.

In section 6.2 of this chapter the epidemiology of take-all was elucidated. The spread of disease involves an initial phase of primary infection on seminal roots followed by secondary infection of both seminal and adventitious roots. A model was derived to

describe the disease progress of *Ggt* on a population of wheat roots (Model 6.2) in which $r_p P$ and $r_s N_i$ are terms for primary and secondary infection respectively. P represents the density and r_p the infectivity of particulate inoculum. Thus pathozone behaviour is subsumed within the parameter r_p . Figure 6.12a demonstrates the effects of controlling primary infection of take-all by reducing the value of r_p . When the epidemic is dominated by primary infection, disease is controlled. As the epidemic switches to secondary infection (after 60 days), disease control is lost. In Figure 6.12b the effects of controlling secondary but not primary infection are predicted by reducing the value of r_s . Although initial infection of the seminal root system is not reduced, overall control of disease is durable, lasting for the entire epidemic. From this I conclude that control of secondary infection is crucial for the long-term control of take-all on wheat.

One of the major factors determining the success of rhizobacteria in suppressing root disease is their ability to colonise the entire root system. Most research has, not surprisingly, involved the early colonisation of seminal roots which can be highly variable (Weller, 1988). Moreover, whilst colonisation of the seminal roots from treated seed is relatively efficient, colonisation of the adventitious roots is poor (Weller, 1984). Variability in the extent of colonisation has been suggested as a potential cause of the inconsistent performance of biological control of root diseases. If control is restricted to primary infection, then variability may also be associated with differences in the contribution of secondary infection during which, disease control is most likely to fail.

Although the adventitious root system may not become colonised by *P. corrugata*, the extent of secondary infection can be suppressed by reducing the infectivity of infected seminal roots. This was not examined. Hence, for a better elucidation of the effects of *P. corrugata* on the spread of *Ggt* a more complete assessment of disease transmission from the different roots (i.e. from seminal to seminal, seminal to adventitious, adventitious to

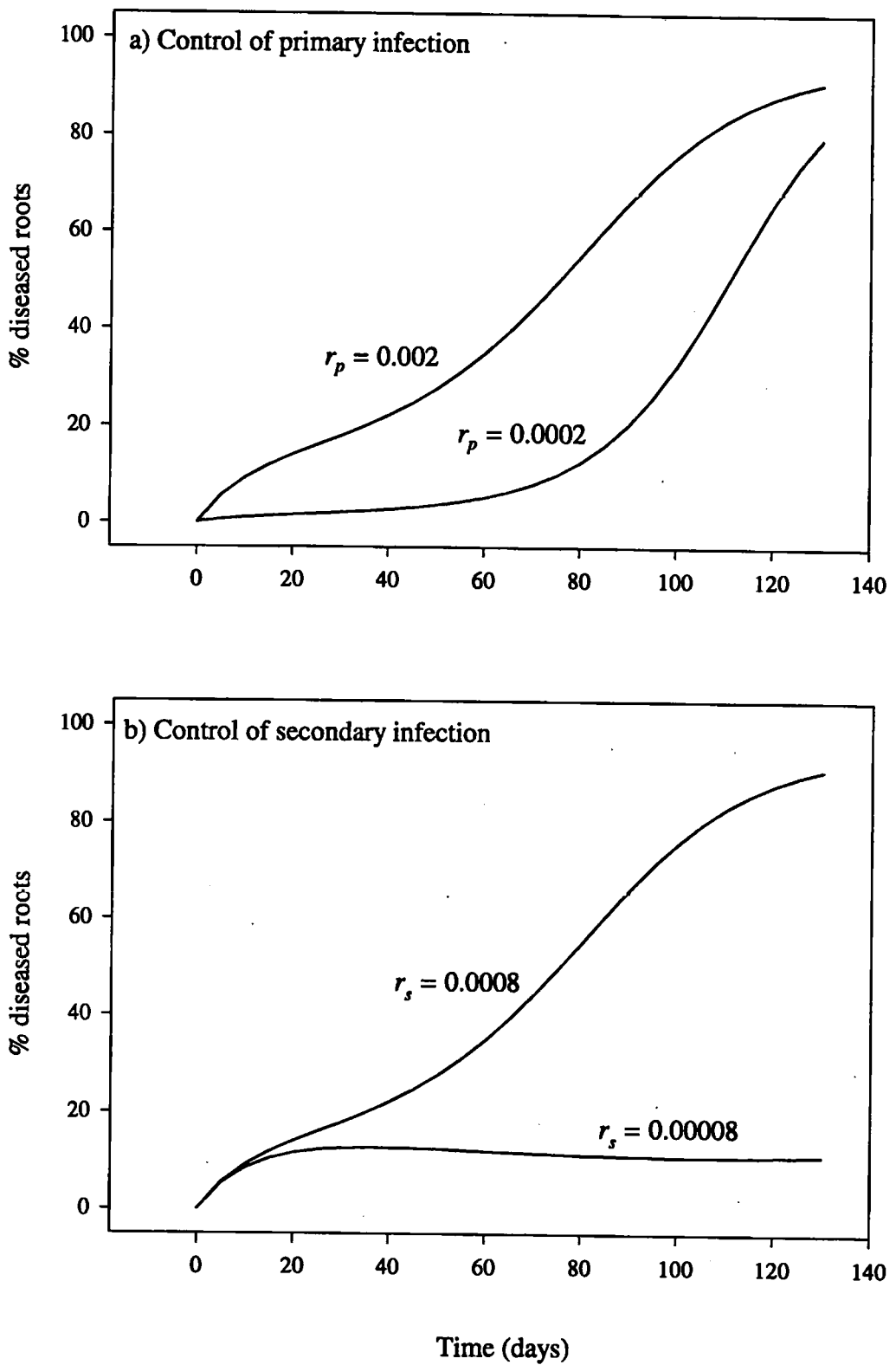


Fig 6.12: The effects of controlling a) primary and b) secondary infection. Simulations were produced using $dN_i / dt = (r_p \cdot P(t) + r_s \cdot N_i) (N(t) - N_i)$ (model 6.2) with default parameters $r_p = 0.002$ and $r_s = 0.0008$.

seminal etc) in the presence and absence of the control agent is necessary.

Chapter seven

Discussion

Following the pioneering work of Vanderplank (1963), disease progress curves, in combination with mathematical modelling, provide a powerful tool for the analysis and mathematical description of disease. The models have become more sophisticated with respect to their biological foundation (Jeger, 1987; Brassett and Gilligan, 1988a; Swinton and Anderson, 1995; Gilligan and Kleczkowski, 1997) but, in contrast to large simulation models, are still constructed with relatively few parameters. This improves the chances of providing analytical solutions, making the models particularly useful for studying conditions that will bring a system to equilibrium and for examining the stability of a system. The improvements of statistical software, for example SAS (Anon, 1982), Genstat (Anon, 1993) and MLP (Ross, 1987), have removed the mathematical constraints imposed by the need for straight-line transformation of data allowing for the direct comparison of non-linear disease progress curves (Gilligan, 1990b). Even the parameters of mathematically intractable models, for which no analytical solutions are available, can be estimated using numerical fitting procedures, for example Facsimile (Anon, 1995). Rarely, however, have the shapes of disease progress curves been related directly to the dynamics of underlying components. Indeed, a detailed knowledge of these components is not only required for the interpretation of parameter estimates but also for the selection of an appropriate model with which to describe the system. This will, in turn, lead ultimately to the optimisation of disease control.

This investigation focused on the behaviour of inoculum and its role in the spread of soil-borne plant disease. Two types of inoculum were identified: particulate inoculum

which causes primary infection; and the infected host which is responsible for secondary infection. The rationale of the study was to examine the behaviour of inoculum in relation to disease progress in two contrasting host-pathogen systems, the infection of radish by *Rhizoctonia solani* and the infection of wheat by *Gaeumannomyces graminis* var. *tritici*. The infection of radish by *R. solani* represents a relatively simple system involving a single cohort of host plants. Growth of *R. solani* is predominantly over the soil surface towards a fixed infection court, the hypocotyl, which is limited in size. Consequently, biological control was relatively easy to effect by placing *Trichoderma viride* close to the hypocotyl. The system was selected for its simplicity to provide the best possible chance with which to establish a clear relationship between the behaviour of inoculum and the progress of disease under controlled conditions. The infection of wheat roots by *Ggt* represents a more complex epidemiological system. Its dynamics are complicated by the growth (movement) of roots through the soil which means that successful biological control by an introduced antagonist, such as *Pseudomonas corrugata*, is more difficult to achieve. The infection court is not restricted to a single site and, following infection, the plant may respond by the production of additional lateral and main roots. Because of the relative complexity of the two systems, the progress of disease involving *R. solani* on radish was predicted from the behaviour of inoculum whilst for the infection of wheat by *Ggt*, inoculum dynamics were used to interpret the shape of disease progress curves.

Types of inoculum vary according to their infectivity which can be characterised by the pathozone profile. The pathozone profile measures changes in the probability of disease, or infection efficiency, when inoculum is placed at different distances from the host. Three major components that dictate the shape of the pathozone for *R. solani* on radish were identified in chapter three. These were: the germinability of inoculum, the density and distribution of mycelium within the fungal colony, and the infectivity of the mycelium that

makes contact with the host. The last of these components, the infectivity of mycelium that makes contact with the host, encompasses both the inoculum potential of the pathogen (*sensu* Garrett, 1970) and the susceptibility of the host. In chapter 3, the means and variances (where appropriate) of the three components were estimated for two types of particulate inoculum and successfully used to predict the shapes of the respective pathozones. Damping-off disease is commonly characterised by a rapid decline in the susceptibility of the host as it ages. However, the decline in the probability of disease with distance (and therefore host age) was not found to be the result of an decline in host susceptibility, but was caused by a reduction in the density of mycelium in the fungal colony as it reaches the host.

The components of pathozone infection can be used to interpret the relative contribution of host and inoculum factors to disease. In this study, the behaviour of inoculum was restricted to a single isolate of *R. solani*, selected for its consistent performance in pathogenicity tests. The isolate, R5, was particularly capable of causing disease even after the seedling had emerged. However, *Rhizoctonia solani* is a species which expresses considerable genetic variation (Cubeta and Vilgalys, 1997) resulting in variable growth and pathogenicity. Thus, one might expect the relative contribution of host and inoculum factors to vary between isolate-host combinations and therefore affect the shape of the profile. For example, when the inoculum potential of isolate R3 (AG-4) was examined by Benson and Baker (1974b), radish seedlings became almost completely resistant to damping-off after only three days. Since the experiment involved assessing disease according to the levels of host emergence, this isolate may only be capable of causing disease during the early stages of host germination. A pathozone profile for such an isolate would be expected to be dominated by changes in host susceptibility.

The growth dynamics of mycelium of *R. solani* from particulate inoculum and an

infected plant were compared using the immunoblotting technique (chapter 4). Growth from an infected radish seedling was rapid achieving a high mycelial density near to the host surface and extending to a radial distance of more than three times that of particulate (mycelial disc) inoculum. Consequently, the inoculum was highly infective when it occurred close to an uninfected radish seedling with a corresponding increase in the width of the pathozone. Immunological (Dewey *et al.*, 1997) and molecular (Keller *et al.*, 1995) techniques for the detailed and specific detection of soil-borne plant pathogens have recently been developed which offer new potential for monitoring fungal dynamics. The results here show a clear application of one such technique in analysing colony dynamics.

The components of pathozone infection from particulate and infected plant inoculum were summarised by the critical exponential and logistic functions respectively. By allowing selected parameters of these equations to vary with time, the pathozone dynamics of individual plants were used to predict disease progress amongst a population of host plants for epidemics dominated by either primary or secondary infection. In this simple system, it was possible to predict disease progress accurately for monocyclic disease both in unprotected crops and in crops protected by *T. viride*. A particular feature of the behaviour of the model describing monocyclic disease was the sensitivity of the asymptotic level of disease to small changes in the outer extent of the profile. By combining a function for changes in the probability of occurrence with distance (based on the distribution of particulate inoculum) with changes in the probability of infection with distance (the pathozone profile), it was possible to identify the portion of particulate inoculum that contributes most to primary infection. Information of this type can then be used to optimise disease control by identifying critical properties of pathozone behaviour that affect disease progress.

The reason that predictions of monocyclic disease were successful was because the

epidemiological system (infectivity of inoculum, susceptibility of the host, placement of inoculum and host) was precisely defined and the growth conditions (light, moisture, temperature) were carefully controlled for the duration of the experiment. Polycyclic disease was also accurately predicted in the absence of biological control but failed in the presence of *T. viride* at the point when the epidemic switched from primary to secondary infection. It is noted, however, that small differences in primary infection caused, for example, by the presence of a biological control agent, may, when combined with a rapid, non-linear increase in secondary infection, together with an interruption of transients (as the host becomes resistant or inoculum becomes less infective) result in large variability in final levels of disease (Kleczkowski *et al.*, 1996). Alternatively, because of the length of such experiments, they are prone to time-dependent factors that are not detected when modelling the behaviour of single plants but which significantly alter the course of disease progress later on in an epidemic. Thus, the minimum requirements that I would recommend for accurate predictions of disease over an extended period, even in this simple system, involve measurement of changes in host susceptibility, the infectivity of inoculum, the biological control agent, the biotic and abiotic environment and the spatial dynamics of each of each component. Unfortunately, mathematical prediction involving such a large number of components will involve many parameters, making fitting of the model to disease data difficult. Hence, the next logical step would be to identify appropriate forms of parsimonious non-linear models which are able to summarise these key processes. This strategy was used in chapter 3 to summarise the behaviour of the infection components that determine the shape of the pathozone.

Much research is currently focused on the detailed behaviour of organisms which exist in the rhizosphere. Typically the work involves examination of single roots or plants at a single time of observation. Little is known about how this behaviour affects a population

of plants. By successfully predicting disease progress and biological control from the pathozone behaviour of single plants, which is, in turn, linked to specific components of infection, the work on *R. solani* and radish provides a highly repeatable model host-parasite system with which to address this and other related problems.

For the progress of take-all disease on winter wheat, the study has identified two distinct phases of infection. There is an initial phase of primary infection by *Ggt* as roots grow through the soil and encounter inoculum but the rate of primary infection slows progressively as particulate inoculum decays. This is followed by an acceleration in the rate of secondary infection stimulated by the increase in availability of infected tissue as a source of inoculum and in the availability of susceptible tissue for infection. Moreover, at a lower density of initial particulate inoculum, primary infection was almost entirely restricted to the seminal root system, whilst secondary infection affected both the seminal and the adventitious roots. This behaviour was consistent with field observations and provides an important biologically driven, mathematical framework with which to examine and optimise disease control. The study also showed that it was possible to suppress primary infection by adding the bacterial antagonist *Pseudomonas corrugata* to the surface of a root. Colonisation of seminal wheat roots by *Pseudomonas* spp. from treated seed is relatively successful (Weller, 1984). However, the model for primary and secondary infection predicts that sustained control can be achieved only by suppressing secondary infection. This does not mean that colonisation of the adventitious roots by *P. corrugata* is crucial. The probability of passing infection from one root to another will depend on the combined infectivity of the donor seminal root and the susceptibility of the recipient root. Whilst colonisation of both root types may provide enhanced control, colonisation of the donor may be sufficient to prevent root to root transmission of disease.

The relative benefits of controlling disease on either the seminal or adventitious roots

also depends on their contributions to the water and mineral requirements and thus the yield of the plant. The seminal roots supply the majority of water and nutrients for the plant to become established. Ultimately, they grow deeper than adventitious roots and may be important during periods of drought when they are able to access water deeper in the soil profile (Innes and Quarrie, 1987). As the wheat plant develops, its water and mineral requirements are increasingly met by the adventitious roots. It follows then, that the contribution of the two root systems to the yield of the plant and the benefits gained by protecting them depends on soil water availability throughout the growing season.

Two areas of research that require urgent attention and are a logical progression from the work described in this study were identified. The first relates to the *R. solani*-radish system. The selection of an appropriate model is crucial if the behaviour of its parameters are to be interpreted with any degree of confidence. Models for botanical epidemics generally assume homogeneous (or complete) mixing. That is to say, the probability of disease transmission from an inoculum unit to a susceptible host is the same for all hosts. This may be a reasonable approximation for primary infection when particulate inoculum is randomly dispersed. It is not, however, tenable for secondary infection where the probability of infection depends on the distance between host and inoculum. For this reason, a cellular automaton was used to model polycyclic disease (Chapter 5). Further work is necessary to identify appropriate functional forms of differential equations with which to model botanical epidemics involving secondary infection and heterogeneous mixing. The *Rhizoctonia*-radish system is well suited for the empirical verification of such models.

Because of its complexity, the *Ggt*-wheat system was not as well defined as the *Rhizoctonia*-radish system. Primary infection was predicted from pathozone profiles, but secondary infection was driven by the growth of roots. There is an urgent need to link

disease transmission with host growth. The *Ggt*-wheat system involves three different types of root (seminal, adventitious and lateral) yet little is known about the transmission of disease from one root to another or for the transmission of a biological control agent between different roots. Further work on a probability matrix for transmission coefficients relating to the different types of root is needed. Once infected, the wheat plant has the capacity to compensate by the production of additional roots. The host functional response (i.e. the relationship between root growth and disease severity) has been introduced theoretically (Gilligan, 1994) and studied experimentally for stem canker on potatoes (Gilligan *et al.*, 1997), and has the potential to offer insight onto the levels of control necessary to allow the host to tolerate disease. This response has not been included in the functional form of models describing disease progress of botanical epidemics in the present work.

In conclusion, the prospects for advancing our understanding of root infecting plant pathogens and their biological control are good. In combination with improved techniques for the mathematical description of disease dynamics, experimental methods for providing relevant data have been enhanced by molecular techniques for detection and quantification. For example, monoclonal antibody (Dewey *et al.*, 1997; Thornton *et al.*, 1993; Thornton *et al.*, 1994; Thornton, 1996) and DNA-based (Keller, 1995) protocols have been developed for detection of *Rhizoctonia*, *Trichoderma* and *Ggt* in soil, *Lux* transformed bacterial control agents are available with which to assess colonisation of the root system by the bacterial antagonist *P. corrugata* (Ratray *et al.*, 1995), and *in situ* scanning techniques have recently been developed to assess the spatial development of wheat roots over time (Grose *et al.*, 1997). This work has shown that, in a well defined and carefully controlled epidemiological system (the infection of radish by *R. solani*), it is possible to scale up from components of disease that affect single plants to the progress of disease amongst a

population of plants. The accurate extrapolation of behaviour at the detailed level to that at the population level is a crucial factor which will contribute to a clearer understanding of the implications of rhizosphere studies. Furthermore, the combination of experimentation and mathematical modelling has provided a lucid explanation for the disease dynamics in a more complex epidemiological system (the infection of wheat by *Ggt* on wheat). These results will ultimately lead to the improvement of disease forecasting and consequently to more effective measures for disease control.

References

- Amorim L, Filho AB, Hau B. 1993.** Analysis of progress curves of sugarcane smut on different cultivars using functions of double sigmoid pattern. *Phytopathology* **83**, 933-936.
- Anon. 1982.** *SAS users guide: Statistics*. SAS Institute Inc, Cary, North Carolina.
- Anon. 1993.** *Genstat 5 Reference Manual*. Oxford University Press, Oxford.
- Anon. 1995.** *Facsimile: Process and chemical reaction modeller*. AEA Technology, Didcot, Oxfordshire.
- Armentrout VN, Downer AJ. 1987.** Infection cushion development by *Rhizoctonia solani* on cotton. *Phytopathology* **77**, 619-23.
- Asher MJC, Shipton PJ. 1981.** *Biology and Control of Take-all*. Academic Press, New York.
- Baker CJ, Bateman DF. 1978.** Cutin degradation by plant pathogenic fungi. *Phytopathology* **68**, 1577-1584.
- Baker KF. 1970.** Types of *Rhizoctonia* diseases and their occurrence. In: Parmeter JR, ed. *Rhizoctonia solani, Biology and Ecology*. University of California Press, Los Angeles. 125-148.
- Baker R. 1971.** Analysis involving inoculum density of soil-borne plant pathogens in epidemiology. *Phytopathology* **61**, 1280-1292.
- Baker R. 1990.** An overview of current strategies and models for biological control In: Hornby D, ed. *An Overview of Current and Future Strategies and Models for Biological Control*. C.A.B International, Wallingford, Oxon. 375-388.
- Baker R, Martinson CA. 1970.** Epidemiology of diseases caused by *Rhizoctonia solani*. In: Parmeter JR, ed. *Biology and Pathology of Rhizoctonia solani*. University of California Press. London. 172-188.
- Baker R, Maurer CL, Maurer RA. 1967.** Ecology of plant pathogens in soil. VII. Mathematical models and inoculum density. *Phytopathology* **57**, 662-66.

- Bald JG. 1969.** Estimation of leaf area and lesion sizes for studies on soil-borne pathogens. *Phytopathology* **59**, 1606-1612.
- Bateman DF, Lumsden RD. 1965.** Relation of calcium content and nature of the pectic substances in bean hypocotyls of different ages to susceptibility to an isolate of *Rhizoctonia solani*. *Phytopathology* **55**, 734-738.
- Benson DM, Baker R. 1974a.** Epidemiology of *Rhizoctonia solani* preemergence damping-off of radish: influence of pentachloronitrobenzene. *Phytopathology* **64**, 38-40.
- Benson DM, Baker R. 1974b.** Epidemiology of *Rhizoctonia solani* preemergence damping-off of radish: inoculum potential and disease potential interaction. *Phytopathology* **64**, 957-62.
- Benson DM, Baker R. 1974c.** Epidemiology of *Rhizoctonia solani* preemergence damping-off of radish: survival. *Phytopathology* **64**, 1163-1168.
- Berger RD, Jones JW. 1985.** A general model for disease progress with functions for variable latency and lesion expansion on growing host plants. *Phytopathology* **75**, 792-97.
- Boddy L. 1993.** Saprotrophic cord-forming fungi: warfare strategies and other ecological aspects. *Mycological Research* **97**, 641-655.
- Bolton RG, Boddy L. 1993.** Characteristics of the spatial aspects of foraging mycelial cord systems using fractal geometry. *Mycological Research* **97**, 762-768.
- Bolton RG, Morris CW, Boddy L. 1991.** Non destructive quantification of growth and regression of mycelial cords using image analysis. *Binary* **3**, 127-132.
- Brassett PR, Gilligan CA. 1988a.** A model for primary and secondary infection in botanical epidemics. *Zeitschrift Fur Pflanzenkrankheiten Und Pflanzenschutz* **95**, 352-60.
- Brassett PR, Gilligan CA. 1988b.** Fitting of simple models for field disease progress data for the take-all fungus. *Plant Pathology* **38**, 397-407.
- Brassett PR, Gilligan CA. 1990.** Effects of self-sown wheat on levels of the take-all disease on seedlings of winter wheat grown in a model system. *Phytopathologische Zeitschrift* **129**, 46-57.

- Brian PW, McGowan JC. 1945.** Viridin: A highly fungistatic substance produced by *Trichoderma viride*. *Nature* **156**, 144-145.
- Bull CT, Weller DM, Thomashow LS. 1991.** Relationship between root colonisation and suppression of *Gaeumannomyces graminis* var. *tritici* by *Pseudomonas fluorescens* strain 2-79. *Phytopathology* **81**, 954-959.
- Bunde A, Havlin S. 1991.** *Percolation I: Epidemics and Forest Fires*. In: Bunde A, Havlin S, eds. *Fractals and Disordered Systems*. Springer-Verlag, Berlin. 51-96.
- Burr TJ, Scroth MN, Suslow T. 1978.** Increased potato yields by treatment of seed pieces with specific strains of *Pseudomonas fluorescens* and *P. putida*. *Phytopathology* **68**, 1377-1383.
- Campbell RC. 1989.** *Statistics for Biologists*. Cambridge University Press, Cambridge.
- Chet I. 1990.** Biological control of soil-borne plant pathogens with fungal antagonists in combination with soil treatments. In: Hornby D, ed. *Biological Control of Soil-borne Plant Pathogens*. CAB International, Wiltshire. 15-26.
- Coley-Smith JR, Ridout CJ, Mitchell CM, Lynch JM. 1991.** Control of bottom rot disease of lettuce (*Rhizoctonia solani*) using preparations of *Trichoderma viride*, *T. harmarum* or tolclofos methyl. *Plant Pathology* **40**, 359-366.
- Cook RJ. 1981.** The effect of soil reaction and physical conditions. In: Asher MJC, Shipton PJ, eds. *Biology and Control of Take-all*. Academic Press, New York. 343-352.
- Cook RJ. 1993.** Making better use of introduced microorganisms for biological control of plant pathogens. *Annual Review of Phytopathology* **31**, 53-80.
- Cook RJ, Rovira AD. 1976.** The role of bacteria in the biological control of *Gaeumannomyces graminis* by suppressive soils. *Soil Biology and Biochemistry* **8**, 269-273.
- Cook RJ, Weller DM. 1987.** Management of take-all in consecutive crops of wheat or barley. In: Chet I, ed. *Innovative Approaches to Plant Disease Control*. Wiley, New York. 41-76.
- Cooke RC, Rayner ADM. 1984.** *Ecology of saprophytic fungi*. Longman, London.

- Cooke RC, Whipps JM. 1993.** *Ecophysiology of fungi*. Blackwell Scientific Publications, London. 210.
- Cooper, RM. 1983.** The mechanisms and significance of enzyme degradation of host cell walls. In: Callow JA, ed. *Biochemical Plant Pathology*. Wiley, Chichester. 101-136.
- Cubeta MA, Vilgalys R. 1997.** Population biology of the *Rhizoctonia solani* complex. *Phytopathology* 4, 480-484.
- Cunningham PC. 1981.** Isolation and culture. In: Asher MJC, Shipton PJ, eds. *Biology and Control of Take-all*. Academic Press, New York. 103-124.
- Deacon JW. 1987.** Programmed cortical senescence: a basis for understanding root infection. In: Pegg CF, Ayres PG, eds. *Fungal Infection of Plants*. Cambridge University Press, Cambridge. 285-297.
- Deacon JW. 1996.** Ecological implications of recognition events in the pre-infection stages of root pathogens. *New Phytologist* 133, 135-145.
- Deacon JW, Henry CM. 1980.** Age of wheat and barley roots and infection by *Gaeumannomyces graminis* var. *tritici*. *Soil Biology and Biochemistry* 12, 113-118.
- Defago G, Berling CH, Burger U, Haas D, Kahr G, Keel C, Voisard C, Wirthner P, Wüthrich B. 1990.** In: Hornby D, ed. *Biological Control of Soil-borne Plant Pathogens*. CAB International, Oxon. 93-108.
- Dennis C, Webster J. 1971.** Antagonistic properties of species-groups of *Trichoderma*. I. Production of non-volatile antibiotics. *Transactions of the British Mycological Society* 57, 25-39.
- Dewey FM, Thornton CR, Gilligan CA. 1997.** Use of monoclonal antibodies to detect, quantify and visualise fungi in soils. In: Tommerup IC, Andrews JH, eds. *Advances in Botanical Research*. Academic Press, London. 276-308.
- Dickinson CH, Bottomley D. 1980.** Germination and growth of *Alternaria* and *Cladosporium* in relation to their activity in the phylloplane. *Transactions of the British Mycological Society* 74, 304-319.

- Dimond AE, Horsfall JG. 1965.** Theory of inoculum. In Baker KF, Snyder WC, eds. *Ecology of Soil-borne Plant Pathogens*. University of California Press, Los Angeles. 404-414.
- Dodman RL, Fentje NT. 1970.** The mechanism and physiology of plant penetration by *Rhizoctonia solani*. In: Parmeter JR, ed. *Rhizoctonia solani, Biology and Pathology*. 149-160.
- Domsch KH, Gams W, Anderson TH. 1980.** *Compendium of Soil Fungi*. Academic press. London.
- Ebel J. 1986.** Phytoalexin synthesis: The biochemical analysis of the induction process. *Annual Review of Phytopathology* **24**, 235-264.
- Elad T, Chet I, Boyle P, Henis Y. 1983.** Parasitism of *Trichoderma* spp. on *Rhizoctonia solani* and *Sclerotium rolfsii* - Scanning electron microscopy and fluorescence microscopy. *Phytopathology* **73**, 85-88.
- Expert JM, Digat B. 1995.** Biocontrol of sclerotinia wilt of sunflower by *Pseudomonas fluorescens* and *Pseudomonas putida* strains. *Canadian Journal of Microbiology* **41**, 685-691.
- Ferris RS. 1981.** Calculating rhizosphere size. *Phytopathology* **71**, 1229-1231.
- Finlay RD, Read DJ. 1985.** The structure and function of the vegetative mycelium of ectomycorrhizal plants. I. Translocation of ¹⁴C-labelled carbon between plants interconnected by a common mycelium. *New Phytologist* **103**, 143-156.
- Garrett SD. 1934.** Factors affecting the severity of take-all. I. The importance of soil micro-organisms. *Journal of the Department of Agriculture, South Australia* **37**, 644-674.
- Garrett SD. 1956.** *Biology of Root Infecting Fungi*. Cambridge University Press, Cambridge.
- Garrett SD. 1970.** *Pathogenic Root Infecting Fungi*. Cambridge University Press, Cambridge.
- Garrett SD. 1981.** The early history and distribution of take-all. In: Asher MJC, Shipton PJ, eds. *Biology and Control of Take-all*. Academic Press, New York. 1-11.

- Ghisalberti EL, Sivasithamparam K. (1991).** Antifungal antibiotics produced by *Trichoderma* spp. *Soil Biology and Biochemistry* **23**, 1011-1020.
- Gilligan CA. 1979.** Modeling rhizosphere infection. *Phytopathology* **69**, 782-784.
- Gilligan CA. 1980a.** Inoculum potential of *Gaeumannomyces graminis* var *tritici* and disease potential of wheat roots. *Transactions of the British Mycological Society* **75**, 419-424.
- Gilligan CA. 1980b.** Zone of potential influence between host roots and inoculum units of the take-all fungus, *Gaeumannomyces graminis* var *tritici*. *Soil Biology and Biochemistry* **12**, 513-514.
- Gilligan CA. 1985.** Probability models for host infection by soil-borne fungi. *Phytopathology* **75**, 61-67.
- Gilligan CA. 1987.** Epidemiology of soil-borne plant pathogens. In: Wolfe MS, Caten CE, eds. *Populations of Plant Pathogens: Their Dynamics and Genetics*. Blackwell, Oxford.
- Gilligan CA. 1990a.** Mathematical models of infection. In: Lynch JM, ed. *The Rhizosphere*. Wiley and Sons, Chichester. 207-232.
- Gilligan CA. 1990b.** Comparison of disease progress curves. *New Phytologist* **115**, 223-242.
- Gilligan CA. 1994.** Temporal aspects of the development of root disease epidemics. In: Campbell CL, Benson DM, eds. *Epidemiology and Management of Root Diseases*. Springer-Verlag, London. 148-194.
- Gilligan CA, Brassett PR, Campbell A. 1994.** Modeling of early infection of cereal roots by the take-all fungus - A detailed mechanistic simulator *New Phytologist* **128**, 515-537.
- Gilligan CA, Simons SA. 1987.** Inoculum efficiency and pathozone width for two host-parasite systems. *New Phytologist* **107**, 549-566.
- Gilligan CA, Simons SA, Gubbins S. 1997.** Analysis and fitting of an SIR model with host response to infection load for plant disease. *Philosophical Transactions of the Royal Society* **352**, 353-364.

- Gilligan CA, Kleczkowski A. 1997.** Population dynamics of botanical epidemics involving primary and secondary infection. *Philosophical Transactions of the Royal Society* **352**, 591-608.
- Gow NAR, Gadd GM. 1995.** (eds). *The Growing Fungus*. Chapman and Hall, London.
- Grainger J. 1956.** Host nutrition and attack by fungal parasites. *Phytopathology* **46**, 445-456.
- Grogan RG, Sall MA, Punja ZK. 1980.** Concepts for modeling root infection by soil-borne fungi. *Phytopathology* **70**, 361-363.
- Grose M, Gilligan CA, Kleczkowski A, Goddard BV, Spencer D. 1997.** Spatial heterogeneity of soil water around single roots: use of CT-scanning to predict fungal growth in the rhizosphere. *New Phytologist* **133**, 261-272.
- Harrison LA, Letendre L, Kovacevich P, Pierson E, Weller D. 1993.** Purification of an antibiotic effective against *Gaeumannomyces graminis* var. *tritici* produced by a biocontrol agent, *Pseudomonas aureofaciens*. *Soil Biology and Biochemistry* **25**, 215-221.
- Hau B, Amorim L, Bergamin Filho A. 1993.** Mathematical functions to describe disease progress curves of double sigmoid pattern. *Phytopathology* **83**, 928-932.
- Henis Y, Ben-Yephet Y. 1970.** Effect of propagule size on saprophytic growth, infectivity and virulence on bean seedlings. *Phytopathology* **60**, 1351-56.
- Hollins TW, Scott PR, Gregory RS. 1986.** The relative resistance of wheat, rye and triticale to take-all caused by *Gaeumannomyces graminis*. *Plant Pathology* **35**, 93-100.
- Horan DP, Chilvers GA. 1990.** Chemotropism- The key to ectomycorrhizal formation. *New Phytologist* **116**, 297-301.
- Hornby D. 1981.** Inoculum. In Asher MJC, Shipton PJ, eds. *Biology and Control of Take-all*. Academic Press, New York. 271-294.
- Hornby D, Fitt DL. 1981.** Effects of root-infecting fungi on structure and function of cereal roots. In: Ayres PG, ed. *Effects of Disease on the Physiology of the Growing Plant*. Cambridge University Press. Cambridge. 101-130.

- Howie WL, Cook RJ, Weller DM. 1987.** Effect of soil matrix potential and cell motility on wheat root colonisation by fluorescent pseudomonads suppressive to take-all. *Phytopathology* **77**, 286-292.
- Innes P, Quarrie SA. 1987.** Water relations. In: Lupton FGH, ed. *Wheat breeding: Its Scientific Basis*. Chapman and Hall, London. 313-338.
- Jeger MJ. 1982.** The relation between total, infectious and post-infectious diseased plant tissue. *Phytopathology* **72**. 1185-1189.
- Jeger MJ. 1986.** The potential of analytic compared with simulation approaches to modeling in plant disease epidemiology. In Leonard KJ, Fry WE, eds. 1986. *Population Dynamics and Management. Vol. 1: Plant Disease Epidemiology*. Macmillan, New York. 255-281.
- Jeger MJ. 1987.** The influence of root growth and inoculum density on the dynamics of root disease epidemics: theoretical analysis. *New Phytologist*. **107**, 459-78.
- Jennings DH, Rayner ADM. 1984. (eds).** *The Ecology and Physiology of the Fungal Mycelium*. Cambridge University Press, Cambridge.
- Keller KO, Engel B, Heinrich K. 1995.** Specific detection of *Gaeumannomyces graminis* in soil using polymerase chain reaction. *Mycological Research* **99**, 1385-1390.
- Kenning LA, Hanchley P. 1980.** Ultrastructure of lesion formation in Rhizoctonia-infected bean hypocotyls. *Phytopathology* **70**, 998-1004.
- Kirk JJ, Deacon JW. 1986.** Early senescence of the root cortex in agricultural grasses and of wheat following root amputation or infection by the take-all fungus. *New Phytologist* **104**, 63-75.
- Kleczkowski A, Bailey DJ, Gilligan CA. 1996.** Dynamically generated variability in plant pathogen systems with biological control. *Proceedings of the Royal Society Series B*. **263**, 777-783.
- Kousik CS, Snow JP, Berggren GT. 1994.** Factors affecting cushion development by *Rhizoctonia solani* AG 1-IA and 1-IB on soybean leaves. *Plant Pathology* **43**, 237-244.

- Ko WH, Lockwood JL. 1967.** Soil fungistasis: relation to fungal spore nutrition. *Phytopathology* **57**, 894-901.
- Leonard KJ. 1980.** A reinterpretation of the mathematical analysis of rhizoplane and rhizosphere effects. *Phytopathology* **70**, 695-696.
- Lewis JA, Lumsden RD, Locke JC. 1996.** Biocontrol of damping off diseases caused by *Rhizoctonia solani* and *Pythium ultimum* with alginate-prills of *Gliocladium virens*, *Trichoderma hamatum* and various food bases. *Biocontrol Science and Technology* **2**, 163-173.
- Lewis JA, Papavizas GC. 1985.** Effect of mycelial preparations of *Trichoderma* and *Gliocladium* on populations of *Rhizoctonia solani* and the incidence of damping off. *Phytopathology* **75**, 812-817.
- Lewis JA, Papavizas GC. 1987.** Reduction of inoculum of *Rhizoctonia solani* in soil by germings of *Trichoderma hamatum*. *Soil Biology and Biochemistry* **19**, 195-201.
- Lewis JA, Papavizas GC. 1991.** Biocontrol of cotton damping off caused by *Rhizoctonia solani* in the field with formulations of *Trichoderma* spp. and *Gliocladium virens*. *Crop Protection* **10**, 396-402.
- Lim HS, Kim SD. 1995.** The role and characterization of beta-1,3-glucanase in biocontrol of *Fusarium solani* by *Pseudomonas stutzeri* ypl-1. *Journal of Microbiology* **33**, 295-301.
- Lingappa BT, Lockwood JL. 1964.** Activation of soil microflora by fungus spores in relation to soil fungistasis. *Journal of General Microbiology* **35**, 215-227.
- Lockwood JL. 1988.** Evolution of concepts associated with soil-borne plant pathogens. *Annual Review of Phytopathology* **26**, 93-121.
- Maloy OC. 1993.** *Plant Disease Control: Principles and Practice*. John Wiley and Sons. New York.
- Maplestone PA, Whipps JM, Lynch JM. 1991.** Effect of peat-bran inoculum of *Trichoderma* species on biological control of *Rhizoctonia solani* in lettuce. *Plant and Soil* **136**, 257-263.

- Marshall DS, Rush MC. 1980.** Infection cushion formation on rice sheaths by *Rhizoctonia solani*. *Phytopathology* **70**, 947-950.
- McCoy RJ, Krafts JM. 1984.** Comparison of techniques and inoculum sources in evaluating peas (*Pisum sativum*) for resistance to stem rot caused by *Rhizoctonia solani*. *Plant Disease* **68**, 53-55.
- McDougall BM, Rovia AD. 1970.** Sites of exudation of ¹⁴C-labelled compounds from wheat roots. *New Phytologist* **69**, 999-1003.
- Mead R, Curnow RN. 1990.** *Statistical Methods in Agriculture and Experimental biology*. Chapman and Hall, London.
- Nelson BD, Hertsgaard DM, Holley RC. 1989.** Disease progress of sclerotinia wilt of sunflower at varying plant populations, inoculum densities and environments. *Phytopathology* **79**, 1358-1363.
- Nicholson RL, Hammerschmidt R. 1992.** Phenolic compounds and their role in disease resistance. *Annual Review of Phytopathology* **30**, 369-389.
- Ogoshi A. 1987.** Ecology and pathogenicity of anastomosis group and intraspecific groups of *Rhizoctonia solani* Kühn. *Annual Review of Phytopathology* **25**, 125-143.
- Ousley MA, Lynch JM, Whipps JM. 1993.** Effect of *Trichoderma* on plant-growth - a balance between inhibition and growth promotion. *Microbial Ecology* **26**, 277-285.
- Parmeter JR, Whitney HS. 1970.** Taxonomy and Nomenclature of the Imperfect State. In: Parmeter JR, ed. *Rhizoctonia solani, Biology and Ecology*. University of California Press, Los Angeles. 7-31.
- Paustian K, Schnurer J. 1987a.** Fungal growth-response to carbon and nitrogen limitation- A theoretical model. *Soil biology & Biochemistry* **19**, 613-620.
- Paustian K, Schnurer J. 1987b.** Fungal growth-response to carbon and nitrogen limitation- Application of a model to laboratory and field data. *Soil biology and Biochemistry* **19**, 621-629.

- Pfender WF. 1982.** Monocyclic and polycyclic root diseases- Distinguishing between the nature of the disease cycle and the shape of the disease progress curve. *Phytopathology* **72**, 31-32.
- Pfender WF, Hagedorn DJ. 1983.** Disease progress and yield loss in *Aphanomyces* root rot of peas. *Phytopathology* **73**, 1109-1113.
- Prosser JI. 1994.** Molecular marker systems for detection of genetically engineered microorganisms in the environment. *Microbiology* **140**, 5-17.
- Prosser JI. 1995.** Kinetics of filamentous growth and branching. In Gow NAR, Gad GM, eds. *The Growing Fungus*. Chapman and Hall, London. 301-335
- Rattray EAS, Prosser JI, Glover LA, Killham K. 1995.** Characterisation of rhizosphere colonisation by luminescent *Enterobacter cloacae* at the population and single-cell levels. *Applied and Environmental Microbiology* **61**, 2950-2957.
- Rayner ADM, Coates D. 1987.** Regulation of mycelial organisation and responses. In: Rayner ADM, Brasier CM, Moore D, eds. *Evolutionary Biology of the Fungi*. Cambridge University Press, Cambridge. 115-136.
- Reddy MN, Roa AS, Rao KN. 1975.** Production of phenolic compounds by *Rhizoctonia solani*. *Transactions of the British Mycological Society* **64**, 146-148.
- Regalado CM, Crawford JW, Ritz K, Sleeman BD. 1996.** The origins of spatial heterogeneity in vegetative mycelia: A reaction-diffusion model. *Mycological Research* **100**, 1473-1480.
- Rengel Z, Graham RD, Pedler JF. 1994.** Time-course of biosynthesis of phenolics and lignin in roots of wheat genotypes differing in manganese efficiency and resistance to take-all fungus. *Annals of Botany* **74**, 471-477.
- Ritz K. 1995.** Growth-responses of some soil fungi to spatially heterogeneous nutrients. *FEMS Microbiology and Ecology* **16**, 269-279.
- Ritz K, Crawford J. 1990.** Quantification of the fractal nature of colonies of *Trichoderma viride*. *Mycological Research* **94**, 1138-1141.

- Robinson RA. 1969.** Disease resistance terminology. *Review of Applied Mycology*. **48**, 593-606.
- Robinson RK, Lucas RL. 1962.** The use of isotopically labelled mycelium to investigate the host range and rate of spread of *Ophiobolus graminis*. *New Phytologist* **62**, 50-53.
- Ross GJS. 1987.** *Maximum Likelihood Program*. Numerical Algorithms Group, Oxford.
- Rouse DI, Baker R. 1978.** Modeling and quantitative analysis of biological control mechanisms. *Phytopathology* **68**, 1297-1302.
- Rovira AD, Wildermuth GB. 1981.** The nature and mechanisms of suppression. In: Asher MJC, Shipton PJ, eds. *Biology and Control of Take-all*. Academic Press, New York. 385-415.
- Rupe JC, Gbur EE. 1995.** The effect of plant age, maturity group, and the environment on disease progress of sudden-death syndrome of soybean. *Plant Disease* **79**, 139-143.
- Russell CN. 1996.** *LUX* gene reporting of the interaction between *Gaeumannomyces graminis* and an antagonistic Pseudomonad in the wheat rhizosphere. *PhD Thesis*. University of Aberdeen.
- Ryder MH, Rovira AD. 1993.** Biological-control of take-all of glasshouse-grown wheat using strains of *Pseudomonas corrugata* isolated from wheat field soil. *Soil Biology and Biochemistry* **25**, 311-320.
- Samuels GJ. 1996.** *Trichoderma* - a review of biology and systematics of the genus. *Mycological Research* **100**, 923-935.
- Schroth MN, Hildbrand DC. 1964.** Influence of plant exudates on root infecting fungi. *Annual Review of Phytopathology* **2**, 101-132.
- Schutte KH. 1956.** Translocation in the fungi. *New Phytologist* **55**, 164-182.
- Scott PR. 1969.** Effects of nitrogen and glucose on saprophytic survival of *Ophiobolus graminis* in buried straw. *Annals of Applied Biology* **63**, 27-36.
- Shipton PJ. 1981.** Saprophytic survival between susceptible crops. In Asher MJC, Shipton PJ, eds. *Biology and Control of Take-all*. Academic Press, New York. 295-316.

Skou JP. 1975. Studies on the take-all fungus *Gaeumannomyces graminis*. V. Development and regeneration of roots in cereal species during the attack. *Kongelige Veterinaer -og Landbohøiskoles Aarsskrift* 142-160.

Skou JP. 1981. Morphology and cytology of the infection process. In Asher MJC, Shipton PJ, eds. *Biology and Control of Take-all*. Academic Press, New York. 175-198.

Slope DB, Salt GA, Broo EW, Gutteridge RJ. 1978. Occurrence of *Phialophora radiculicola* var. *graminicola* and *Gaeumannomyces graminis* var. *tritici* on wheat roots in field crops. *Annals of Applied Biology* **88**, 239-246.

Smalla K, Cresswell N, Mendoncahagler LC, Wolters A, Vanelsas JD. 1993. Rapid DNA extraction protocol from soil for polymerase chain reaction mediated amplification. *Journal of Applied Bacteriology*. **74**, 78-85.

Speakman JB, Lewis BJ. 1978. Limitation of *Gaeumannomyces graminis* by wheat root responses to *Phialophora radiculicola*. *New Phytologist* **80**, 373-380.

Swinton, Anderson. 1995. Model frameworks for plant-pathogen interactions. In Grenfell BT, Dobson AP, eds. *Ecology of Infectious Diseases in Natural Populations*. Cambridge University Press. 280-294.

Thomashow LS, Weller DM, Bonsall RF, Pierson LS. 1990. Production of the antibiotic phenazine-1-carboxylic acid by fluorescent *Pseudomonas* species in the rhizosphere of wheat. *Applied Environmental Microbiology* **56**, 908-912.

Thornton CR. 1996. Detection and quantification of *Rhizoctonia solani* in soil by monoclonal antibody-based immuno-magnetic bead assay. *Soil Biology & Biochemistry*. **28**, 527-532.

Thornton CR, Dewey FM, Gilligan CA. 1993. Development of monoclonal antibody-based immunological assays for the detection of live propagules of *Rhizoctonia solani* in soil. *Plant Pathology* **42**, 763-773.

Thornton CR, Dewey FM, Gilligan CA. 1994. Development of monoclonal antibody-based immunosorbent assay for the detection of live propagules of *Trichoderma harzianum* in a peat-bran medium. *Soil Biology and Biochemistry* **26**, 909-920.

- Trinci APJ. 1971.** Influence of the peripheral growth zone on the radial growth rate of fungal colonies. *Journal of General Microbiology* **67**, 325-344
- Trinci APJ. 1979.** The duplication cycle and branching in fungi. In: Burnett JH, Trinci APJ, eds. *Fungal Walls and Hyphal Growth*. Cambridge University Press, Cambridge. 319-358
- Trinci APJ. 1984.** Regulation of hyphal branching and hyphal orientation. In: Jennings DH and Rayner ADM, eds. *The Ecology and Physiology of the Fungal Mycelium*. 23-52. Cambridge University Press, Cambridge.
- Trinci APJ, Saunders PT, Gosrani R, Campbell KAS. 1979.** Spiral growth of mycelium and reproductive hyphae. *Transactions of the British Mycological Society* **73**, 283-293.
- Vance CP, Kirk TK, Sherwood RT. 1980.** Lignification as a mechanism of disease resistance. *Annual Review of Phytopathology* **18**, 259-288.
- Vanderplank JE. 1963.** *Plant Diseases: Epidemics and Control*. New York: Academic.
- Vanderplank JE. 1975.** *Principles of Plant Infection*. New York. Academic.
- Van Fleet DS. 1961.** Histochemistry and function of the endodermis. *Botanical Reviews* **27**, 165-220.
- Vilgalys R, Cubeta MA. 1994.** Molecular systematics and population biology of *Rhizoctonia*. *Annual Review of Phytopathology* **32**, 135-55.
- Waggoner PE. 1986.** Progress curves of foliar diseases: their interpretation and use. In: Leonard KJ, Fry WE, eds. 1986. *Population Dynamics and Management. Vol. 1: Plant Disease Epidemiology*. New York: Macmillan. 3-37.
- Walker J. 1972.** Type studies on *Gaeumannomyces graminis* and related fungi. *Transactions of the British Mycological Society* **58**, 427-457.
- Walker J. 1975.** Take all diseases of Gramineae: a review of recent work. *Review of Plant Pathology* **54**, 113-144.

Weindling R. 1934. Studies on a lethal principle effective in the parasitic action of *Trichoderma lignorum* on *Rhizoctonia solani* and other soil fungi. *Phytopathology* **24**, 1152-1179.

Weinhold AR, Motta J. 1973. Initial host responses in cotton to infection by *Rhizoctonia solani*. *Phytopathology* **63**, 157-162.

Weinhold AR, Sinclair JB. 1996. *Rhizoctonia solani*: Penetration, colonization and host response. In: Sneh B, Jabaji-Hare S, Neate S, Dijkstra G, eds. *Rhizoctonia Species: Taxonomy, Molecular Biology, Ecology, Pathology and Disease Control*. Kluwer Academic Publishers, Dordrecht.

Weller DM. 1984. Distribution of a take-all suppressive strain of *Pseudomonas fluorescens* on seminal roots of winter wheat. *Applied Environmental Microbiology* **48**, 897-899.

Weller DM. 1988. Biological control of soil-borne pathogens in the rhizosphere with bacteria. *Annual Review of Phytopathology* **26**, 379-407.

Werker AR, Gilligan CA, Hornby D. 1991. Analysis of disease progress curves for take-all in consecutive crops of winter wheat. *Plant Pathology* **40**, 8-24.

Whipps JM. 1990. Carbon economy. In: Lynch JM, ed. *The Rhizosphere*. Wiley and Sons, Chichester. 59-97.

Whipps AR, Lewis K, Cooke RC. 1988. Mycoparasitism and plant disease control. In: Burge MN, ed. *Fungi in Biological Control Systems*. Manchester University Press, Manchester.

Whipps JM, Lynch JM. 1985. Energy losses in the plant by rhizodeposition. *Annual Proceedings of the Phytochemical Society of Europe* **26**, 59-71.

Yarham DJ. 1981. Practical aspects of epidemiology and control. In Asher MJC, Shipton PJ, eds. *Biology and Control of Take-all*. Academic Press, New York. 353-384.

Yarwood CE, Sylvester ES. 1959. The half life concept of longevity of plant pathogens. *Plant Disease* **43**, 125-128.

Zadoks JC, Schein RD. 1979. *Epidemiology and Plant Disease Management*. New York. Oxford University Press.

Zhou T, Paulitz TC. 1994. Induced resistance in the biocontrol of *Pythium aphanidermatum* by *Pseudomonas* spp on cucumber. *Phytopathologische Zeitschrift* **142**, 51-63.

Appendix I

Soils

Soil	Location	Type*	Class	Content	pH
Soil 1	Cambridge University Farm	Evesham 3	Sandy loam	Clay = 17.0 % Organic matter = 2.0 %	7.0
Soil 2	Cambridge University Farm	Hanslope	Sandy clay loam	Clay = 23.8% Organic matter = 2.1%	7.5
Soil 3	Woburn Experimental Farm	Bearsted	Loamy sand	Clay = 6.85% Organic matter = 1.1%	6.7

* Classification from the Soil Survey of England and Wales, 1983 (Rothamsted Experimental Station).

Appendix II

Isolates

1. *Gaeumannomyces graminis*

Isolate	Location	Host	Source
Av	Unknown	Unknown	CAG
BF1	CUF (Brookfields)	10 th wheat	-
BF3	CUF (Brookfields)	10 th wheat	-
BF4	CUF (Brookfields)	10 th wheat	-
Cv	Unknown	Unknown	CAG
ML1	CUF (Meadowlands)	2 nd wheat	-
ML2	CUF (Meadowlands)	2 nd wheat	-
ML3	CUF (Meadowlands)	2 nd wheat	-
ML5	CUF (Meadowlands)	2 nd wheat	-
NM1	CUF (Nomans)	4 th wheat	-
NM2	CUF (Nomans)	4 th wheat	-
NM5	CUF (Nomans)	4 th wheat	-

CUF = Cambridge University Farm;

CAG = Dr C. A. Gilligan, University of Cambridge

2. *Rhizoctonia solani*

Isolate	Anastomosis group	Host	Source
R1	4	<i>Solanum tuberosum</i>	CAG
R2	2-1	<i>Solanum tuberosum</i>	CAG
R3	4	NA	RB
R5	2-1	<i>Solanum tuberosum</i>	CAG
R8	3	<i>Solanum tuberosum</i>	CAG
R10	3	<i>Solanum tuberosum</i>	CAG
R13	3	<i>Solanum tuberosum</i>	CAG
R14	3	<i>Solanum tuberosum</i>	CAG
J262	3	NA	CAG
J312	4	NA	CAG
J317	2-1	NA	CAG
AG1	1	<i>Beta vulgaris</i>	IMI (303154)
AG 2-1	2-1	<i>Linum usitatissimum</i>	IMI (303155)
AG 2-2	2-2	<i>Arachis hypogaea</i>	IMI (303156)
AG3	3	<i>Solanum tuberosum</i>	IMI (303158)
AG4	4	<i>Phaseolus spp.</i>	IMI (303162)

NA = information unavailable

CAG = Dr C. A. Gilligan, University of Cambridge, Cambridge, UK.

RB = Dr R. Baker, Colorado State University, USA.

IMI = International Mycological Institute, Egham, Surrey, UK.

3. *Trichoderma* and *Gliocladium*

Isolate	Species	Source
Ex_PM	<i>Trichoderma viride</i>	Dr P. Mills. Horticultural Research International, Wellesbourne, Warwickshire, UK.
TMD	<i>Gliocladium repens</i>	Dr F.M. Dewey. University of Oxford, Oxford, UK.

Appendix III

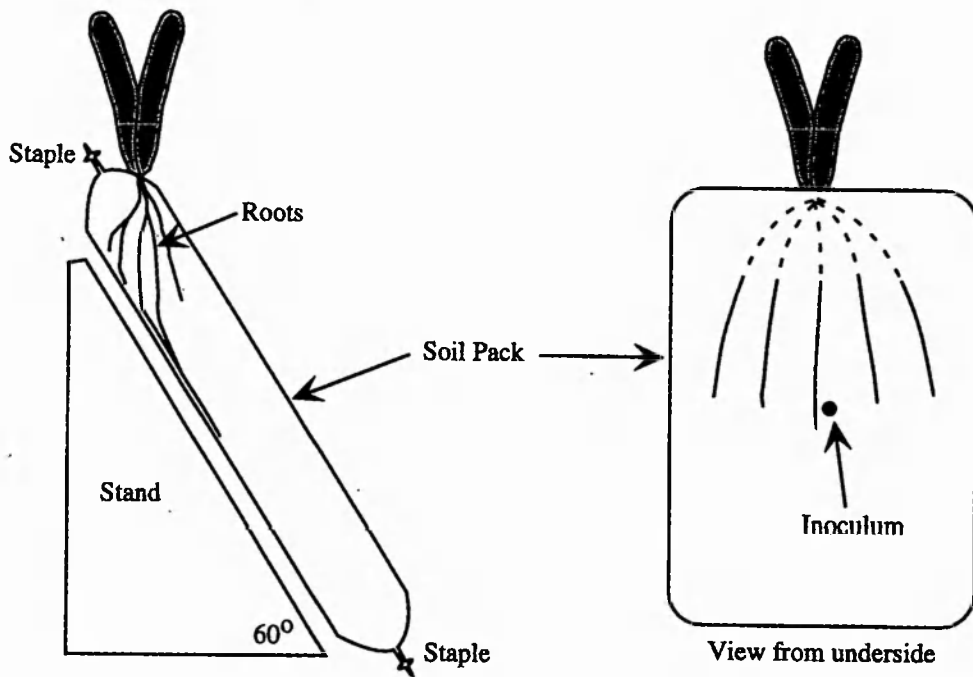


Diagram showing the soil pack system used for the derivation of pathozone profiles for *Gaeumannomyces graminis* var. *tritici* on wheat. The pathozone describes changes in the probability of infection with distance between inoculum and host.